DCU

Dublin City University

Ollscoil Chathair Bhaile Átha Cliath

INVESTIGATION OF A NOVEL ELECTROCATALYST FOR HYDROGEN PEROXIDE REDUCTION AND ITS APPLICATION TO SENSING AND BIOSENSING

by

Laura Gonzalez-Macia

Thesis submitted for the Degree of Doctor of Philosophy

Supervisors:
Prof. Anthony J. Killard
&
Prof. Malcolm R. Smyth

School of Chemical Sciences   **May 2011**

DECLARATION

I hereby certify that this material, which I now submit for assessment on the programme of study leading to the award of PhD, is entirely my own work, that I have exercised reasonable care to ensure that the work is original, and does not to the best of my knowledge breach any law copyright, and has not been taken from the work of others save and to the extend that such work has been cited and acknowledged within the text of my work.

Signed: _____

(Candidate) ID No.: ___57115982_____

Date: _____10 / 05 / 11 _____

ACKNOWLEDGEMENTS

First of all, I would like to thank Prof. Malcolm Smyth for giving me the opportunity to join his research group and develop this work in Dublin City University.

The second person I would like to acknowledge is Prof. Tony Killard for his guidance and discussions during all these years. Thank you so much Tony for your constant support and optimism, which were indispensable for the development of this thesis.

I would like also to thank Dr. Aoife Morrin, Dr. Blanaid White and Dr. Karl Crowley for their invaluable help and support during the last three years.

Thanks to all the members of sensors and separations group I have met during these years in DCU. A special thanks to Kyriaki, Agnieszka, Ewa, Hannah and Jeremy for their support and for sharing laughs and tears with me. Because of them I remember my time in DCU with a smile.

Special thanks to my friends back in Seville: Maria, Myriam, Cristina, Jose and Rocio for their long distance support and for all the things we have shared since we started the "big adventure" in the Faculty of Chemistry together. Particular thanks to Emilio for his discussions about chemistry, research and life in general.

I also would like to thank my friends in Dublin: Dessi, Leti, Xaira, Bea, Pili, Ana… for all the moments that we have shared during the last years. They have been my closest support all this time and made me laugh even in the bad moments.

Finally, I would like to thank my parents for their wholehearted encouragement throughout all my life. They have been an unconditional support for me, even long distance, and I really feel very lucky to have them. Thanks also to my sister, Bea, and

DEDICATION

To my parents and to my sister and brother,

for all their support

TABLE OF CONTENTS

Abbreviations

α	Reaction order
A	Ampere, electrode area
A_{cat}	Surface area of the catalyst
a_{Ox}	Chemical activity for the oxidant species
a_{Red}	Chemical activity for the reductant species
AFM	Atomic force microscopy
Ag/AgCl	Silver/silver chloride reference electrode
AgNPs	Silver nanoparticles
Ag SPE	Silver screen printed electrode
Au SPE	Gold screen printed electrode
Au SPE AT	Gold screen printed electrode cured at high temperature
Au SPE BT	Gold screen printed electrode cured at low temperature
β	Reaction order
BCA	Bicinchoninic acid
BET	Brunauer-Emmett-Teller analysis
BSA	Bovine serum albumin
C SPE	Carbon screen printed electrode
CA	Cellulose acetate
CD	β-cyclodextrin
CHIT	Chitosan
ChOx	Cholesterol oxidase
CILE	Carbon ionic liquid electrodes
CL	Chemiluminescence
CMC	Critical micelle concentration
CNTs	Carbon nanotubes
CoPC	Cobalt phthalocyanine
COs	Chitosan oligomers
CPE	Carbon paste electrode

cryo-FESEM	Cryo-field emission scanning electrode microscopy
CTAB	Cetyltrimethylammonium bromide
Cu SPE	Copper-plated screen printed electrode
DBF	Dibutylphtalate
DBSA	Dodecylbenzenesulphonic acid
dpi	Drops per inch
DS	Degree of substitution
E	Cell potential
E^0	Standard cell potential
Ea	Energy of activation
EDC	1-ethyl-3-(3-dimethylaminopropyl) carbodiimide hydrochloride
EDTA	Ethylenediaminetetraacetic acid
EDX	Energy Dispersive X-ray
EM	Electron microscopy
F	Faraday constant
FCE	Ferrocene-modified carbon paste electrode
FFTCCV	Fast Fourier transformation continuous cyclic voltammetry
FIA	Flow injection analysis
GA	Glutaraldehyde
GC	Glassy carbon
GCE	Glassy carbon electrode
GNp	Gold nanoparticles
GOx	Glucose oxidase
HGPM	Hydrophobic gas permeable membrane
HMDA	Hexamethylenediamine
H_2O_2	Hydrogen peroxide
HPPA	3-(4-hydroxyphenyl)propionic acid
HRP	Horseradish peroxidase
i	Current
i_{cat}	Catalytic reduction current
IJP	Inkjet printing

ISE	Ion-selective electrode
ITO	Indium tin oxide
j	Current density
k	Rate constant for a reaction
k_{app}	Apparent first-order rate constant
k_s	Heterogeneous rate constant
LOD	Limit of detection
MEMs	Microelectromechanical Systems
MWCNTs	Multiwalled carbon nanotubes
n	Number of electrons transferred
N	Moles of electroactive species reacted
NAD^+	Nicotinamide adenine dinucleotide
NaDoBS	Sodium dodecylbenzenesulfonate
Nf	Nafion
OLED	Organic Light-Emitting Diode
OPD	o-phenylenediamine
ORC	Oxidation-reducton cycles
PABS	p-aminobenzene sulfonic acid
PANI	Polyaniline
PB	Prussian blue
PBS	Phosphate buffer solution
PEDOT	Poly(3,4-ethylenedioxythiophene)
PEM	Polymer electrolyte membrane
PET	Poly(ethylene) terephthalate
PNR	Poly(neutral red)
PPy	Polypirrole
PSA	Polyester pressure sensitive adhesive
PSS	Poly(styrenesulfonate)
Pt	Platinum
Pt SPE	Platinum screen printed electrode
PVA	Polyvinyl alcohol

PVC	Polyvinyl chloride
PVP	Poly(vinylpirrolidone)
Q	Charge
R	Intensive reaction rate
R&D	Research and development
r.s.d.	Relative standard deviation
ROS	Reactive oxygen species
SAMs	Self-assembled monolayers
S/B	Signal-to-background
SDS	Sodium dodecyl sulphonate
SE	Secondary Electron
SEM	Scanning electron microscopy
ssDNA	Single-stranded deoxyribonucleic acid
SWCNTs	Single-walled carbon nanotubes
t	Time
TDMAI	Tridodecylmethylammoniumiodide
TEM	Transmission electron microscopy
ttb-CuPc	tetra-*terc*-butyl copper phthalocyanine
UV	Ultra violet
v_i	stoichiometric coefficient of species i
V	Volt
V_{liq}	Volume of solution
XPS	X-Ray Photoelectron Spectroscopy
XRD	X-ray powder diffraction
YSI	Yellow Spring Instruments
z	Number of moles of electrons transferred in a cell reaction

ABSTRACT

Hydrogen peroxide has, for many years, been shown to be a very important compound due to its wide and varied applications in many industrial processes as well as biological systems. Therefore, its detection and measurement represents an important analytical issue. Traditional methods such as titrimetry or spectrophotometry have more recently been displaced by electrochemical techniques, which have proven to be an inexpensive and effective means of hydrogen peroxide determination. Hydrogen peroxide is also the final product in many biochemical processes, most notably in oxidation reactions employing enzymes such as glucose oxidase where it is used extensively as a reporter molecule which is amenable to electrochemical detection.

In this work, a novel electrocatalyst for the reduction of hydrogen peroxide was employed as the foundation for the development of an electrochemical biosensor for glucose determination. Critical to this development was to understand the nature of the novel catalytic material which was based on a modification of silver paste electrodes, and the fabrication of an enzyme biosensor platform capable of operating on this material. A further key theme that was explored in this work was to make the biosensor amenable to fabrication using printing techniques, including screen printing and inkjet printing.

With regard to the novel electrocatalyst, it was shown that the modification of silver screen printed electrodes (Ag SPEs) with a solution of dodecylbenzenesulphonic acid (DBSA) and potassium chloride (KCl) significantly improved the catalytic activity of those electrodes towards the electrochemical reduction and decomposition of hydrogen peroxide. Characterisation of the modified electrodes was performed by surface analysis and electrochemical techniques. Other surfactant/salt combinations were also assessed and showed an analogous catalytic effect on the hydrogen peroxide reactions. The application of such a phenomenon for the development of novel hydrogen peroxide sensors was evaluated.

DBSA/KCl modification was further performed on a range of metallic and metal paste electrodes in order to better understand the catalytic process as well as to assess the feasibility of other modified materials as hydrogen peroxide sensors. Both the electrochemical reduction and decomposition processes were studied and the electrode surfaces were also analyzed by microscopic techniques. A kinetic study of the hydrogen peroxide decomposition process was also performed. The apparent and heterogeneous rate constants for this process were calculated and comparisons between materials were carried out. Possible mechanisms for the catalysis are proposed along with identification of the most optimal materials and processing methodologies. Further work was performed on the DBSA/KCl-modified Ag SPEs.

The most common enzyme used for the development of glucose biosensors is glucose oxidase, which oxidizes glucose to gluconolactone in the presence of oxygen, leading to the formation of hydrogen peroxide as a product. DBSA/KCl modified Ag SPEs were assessed as platforms for the development of a glucose biosensor. A cellulose acetate membrane was found to be required to separate enzyme from glucose substrate at the electrode surface as well as to form the site for enzyme immobilization. Analytical parameters of the glucose biosensor such as limit of detection (LOD), sensitivity and reproducibility were evaluated and compared to other systems in the literature.

The application of the inkjet printing technique to the deposition of the modification solution was investigated to improve the reproducibility of the biosensor devices since such a technique enhances the control of the reagent volume. Comparisons with glucose biosensors fabricated by drop-coating were presented. The potential application of inkjet printing for the manufacture of an all-printed biosensor was also assessed. In general, the notable enhancement towards hydrogen peroxide reactions of Ag SPEs following exposure to DBSA/KCl solutions was used for the development of novel enzyme-less hydrogen peroxide sensors. These devices were subsequently employed in the fabrication of glucose biosensors by immobilization of glucose oxidase onto the modified electrode surfaces. Inkjet printing was proven to be a feasible technique for

DBSA/KCl modification of Ag SPEs, which represented the first step towards an all-printed glucose biosensor device.

Although successful in principle, for the fabrication of a glucose biosensor, improvements are required to improve the analytical properties of the device which may be brought about by further understanding and improvement of the catalytic material.

Chapter 1

Electrocatalysis and detection of hydrogen peroxide:
A Literature Review

1.1. INTRODUCTION

Hydrogen peroxide has, for many years, been shown to be a very important compound as an intermediate in many industrial processes as well as in many biological systems. This has made it highly relevant in the food, environmental, clinical and pharmaceutical industries and related areas of research.[1, 2] The importance of H_2O_2 is related to its unique oxidising properties. Hydroxyl radicals formed during the decomposition of H_2O_2 are used as oxidising agents in the degradation of organic pollutants from water such as the azo dye compounds used in the textile industry, which are toxic to aquatic life and carcinogenic to humans.[1, 3] H_2O_2 and its derivatives can also be employed as powerful oxidising agents in the synthesis of many organic compounds.[4] Moreover, the decomposition of H_2O_2 plays a very important role in the manufacture of industrial water electrolysers, secondary metal-air batteries and fuel cells.[5, 6] Besides its many industrial applications, H_2O_2 can also create problems; its excessive concentration as a product of industrial and atomic power stations affects the environment.[7] Polymer electrolyte membranes (PEM) used in fuel cells may be degraded by the chemical attack of hydroxyl free radicals generated from H_2O_2.[8] Regarding medical applications, H_2O_2 is a major reactive oxygen species (ROS) in living organisms and plays a central role in causing several life-threatening human diseases. H_2O_2 is the most valuable marker for oxidative stress, which is connected to aging and severe human diseases such as cancer, cardiovascular disorders, Alzheimer and related neurodegenerative diseases.[7, 9, 10] Many enzymatic reactions also create H_2O_2 as an end-product so its concentration may be used as an indicator of the progress of the reaction.[4] Due to these wide and varied applications, its determination represents an important analytical issue.

In the present review, a detailed look at the detection methods of H_2O_2 is taken, with particular emphasis on electrochemical techniques. The most significant materials and catalytic mechanisms in the literature to date are discussed, along with the main applications of H_2O_2 detection.

1.2. METHODS FOR HYDROGEN PEROXIDE DETECTION

Numerous processes for H_2O_2 detection have been published in the literature and successfully used for specific applications. The techniques employed in the measurement of H_2O_2 tend to consist either of the direct chemical detection of H_2O_2 or indirect measurement as a consequence of its reaction with enzymes, mainly horseradish peroxidase (HRP). Direct detection methods are generally prone to interferences and are sometimes time-consuming and difficult for automated detection.[11] In contrast to this, the specific character of the enzymatic reaction between HRP and H_2O_2 allows H_2O_2 determination in the presence of interferences. However, the use of an enzyme brings about several drawbacks such as reduced stability (special requirements of temperature, pH, and concentration), electron transfer issues and substrate saturation, which affects linear calibration range.[7, 12]

Laboratory methods for the determination of H_2O_2 concentrations may be classified into five categories as follows: Titrimetry; Spectrophotometry; Fluorescence; Chemiluminescence and Electrochemical methods. These will be reviewed, with special attention given to electrochemical methods.

1.2.1. Titration methods

Several titration schemes have traditionally been used for the determination of H_2O_2. In the permanganate method, a peroxide solution is titrated with permanganate (VII), which is reduced to manganese (II) in the presence of H_2O_2.[13] This method is subject to interferences caused by both organic and inorganic substances that react with permanganate. Hurdis et al.[14] reported the determination of H_2O_2 by cerate oxidimetry. The method consists of the reduction of cerium (IV) in the form of ceric sulfate ($Ce[SO_4]_2$) to cerium (III) by H_2O_2 under acidic conditions in the presence of a ferroin indicator. No significant difference in results by the cerate and permanganate methods was found.[15] The iodometric method has been widely used since it was first proposed by Kingzett in 1880.[16] The method is based on the oxidation of iodide to iodine by H_2O_2 in the presence of a molybdate catalyst and the subsequent titration of the iodine formed

with a thiosulfate solution using a starch indicator to indicate the endpoint. Catalysis or interference from transition metals such as iron, copper, nickel and chromium as well as the fading of colour are possible issues that may affect the accuracy of this method.

1.2.2. Spectrophotometric methods

Matsubara et al.[17] used a water-soluble titanium (IV)-porphyrin complex, $[TiO(tpypH_4)^{4+}]$, to determine trace amounts of H_2O_2. It was observed that the absorbance of $TiO(tpypH_4)^{4+}$ at 432 nm decreased significantly in proportion to the concentration of H_2O_2 added, this being due to the consumption of $TiO(tpypH_4)^{4+}$ accompanied by the formation of $TiO_2(tpypH_4)^{4+}$. This reagent was used for the determination of H_2O_2 in water samples such as tap water and rainwater and absorbance was found to be proportional to H_2O_2 concentration in the range $1.0 \cdot 10^{-8}$ to $2.8 \cdot 10^{-6}$ M. Seller[18] reported the use of potassium titanium (IV) oxalate for the spectrophotometric determination of H_2O_2 concentrations down to 10 µM. The method seemed to be particularly suitable for the determination of H_2O_2 in the presence of complexing and reducing agents, although interference by fluoride was observed. The iodometric method is similar to the iodometric titration in that iodide is oxidized to iodine in the presence of molybdate catalyst. Then, the I_3^- species, which is in equilibrium with I_2 and I^-, is measured spectrophotometrically at 351 nm.[15] More recently, Sunil and Narayana[19] reported a variation of the iodometric method using toluidine blue as a reagent. The liberated iodine bleached the blue colour of toluidine blue measured at 628 nm and the decrease in absorbance was directly proportional to H_2O_2 concentration. The modification of the spectrophotometric method improved the measurement of H_2O_2 at low concentrations. Possible interfering agents for this method included transitions metals and oxidants such as chlorine.

1.2.3. Fluorescence methods

The spectrofluorimetric determination of H_2O_2 is generally based on an enzyme catalytic oxidation reaction of a fluorogenic substrate by H_2O_2. Horseradish peroxidase

(HRP) is a haem-containing enzyme and the most commonly used enzyme in H_2O_2 determination due to its high selectivity.[20] Chang et al.[21] developed a sensing probe for H_2O_2 based on the HRP immobilization on Fe_3O_4/SiO_2 magnetic nanoparticles. H_2O_2 was activated in the presence of HRP and oxidized non-fluorescent 3-(4-hydroxyphenyl)propionic acid (HPPA) to a fluorescent product with an emission maximum at 409 nm. Liu et al.[20] used β-cyclodextrin (CD)-hemin instead of HRP as the catalyst in the spectrofluorometric determination of H_2O_2. 4-methylphenol (*p*-cresol) was used as the substrate because it presented low fluorescence whereas the oxidation product showed high fluorescence intensity with a maximum at 410 nm. The use of β-cyclodextrin solved some of the drawbacks shown by HRP such as its cost and instability in solution. Demirata-Öztürk et al.[22] reported the determination of H_2O_2 by fluorimetry in the presence of ceric ions. H_2O_2 was oxidized by ceric ions (nonfluorescent) in acid solution and the Ce(III) ions produced were determined by a fluorimetric method at an emission maximum of 360 nm. The spectrofluorimetric methods resulted in LODs for H_2O_2 in the order of nM. However, they were susceptible to interference from organic matter in water.[15, 21]

1.2.4. Chemiluminescence methods

Several chemiluminescence methods for H_2O_2 determination involve the use of 5-amino-2,3-dihydro-1,4-phathlazinedione (luminol). When H_2O_2 is mixed with luminol in the presence of a catalyst, the decomposition of H_2O_2 leads to a sequence of reactions resulting in the release of photons from a luminol by-product. Either Co(II) or Cu(II) can be used as a catalysts for H_2O_2 decomposition.[15] Hanaoka et al.[23] reported the determination of H_2O_2 by chemiluminescence (CL), using a heterogeneous catalyst, Co(II)-monoethanolamine complex immobilized on Dowex-50W resin. They developed a H_2O_2 flow sensor, which showed a linear ratio of CL versus the concentration of H_2O_2 in the range $2 \cdot 10^{-7} \rightarrow 2 \cdot 10^{-5}$ M and a detection limit of $1 \cdot 10^{-7}$ M (S/N = 3). The application of the device to determine H_2O_2 in rainwater samples yielded satisfactory results. The use of luminol is subject to interferences in natural water.

Chemiluminescence provided a LOD lower than the titration and spectrophotometric methods, although the best values were reported by fluorescence methods, down to 10^{-9} M.[21] Titration methods seemed to be suitable for H_2O_2 detection at high concentrations, being inaccurate for the determination of H_2O_2 below 10^{-3} M. However, spectrophotometry allowed H_2O_2 detection down to 10^{-6} M, whereas 10^{-8} M H_2O_2 was achievable by fluorescence and chemiluminescence.[15] However, most of these techniques employed a partial or total human operation, making the automated quantification of H_2O_2 difficult. Moreover, the above-mentioned methods have proved to be time-consuming and highly prone to interferences.[24] All these drawbacks have led the search for alternative methods for H_2O_2 detection.

1.2.5. Electrochemical methods

As was mentioned above, the challenge associated with H_2O_2 detection was its accurate quantification at low concentration[7] in samples containing possible interferences. Thus, one of main drawbacks of the traditional techniques was their inability to give precise results in the presence of interferences such as chlorine, which is very common in water samples. Recently, electrochemical methods have exhibited the potential to be inexpensive and of high sensitivity, resulting in an effective way to examine the reactions of many substances.[2, 4, 12, 25] Moreover, they are quite selective techniques, which allow the determination of a particular analyte by choosing the appropriate applied potential, eliminating possible interferences.

As is well-known, a chemical sensor is a device that transforms real-time chemical information of its surrounding environment (from the concentration of a specific sample component to total composition analysis), into an analytically useful signal.[26, 27] Generally, chemical sensors contain two basic components connected in series: a chemical recognition system (receptor) and a physico-chemical transducer. In the case of electrochemical sensors, the analytical information is obtained from the electrical signal that results from the interaction of the target analyte and the receptor. According to the nature of the electrical signal, the electrochemical sensors can be classified into the following categories: Amperometric sensors; Potentiometric sensors; Conductimetric

sensors. The main characteristics and transduction mechanisms for such electrochemical sensors are shown in Table 1.1.

Table 1.1. Characteristics of electrochemical sensors[28]

Transducer	Mechanism	Signal	Example
Amperometric	Electron charge transfer reaction (Faraday´s law)	Current (due to production or consumption of electroactive species)	Clark electrode (Oxygen), fuel cells, H_2O_2
Potentiometric	Multiphase equilibrium (Nernst equation)	Potential (due to distribution of ionic species across phases)	Glass pH electrode, ion selective electrodes, gas sensors
Conductimetric	Variation of resistance with composition	Conductance or resistance (due to changes in resistive elements with absorption-adsorption events)	Gas and humidity sensors

1.2.5.1. Amperometric sensors

Amperometric sensors are based on the measurement of the current resulting from the electrochemical oxidation or reduction of an electroactive species. The signal transduction process is accomplished by controlling the potential of the working electrode at a fixed value (relative to a reference electrode) and monitoring the current as a function of time. The applied potential provides the driving force for the electron transfer reaction of the electroactive species.[26] The resulting current is directly proportional to the rate of the electron transfer reaction and, therefore, to the bulk concentration of the electroactive species. The relationship between the moles, N, of electroactive species reacted (either oxidized or reduced) and the charge passed through the sensor, Q, is known as Faraday's Law:

$$N = Q/nF \qquad \text{(Equation 1.1)}$$

where n is the number of electrons transferred per mole and F is the Faraday constant ($F = 96487$ C/mol).[28]

Many of the current devices for the determination of H_2O_2 are based on amperometric sensors. Li et al.[29] reported the development of a disposable amperometric biosensor based on the screen printing technique for the commercial detection of H_2O_2 at –0.3 V (vs. a screen-printed Ag/AgCl pseudo-reference electrode). Horseradish peroxidase (HRP) was entrapped in a polypyrrole (PPy) film electropolymerized on the surface of the carbon screen printed electrode. Potassium ferrocyanide was used as a mediator to improve the electron transfer between the enzyme and the electrode. The sensor showed a sensitivity of $3.3 \cdot 10^{-2}$ AM^{-1}cm^{-2} and a relative standard deviation (r.s.d.) of 10.24% (n = 5). Mattos et al.[30] described the fabrication of amperometric sensors selective for H_2O_2 based on Prussian blue (PB) modified gold (Au) and platinum (Pt) screen printed electrodes. Tetrabutylammonium toluene-4-sulphonate when added to the buffer was shown to improve the long term stability of the PB films on both Au and Pt electrodes. H_2O_2 determination was performed at –0.05 V (vs. Ag/AgCl) and the sensitivities exhibited by the sensors were 2 and 1 AM^{-1}cm^{-2} for Au and Pt electrodes, respectively. Zhang et al.[31] developed a sensitive amperometric H_2O_2 sensor based on a glassy carbon electrode modified with a composite made from thionin, EDTA, multiwalled carbon nanotubes (MWCNTs) and chitosan (CHIT). Thionin was used as a mediator and was covalently immobilized onto the MWCNTs-CHIT film by means of EDTA activated by carbodiimide (EDC). The amperometric detection of H_2O_2 was carried out at approx. –0.4 V (vs. Ag/AgCl). The sensor showed high sensitivity with a LOD of $6.5 \cdot 10^{-8}$ M (S/N=3) and a reproducibility of 5.6% (r.s.d.) for n = 3. Lately, there is an increasing amount of research focus on amperometric probes due to their high sensitivity and rapid performance. This has seen amperometric sensors become widely used for the determination of H_2O_2 compared to other electrochemical techniques, as will be discussed below.

1.2.5.2. Potentiometric sensors

Potentiometric measurements rely on the determination of the potential difference at zero current between either an indicator and a reference electrode or two reference electrodes separated by a permselective membrane.[27] The analytical information is obtained by converting the recognition process into a potential difference, which is proportional (in a logarithmic fashion) to the concentration (activity) of species generated or consumed in the recognition event. The most important feature in a potentiometric measurement is that equilibrium conditions are established between electroactive species in solution and at the electrode. This is in contrast to the diffusion-limited condition characteristic of amperometric measurements and leads to relations between voltage and concentration that are logarithmic rather than linear. The relationship between the potential and the ionic concentration in solution in a potentiometric chemical sensor is given by the Nernst equation:

$$E = E^0 - \frac{0.05916 \text{ V}}{z} \log_{10} \frac{a_{\text{Red}}}{a_{\text{Ox}}}.$$

(Equation 1.2)

where E is the cell potential, E° is the standard cell potential, z is the number of moles of electrons transferred in the cell reaction, and a_{Red} and a_{Ox} are the chemical activities for the reductant and oxidant species, respectively.

Potentiometric sensors generally involve the use of ion-selective electrodes (ISEs) for obtaining the potential signal.[26] An ISE is an electrochemical sensor based on thin films or selective membranes as recognition elements. Common potentiometric devices are pH electrodes, several other ion (F^-, I^-, CN^-, Na^+, K^+, Ca^{2+}, NH_4^+) and gas (CO_2, NH_3) selective electrodes.[27] Ngeontae et al.[32] reported the use of a Ag-ISE modified with a polymeric membrane of benzothiazole calyx[4]arene as an ionophore for the detection of H_2O_2 and its application to the fabrication of a glucose biosensor. Silver nanoparticles (AgNPs) were used as a redox marker and were oxidized to free Ag^+ ions by H_2O_2. The log-linear relationship between H_2O_2 concentration and activity of free Ag^+ was followed by direct potentiometry. The working linear range for glucose was found to be

from $1\cdot10^{-4}$ to $3\cdot10^{-3}$ M when the electrodes were measured in $1\cdot10^{-2}$ M magnesium acetate buffer, pH 6.0, with the enzyme in solution. The sensor showed a LOD of $1\cdot10^{-5}$ M and a reproducibility below 7% (r.s.d.) Zheng et al.[33] developed a potentiometric H_2O_2 sensor by doping a carbon paste electrode (CPE) with MnO_2 and using solid paraffin as gluing material. The sensor exhibited a LOD of $1.2\cdot10^{-7}$ M and many potentially interfering ionic species were shown not to interfere in H_2O_2 determination, except Co^{2+} and PO_4^{3-}. The sensor was applied to the quantitative determination of H_2O_2 in rainwater samples and good agreement was obtained by comparing the results with those of the chemiluminescence method. Kalayci et al.[34, 35] used an iodide selective electrode for the detection of H_2O_2 and its subsequent application for glucose determination. The iodide selective electrode consisted of 10% of the ion exchanger tridodecylmethylammoniumiodide (TDMAI) as the active material, dibutylphtalate (DBF) as the plasticiser and PVC as the membrane matrix. Iodide was oxidized by H_2O_2 in the presence of a molybdenum (VI) catalyst and therefore, the decrease of iodide concentration was proportional to the concentration of H_2O_2 in the bulk solution. By immobilizing glucose oxidase (GOx) on the surface the iodide selective electrode, it was used as a biosensor for the determination of glucose content in blood. Potentiometric sensors are often very attractive because of their high selectivity, simplicity and low cost and they have been more widely used in the past. However, their lower sensitivity and often slower response compared to amperometric sensors have lately shifted the balance towards the latter.

1.2.5.3. Conductimetric sensors

Conductimetric (or resistive) sensors rely on the electrical resistance change that accompanies the interaction of a target analyte with a conductive layer (typically a polymer or ceramic) held between two electrodes.[28] In the case of conductimetric biosensors, changes in substrate and product concentrations resulting from the catalytic action of enzymes may bring about a net change in solution electrical conductivity. This conductivity change may result from a number of mechanisms: 1. The generation of ionic groups; 2. The separation of unlike charges; 3. Proton generation and buffering; 4.

Changes in the size of charge-carrying groups, and 5. Changes in the degree of association of ionic species.[36] In order to thoroughly define the selectivity of the sensors and improve their commercial utility, meticulous calibration with a variety of potential interferents is required. Conductimetric sensors are generally inexpensive and quite simple to construct since they do not need a reference electrode. The conductimetric transducers can be manufactured using simple thin film technology, and the voltage can be rather small to substantially decrease the power consumption and to reduce safety risks when used in living organisms.[37, 38] Few conductimetric sensors for H_2O_2 determination can be found in the literature because the relatively low impedance of aqueous media hinders the proper operation of the sensor. Sergeyeva et al.[37] reported the fabrication of a conductimetric biosensor for H_2O_2 determination using tetra-*tert*-butyl copper phthalocyanine (ttb-CuPc) thin film and horseradish peroxidise (HRP) as the sensitive element. The ttb-CuPc film is able to change its conductivity in the presence of molecular iodine. The sensor was then based on the detection of molecular iodine produced as a result of the oxidation of iodide ions by H_2O_2 in the presence of HRP. A scheme of the conductimetric biosensor is shown in Fig. 1.1.

$$H_2O_2 + 2I^- + 2H^+ \qquad 2H_2O + I_2$$

HRP

HGPM, 100 nm

ttb-CuPc film, 200 μm

Au/Cr electrodes, 1 μm

ceramics, 200 μm
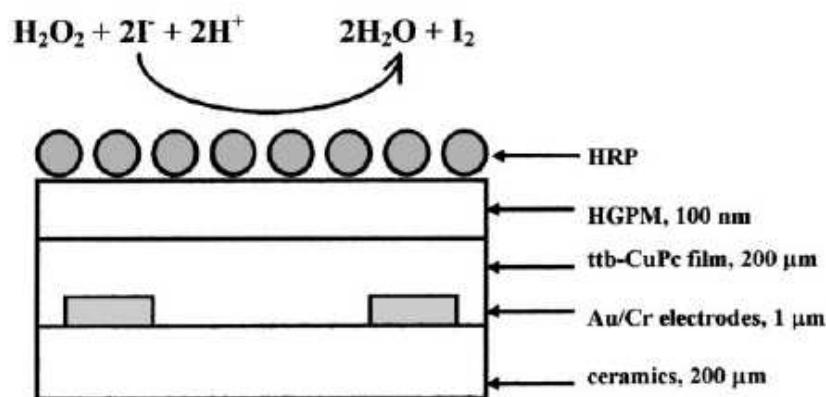
Figure 1.1. **Scheme of a conductimetric biosensor for H_2O_2 determination.**[37]

A hydrophobic gas-permeable membrane (HGPM) was placed on to the iodine-sensitive film to avoid interferences from the ionic strength and buffer capacity of the

aqueous media. A linear range of H_2O_2 concentration from 0.05 to $3 \cdot 10^{-4}$ M and a standard deviation below 10% were obtained with the conductimetric device.

The high dependence of the conductimetric measurements on the buffering capacity of the aqueous solutions has limited their use to gas-sensing applications whereas potentiometric and, more particularly, amperometric devices are predominant in aqueous-sensing applications.

1.3. MATERIALS FOR H_2O_2 ELECTROCATALYSIS

The main purpose of a sensor recognition system is to provide the sensor with a high degree of selectivity for the analyte to be measured.[27] Apart from the inherent catalytic characteristics of a material towards the analyte, its selectivity may be improved by the choice of a suitable electrical potential, by the introduction of a catalytic reaction step, through the addition of permselective membranes or by further modifications.[28] Many materials have been used in the literature for the electrocatalytic detection of H_2O_2. This section will review the most important materials with particular interest in the analytical parameters of the sensing devices fabricated from them.

1.3.1. Platinum

Electrochemical detection of H_2O_2 has been traditionally performed at platinum electrodes because of its excellent electrocatalytic properties towards H_2O_2. Zhang et al.[39] studied the electrochemical oxidation of H_2O_2 on Pt disk electrodes in physiological buffer at pH 7.4. Amperometric measurements were performed by applying a constant potential of 0.65 V (vs. Ag/AglCl). The phenomenon was shown to be strongly influenced by factors such as pH, temperature and surface conditioning. Hall et al.[40] also reported the study of the electrochemical oxidation of H_2O_2 at a Pt rotating disk electrode over a range of concentration and rotation rates. Details about the proposed mechanisms for H_2O_2 oxidation will be given in the next section. Many other H_2O_2 sensors are based on further modifications of Pt electrodes. For example, Wang et al.[41]

reported the development of a non-enzymatic electrode for H_2O_2 sensing based on the electro-polymerization of aniline and single-walled carbon nanotubes (SWCNTs) on a Pt electrode. The composite film was synthesized in an ionic liquid and provided excellent stability and enhanced selectivity towards H_2O_2 detection. A detection limit of $1.2 \cdot 10^{-6}$ M and a response time of 4 s were observed by chronoamperometry at approx. -0.35 V (vs. Ag/AgCl).

However, Pt electrodes are expensive and susceptible to poisoning, so require meticulous cleaning pretreatment procedures. Also, a resistive oxide film is created on Pt surfaces over time at constant potential, altering the electrode response, so measurements must either take this into account or allow for the film to reach a stable equilibrium before commencing experimentation.[4, 42] Moreover, the potential applied for H_2O_2 detection on Pt is inside the potential range for the oxidation of some common interfering species, such as ascorbic acid, urea and paracetamol. Therefore, other types of electrodes have been studied for the determination of H_2O_2.

1.3.2. Silver

Silver has proved to be an excellent material for the direct electro-analytical detection of H_2O_2.[4, 12] Lian et al.[12] reported the enhanced characteristics of a Ag electrode towards H_2O_2 reduction after it was roughened by electrochemical oxidation-reduction cycles (ORC) in a KCl solution. The improvement in the catalytic activity of the roughened electrode was ascribed to the small Ag nanoparticles produced from the electrodeposition of Ag^+ during the oxidation-reduction process. A LOD of $6 \cdot 10^{-6}$ M, a response time of 2 s and a reproducibility of 4.6% (r.s.d., n = 10) were the analytical parameters of the sensor obtained at an applied potential of approx. –0.35 V (vs. Ag/AgCl). Zhao et al.[43] synthesized 'flowerlike' silver microspheres, which were used to fabricate a H_2O_2 sensor by immobilization on a glassy carbon electrode. Silver structures were obtained by reduction of $AgNO_3$ in the presence of ascorbic acid as reductant and poly(vinylpyrrolidone) (PVP) as the stabilizer. Fig. 1.2 shows a typical SEM picture of the flowerlike silver microspheres. The sensor exhibited a LOD of $1.2 \cdot 10^{-6}$ M (estimated at S/N = 3), a response time of 3.5 s and a relative standard

deviation less than 5% when the electrode was measured at approx. –0.55 V in PBS pH 7.0.
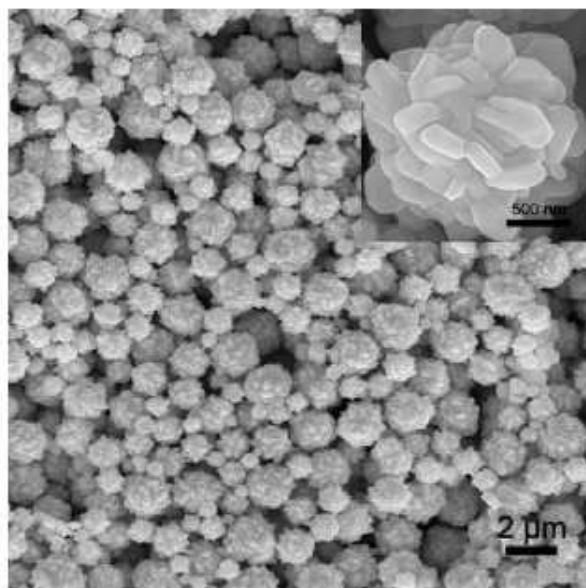
Figure 1.2. **SEM image of flowerlike silver microspheres used for the reduction of hydrogen peroxide. Inset: high magnification SEM image.[43]**

Recently, interest has been shown in using silver nanoparticles for the electro-analytical detection of H_2O_2.[2, 4, 44] The microelectrode arrays created by the deposition of metallic nanoparticles on electrodes have been shown to significantly improve the sensitivity of electro-analytical sensing methods due to their large specific surface areas, excellent conductivities and biocompatibilities. Welch et al.[4] recently reported the application of silver nanoparticles (AgNPs) on glassy carbon (GC) electrodes to detect H_2O_2. The nanoparticles were deposited on GC electrodes from a solution containing silver nitrate and tetra-n-butylammonium perchlorate in acetonitrile after the application of –0.5 V vs. Ag/AgCl for 1 min. A H_2O_2 reduction wave at approx. –0.7 V vs Ag/AgCl was observed by cyclic voltammetry. The LOD of the AgNP-GC device in phosphate buffer pH 7.4 was $2.0 \cdot 10^{-6}$ M, with a five times higher sensitivity than that observed at a

silver macroelectrode. They also studied how different stripping times influenced the distribution and size of the Ag nanoparticles on the electrode surface. In each case Ag was deposited for 1 min and they found that longer stripping times led to smaller particle sizes. When the Ag nanoparticles were not stripped, the electrode behaved as a Ag macro-electrode and H_2O_2 was reduced directly on the Ag via a mechanism analogous to that proposed by Honda et al.[45] (see reactions 1.15-1.17 on p20). However, when the Ag nanoparticles were stripped, a negative shift in the peak potential and the presence of a shoulder in the reduction wave were observed during the determination of H_2O_2 by cyclic voltammetry. The shoulder was attributed to the electrode-reduction of oxygen on glassy carbon, produced via the silver-catalysed decomposition of H_2O_2. Guascito et al.[2] have also reported the use of AgNPs for the analytical determination of H_2O_2. The sensor was fabricated by immobilizing AgNPs in a polyvinyl alcohol (PVA) film on a platinum electrode. Cyclic voltammograms and voltammetry showed that AgNPs facilitated H_2O_2 reduction, exhibiting catalytic activity at –0.55 V vs Ag/AgCl. The estimated LOD for this electrode was $1.0 \cdot 10^{-6}$ M, based on S/N = 3.

However, Ag is prone to oxidation when it is in contact with the air and the increase in the degree of the electrode oxidation on Ag electrodes leads to a retardation in the H_2O_2 reduction process.[45] Ag as a commodity has also seen a recent dramatic increase in price which is impacting on its cost-effectiveness as a catalytic substrate.

1.3.3. Other metals and metal alloys

Besides Pt and Ag, many other metals such as Fe, Zn, Cu[46] and Pd[47] and metal alloys such as Pd/Au,[48] Pd/Ir, and Au/Pt[4] have been employed as catalysts for hydrogen peroxide reactions. For example, Zen et al.[49] developed a disposable copper-plated screen printed carbon electrode (CuSPE) for H_2O_2 determination at ambient temperature. The electrode was prepared by electrochemical deposition of a Cu layer at –0.7 V (vs. Ag/AgCl) from a solution containing $Cu(NO_3)_2$ on to a carbon screen printed electrode. The detection of H_2O_2 was performed by flow injection analysis (FIA) at a poised potential of –0.3 V (vs Ag/AgCl) and a flow rate of 2 ml·min^{-1}. A LOD of $9.7 \cdot 10^{-7}$ M (S/N = 3), a sensitivity of $3.45 \cdot 10^{-2}$ AM^{-1} and a reproducibility of 1.1% (r.s.d., n = 10)

were obtained by the device in PBS pH 7.4. Considerable interferences due to Cl^- and O^- ions were reported. Kumar and Sornambikai[50] reported the amperometric detection of H_2O_2 in physiological solution (pH 7) by means of a Nafion/Cu particulate modified glassy carbon electrode (GCE). The GCE/Nf was first doped with copper (II) ions, which were subsequently converted into copper cluster particulate islands by applying a potential of –0.7 V (vs. Ag/AgCl) for a determined time. The electrochemical sensing experiments were carried out at –0.2 V (vs. Ag/AgCl) and a LOD of $1.63 \cdot 10^{-6}$ M (S/N = 3) was obtained. The determination of H_2O_2 in real sample solutions such as milk, human urine and green tea was successfully demonstrated with this system.

Pd, Ru and Pd-Ru nanoparticles have been also investigated as electrocatalysts for H_2O_2.[51] The nanoparticles were supported on Vulcan XC-72 carbon and the system was characterized by transmission electron microscopy (TEM), X-ray powder diffraction (XRD) and electrochemical techniques. After 30 min measurement in $3 \cdot 10^{-2}$ M H_2O_2, Pd-Ru/C catalyst showed higher catalytic activity for H_2O_2 electroreduction than Pd/C and Ru/C.

1.3.4. Protein and enzyme-based sensors

In trying to mimic biological systems, H_2O_2 has been determined by electrodes modified with redox proteins and enzymes such as haemoglobin, soybean peroxidase, myoglobin[24, 52, 53] and horseradish peroxidase (HRP).[24, 54, 55] The latter enzyme has been the most commonly used enzyme for construction of H_2O_2 biosensors due to its ready commercial availability in high purity and low cost. Many methods and materials including absorption, cross-linking, self-assembly, and gel or polymer entrappment have been studied to improve HRP immobilization and transduction in the manufacture of H_2O_2 biosensors, with the aim of achieving high enzyme activity and a sensitive electron transducer.[56] Yemini et al.[57] recently reported the use of well-organized peptide monolayers to anchor HRP enzyme molecules on gold electrode surfaces. The electrodes were first soaked in a peptide-containing solution for 2 min. They were then rinsed and treated with 1-ethyl-3-(3-dimethylaminopropyl) carbodiimide hydrochloride (EDC) to subsequently immobilize HRP molecules by covalent bonds. Fig. 1.3 shows the HRP

immobilization process onto the collagen-like peptide. The enzymatic activity of the immobilized HRP was measured by spectroscopy and a typical current-time curve for successive additions of H_2O_2 was registered at –0.1 V (vs. Ag/AgCl) with response time lower than 10 s.
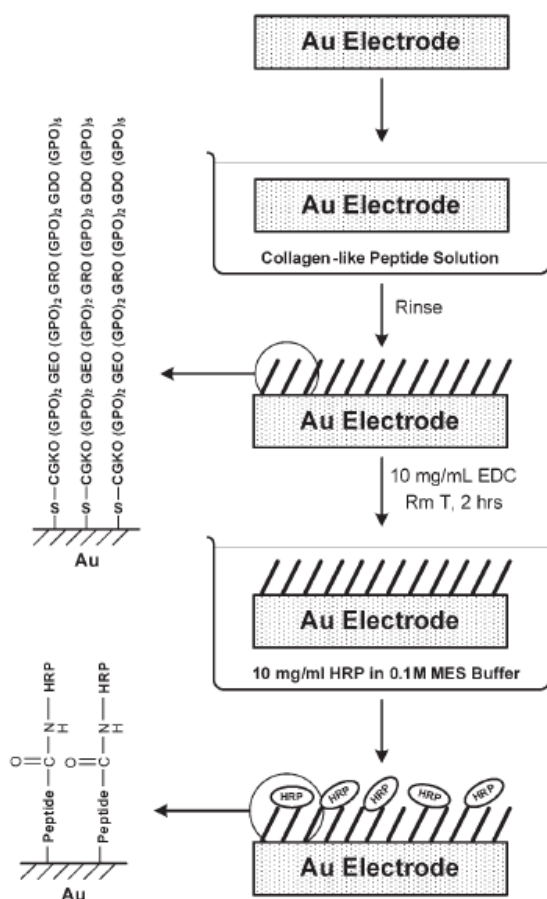
Figure 1.3. **Scheme of the electrode preparation: first, the collagen-like peptide is immobilized onto the Au electrode; then, the functionalized electrodes are activated with carbodiimide (EDC) and HRP is deposited on top. After the process, the electrodes were rinsed and air dried.**[57]

Several studies have employed self-assembled monolayers (SAMs) for HRP immobilization on electrode surfaces[57, 58] with the limitations of low biocompatibility

and partial activity loss due to the covalent attachment of the enzyme to the monolayer. Li et al.[56] reported the fabrication of an amperometric biosensor where HRP was immobilized on a sandwiched nano-Au particle/ *m*-phenylenediamine polymer film by glutaraldehyde cross-linking. The poly (*m*-phenylenediamine) film was potentiostatically electropolymerized on the surface of a home-made ferrocene-modified carbon paste electrode (FCE). Au colloid particles were spread on the electrode surface and a new *m*-phenylenediamine polymerization was then carried out. Once rinsed, the enzyme was immobilized on the surface, showing still more than 90% of its initial activity after two weeks storage. The sensor presented a detection limit of $1.3 \cdot 10^{-7}$ M and was used to determine H_2O_2 concentration in plant leaf samples. Interfering substances such as glucose, ethanol or ascorbic acid were tested, showing less than 1% interference.

Chen et al.[59] reported the incorporation of HRP into a poly(3,4-ethylenedioxy thiophene) (PEDT) film and their subsequent use as an amperometric biosensor for H_2O_2 sensing. The vapour phase polymerized PEDT films could shrink to 5% of their original thickness during a washing step. This advantage was used to successfully entrap HRP molecules within a PEDT film following exposure to an ethanol solution containing such enzyme. The sensing activity of the device towards H_2O_2 detection was demonstrated by sensing $5 \cdot 10^{-3}$ M H_2O_2 in phosphate buffered saline solution with a sensitivity of 190 μA cm^{-2}.

However, the special requirements of temperature, concentration and pH to maintain enzyme stability and the difficulties in finding an appropriate method of immobilization of the enzyme on a solid surface as well as the saturation with the substrate, which affects linear calibration range, have led the search for alternative non-enzymatic process to H_2O_2 determination.[7, 12]

1.3.5. Other materials

Another widely used material in H_2O_2 detection is ferric hexacyanoferrate or Prussian blue (PB). This reagent was first used for selective detection of H_2O_2 by its reduction in the presence of oxygen by Karyakin's group.[60] Thereafter, many studies of the electrocatalytic reduction of H_2O_2 by PB have been performed. It has been shown as

the most advantageous peroxide transducer. Thus, compared to platinum, PB modified electrodes are three orders of magnitude more active in H_2O_2 reduction and oxidation in neutral media and three orders of magnitude more selective for H_2O_2 reduction in the presence of O_2.[7, 61] Recently, the possibility for nanostructuring of PB by its electrochemical deposition through lyotropic liquid crystal templates has been reported. The detection limit of the resulting sensor was $1 \cdot 10^{-8}$ M and a linear calibration range for H_2O_2 concentrations from $1 \cdot 10^{-8}$ to $1 \cdot 10^{-2}$ M was shown.[7]

Many polymers have also been used in the catalytic detection of H_2O_2. For example, the electrochemical H_2O_2 reduction on poly (*p*-aminobenzene sulphonic acid) (PABS)-modified glassy carbon electrodes was studied. The enzyme-less amperometric sensor showed a linear range of detection of 0.5 to $5 \cdot 10^{-4}$ M H_2O_2 and a LOD of $1 \cdot 10^{-5}$ M (S/N = 3) from the amperometric curves obtained at –0.7 V vs. Ag/AgCl.[25] This polymer-based H_2O_2 sensor device showed worse sensing parameters than previously reported examples. Daly et al.[62] evaluated the use of three polymers (polypyrrole, polyaniline and 1,3-diaminobenzene) for the suppression of interferents during H_2O_2 detection on metallised (Ru, Rh, Pt) carbon electrodes. The electrodes were measured at +0.65 V (the potential required for electrocatalysis of H_2O_2 using non-membrane electrodes) and at +0.10 V (vs. Ag/AgCl) in the presence of H_2O_2 and interferents such as L-ascorbic acid, acetaminophen, L-cysteine and uric acid. The latter applied potential was shown to provide the maximum H_2O_2: interferent ratio.

1.4. CATALYTIC MECHANISMS FOR H_2O_2 DETECTION

H_2O_2 is a colourless liquid, slightly more viscous than water (density = 1.11 g/ml, giving a molarity of 9.8 M)[63] and completely miscible in water and alcohol. It behaves as a weak acid (pK_a = 11.6) and at alkaline pH's it deprotonates to form a perhydroxyl ion along with a hydrogen ion:[15, 64]

$$H_2O_2 \rightleftharpoons H^+ + HO_2^- \hspace{3cm} \text{(reaction 1.1)}$$

H_2O_2 is unstable with respect to disproportionation and it decomposes to oxygen and water exothermically. In practice, however, it is not very labile and survives reasonably well at moderate temperatures and low and moderate pH. Nevertheless, it will rapidly decompose when catalytic agents (like iron) are present.[65] The reaction corresponding to the decomposition of H_2O_2 is the following:

$$2 H_2O_2 \rightarrow O_2 + 2H_2O \qquad \text{(reaction 1.2)}$$

H_2O_2 is considered a strong oxidizing agent, but is dependent on the pH. The half-cell reaction for H_2O_2 in acidic and neutral aqueous solutions is as follows:[39]

$$H_2O_2 + 2H^+ + 2e^- \rightarrow 2H_2O \qquad \text{(reaction 1.3)}$$

The standard potential for reaction 1.3 is 1.76 V, so H_2O_2 behaves as a powerful oxidizing agent in acid solutions, although generally it requires activation to exhibit such properties.[15, 64] In basic solutions, however, the half-cell potential is lower ($E^0 = 0.87$ V) because of the presence of the perhydroxyl ion rather than of the H_2O_2 molecule:

$$HO_2^- + H_2O + 2e^- \rightarrow 3OH^- \qquad \text{(reaction 1.4)}$$

H_2O_2 can also behave as a reducing agent. The half-cell reaction in acid solutions is the following:

$$H_2O_2 \rightarrow 2H^+ + O_2 + 2e^- \qquad \text{(reaction 1.5)}$$

The standard potential for reaction 1.5 is –0.69 V.[64] The corresponding half-cell reaction in basic conditions has a standard potential of –0.08 V and is:[66]

$$HO_2^- + OH^- \rightarrow O_2 + H_2O + 2e^- \qquad \text{(reaction 1.6)}$$
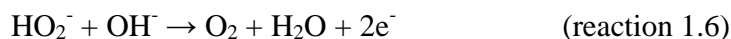
Generally, electrochemical reactions of H_2O_2 presents slow electrode kinetics on many electrode materials and as a result, high overpotentials are required.[4]

Many mechanisms have been proposed in the literature for the electrochemical oxidation and reduction of H_2O_2, which are reliant on the catalyst material. Some of the most important mechanism will be reported below.

Pt has been widely used as a catalyst for the electrochemical oxidation of H_2O_2.[40] However, the electro-oxidation of H_2O_2 in the neutral pH range is not yet fully understood. Most studies were performed under extreme pH conditions which simplified the electrode mechanism because either $[H^+]$ or $[OH^-]$ was high enough to give reproducible results. Moreover, the catalytic decomposition of H_2O_2 on a Pt electrode has been a major problem for the oxidative detection of H_2O_2 as the current efficiency depends on the rate of catalytic decomposition.[39] On the other hand, the oxidation of H_2O_2 is favoured on oxidized Pt surfaces as the potential region had previously been shown to correspond to platinum oxide film formation. Hickling and Wilson[67] first, and Lingane and Lingane[68] later suggested that the oxidation of H_2O_2 on Pt occurred through the initial reduction of the Pt oxide film by H_2O_2 followed by the re-oxidation of Pt to Pt oxides, according to the following scheme:

$$PtO + H_2O_2 \rightarrow Pt + H_2O + O_2 \qquad \text{(reaction 1.7)}$$
$$Pt + 2OH^- - 2e^- \rightarrow PtO + 2H_2O \qquad \text{(reaction 1.8)}$$

Gorton[48] proposed a similar mechanism for the oxidation of H_2O_2 at Pd. A carbon electrode was modified by vapour deposition of a thin layer of a mixture of Pd and Au. Assuming that Au only acts to aid dispersion of Pd, H_2O_2 oxidation was proposed to be dependent on surface oxide films in a similar manner to that previously reported for Pt and follows the scheme:[40, 48]

$$Pd(OH)_2 + H_2O_2 \rightarrow Pd + 2H_2O + O_2 \qquad \text{(reaction 1.9)}$$
$$Pd + 2H_2O \rightarrow Pd(OH)_2 + 2e^- + 2H^+ \qquad \text{(reaction 1.10)}$$
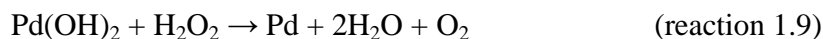
H_2O_2 reduces the metal oxide film to the metal, which is re-oxidized electrochemically. Johnston et al.[69] also studied H_2O_2 oxidation on Pd/Au thin-film electrodes. They found similar results to those of Gorton and suggested a surface binding site model incorporating reactions 1.11 and 1.12 to correct the deviation of the linearity observed by the latter:

$$H_2O_{2\ bulk} \rightarrow H_2O_{2\ surface} \qquad \text{(reaction 1.11)}$$

$$H_2O_{2\ surface} + Pd(OH)_2 \rightleftarrows Pd(OH)_2 \cdot H_2O_2 \qquad \text{(reaction 1.12)}$$

$$Pd(OH)_2 \cdot H_2O_2 \rightarrow Pd + 2H_2O + O_2 \qquad \text{(reaction 1.13)}$$

$$Pd + 2H_2O \rightarrow Pd(OH)_2 + 2H^+ + 2e^- \qquad \text{(reaction 1.14)}$$
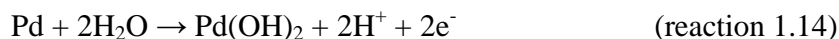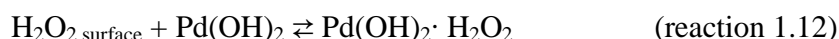
The first step of the mechanism involved the diffusion of H_2O_2 to the electrode surface. The surface complex was assumed to be in rapid equilibrium and the anodic potential was high enough so that reaction 1.14 was more rapid than 1.13.

Honda et al.[45] studied the electrochemical reduction of H_2O_2 at a Ag electrode in acidic solution. The proposed mechanism for the cathodic reaction was the following:

$$H_2O_2 + e^- \rightarrow OH_{(a)} + OH^- \qquad \text{(reaction 1.15)}$$

$$OH_{(a)} + e^- \rightarrow OH^- \qquad \text{(reaction 1.16)}$$

$$2OH^- + 2H^+ \rightarrow 2H_2O \qquad \text{(reaction 1.17)}$$

where $OH_{(a)}$ designates the adsorbed state. Reaction 1.15 was considered as the rate-determining step and the whole mechanism was the same as suggested for the reaction on Ag in alkaline solution[66] and on other metal electrodes. The mechanism concluded for the anodic reaction was:

$$Ag \rightleftarrows Ag^+_{(s)} + e^- \qquad \text{(reaction 1.18)}$$

$$Ag^+_{(s)} \rightarrow Ag^+_{(b)} \qquad \text{(reaction 1.19)}$$

where (s) and (b) designate the state of Ag^+ near the electrode surface and in the bulk of the solution, respectively. The detection of Ag^+ by chemical analysis confirmed the dissolution of Ag, although reaction 1.19 was considered as the rate-determining step.

1.5. APPLICATIONS OF THE DETECTION AND ELECTROCATALYSIS OF H_2O_2

As was mentioned above, H_2O_2 determination has become extremely relevant in recent years because of its wide and varied applications. Two of the main applications of H_2O_2 detection are in biosensors and fuel cells.

1.5.1. Biosensors

Many enzymatic reactions produce H_2O_2 as an end-product so its concentration may be used as an indicator of the progress of the reaction.[4] The coupling of H_2O_2 electrochemical detection to amperometric biosensors as the signal transducing device has contributed significantly to the development of the sensor industry. One of the most frequently used biosensors to date has, of course, been the glucose sensor with glucose oxidase (GOx) as the biospecific reagent. Fig. 1.4 shows the scheme of a glucose biosensor. The reactions involved in the process are:[39, 40]

Glucose + $O_2 \rightarrow$ gluconic acid + H_2O_2 (reaction 1.20)

$H_2O_2 \rightarrow O_2 + 2H^+ + 2e^-$ (reaction 1.21)
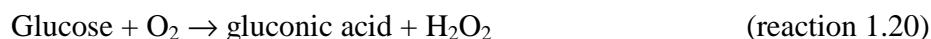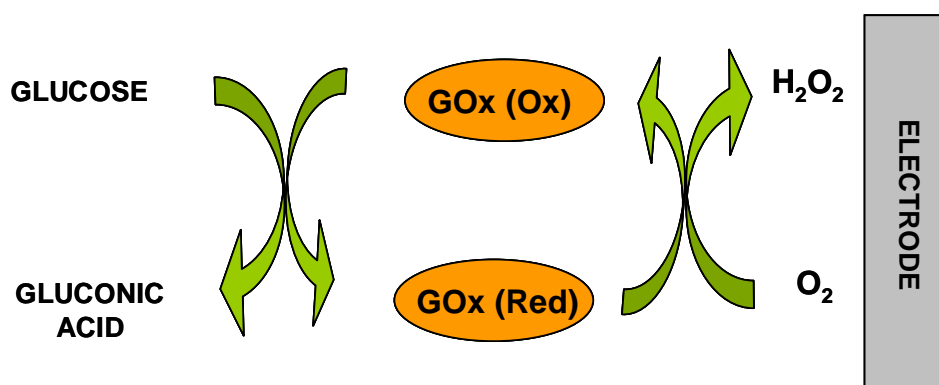
Figure 1.4. **General scheme of a glucose biosensor.**

The first glucose biosensor was developed in 1962 by Clarks and Lyons[70] and was based on the monitoring of the oxygen consumed by the enzyme-catalyzed reaction. The enzyme electrode consisted of a thin layer of GOx entrapped over an oxygen electrode via a semipermeable dialysis membrane. However, measurements of H_2O_2 formation have the advantage of being simpler, especially where miniaturized devices are concerned, as well as providing higher sensitivity. A very common configuration has been the YSI probe based on a Pt electrode. The biosensor involved the entrapment of GOx between an inner anti-interference cellulose acetate membrane and an outer diffusion-limiting/biocompatible one (such as Nucleopore polycarbonate membrane) to form an enzyme sandwich.[71, 72] Since then, many glucose sensing devices have been fabricated by the immobilization of GOx on an electrode surface which had previously been shown to be ultrasensitive to H_2O_2 detection. Thus, Cao et al.[73] fabricated a glucose biosensor based on ultrafine Pt nanoparticles dispersed on a glassy carbon electrode. Pt nanoparticles have been shown to facilitate the electron transfer and increase the surface area, which enhances the catalytic activity towards H_2O_2. The enzyme was then immobilized on to the modified electrode and a mixture of glutaraldehyde and Nafion was placed on top as a protective film. The biosensor showed a LOD of $5 \cdot 10^{-6}$ M and an elevated sensitivity, which was mostly attributed to the high H_2O_2 electro-oxidation efficiency. Karyakin et al.[74] reported the use of a PB-modified GC electrode for the fabrication of a glucose biosensor. As described earlier, PB has proved to be an excellent

electrocatalyst for H_2O_2 – even better than Pt – facilitating its detection at low applied potential (approx. 0 V vs. Ag/AgCl). Such a low potential enhances the immunity against ascorbic acid interference during blood sugar testing.[75] A glucose biosensor was developed by GOx immobilization into a Nafion membrane that was subsequently deposited onto the PB-modified electrode. Glucose detection was performed at 0.18 V (vs. Ag/AgCl) and a linear response from $1 \cdot 10^{-6}$ to $5 \cdot 10^{-3}$ M was observed. More recently, Ricci et al.[76] modified carbon screen printed electrodes with PB before enzyme immobilization by cross-linking employing glutaraldehyde and Nafion. This allowed the detection of H_2O_2 produced by the enzymatic reaction at approx. 0 V (vs. Ag/AgCl) and a LOD of $2 \cdot 10^{-5}$ M together with a sensitivity of $5.4 \cdot 10^{-2}$ $AM^{-1}cm^{-2}$ were obtained.

A cholesterol biosensor is another H_2O_2-based device due to the fact that the side product of the cholesterol oxidase reaction is also H_2O_2, formed by the enzyme-catalyzed oxidation of the cholesterol by dissolved molecular oxygen. Vidal et al.[77] reported the fabrication of a cholesterol biosensor based on the electrodeposition of a PB layer on a Pt electrode. The cholesterol oxidase was then immobilized by electropolymerization of a polypyrrole film (PPy) and a Nafion layer was formed on top to exclude molecular and anionic species from reaching the electrode surface. The so-created biosensor provided a LOD of $1.2 \cdot 10^{-5}$ M and a sensitivity of $8.6 \cdot 10^{-3}$ $AM^{-1}cm^{-2}$ when the applied potential was –0.05 V (vs. Ag/AgCl).

1.5.2. Fuel cells

In order to improve fuel cell performance, much effort has been focused on the development of electrode materials with high catalytic activity for the electrochemical reduction of oxygen.[5] Generally, noble metals in high surface-area forms have been used for such purpose. However, they turned out to be very expensive and difficult to operate over long periods of time. Porous electrodes fabricated with high-area carbon have subsequently been used as catalysts in alkaline solution for the two-electron reduction of oxygen:[78]

$$O_2 + H_2O + 2e^- \rightarrow HO_2^- + OH^- \qquad \text{(reaction 19)}$$

In order to decrease the polarization created in the cathode, to improve the electrode life and to reach high operation potentials, the H_2O_2 concentration should be reduced. The use of a catalyst enhances the elimination of H_2O_2 and therefore, the rest of the process where it is involved. Venkatachalapathy et al.[78] investigated the catalytic activity of several materials (carbon, Pt-supported on high-area carbon, Pt, lead ruthenate and ruthenium oxide) towards H_2O_2 decomposition. Pt showed the best catalytic effect although ruthenate activity was also comparable. Therefore, lead ruthenate might be used as a second catalyst on the cathode side of fuel cells to decompose H_2O_2. Kjeang et al.[79] developed a microfluidic fuel cell incorporating H_2O_2 as an oxidant. High-surface area electrodeposited Pt and Pd on Au electrodes were evaluated as catalysts showing similar catalytic activity towards H_2O_2 reduction. The H_2O_2-based fuel cell showed higher power and current densities than cells based on dissolved oxygen, and so they might be employed in anaerobic conditions such as submersible and space applications.

Further developments in H_2O_2 catalysts might be applied in the fabrication of fuel cells with improved and more customized properties, particularly as an oxidant in liquid-liquid fuel cells employing methanol or borohydride as fuels.

1.6. CONCLUSIONS

The numerous applications of H_2O_2 in industry and biotechnological processes have brought about an increase in the number of techniques focused on its analytical detection and quantification. Traditional techniques such as titrimetry or spectrophotometry are being replaced by electrochemical techniques which are faster, more convenient and less prone to interferences. Although there are already several potentiometric and conductimetric sensors reported in the literature, amperometric sensors have become the focus of research interest for H_2O_2 detection due to their high sensitivity and rapid responses. Many materials have been employed in the fabrication of H_2O_2 sensors such as metals, proteins, enzymes, polymers and other catalysts such as Prussian blue. Lately, growing interest has been shown towards nanoparticulate materials, which enhance the sensitivity of the sensing devices because of the increase of their specific surface areas.

Regarding the driving mechanism for the electrochemical oxidation or reduction of H_2O_2, many systems have been proposed depending on the catalytic material. Some of them have been reported and compared along previous sections of the review. Finally, the application of H_2O_2 sensing devices in the fabrication of biosensors and fuel cells has been discussed as examples of the importance that H_2O_2 detection has in our time.

1.7. THESIS OUTLINE

The purpose of the present work was to understand the nature of a new electrocatalyst for the electrochemical reduction of hydrogen peroxide and apply this as the basis of an enzyme-based biosensor for glucose determination. Another aim was to investigate how the catalytic modification would be amenable to print fabrication.

Chapter 1 presents a literature survey on the topic of the electrocatalysis and detection of hydrogen peroxide.

In Chapter 2, the materials, instrumentation and methods used throughout this thesis are outlined.

Chapter 3 describes the development of a novel catalyst for the electrochemical reduction of H_2O_2 based on the surfactant/salt modification of silver screen printed electrodes (Ag SPEs). Optimization of the modification process was performed through electrochemical and microscopic techniques to assess the effects of varying parameters such as surfactant and salt concentrations and modification times. Enhancement of the H_2O_2 decomposition process was also observed by Ag SPEs following the exposure to the modification solution.

Chapter 4 addresses the surfactant/salt modification on a range of substrates such as Ag, Au, Pt metal and paste electrodes and their catalytic effect towards the electrochemical reduction and decomposition of H_2O_2. A kinetic study of the decomposition process including the calculation of the apparent and heterogeneous rate constants for the process will be also provided.

The application of surfactant/salt modified Ag SPEs for the development of a glucose biosensor is outlined in Chapter 5. GOx was used as the glucose recognition

element. Much of the work focuses on the optimization of a membrane layer and immobilization of the enzyme. Analytical parameters such as LOD, reproducibility and sensitivity will be highlighted.

The use of inkjet printing for the deposition of the surfactant/salt modification solution onto the Ag SPEs is explored in Chapter 6. Attempts to minimize the high variability observed in Chapter 5 through the fabrication of all-printed sensors will be illustrated. Comparisons of the H_2O_2 sensors and glucose biosensors fabricated by both dip-coating and inkjet printing will be addressed.

Recommendations for future work developments emerging from this thesis are presented in Chapter 7.

1.8. REFERENCES

1.   C. P. Huang, Y. F. Huang, H. P. Cheng and Y. H. Huang, *Catalysis Communications*, 2009, **10**, 561-566.
2.   M. R. Guascito, E. Filippo, C. Malitesta, D. Manno, A. Serra and A. Turco, *Biosensors & Bioelectronics*, 2008, **24**, 1057-1063.
3.   Z.-q. Lei and R.-r. Wang, *Catalysis Communications*, 2008, **9**, 740-742.
4.   C. M. Welch, C. E. Banks, A. O. Simm and R. G. Compton, *Analytical and Bioanalytical Chemistry*, 2005, **382**, 12-21.
5.   H. Falcon and R. E. Carbonio, *Journal of Electroanalytical Chemistry*, 1992, **339**, 69-83.
6.   Y. Shimizu, K. Uemura, H. Matsuda, N. Miura and N. Yamazoe, *Journal of The Electrochemical Society*, 1990, **137**, 3430-3433.
7.   A. A. Karyakin, E. A. Puganova, I. A. Budashov, I. N. Kurochkin, E. E. Karyakina, V. A. Levchenko, V. N. Matveyenko and S. D. Varfolomeyev, *Analytical Chemistry*, 2003, **76**, 474-478.
8.   W. Liu and D. Zuckerbrod, Fourth international symposium on proton conducting membrane fuel cells, 2004.
9.   D. Lee, V. R. Erigala, M. Dasari, J. Yu, R. M. Dickson and N. Murthy, *International journal of nanomedicine*, 2008, **3**, 471-476.
10.   M. C. Y. Chang, A. Pralle, E. Y. Isacoff and C. J. Chang, *Journal of the American Chemical Society*, 2004, **126**, 15392-15393.
11.   X. Wang, T. Yang, Y. GFeng, K. Jiao and G. Li, *Electroanalysis*, 2009, **21**, 819-825.
12.   W. Lian, L. Wang, Y. Song, H. Yuan, S. Zhao, P. Li and L. Chen, *Electrochimica Acta*, 2009, **54**, 4334-4339.
13.   N. V. Klassen, D. Marchington and H. C. E. McGowan, *Analytical Chemistry*, 1994, **66**, 2921-2925.
14.   E. C. Hurdis and H. Romeyn, *Analytical Chemistry*, 1954, **26**, 320-325.
15.   P. J. Brandhuber and G. Korshin, eds., *Methods for the detection of residual concentrations od hydrogen peroxide in advanced oxidation processes*, WateReuse Foundation, Alexandria, VA.
16.   C. Kingzett, *J. Chem. Soc.*, 1880, **37**.
17.   C. Matsubara, N. Kawamoto and K. Takamura, *Analyst*, 1992, **117**, 1781-1784.
18.   R. M. Sellers, *Analyst*, 1980, **105**, 950-954.
19.   K. Sunil and B. Narayana, *Bulletin of Environmental Contamination and Toxicology*, 2008, **81**, 422-426.
20.   Z. Liu, R. Cai, L. Mao, H. Huang and W. Ma, *Analyst*, 1999, **124**, 173-176.
21.   Q. Chang, L. Zhu, G. Jiang and H. Tang, *Analytical and Bioanalytical Chemistry*, 2009, **395**, 2377-2385.
22.   B. Demirata-Öztürk, G. Özen, H. Filik, I. Tor and H. Afsar, *Journal of Fluorescence*, 1998, **8**, 185-189.
23.   S. Hanaoka, J.-M. Lin and M. Yamada, *Analytica Chimica Acta*, 2001, **426**, 57-64.

24. X. Wang, T. Yang, Y. Feng, K. Jiao and G. Li, *Electroanalysis*, 2009, **21**, 819-825.

25. S. A. Kumar and S.-M. Chen, *Journal of Molecular Catalysis A: Chemical*, 2007, **278**, 244-250.

26. J. Wang, *Electrochemical sensors for environmental monitoring: a review of recent technology*, National Exposure Research Laboratory, Office of research and development, U.S. Environmental Protection Agency, 2004.

27. D. Thevenot, K. Toth, R. Durst and G. Wilson, *Analytical Letters*, 2001, **34**, 635.

28. S. A. Dyer, *Survey of instrumentation and measurement*, Wiley-Interscience, John Wiley & Sons, Inc., 2001.

29. G. Li, Y. Wang and H. Xu, *Sensors*, 2007, **7**, 239-250.

30. I. L. de Mattos, L. Gorton and T. Ruzgas, *Biosensors and Bioelectronics*, 2003, **18**, 193-200.

31. K. Zhang, L. Zhang, J. Xu, C. Wang, T. Geng, H. Wang and J. Zhu, *Microchimica Acta*, 2010, **171**, 139-144.

32. W. Ngeontae, W. Janrungroatsakul, P. Maneewattanapinyo, S. Ekgasit, W. Aeungmaitrepirom and T. Tuntulani, *Sensors and Actuators B: Chemical*, 2009, **137**, 320-326.

33. X. Zheng and Z. Guo, *Talanta*, 2000, **50**, 1157-1162.

34. S. Kalayci, G. Somer and G. Ekmekci, *Talanta*, 2005, **65**, 87-91.

35. G. Somer, S. KalaycI and G. Ekmekci, *Sensors and Actuators B: Chemical*, 2001, **81**, 122-127.

36. N. F. Sheppard and A. Guiseppi-Elie, *Enzyme sensors based on conductimetric measurement In Enzyme and microbial biosensors: techniques and protocols*, Humana Press, 1998.

37. T. A. Sergeyeva, N. V. Lavrik, A. E. Rachkov, Z. I. Kazantseva, S. A. Piletsky and A. V. El'skaya, *Analytica Chimica Acta*, 1999, **391**, 289-297.

38. S. V. Dzyadevich, V. N. Arkhipova, A. P. Soldatkin, A. V. El'skaya and A. A. Shul'ga, *Analytica Chimica Acta*, 1998, **374**, 11-18.

39. Y. Zhang and G. S. Wilson, *J. Electroanal. Chem*, 1993, **345**, 253-271.

40. S. B. Hall, E. A. Khudaish and A. L. Hart, *Electrochimica Acta*, 1998, **43**, 579-588.

41. Q. Wang, Y. Yun and J. Zheng, *Microchimica Acta*, 2009, **167**, 153-157.

42. H. Elzanowska, E. Abu-Irhayem, B. Skrzynecka and V. I. Birss, *Electroanalysis*, 2004, **16**, 478-490.

43. B. Zhao, Z. Liu, Z. Liu, G. Liu, Z. Li, J. Wang and X. Dong, *Electrochemistry Communications*, 2009, **11**, 1707-1710.

44. F. Wang, R. Yuan, Y. Chai and D. Tang, *Analytical and Bioanalytical Chemistry*, 2007, **387**, 709-717.

45. M. Honda, T. Kodera and H. Kita, *Electrochimica Acta*, 1986, **31**, 377-383.

46. J. F. Perez-Benito, *Monatshefte für Chemie / Chemical Monthly*, 2001, **132**, 1477-1492.

47. D. Cao, L. Sun, G. Wang, Y. Lv and M. Zhang, *Journal of Electroanalytical Chemistry*, 2008, **621**, 31-37.

48. L. Gorton, *Analytica Chimica Acta*, 1985, **178**, 247-253.

49. J.-M. Zen, H.-H. Chung and A. S. Kumar, *Analyst*, 2000, **125**, 1633-1637.

50. A. S. Kumar and S. Sornambikai, *Indian Journal of Chemistry*, 2009, **48A**, 940-945.

51. L. Sun, D. Cao and G. Wang, *Journal of Applied Electrochemistry*, 2008, **38**, 1415-1419.

52. B. Wang, B. Li, Z. Wang, G. Xu, Q. Wang and S. Dong, *Analytical Chemistry*, 1999, **71**, 1935-1939.

53. W. Yang, Y. Li, Y. Bai and C. Sun, *Sensors and Actuators B: Chemical*, 2006, **115**, 42-48.

54. N. G. R. Mathebe, A. Morrin and E. I. Iwuoha, *Talanta*, 2004, **64**, 115-120.

55. A.-E. Radi, X. Muñoz-Berbel, M. Cortina-Puig and J.-L. Marty, *Electroanalysis*, 2009, **21**, 696-700.

56. J. Li, L.-T. Xiao, X.-M. Liu, G.-M. Zeng, G.-H. Huang, G.-L. Shen and R.-Q. Yu, *Analytical and Bioanalytical Chemistry*, 2003, **376**, 902-907.

57. M. Yemini, P. Xu, D. L. Kaplan and J. Rishpon, *Electroanalysis*, 2006, **18**, 2049-2054.

58. Z.-M. Liu, Y. Yang, H. Wang, Y.-L. Liu, G.-L. Shen and R.-Q. Yu, *Sensors and Actuators B: Chemical*, 2005, **106**, 394-400.

59. J. Chen, B. Winther-Jensen, C. Lynam, O. Ngamna, S. Moulton, W. Zhang and G. G. Wallace, *Electrochemical and Solid-State Letters*, 2006, **9**, H68-H70.

60. A. A. Karyakin, O. V. Gitelmacher and E. E. Karyakina, *Analytical Letters*, 1994, **27**, 2861 - 2869.

61. A. A. Karyakin, *Electroanalysis*, 2001, **13**, 813-819.

62. D. J. Daly, C. K. O'Sullivan and G. G. Guilbault, *Talanta*, 1999, **49**, 667-678.

63. *Merck Index*, 12th Ed., #4839 and #4391 edn., 1996.

64. D. J. Marks and J. Donnelly, *Introduction to physical inorganic chemistry*, 4th Ed. edn., Longman Inc., New York, 1978.

65. D. F. Shriver and P. W. Atkins, *Inorganic chemistry*, 3rd Ed. edn., Oxford University Press, Oxford, 2001.

66. M. Honda, T. Kodera and H. Kita, *Electrochimica Acta*, 1983, **28**, 727-733.

67. A. Hickling and W. H. Wilson, *Journal of The Electrochemical Society*, 1951, **98**, 425-433.

68. J. J. Lingane and P. J. Lingane, *Journal of Electroanalytical Chemistry (1959)*, 1963, **5**, 411-419.

69. D. A. Johnston, M. F. Cardosi and D. H. Vaughan, *Electroanalysis*, 1995, **7**, 520-526.

70. L. Clark, Jr. and C. Lyons, *Ann. NY Acad. Sci.*, 1962, **102**, 29.

71. A. P. F. Turner, I. Karube and G. S. Wilson, *Biosensors: Fundamentals and Applications*, Oxford University Press, Oxford, 1987.

72. J. Wang, *Chemical Reviews*, 2008, **108**, 814-825.

73. Z. Cao, Y. Zou, C. Xiang, L.-X. Sun and F. Xu, *Analytical Letters*, 2007, **40**, 2116-2127.

74. A. A. Karyakin, O. V. Gitelmacher and E. E. Karyakina, *Analytical Chemistry*, 1995, **67**, 2419-2423.

75. J.-Y. Chiu, C.-M. Yu, M.-J. Yen and L.-C. Chen, *Biosensors and Bioelectronics*, 2009, **24**, 2015-2020.

76. F. Ricci, D. Moscone, C. S. Tuta, G. Palleschi, A. Amine, A. Poscia, F. Valgimigli and D. Messeri, *Biosensors and Bioelectronics*, 2005, **20**, 1993-2000.

77. J.-C. Vidal, J. Espuelas, E. Garcia-Ruiz and J.-R. Castillo, *Talanta*, 2004, **64**, 655-664.

78. R. Venkatachalapathy, G. P. Davila and J. Prakash, *Electrochemistry Communications*, 1999, **1**, 614-617.

79. E. Kjeang, A. G. Brolo, D. A. Harrington, N. Djilali and D. Sinton, *Journal of The Electrochemical Society*, 2007, **154**, B1220-B1226.

Chapter 2

Materials and Methods

2.1. MATERIALS

2.1.1. Materials

Dodecylbenzenesulphonic acid (DBSA) was purchased from TCI Europe. Sodium dodecyl sulphonate (SDS), cetyltrimethylammonium bromide (CTAB), Triton X-100, lithium, sodium, potassium and caesium chloride (LiCl, NaCl, KCl, CsCl), sodium bromide (NaBr), potassium dihydrogen phosphate (KH_2PO_4), D-(+)-glucose, cellulose acetate (CA), chitosan, hexamethylenediamine (HMDA), acetone and glucose oxidase (GOx, Type II-S: from Aspergillus niger, 20% protein) were purchased from Sigma-Aldrich. Di-sodium hydrogen phosphate (Na_2HPO_4) was purchased from Riedel-de Haen. 30% (v/v) hydrogen peroxide (H_2O_2) solution was purchased from Merck. Glutaraldehyde (GA) and Nafion® 117 solution (~5% in a mixture of lower aliphatic alcohols and water) were purchased from Fluka Chemika. Acetic acid glacial was purchased from Fisher Scientific. Silver conductive ink (Electrodag® PF-410) was purchased from Henkel (Scheemda, The Netherlands). Sterling silver (92.5%, 300 µm-thick) was purchased from NN Enterprises (Dublin, Ireland) and it was cut into 0.6 cm^2 substrates (unless otherwise is stated). 0.5 mm diameter silver wire (99.9%) was purchased from Sigma-Aldrich and 1.1 cm long electrodes were prepared as working electrodes using isolating tape. Silver (CHI103, 99.9%, A = 0.031 cm^2) and gold (CHI101, 99.9%, A = 0.031 cm^2) metallic electrodes were purchased from IJ Cambria Scientific Ltd. (Carms, UK). Gold and platinum screen printed electrodes (A = 0.1 cm^2) were purchased from DuPont (Delaware, US). Gold and platinum screen printed electrodes (4 mm diameter) were purchased from DropSens (Asturias, Spain). Poly(ethylene) terephthalate (PET) substrates were Melinex® films obtained from HiFi Industrial Film Ltd. (Dublin, Ireland). Polyester pressure sensitive adhesive (PSA, ARcare® 92712) was purchased from Adhesives Research Ireland Ltd. (Limerick, Ireland). Seriwash universal screen wash was purchased from Sericol Ltd., (Kent, UK). 0.3 µm and 0.05 µm alumina powders were purchased from Buehler (Dorset, UK). Silver/silver chloride electrodes were purchased from Bioanalytical Systems Ltd.

(Cheshire, UK). The platinum mesh was purchased from Sigma-Aldrich. All the solutions were prepared using 18 MΩ Milli-Q water.

2.1.2. Buffers and solutions

Unless otherwise stated, all electrochemical measurements were carried out in phosphate buffered saline solution (PBS). The buffer solution was 10^{-1} M phosphate, $1.37 \cdot 10^{-1}$ M NaCl and $2.7 \cdot 10^{-3}$ M KCl. This was prepared by mixing solution 1 (10^{-1} M Na_2HPO_4, $1.37 \cdot 10^{-1}$ M NaCl and $2.7 \cdot 10^{-3}$ M KCl) and solution 2 (10^{-1} M KH_2PO_4, $1.37 \cdot 10^{-1}$ M NaCl and $2.7 \cdot 10^{-3}$ M KCl) to a pH of 6.8.

Unless otherwise stated, GOx enzyme solution was prepared in PBS pH 5.0. Such buffer was prepared in the same way but adjusting the final pH to 5.0.

1 M H_2O_2 solution was prepared daily by diluting 20-times the stock solution with distilled water.

0.2 M glucose solution was prepared and left overnight to allow equilibration of the anomers to the stable ratio of α:β 36:64.[1-3]

2.2. INSTRUMENTATION

Silver screen-printed electrodes (Ag SPE) were fabricated using an automated DEK 248 machine (Weymouth, UK). Briefly, a layer of silver paste was deposited onto PET substrate and cured in a convection oven at 120 ^{o}C for 5 minutes. Then, an isolating tape layer was deposited to define the working electrode area (0.126 cm^2).

All electrochemical measurements were performed in a three-electrode electrochemical batch cell, using a Ag/AgCl/NaCl (saturated) electrode and a platinum mesh electrode as reference and auxiliary electrodes, respectively. Cyclic voltammetry and time-based amperometric measurements were carried out with a CHI601C electrochemical analyzer with CHI601C software (IJ Cambria Scientific Ltd., UK). Measurements were performed at a room temperature of 18 ± 2 $^{\circ}$C. Unless otherwise stated, all potential values are referred to the Ag/AgCl/NaCl (saturated) electrode.

Scanning Electron Microscopy (SEM) using Secondary Electron (SE) and Energy Dispersive X-ray (EDX) detection was carried out with a Hitachi S-3400N. Acceleration voltage of 20 kV and working distance of approx. 10.5 mm were employed to obtain the surface images. For the analysis of Ag metallic electrodes, electrodes were fixed to stubs using conductive carbon cement.

X-Ray Photoelectron Spectroscopy (XPS) measurements were performed using a Kratos AXIS 165 spectrometer (University of Limerick, Ireland).

Surface area determinations were performed by BET analysis by Ceram (Staffordshire, UK) using a Gemini VI instrument (Micromeritics). The standard error on the mean uncertainty with a coverage factor of k=2.20 is 0.3458% for the multipoint determination and 0.3327% for the single point determination.

A Sartorius CP225D analytical balance was employed to register the mass differences during H_2O_2 decomposition.

A Graphtec Robo Pro S (Model no. CE50000-4-CRP) cutting plotter and a Robo Master Pro software (Wrexham, UK) were used to prepare the PSA patterns for biosensor fabrication. Electrode patterns were drawn using AutoCAD and uploaded into the Robo Master software. A 3 cm x 12 cm PSA substrate was designed with ten circular (0.4 cm diameter) patterns so ten electrodes could be modified simultaneously, increasing the reproducibility of the devices.

Inkjet printing was performed using a Dimatix Materials Printer DMP-2831 (FujiFilm Dimatix, Inc.) and a Dimatix Drop Manager DMP-2800 series software. The Dimatix cartridges used for printing were MEMs-based, with 16 nozzles (20 µm diameter) spaced at 254 µm. The droplet volume was quoted at being 10 pl.

2.3. METHODS

2.3.1. Electrode modification with surfactant/salt-based solutions

Screen-printed (Au, Pt, Ag) and sterling 92.5% Ag electrodes were dipped into a freshly-prepared solution of a surfactant (DBSA, SDS, CTAB, Triton X-100) and a salt

(LiCl, NaCl, KCl, CsCl) at a range of concentrations (modification solution) for 3 hours. The electrodes were then rinsed with water to remove the excess of modification solution and employed directly. Au and Ag metallic (99.9%) electrodes were initially polished using 0.3 and 0.05 µm alumina. They were then sonicated for 5 min in distilled water and subsequently dipped into the modification solution for 3 hours, following the same procedure used for SPEs. These electrodes were first used as H_2O_2 sensors and subsequently, as platforms for GOx immobilization.

2.3.2. Electrochemical characterisation

All electrochemical measurements were carried out in a stirred batch system with a three-electrode configuration. Unless otherwise stated, the electrodes were measured in 2.5 ml PBS pH 6.8. Cyclic voltammograms were obtained in the potential range from -0.200 to 0.025 V (vs Ag/AgCl) at a scan rate of 0.1 V/s and a sensitivity of $1 \cdot 10^{-5}$ V/A. Amperometry was performed at -0.1 V (vs Ag/AgCl) with a sensitivity of $1 \cdot 10^{-5}$ V/A for H_2O_2 and $1 \cdot 10^{-6}$ V/A for glucose measurements. 1 M stock solution of H_2O_2 was prepared daily and then aliquots from this solution were added to the working cell during amperometric measurements in order to characterize the sensor parameters. For the glucose sensing, aliquots of 0.2 M glucose solution were added to the bulk to obtain the electrochemical responses at the same applied potential.

2.3.3. Measurement of H_2O_2 decomposition

H_2O_2 decomposition was assessed by the decrease in mass registered when the electrodes were placed in 2 ml of 1 M H_2O_2. The electrodes were dipped into the H_2O_2 solution and the vials were covered with laboratory film to avoid losses due to evaporation. In order to allow the O_2 formed during the decomposition to release from the devices, a small hole was made in the laboratory film. The mass data were registered every minute for 1 hour and each electrode was measured three times, with a resting time of 10-15 minutes between measurements.

2.3.4. Immobilization of GOx onto silver screen-printed electrodes

Unless otherwise stated, the glucose biosensor was prepared by immersing the DBSA/KCl modified electrode in a CA solution ($2 \cdot 10^{-2}$% CA in glacial acetic acid) for 3 s to create a thin and uniform layer of the polymer on the electrode. After the immersion, the electrode was placed for ten minutes in cold deionised water to accelerate the polymer solidification phase. Activation of the CA layer was carried out by immersing the electrode into a 5% (w/v) HMDA aqueous solution for 20 min. After washing in deionised water, the electrode was immersed for 20 min in 2.5% (v/v) GA aqueous solution. After further rinsing with deionised water, the electrode was kept overnight at 4 °C in a 25 mg/ml GOx solution in PBS pH 5 for enzyme immobilization.[4] A diagram of the electrode design is shown in Appendix 1.

2.3.5. Inkjet printing of DBSA/KCl solution

DBSA/KCl solution was inkjet printed by placing the freshly prepared solution at the corresponding concentration in a Dimatix cartridge. No prior filtering was performed in order to avoid any possible breaking-down of the micelle/lamellar structures created in the surfactant-based solution. Unless otherwise stated, the solution was printed onto the Ag SPEs using circular patterns (5.04 mm diameter) and 20 µm resolution (dot spacing), which was equivalent to approx. 1270 dpi (drops per inch). Electrodes were then rinsed to remove the excess of modification solution that did not interact with the electrode surface.

2.4. REFERENCES

1.   R. U. Lemieux and J. D. Stevens, *Canadian Journal of Chemistry*, 1966, **44**, 249-262.
2.   N. Le Barc'H, J. M. Grossel, P. Looten and M. Mathlouthi, *Food Chemistry*, 2001, **74**, 119-124.
3.   S.-H. Lee, H.-Y. Fang and W.-C. Chen, *Sensors and Actuators B: Chemical*, 2006, **117**, 236-243.
4.   M. Portaccio, D. Durante, A. Viggiano, S. Di Martino, P. De Luca, D. Di Tuoro, U. Bencivenga, S. Rossi, P. Canciglia, B. De Luca and D. G. Mita, *Electroanalysis*, 2007, **19**, 1787-1793.

Chapter 3

Investigation of a novel electrode surface modification and its catalysis of the decomposition and electrochemical reduction of hydrogen peroxide

3.1. INTRODUCTION

As was set out in Chapter 1, detection and measurement of H_2O_2 is of major scientific, social and economic importance.[1-3] Thus, the continuing search for novel and better ways of detecting or measuring it are important research goals. In particular, its use in electrochemical sensing devices requires that such sensors be of low cost and be amenable to rapid production. To date, this has been primarily achieved through the fabrication of the screen printed electrode. In this regard, the need for compatibility with screen printable materials such as conductive inks and pastes is a critical feature.

The major theme of the work presented in this thesis developed out of the initial observation that carbon paste screen printed electrodes modified with polyaniline (PANI) nanoparticles appeared to show enhanced catalysis towards H_2O_2 reduction. The synthesis of PANI nanoparticles using dodecylbenzenesulphonic acid (DBSA) as both dopant and surfactant was employed to allow the use of this polymer in aqueous media, improving its processability. It enabled PANI nanoparticles to be deposited onto electrodes by means of traditional methods, such as drop coating,[4, 5] or using more sophisticated techniques, such as inkjet printing.[6, 7]

The initial objective of the project was the assessment of the PANI nanoparticles deposited onto the carbon paste screen printed electrode as a sensor platform for the H_2O_2 detection. Early data showed an enhancement of the cathodic current at –0.1 V when the PANI-modified electrodes where measured in the presence of H_2O_2. However, subsequent investigations showed that the catalytic responses were, in fact, associated with the silver ink layer underlying the carbon paste. Screen printing can sometimes lead to the formation of pinholes on the printed surfaces depending on the viscosity of the material and the curing conditions. Here, it was noted that the real catalytic surface that enhanced the H_2O_2 electrochemical reduction was the silver paste layer. Moreover, it was found that PANI nanoparticles themselves were not involved in the H_2O_2 catalysis, but that this was due to the combination of the doping surfactant used in the PANI nanoparticles synthesis (DBSA) and a salt present in the phosphate buffer (KCl).

Thus, in the present work, silver screen printed electrodes (Ag SPEs) were evaluated as platforms for H_2O_2 determination due to their cost-effectiveness and ease of

fabrication and manufacture. To achieve this, however, the nature of the observed catalysis required an initial detailed study to aid in an understanding of the relationship between the catalysis and the materials involved, and an optimisation of the system. Initial investigations suggested that this catalysis was novel and had no precedent in the literature. Thus, in this chapter, the nature of the catalysis is thoroughly investigated, looking initially at the silver paste as the catalytic substrate material and looking at the nature of the surfactant/salt solutions and their impact on both electrochemical reduction and chemical decomposition rates at the surface.

Modifications of the above-mentioned devices were performed by dipping the electrodes in a combined surfactant/salt solution. The effect of the modification on the reduction of H_2O_2 was assessed by cyclic voltammetry and amperometry. In addition, Scanning Electron Microscopy (SEM), Energy Dispersive X-Ray (EDX) Analysis, BET analysis and X-Ray Photoelectron Spectroscopy (XPS) measurements were performed to characterize the electrode surfaces before and after the modification and exposure to H_2O_2. A study of the enhancement on the H_2O_2 decomposition process following modification of the Ag SPEs was carried out using gravimetric analysis. The optimised material was assessed for its ability to quantify H_2O_2.

3.2. RESULTS AND DISCUSSION

As was mentioned earlier, a catalytic effect on H_2O_2 decomposition and electrochemical reduction was observed when Ag SPEs were modified with a combination of surfactant and salt. This finding led to the assessment of the catalysis by varying different modification parameters such as surfactant and salt concentrations, modification times as well as the type of surfactant and salt. The motivations of using these modified SPEs were their low cost, rapid fabrication and ease of use, which would allow the rapid manufacture of H_2O_2 sensor devices.

3.2.1. Electrochemical characterisation of the catalytic enhancement toward H_2O_2 at Ag SPEs

Cyclic voltammetry and time-based amperometry were carried out in order to assess the catalytic effect observed when Ag SPEs had been modified with surfactant/salt-based solutions. These were performed on the unmodified home-made electrodes in PBS pH 6.8 as controls. Subsequently, Ag SPEs were dipped into a solution of $3.3 \cdot 10^{-2}$ M DBSA/ 0.1 M KCl for 3 h and rinsed with distilled water to remove any excess of the modification solution from the surface prior to characterisation by cyclic voltammetry and amperometry in PBS pH 6.8. For amperometric measurements, H_2O_2 was added to the solution at concentrations from $1 \cdot 10^{-3}$ to $5 \cdot 10^{-3}$ M. One of the main requirements of a substrate to be used as a platform in an electrochemical sensing process is that it be electrochemically inert in the selected range of potential. Here, a narrow window of potential was chosen for the voltammetric measurements (–0.2 to +0.025 V vs. Ag/AgCl), as a wider potential range would lead to the oxidation of Ag (at more positive potentials) or O_2 interferences (at more negative potentials), thus distorting H_2O_2 responses. Fig. 3.1 shows the cyclic voltammograms for unmodified and DBSA/KCl modified Ag SPEs in the presence and absence of $5 \cdot 10^{-3}$ M H_2O_2. As can be seen, the non-faradaic or charging current from the cyclic voltammograms in the absence of H_2O_2, is up to ten times higher for the modified electrodes than that for the unmodified ones. This indicates that the Ag SPE surface had undergone a modification after being dipped

into surfactant-based solutions. Moreover, the cathodic current in the presence of $5 \cdot 10^{-3}$ M H_2O_2 was more than 100 times higher for electrodes after being modified with $3.3 \cdot 10^{-2}$ M DBSA/ 0.1 M KCl when compared to unmodified electrodes. Thus, the cathodic current at –0.1 V from the cyclic voltammograms in the presence of $5 \cdot 10^{-3}$ M H_2O_2 was approx. $4.4 \cdot 10^{-5}$ A for the modified electrode, after subtracting the background current, whereas the modified one exhibited only a $3.8 \cdot 10^{-7}$ A current at the same potential.
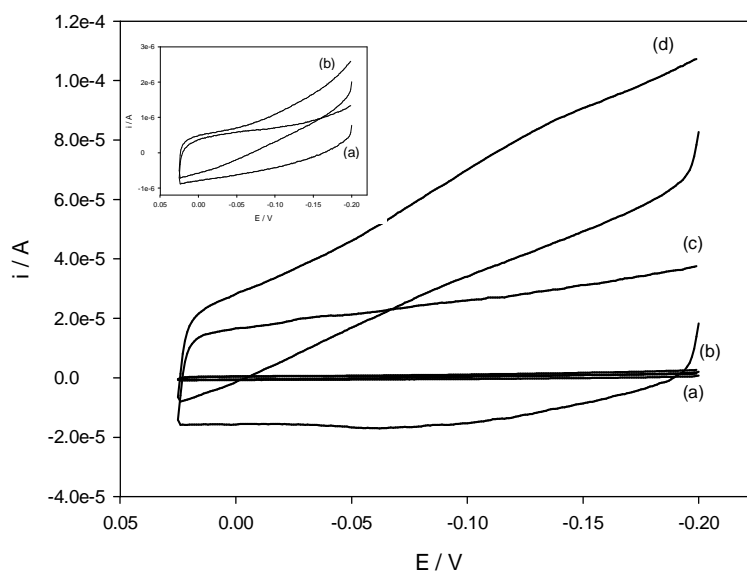
Figure 3.1. **Cyclic voltammograms of Ag SPEs measured in PBS pH 6.8 solution: (a) unmodified, in the absence of H_2O_2; (b) unmodified, $[H_2O_2] = 5 \cdot 10^{-3}$ M; (c) $3.3 \cdot 10^{-2}$ M DBSA/ 0.1 M KCl modified, in the absence of H_2O_2; (d) $3.3 \cdot 10^{-2}$ M DBSA/ 0.1 M KCl modified, $[H_2O_2] = 5 \cdot 10^{-3}$ M. Inset: magnified diagram of voltammograms (a) and (b).**

This catalytic effect for the surfactant/salt-based pre-treated electrodes is also presented in Fig. 3.2, where the amperometric responses following additions of $1 \cdot 10^{-3}$ M H_2O_2 for the unmodified and DBSA/KCl modified electrodes is shown. These were performed at –0.1 V (vs Ag/AgCl). Although a catalytic effect is seen by the modified electrodes from +0.025 V in Fig. 3.1, the current increased quite linearly within the

cathodic potential window with a discernible peak between –0.1 and –0.15 V. Given the significant current increases at these potentials, the narrow potential window of the Ag paste electrodes and the desire to avoid interferences at lower potentials, –0.1 V seemed to be a suitable potential for further study of the catalytic effect of the surfactant/salt-based modification on Ag SPEs towards H_2O_2 reduction. Examples of applied potentials used for the amperometric determination of H_2O_2 reduction in the literature include –0.7 V (GC/PABS-modified electrodes),[3, 8] –0.5 V (Ag nanoparticles in a polyvinyl alcohol film on a Pt electrode)[9], –0.1 V commonly applied in enzymatic biosensors (such as a HRP-modified electrodes)[10, 11] and up to 0 V with Prussian blue (PB).[12] The fact that H_2O_2 reduction can be detected at this potential in the absence of enzymes represents a unique advantage as it avoids the more challenging requirements of temperature, concentration and pH required by the enzymatic compounds and broadens its application field.
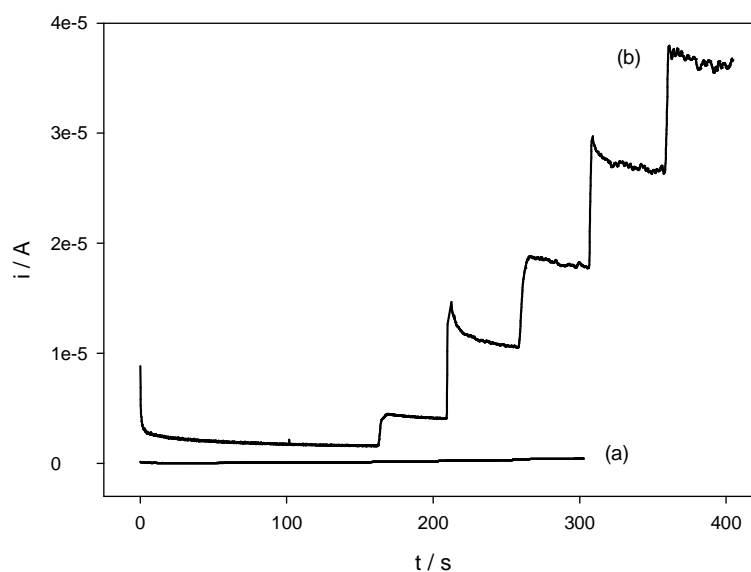
Figure 3.2. **Amperometric responses of Ag SPEs measured at –0.1 V (vs Ag/AgCl) in PBS pH 6.8: (a) unmodified and (b) modified with 3.3·10^{-2} M DBSA/ 0.1 M KCl at H$_2$O$_2$ concentration from 1 to 5·10^{-3} M.**

Modified Ag SPEs showed cathodic currents of approx. $3.6 \cdot 10^{-5}$ A at -0.1 V in the presence of $5 \cdot 10^{-3}$ M H_2O_2 whereas the current obtained with the unmodified electrodes reached approx. $4.2 \cdot 10^{-7}$ A. This difference of almost two orders of magnitude was previously observed in the cyclic voltammograms in Fig. 3.1. Moreover, the greater steady state background current exhibited by the modified electrodes (approx. $1.6 \cdot 10^{-6}$ A) compared to the unmodified one (approx. $9.0 \cdot 10^{-8}$ A) makes it evident that the Ag SPE surface undergoes a modification following the exposure to DBSA/KCl solution.

Further controls employing DBSA or KCl alone were performed. Figure 3.3 shows the amperometric responses of an unmodified Ag SPE and with DBSA ($3.3 \cdot 10^{-2}$ M) and KCl (0.1 M) together and separately. As can be seen, there was no a notable enhancement in the cathodic current corresponding to the DBSA modified electrode compared to the unmodified one. Thus, the latter showed a cathodic current in the presence of $5 \cdot 10^{-3}$ M H_2O_2 of $4.2 \cdot 10^{-7}$ A, which was only five-fold lower than that exhibited by the DBSA modified electrode, $2.4 \cdot 10^{-6}$ A. However, enhanced responses were obtained when the Ag SPE electrode had been exposed to KCl, showing $9.4 \cdot 10^{-6}$ A as cathodic current at $5 \cdot 10^{-3}$ M H_2O_2. However, the highest cathodic current was obtained when the Ag SPE was modified with a mixture of both DBSA and KCl. Such pre-treated electrodes provided cathodic responses of $3.6 \cdot 10^{-5}$ A, which represented a more than eighty-fold greater response to H_2O_2 than those without any modification. Therefore, the relative order of the modified Ag SPEs regarding the catalytic response to $5 \cdot 10^{-3}$ M H_2O_2 is the following:

Unmodified $<$ $3.3 \cdot 10^{-2}$ M DBSA modified $<$ 0.1 M KCl modified $<$ $3.3 \cdot 10^{-2}$ M DBSA/ 0.1 M KCl modified

The same relative order was observed with respect to the steady state background current of the amperometric responses, where unmodified electrodes showed the lowest value ($4.8 \cdot 10^{-8}$ A) whereas the DBSA/KCl modified showed the greatest (approx. $1.6 \cdot 10^{-6}$ A). Once again, the background or charging current was proportional to the catalytic effect shown by the electrodes and, therefore, the degree of modification of the electrode surfaces.
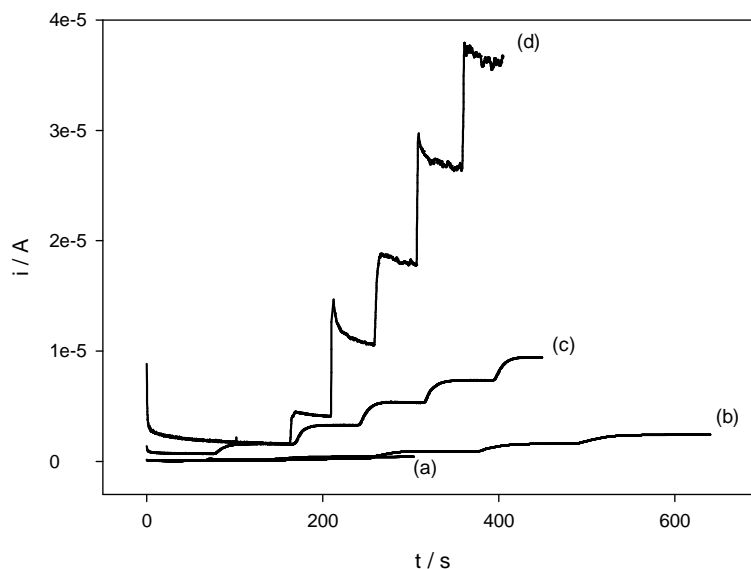
Figure 3.3. **Amperometric responses of Ag SPEs measured at –0.1 V (vs Ag/AgCl) in PBS pH 6.8: (a) unmodified; (b) $3.3 \cdot 10^{-2}$ M DBSA (c) 0.1 M KCl and (d) $3.3 \cdot 10^{-2}$ M DBSA/ 0.1 M KCl modified electrodes, at H_2O_2 concentration ranges from 1 to $5 \cdot 10^{-3}$ M.**

Having established that both DBSA and KCl were necessary for full catalytic effect, the concentrations of DBSA and KCl were optimised. Cyclic voltammetry and amperometry were performed using first 0.1 M KCl over a range of DBSA concentrations followed by $3.3 \cdot 10^{-2}$ M DBSA over a range of KCl concentrations. The cathodic responses to $5 \cdot 10^{-3}$ M H_2O_2 were correlated with DBSA or KCl concentrations. Fig. 3.4 shows the responses of Ag SPEs after dipping into solutions of DBSA at several concentrations for 3h, in the absence and the presence of 0.1 M KCl in the modification solutions. At low DBSA concentrations, the presence of KCl provided approx. six-fold higher responses, being $5.5 \cdot 10^{-6}$ A at $5 \cdot 10^{-3}$ M H_2O_2 whereas the electrode modified in the absence of KCl showed only $9 \cdot 10^{-7}$ A. However, from 10^{-4} M DBSA and above, the difference between the reduction currents obtained from the electrodes without and with KCl in their modification solution increased to more than 20-fold. Thus, at 10^{-3} M DBSA the cathodic current exhibited by the electrode modified in the absence of KCl

was approx. $1.4 \cdot 10^{-6}$ A, whereas the current from the electrode modified with DBSA/KCl rose to $3.1 \cdot 10^{-5}$ A. Even at 10^{-2} M DBSA, where the electrode modified in the absence of KCl showed the highest response, the cathodic current of the electrode modified with the DBSA/KCl mixture was still six-fold greater than the former. This confirmed that the presence of both DBSA and KCl reagents in the pre-treatment solution was essential for the full catalytic reduction effect of H_2O_2 observed on the Ag SPEs.
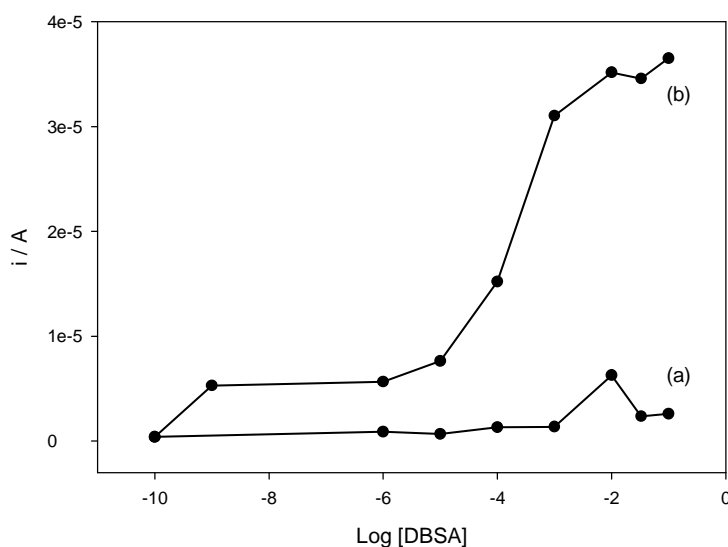
Figure 3.4. **Plot of current vs log [DBSA] obtained during amperometric measurements of Ag SPEs at –0.1 V (vs Ag/AgCl) at $5 \cdot 10^{-3}$ M H_2O_2. The electrodes were modified only with DBSA (a) or 0.1 M KCl and DBSA (b).**

Fig. 3.5 shows the results of a similar study, using three DBSA concentrations and a range of KCl concentrations. Fig. 3.4 highlighted that the optimum DBSA concentration in the modification solution was between 0.1 and 0.01 M. Therefore, DBSA concentrations of 0.1, $3.3 \cdot 10^{-2}$ and 10^{-2} M were studied. Fig. 3.5 presents the results for these experiments and compares them to those obtained using KCl alone. The catalytic effect on H_2O_2 reduction was again observed for those electrodes modified with both DBSA and KCl reagents whereas those electrodes pre-treated only with KCl displayed a

small catalytic increase at 0.1 M, which was also seen by amperometry in Fig. 3.3. The enhancement of the H_2O_2 reduction current was shown to be dependent on KCl concentrations greater than 10^{-4} M. Thus, at 10^{-4} M KCl the cathodic currents observed for the unmodified, 10^{-2} M DBSA/KCl, $3.3 \cdot 10^{-2}$ M DBSA/KCl and 0.1 M DBSA/KCl modified electrodes were $1.4 \cdot 10^{-6}$ A, $2.1 \cdot 10^{-6}$ A, $5.0 \cdot 10^{-6}$ A and $2.2 \cdot 10^{-5}$ A, respectively, whereas at 10^{-3} M KCl the reduction currents were $1.3 \cdot 10^{-6}$ A, $1.5 \cdot 10^{-5}$ A, $2.8 \cdot 10^{-5}$ A and $3.2 \cdot 10^{-5}$ A, respectively. The optimum KCl concentration in the modification solution was found to be approx. 0.1 M, where the cathodic currents for the studied electrodes reached values of $8.7 \cdot 10^{-6}$ A, $3.1 \cdot 10^{-5}$ A, $3.5 \cdot 10^{-5}$ A and $3.5 \cdot 10^{-5}$ A, respectively. Further increases in KCl concentration in the modification solutions led to a decrease in the reduction current, as can be seen in Fig. 3.5 for 1 M KCl. The onset of the enhanced catalysis was also dependent on DBSA concentration, as is shown by the above-mentioned cathodic current data at 10^{-4} M KCl. At this value, the catalytic ratio shown by the modified electrodes went along the following relative order: unmodified $< 10^{-2}$ M DBSA/KCl $< 3.3 \cdot 10^{-2}$ M DBSA/KCl $<$ 0.1 M DBSA/KCl. Electrodes exhibited enhanced catalysis at lower KCl concentrations when DBSA concentrations were increased. Electrodes modified with 0.1 M DBSA/KCl solutions showed catalytic activity from approx. 10^{-4} M KCl concentrations whereas the onset of the catalysis occurred from 10^{-3} M KCl for the electrodes modified in $3.3 \cdot 10^{-2}$ M DBSA/KCl or 10^{-2} M DBSA/KCl solutions. As will be commented upon later in this section, surfactants are well-known to form organized structures when they are in aqueous solution.[13, 14] At low concentrations but above the critical micelle concentration (CMC), typical surfactant aggregations are in the form of spheroidal micelles. As the concentration of surfactant in solution increases, greater aggregations such as hexagonal or lamellar structures are observed. The addition of a salt or cosurfactant to the solution allows the formation of these high-aggregation structures at lower surfactant concentrations. This was observed by Sein and Engberts[15] with sodium dodecylbenzenesulfonate (NaDoBS) in the presence of several chloride salts. The CMC for DBSA is approx. 1.6-$2 \cdot 10^{-3}$ M,[15, 16] so at least micellar structures should be observed in all the modification solutions used. The fact that greater catalytic responses are obtained when both the surfactant and salt concentrations in the modification solution are increased might be directly related to the

early formation of hexagonal or lamellar structures in the solution, which may bring about the modification of the Ag SPE surface in some way. This initial hypothesis will be further discussed. Hence, a solution of $3.3 \cdot 10^{-2}$ M DBSA and 0.1 M KCl was established as the optimum modification solution, which provided the highest electrocatalysis of H_2O_2 reduction on Ag SPEs and this was used in subsequent experiments.
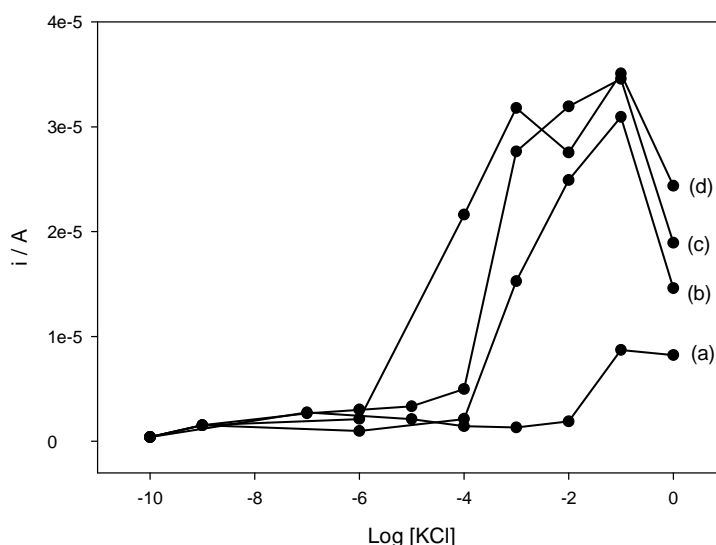
Figure 3.5. **Plot of current vs log [KCl] obtained during amperometric measurements of Ag SPEs at –0.1 V (vs Ag/AgCl) at $5 \cdot 10^{-3}$ M H_2O_2. The electrodes were modified only with KCl (a), 10^{-2} M DBSA/ KCl (b), $3.3 \cdot 10^{-2}$ M DBSA/ KCl (c) and 0.1 M DBSA/ KCl (d). Value at log [salt] = – 10 corresponds to unmodified Ag SPEs.**

Another parameter of the deposition process which needed to be optimized and studied was the modification time, i.e. the time Ag SPEs were deposited in the DBSA/KCl solution before their application to H_2O_2 detection. Several Ag SPEs were immersed into solutions of $3.3 \cdot 10^{-2}$ M DBSA/ 0.1 M KCl for different periods of time, from a few seconds to one day. Then, the electrodes were rinsed thoroughly with distilled water to remove any non-adherent species which might remain on the surface

and these were measured amperometrically in $5 \cdot 10^{-3}$ M H_2O_2 in PBS pH 6.8. Fig. 3.6 shows the plot of these data vs. modification time. As can be seen, the catalytic effect on H_2O_2 reduction was noticeable even when the electrodes had been immersed for a very short period of time (2-10 s) into the DBSA/KCl solution. These electrodes exhibited a response of approx. $2.2 \cdot 10^{-5}$ A; more than 20 times greater reduction currents when they were measured in the presence of $5 \cdot 10^{-3}$ M H_2O_2 compared to unmodified electrodes, which only exhibited $7.5 \cdot 10^{-7}$ A. This suggested that whatever process was taking place between the electrodes and the DBSA/KCl was extremely rapid.
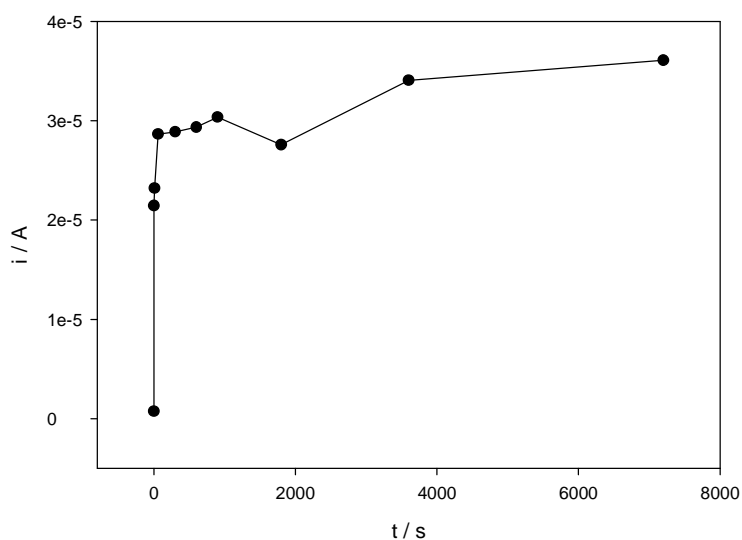
Figure 3.6. **Plot of current vs modification time obtained during amperometric measurements of Ag SPEs at –0.1 V (vs Ag/AgCl) at $5 \cdot 10^{-3}$ M H_2O_2. Data at 0 s corresponds to unmodified electrode.**

The catalytic reduction current increased with modification time but quickly reached a plateau where the current rise was not as marked as before. The cathodic currents displayed by Ag SPEs after 60, 300 and 600 s modification time were all approx. $2.9 \cdot 10^{-5}$ A. The highest cathodic current value of $3.4 \cdot 10^{-5}$ A was obtained with electrodes following exposure to DBSA/KCl modification solution for 2 hours. Further exposure times such as 1 day or 1 week did not improved the response; on the contrary, the

catalytic current started to decrease. To ensure that the highest catalytic currents were obtained, 3 hours was chosen as the optimum modification time for the experiments. This was used for all subsequent experiments where DBSA/KCl modification was performed by dip-coating.

3.2.1.1. Influence of pH on the catalytic process

The influence of the pH of the bulk electrolyte solution during the reduction of $5·10^{-3}$ M H_2O_2 was investigated for both unmodified and DBSA/KCl modified Ag SPEs. Amperometric measurements at -0.1 V were performed (Fig. 3.7) using the same electrode while changing the pH. H_2O_2 reduction at the unmodified Ag SPE showed little catalytic response in the pH range from 2 to 10, unlike the DBSA/KCl modified electrodes. Thus, the cathodic currents of the unmodified electrodes ranged from $3.4·10^{-7}$ A at pH 2 to $3.6·10^{-6}$ A at pH 10, with a maximum value of $4.4·10^{-6}$ A at pH 6.8. The DBSA/KCl modified electrodes showed no catalytic activity at very acidic solutions (pH $= 2$), $6.0·10^{-7}$ A, whereas the cathodic current increased approx. 50-fold up to $3.3·10^{-5}$ A as the bulk solution pH increased up to 10. This suggested that the catalytic mechanism of H_2O_2 reduction is significantly enhanced by the presence of OH^- or suppressed in the presence of H^+. This pH-dependence of H_2O_2 reduction has been observed previously[17, 18] and has been explained by the effect of the pH on the reduction potential. At high concentrations of H^+ in solution, H_2O_2 reduction occurs at more negative potentials than when the concentration is lower. This behaviour is typical of a reaction mechanism in which H^+ appear as a product or OH^- as a reactant.

Therefore, at -0.1 V the rate of H_2O_2 reduction was higher when the reaction took place in more basic solution rather than in more acidic ones. pH 6.8 was selected for the electrolyte measurement solutions in further work as it exhibited more than thirty-fold higher catalytic currents and is a suitable pH for the study of biological systems, such as enzyme-based biosensors, for which this system will form a platform.
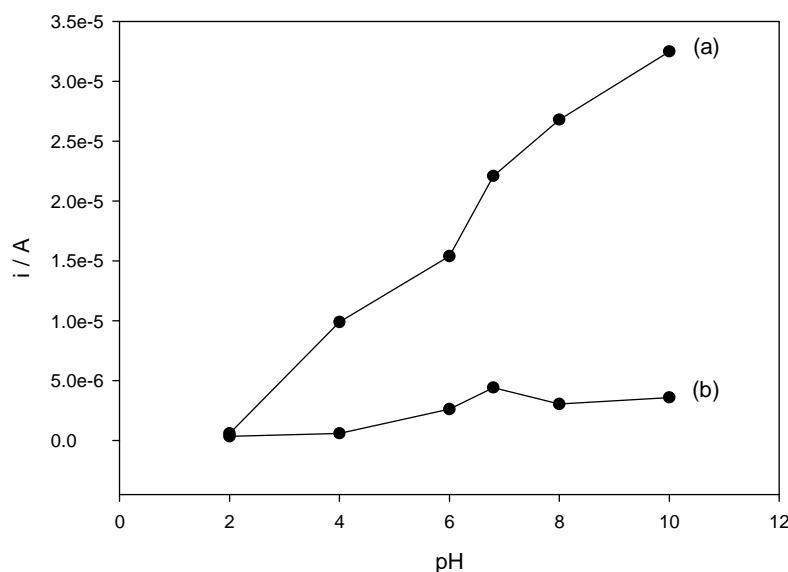
Figure 3.7. **Plot i_{cat} vs electrolyte pH for Ag SPEs (a) with and (b) without DBSA/KCl modification in $5·10^{-3}$ M H_2O_2 at –0.1 V vs Ag/AgCl.**

3.2.1.2. Analytical characterisation of the electrocatalyst as a H_2O_2 sensing electrode

Subsequently, the feasibility of the Ag SPEs electrodes modified with DBSA/ KCl to be used as H_2O_2 sensors was assessed and preliminary studies were carried out to determine their limit of detection (LOD) and reproducibility characteristics. Three Ag SPEs were modified in $3.3·10^{-2}$ M DBSA/ 0.1 M KCl solutions for 3 h, according to the adopted standard protocol. After rinsing, they were measured in PBS pH 6.8. Amperometric responses to H_2O_2 (2 to $16·10^{-5}$ M) are shown in Fig. 3.8, where typical response times of 10-15 s were observed. Experiments were repeated three times with each electrode and the data were compared to check the intra- and inter- electrode reproducibility. Although the lowest concentration measured was $2·10^{-5}$ M, the lowest theoretical LOD of the sensor devices was found to be $1.1·10^{-6}$ M, with a signal-to-noise ratio of 3. The LOD was calculated from the regression line obtained from the plot of the cathodic currents vs. H_2O_2 concentration.[19] These data are presented in the inset of Fig.

3.8. A comparison of the analytical parameters of the developed H_2O_2 sensor with other devices reported in the literature is shown in Appendix 2.
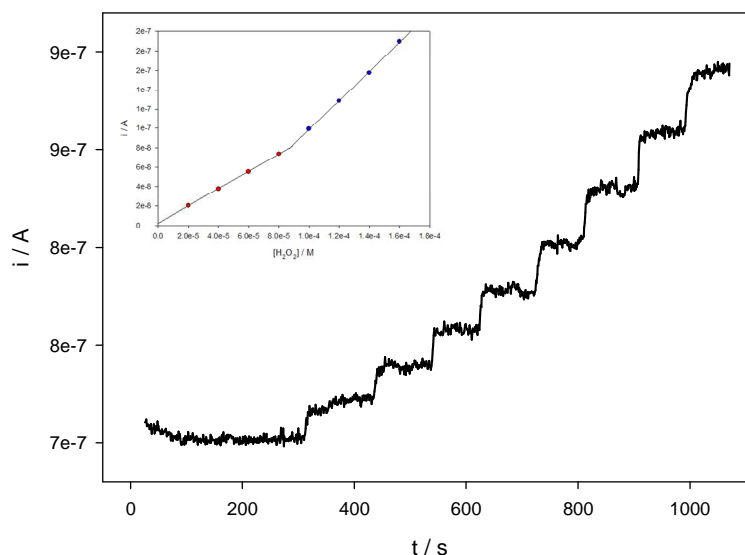
Figure 3.8. **Amperometric responses of the DBSA/KCl modified electrodes in 20·10^{-6} M aliquots of H_2O_2 (20 - 160 ·10^{-6} M) at –0.1 V (vs Ag/AgCl) in PBS pH 6.8. Input: Plot of cathodic current vs H_2O_2 concentration at –0.1 V (vs Ag/AgCl) in PBS pH 6.8.**

Other recent studies have demonstrated the direct detection of H_2O_2 using silver nanoparticles (AgNPs) on glassy carbon (GC) electrodes at –0.7 V vs Ag/AgCl with a LOD in phosphate buffer pH 7.4 of 2.0·10^{-6} M.[3] Ag NPs were also used to determine H_2O_2 at –0.55 V vs Ag/AgCl by immobilization in a polyvinyl alcohol (PVA) film on a platinum electrode, showing a LOD of 1.0·10^{-6} M [9]. Safavi et al.[20] reported the excellent electrocatalytic activity towards H_2O_2 reduction of Ag NPs electrodeposited on carbon ionic liquid electrodes (CILE). The sensor exhibited a detection limit of 7·10^{-7} M at an applied potential of –0.35 V vs. Ag/AgCl. Another widely used material in H_2O_2 detection is ferric hexacyanoferrate or Prussian blue (PB) [2, 12, 21]. It has demonstrated an LOD of 1.0·10^{-8} M and a linear calibration range for H_2O_2 concentrations from 1.0·10^{-8} to 1.0·10^{-2} M when nanostructured by electrochemical deposition through lyotropic

liquid crystal templates.[2] Recently, a detection limit of $1 \cdot 10^{-11}$ M was achieved by using a GC electrode modified with NAD^+ and single walled carbon nanotubes at –0.25 V vs. Ag/AgCl.[22] It should be noted that the values determined in the present study represent practical detection limits using moderate conditions of pH (6.8), on disposable screen printed electrodes and at low applied potentials (–0.1 V) to avoid electrochemical interferences. Due to the fact that measurements were performed on mass-producible screen printed electrodes and not on idealised rotating disk electrodes, these represent real and practical electrode materials for sensor fabrication and other applications with significant potential for further improvement or optimisation depending on the required application.

The response across this range of concentrations of H_2O_2 (2 to $16 \cdot 10^{-5}$ M) was non-linear, as is shown in the inset of Fig. 3.8. The upward curvature observed here is different from the downward curvature found for substrate limitation at enzyme electrodes and might be explained by an autocatalytic process during the H_2O_2 reduction. The autocatalytic reduction of H_2O_2 on Ag electrodes has been previously reported by Flätgen et al.[23] They observed two mechanisms of H_2O_2 reduction operating at different overvoltages. At potentials more negative than –0.8 V (vs Ag/AgCl) the "normal" reduction took place whereas a second mechanism was operative at E > –0.7 V. They proposed that the rate of H_2O_2 reduction in this second case was increased by the presence of the adsorbate $(OH)_{ad}$ formed during the reduction process on the Ag surface, leading to an autocatalytic reaction on the electrode. Moreover, the catalytic activity of the modified Ag SPEs seemed to improve with the number of repeat measurements. This behaviour was not observed at H_2O_2 concentrations > 10^{-3} M, where the catalytic responses decreased with the number of repeats. Moreover, the shape of the curvature adopted a downward trend at H_2O_2 concentrations in the range $10^{-2} – 10^{-1}$ M, which might be explained by the saturation of the electrode at such high analyte concentrations. Fig. 3.9 shows the three data point collection obtained for each of the electrodes in the range of H_2O_2 concentrations 2 to $16 \cdot 10^{-5}$ M. In the three cases, the highest catalytic responses for H_2O_2 reduction were obtained in the last repeat.

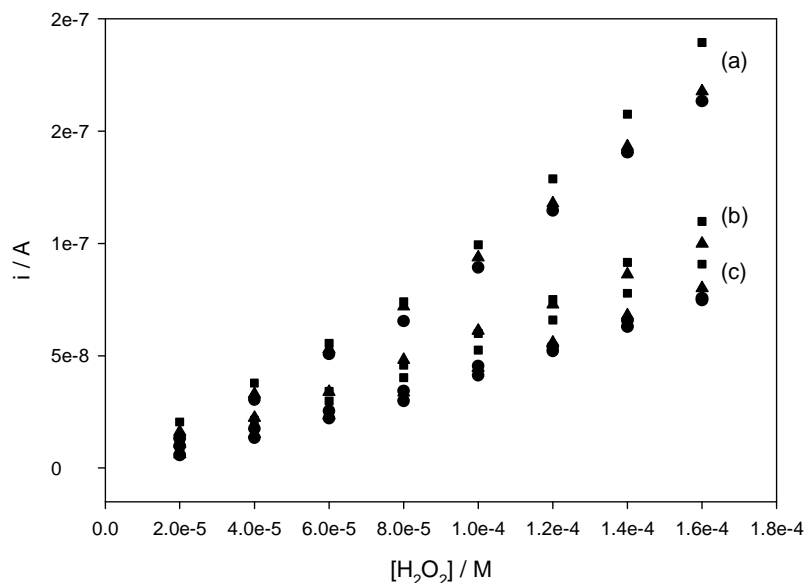*Figure 3.9.* **Reproducibility study using three different electrodes: (a) electrode 1; (b) electrode 2; (c) electrode 3. Amperometric responses of the DBSA/KCl modified electrodes in $20 \cdot 10^{-6}$ M aliquots of H_2O_2 (20 - 160 $\cdot 10^{-6}$ M) at –0.1 V (vs Ag/AgCl) in PBS pH 6.8. Each electrode was measured three times: (●) repeat 1; (▲) repeat 2; (■) repeat 3.**

3.2.2. Surface characterisation

Scanning electron micrographs and EDX spectra of Ag SPE before and after DBSA/KCl modification and following electrocatalytic reduction of H_2O_2 are shown in Fig. 3.10. SEM was performed in Secondary Electron (SE) detection mode. Due to the conductive character of the silver-based ink, no gold-sputtering was required on these surfaces. KCl-modified electrodes and AgCl-modified electrodes are also shown as controls. The unmodified screen printed electrode (Fig. 3.10a) shows the typical morphology of a metallic silver paste. It is known that the ink used contains metallic Ag particles, an organic binder and solvent.[24] Thus, SEM shows amorphous metallic Ag suspended in an organic paste. Following exposure to the DBSA/KCl solution, spheroidal structures became visible on the DBSA/KCl modified electrodes. These

structures were not present on the KCl-modified surfaces, although these electrodes did show some structural differences to controls – they also showed some catalysis. The spheroidal structures varied in size with typical diameters of approx. 1 μm. These modifications were observed on electrodes which exhibited the catalytic effect on H_2O_2 reduction. In addition, the morphology of the structures appeared to change following reduction of H_2O_2, which might be explained by the interaction between H_2O_2 and the structures during the reduction process.

With EDX, Ag was shown to be the major component in the unmodified electrodes, where C was also detected, as one might expect due to the metallic/organic binder composition required to obtain the rheological and curing characteristics for the printing process. When DBSA/KCl modified electrodes were analysed, Cl was detected as well as Ag, which was more significant in the areas with greater numbers of spheroidal structures. However, no Cl could be identified in the spectrum corresponding to DBSA/KCl modified electrodes following exposure to H_2O_2 reduction. Therefore, the spheroidal structures formed after DBSA/KCl pre-treatment appear to result from or result in an increase in surface Cl levels and may be involved in the catalytic process of H_2O_2 reduction.
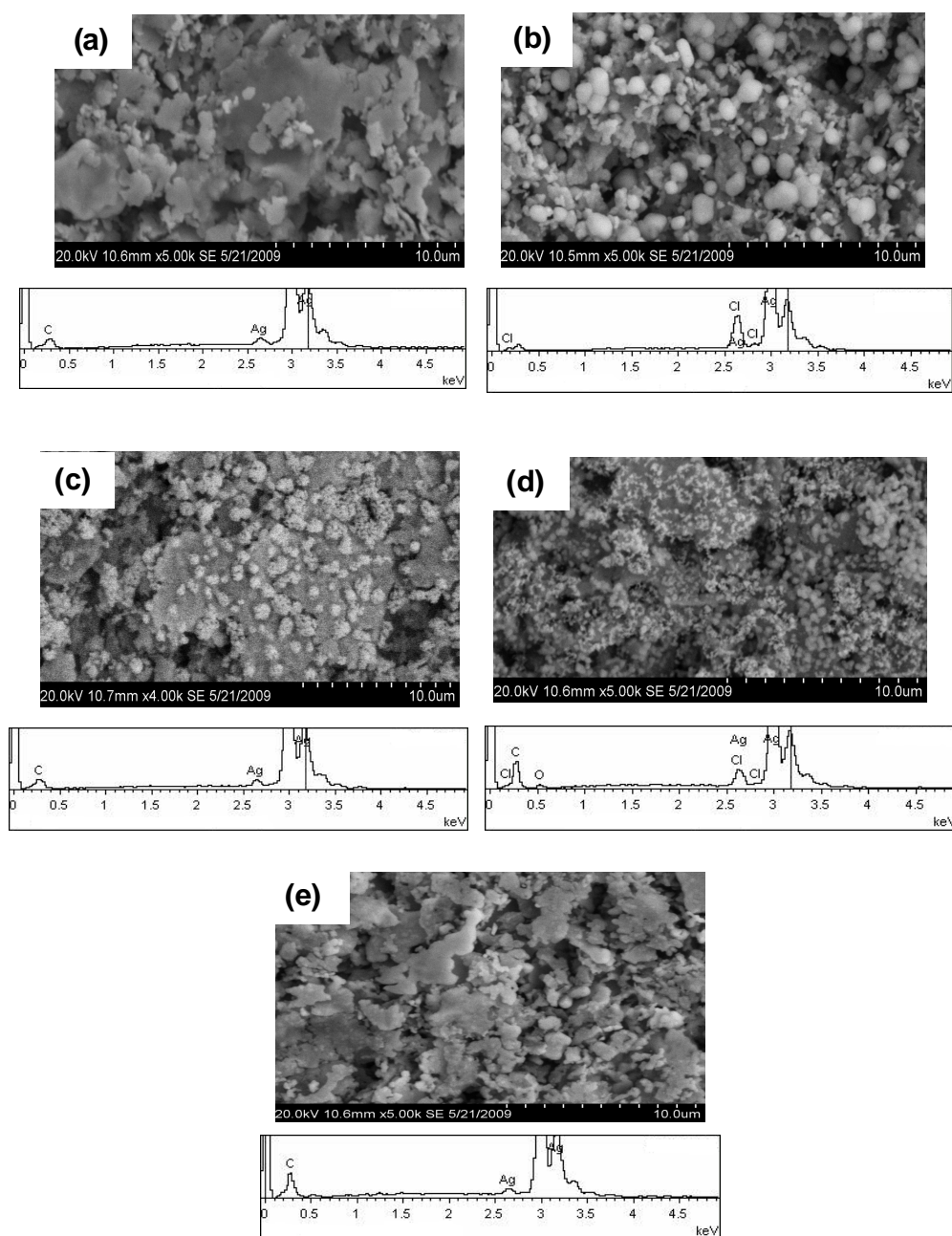
Figure 3.10. **SEM images using secondary electron (SE) detection of Ag SPEs (a) unmodified; (b) DBSA/KCl-modified; (c) DBSA/KCl-modified after electrochemical reduction of $5 \cdot 10^{-3}$ M H_2O_2; (d) AgCl electrochemically deposited; (e) KCl modified. Accelerating voltage of 20 kV. (5.0k x magnification). Below, the respective EDX spectrum for each sample. Binding energies in keV.**

X-Ray Photoelectron Spectroscopy (XPS) measurements were performed using a Kratos AXIS 165 spectrometer (University of Limerick). The samples analysed were unmodified and DBSA/KCl modified Ag SPEs. Spectra and concentration percentages are presented in Fig. 3.11 and Table 3.1, respectively. As might be expected, Ag SPE surfaces showed the presence of Cl, K and S after the modification in DBSA/KCl solutions. However, a higher proportion of Cl (4.3%) over K (0.6%) was detected on the electrode surface, which is approx. 7.5-fold greater than that which would be expected on stoichiometric basis. This fact could be explained by the formation of AgCl on the substrates during the modification which, unlike K would remain on the surface after the electrodes were rinsed.

Table 3.1. XPS data for unmodified and DBSA/KCl modified Ag SPEs.

Unmodified Ag SPE			DBSA/KCl modified Ag SPE		
Name	Position (eV)	% Conc.	Name	Position (eV)	% Conc.
O 1s	533.3	12.9	O 1s	531.4	11.7
Ag 3d	368.2	24.5	Ag 3d	367.7	26.1
C 1s	284.5	62.5	C 1s	284.6	55.8
--	--	--	K 2p	291.8	0.6
--	--	--	Cl 2p	197.5	4.3
--	--	--	S 2p	167.5	1.6
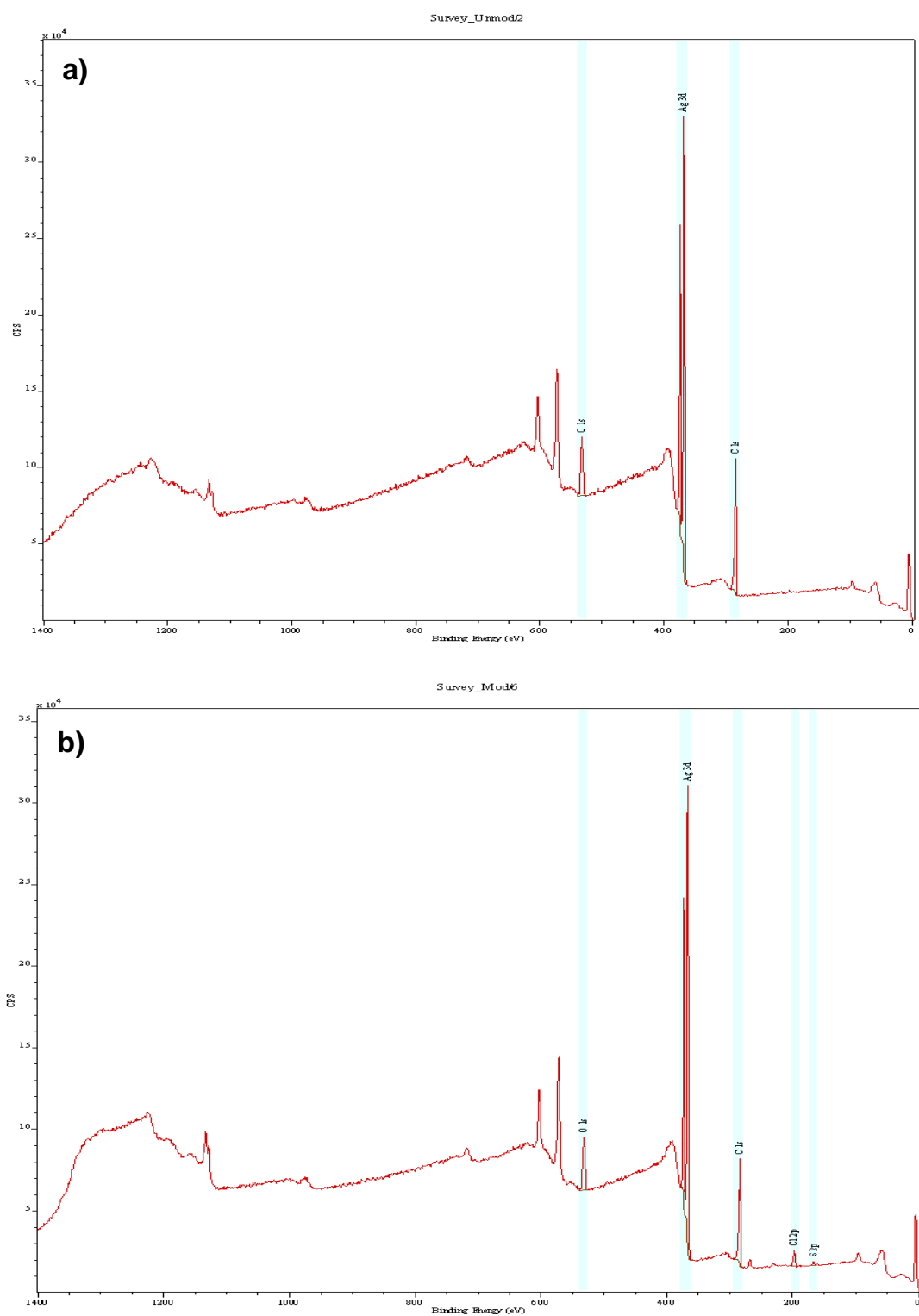
Figure 3.11. **XPS images of Ag SPEs (a) unmodified and (b) DBSA/KCl modified.**

Consequently, to check if the catalysis observed on modified Ag SPEs was due to the effect of Cl$^-$ ions and the formation of AgCl on the surface, Ag SPEs were dipped into 0.1 M HCl and a potential of 1 V was applied for 5 s.[25] Such conditions are usually applied to coat Ag electrodes with AgCl during the fabrication of Ag/AgCl references electrodes. Ag SPEs after this pre-treatment became darker due to the formation of the AgCl salt on the surface.[26, 27] Then, the electrodes were rinsed and placed in PBS pH 6.8 to the electrochemical analysis. H$_2$O$_2$ was added to the solution during amperometry performed at –0.1 V to a final H$_2$O$_2$ concentration of $5 \cdot 10^{-3}$ M in solution. The amperometric responses for these electrodes were compared to those obtained for the unmodified and DBSA/KCl modified ones (Fig. 3.12).
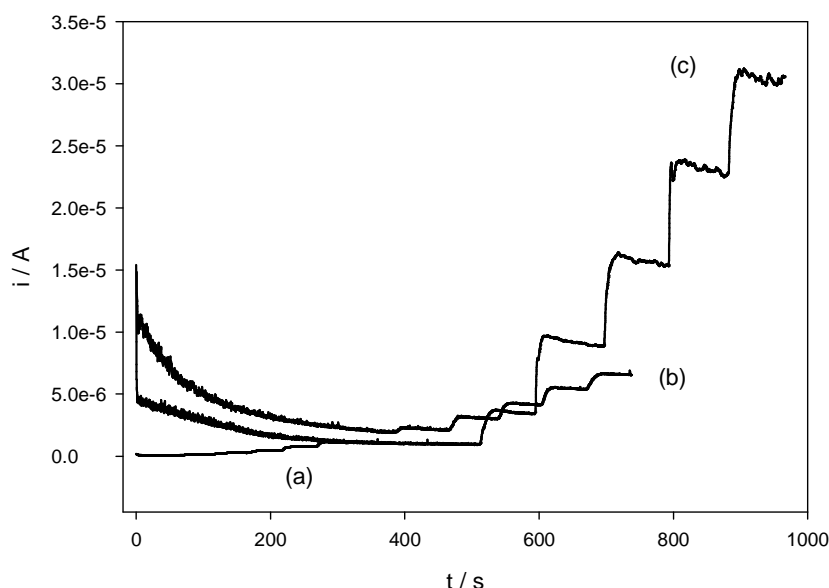
Figure 3.12. **Amperometric responses of Ag SPEs measured at –0.1 V (vs Ag/AgCl) in PBS pH 6.8: (a) unmodified; (b) AgCl electrodeposited and (c) DBSA/KCl modified electrodes, at H$_2$O$_2$ concentrations from 1 to $5 \cdot 10^{-3}$ M.**

The reduction current corresponding to $5 \cdot 10^{-3}$ M H$_2$O$_2$ solution obtained with the AgCl modified SPE was about four times higher than that shown by the unmodified

electrode, whereas for the DBSA/KCl modified one, this was about thirty times greater. The slight catalytic effect of the AgCl modified electrode could be explained as the response expected due to an increase of the Ag metallic area available to H_2O_2. An increase in the catalysis had been earlier observed when the electrodes were modified in a KCl alone solution, but then the catalysis enhancement was higher than now. However, it is clear that the catalysis is not solely due to the formation of AgCl at the electrode, although this may play a role in the process. Lian et al.[28] recently reported the increasing roughness of Ag electrodes by electrochemical oxidation-reduction cycles (ORC) in a KCl solution and their application to the quantitative determination of H_2O_2. The process began with the stripping of Ag to form Ag-Cl complex and the subsequent cathodic electrodeposition of Ag^+ to form Ag nanoparticles on the Ag substrate. The Ag-Cl complex decreased the diffusion rate of Ag^+ and made the reduction of Ag^+ more difficult, which was helpful in the formation of small Ag nanoparticles. The activity of the roughed electrodes towards H_2O_2 reduction was assessed as a function of the number of cycles, KCl concentration and scan rate during the cyclic voltammetry. The catalytic current due to H_2O_2 reduction increased with cycle number and, therefore, Ag surface area of the electrodes.[3, 29, 30]

The extreme conditions (1 V for 5 s) required for the electrochemical formation of AgCl on the electrodes in the present work could also generate the decomposition of the organic compounds which bind the metallic particles of Ag in the paste, rendering more Ag sites free to perform the reduction of H_2O_2. With regard to the chemical analysis of the surface, EDX data in Fig. 3.10d showed the presence of Ag and Cl as predominant components in the AgCl modified Ag SPEs. However, unlike the DBSA/KCl modified electrodes, the spherical structures formed on the surfaces were smaller for the Ag/AgCl SPE, as is shown in the SEM images for both substrates. Such differences in the morphology could be expected as the modification procedures were very dissimilar. Indeed, the structures from these two processes may be completely unrelated. The electrochemical deposition of Ag/AgCl was the result of intense conditions by the application of a very high oxidising potential, whereas the DBSA/KCl modification was performed under much milder conditions. The formation of the larger spheroidal aggregates on the surface of Ag SPEs seemed to be favoured by the presence of the

surfactants at certain concentrations in the modification solution. Such structures may be implicated in the catalytic process for the electrochemical reduction of H_2O_2, providing responses up to eighty times higher than those obtained with the unmodified electrodes. One possible explanation could be that micellar, hexagonal or lamellar structures often formed by the surfactants when they are in solution may have become deposited onto the Ag SPE in some way, creating an enhanced surface for the catalytic process. These structures or processes appear to create the appropriate environment for the subsequent formation of AgCl due to the presence of Cl^- in the modification solution. This would explain the presence of a higher concentration of Cl on the electrode surface following DBSA/KCl modification.

Another explanation for the catalytic process could be that the interactions of DBSA/KCl with the electrode surface may have changed the Ag morphology by creating a high surface area, nanostructure. This would provide nanoparticulate silver structures, increasing the active surface area available to perform the H_2O_2 reduction. However, BET analysis demonstrated that the surface modification did not appear to increase surface area. BET analysis is a technique for the measurement of the specific surface area of a material that is based on the physical adsorption of gas molecules on a solid surface.[31] BET nitrogen adsorption analysis performed on the modified and unmodified electrodes showed that the surface areas were 0.65 and 0.78 m^2/g, respectively, demonstrating no significant, or even a small decrease in microscopic surface area. That suggested that surface area enhancement was not the source of the enhanced catalysis, but a real electrocatalytic effect of Ag SPEs after DBSA/KCl modification. One should note that, according to the earlier voltammetric data, the electrode surface had significantly increased capacitance which can only occur as a result of a change in the dielectric constant of the surface, or a change in the surface area. The BET data suggests that no change in surface area resulted. However, if the surface was modified by the presence of a film composed of DBSA and KCl, this may block gas adsorption, leading to the observed decrease in adsorbed surface area. In addition, it should also be noted that SEM only detects materials with high electron density; namely metallics, and would not visually show the presence of organic materials such as the DBSA if it were present on the electrode.

However, the BET surface area can be different from the electroactive area. To assess a possible increase of the electroactive surface area, cyclic voltammetry of the unmodified and modified electrodes in the presence of a reversible redox probe (benzoquinone, BQ) was performed. No electrocatalysis was expected to affect a process already reversible, but only changes of electroactive area would play a role. The electrodes were measured in $1 \cdot 10^{-3}$ M BQ/ 0.5 M KCl in the potential range from –0.4 to 0.05 V (vs. Ag/AgCl) (Fig. 3.13). Rough calculations using the Randles-Sevcik equation, at room T, considering the BQ diffusion coefficient[32] as $4.2 \cdot 10^{-6}$ $cm^2 s^{-1}$ provided surfaces areas of 0.105 and 0.085 cm^2 for the modified and unmodified electrodes, respectively. No remarkable changes in the calculated surface areas were observed, indicating that there was no increase in the electroactive surface area, but a real electrocatalytic effect of Ag SPEs after DBSA/KCl modification
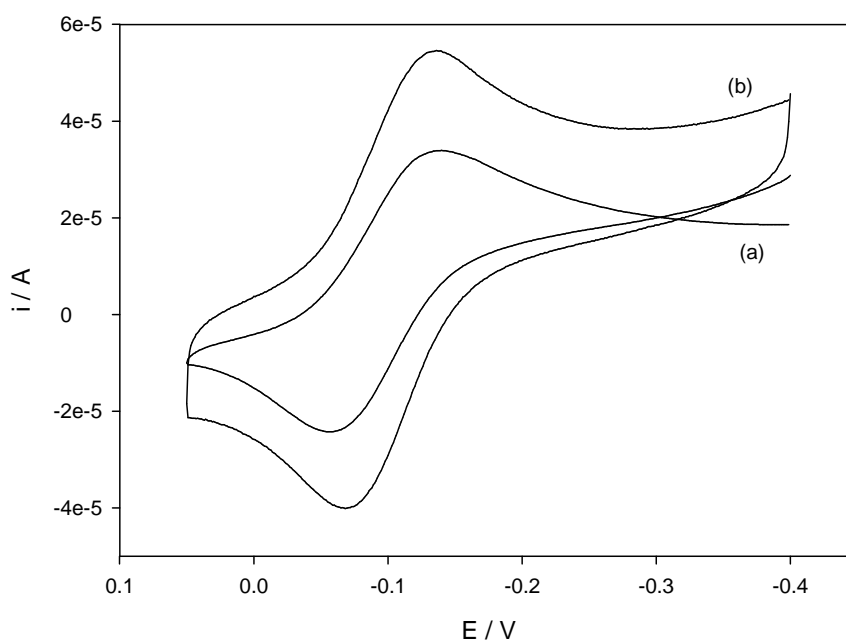
Figure 3.13. **Cyclic voltammograms of Ag SPEs measured in $1 \cdot 10^{-3}$ M BQ/ 0.5 M KCl solution: (a) unmodified; (b) $3.3 \cdot 10^{-2}$ M DBSA/ 0.1 M KCl modified. Scan rate: $5 \cdot 10^{-2}$ Vs^{-1}.**

The fact that no surfactants were detected on the substrates (i.e. no S from DBSA) using EDX analysis may be an artefact of the EM imaging process. When Ag SPEs are modified, rinsed and used directly in the cell to carry out the electrochemical techniques, these hexagonal or lamellar structures may be present on the surface because it always remains wet. However, the SEM technique requires dry surfaces to take images of the substrates, or else the detector may not have been sufficiently sensitive at the deposited concentrations. Therefore, once the surface is dried, the possible structures responsible for the surface modification could be broken down, making their detection more difficult. In fact, XPS data showed the presence of S on the DBSA/KCl modified Ag SPE, which was not detected on the unmodified one. Although its concentration (1.6%) was not so high as Cl concentration (4.3%), its presence cannot be ignored and further studies should be performed to conclude if the presence of S on the modified electrode surface is due to either the real surface modification or the remaining modification solution which has not been rinsed thoroughly enough. This would require more sophisticated preparation of samples for SEM, such as cryo-field emission scanning electrode microscopy (cryo-FESEM), which has been already used to characterize water/oil microemulsion structures.[33, 34] Other techniques already applied for the characterization of surfactant deposited on surfaces is atomic force microscopy (AFM), which has been used to image surfaces coated with different surfactants to determine their aggregate morphology.[35-37]

DBSA/KCl modified Ag SPEs were shown by contact angle measurements in water to be more hydrophilic compared to the unmodified electrodes, as is shown in Fig. 3.14.

Figure 3.14. **Comparison of the surface hydrophilicity of an unmodified (on the right) and a DBSA/KCl modified Ag SPE when $2 \cdot 10^{-6}$ l H_2O was deposited onto the surface (surface area = 0.126 cm^2)**

This increase in hydrophilicity and thus, surface energy would be consistent with modification with an amphiphile in a "head-up" orientation. Dominguez[38] has already reported the difference in contact angle for unmodified and surfactant modified surfaces. He performed contact angle measurements on graphite surfaces modified with SDS in the presence and the absence of different NaCl concentrations to show the different characteristics of the aggregates on the electrode surface. He found that the contact angle decreased as the salt concentration was increased. This indicated that the SDS aggregates wet the surface more thoroughly as the salt concentration is increased. This agreed with a more dense surface coverage with less hydrophobic graphite exposed to solution reported by Wanless and Ducker[36] for the same system. They proposed that a decrease in SDS aggregate separation on the surface occurred when the salt concentration was increased because the electrolyte screened the interactions between charged head groups.

3.2.3. Effect of DBSA/KCl modification of Ag SPEs on H_2O_2 decomposition

During studies on the electrochemical reduction of H_2O_2 on the DBSA/KCl modified electrodes, it was observed that there was also an increase in O_2 evolution as a result of accelerated decomposition. Therefore, the surface shared both increased chemical catalytic decomposition and coupled electrocatalytic reduction of H_2O_2. As a consequence of this observation, the catalytic effect on the chemical decomposition of H_2O_2 was also assessed. Gravimetric measurements of H_2O_2 decomposition on Ag SPEs were carried out before and after modification of the substrates in freshly prepared $3.3 \cdot 10^{-2}$ M DBSA/ 0.1 M KCl solutions. The mass differences due to O_2 evolution after the break-down of H_2O_2 were plotted versus time to compare the effect that the surfactant-based solution had on the decomposition process. Figure 3.15 shows the different behaviour of a Ag SPE before and after the modification. As can be observed, the modified electrode showed faster H_2O_2 decomposition (and therefore greater loss of O_2) than the unmodified one. This could also be observed visually by the formation of gas bubbles at the electrode surface. The amount of O_2 evolved from the solution was approx. eight times higher for the modified electrode after a 1 hour reaction. The

degradation showed significant non-linearity of the responses with time exhibited by the modified electrodes. These electrodes showed a linear dependence with time during the first 5-6 minutes, after which the amount of O_2 released per unit time seemed to decrease drastically. This effect, which appears only with modified electrodes, was further analysed.
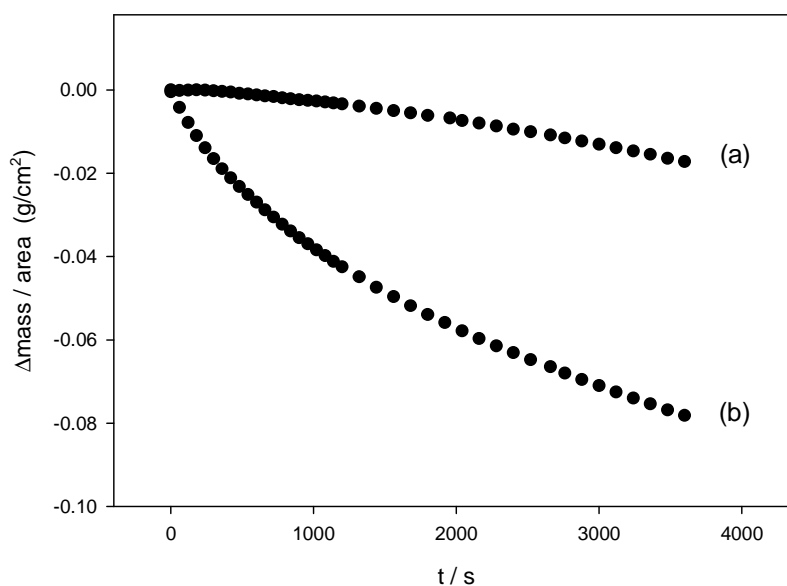
Figure 3.15. **Plot of change in mass per unit area versus time of (a) unmodified and (b) modified Ag SPE in 2 ml 1M H_2O_2.**

Each electrode was tested three times in order to analyze the stability and reproducibility of the measurements in fresh H_2O_2 solutions (Figure 3.16). Both modified and unmodified Ag SPEs showed decreasing responses as the number of repetitions increased. Significant decreases were observed for the modified SPE as compared to the unmodified one and this may suggest that the decomposition process is not truly catalytic as the surface may lose its catalytic properties over time.

Therefore, the use of DBSA/KCl solution as a modification agent for Ag SPEs resulted in the acceleration of the decomposition process when the electrodes were placed in H_2O_2, resulting in faster O_2 release compared to the unmodified ones.
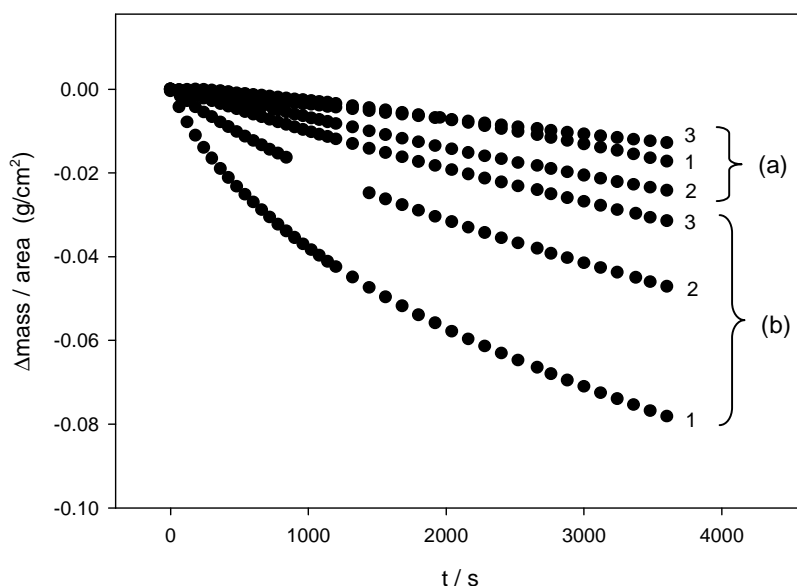
Figure 3.16. **Change in mass per unit area versus time of (a) unmodified and (b) modified Ag SPE in 2ml 1M H₂O₂ solution for 1 hour. Each electrode was measured three times and the number of the repetition is indicated besides each graph.**

Scanning electron microscopic images of the unmodified and DBSA/KCl modified Ag SPEs were obtained before and after exposure to 1 M H_2O_2 solution (Figure 3.17). As can be observed, Ag SPE electrodes presented very rough surfaces. Ag paste ink used to manufacture these electrodes consists of metallic Ag as well as an organic solvent and a vinyl or epoxy-based polymeric binder to maintain the structure of the ink and make it printable.[24] The purpose of the binder is to ensure the ink's affinity for the substrate in terms of adhesion properties. After screen printing, the fresh electrodes are cured in the oven so the organic solvent from the ink is evaporated. Moreover, as Grennan et al. (2001) reported using carbon-paste screen printed electrodes,[39] as the temperature of curing is increased, the surface roughness increases because the microparticulate nature of the Ag ink is consequently increased. Regarding the SEM images after H_2O_2 measurements, rougher surfaces of both types of electrodes were

observed after the reaction either due to the formation of a reaction product on the surfaces or because something on the electrode surface reacts with H_2O_2, provoking its decomposition and increasing the amount of holes on the surface. This increase of the surface roughness during H_2O_2 decomposition process was already reported by Schmidt et al.[40] They observed a micro-roughening effect occurred on hydrophobic silicon wafers after being immersed into H_2O_2/NH_4OH (SC1) cleaning solutions. They believed that small O_2 bubbles were stuck on the initially hydrophobic silicon surfaces preventing them from the etching action of the SC1 chemistry and making them responsible of the micro-masking effect.

It should be noted, however, that although unmodified Ag SPEs underwent a morphological change upon exposure to H_2O_2, this was not associated with an increase in catalytic decomposition.

Before the reaction, the DBSA/KCl modification appeared to produce some structural alteration on Ag SPEs (Fig. 3.17C) which did not appear on the unmodified electrodes (Fig. 3.17A). Moreover, Ag SPEs after modification did exhibit greater increases in levels of O_2 evolution from the solution due to H_2O_2 decomposition than those observed with the same electrodes without modification. The appearance of smaller structures in the same place as those formed prior to modification after the reaction with H_2O_2 seems to indicate that these surfactant-based structures formed on the electrode surfaces after the modification are in some way responsible for, or are a result of the catalytic effect on H_2O_2 decomposition observed on the modified Ag electrodes. In addition, the two structural morphologies exhibited for unmodified electrodes following H_2O_2 exposure and modified electrodes prior to H_2O_2 exposure cannot be equated and do not result in similar catalytic behaviours.
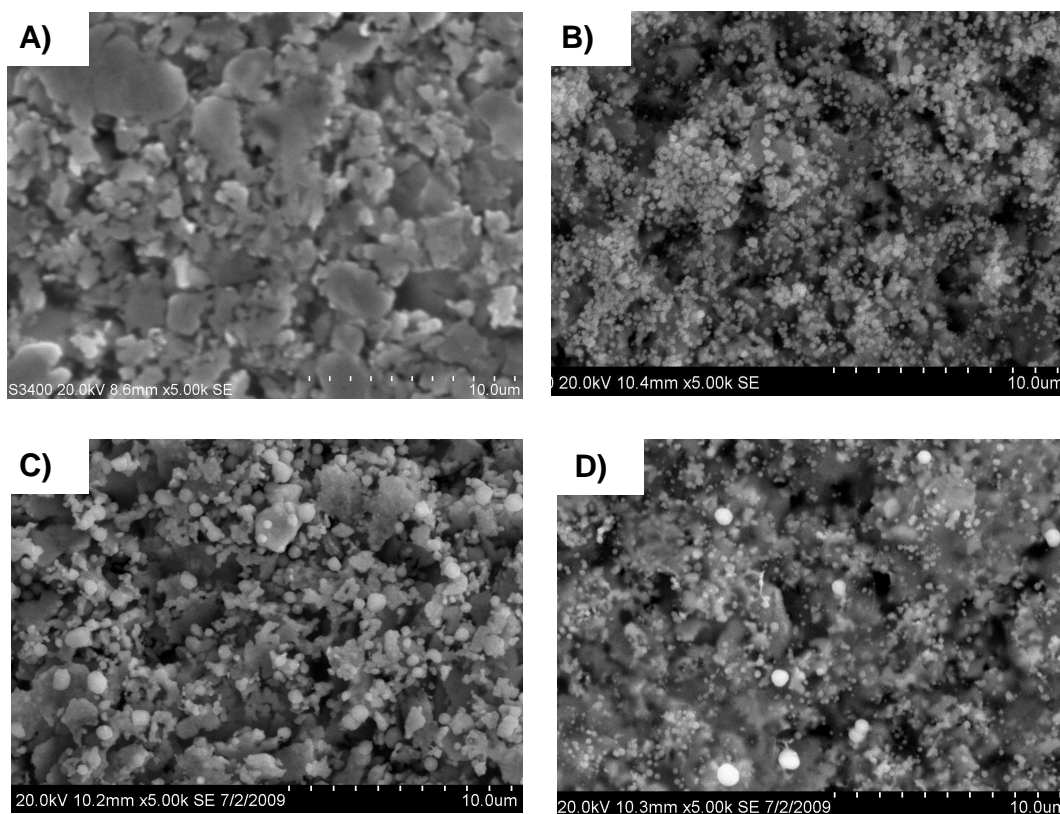
Figure 3.17. **SEM images of unmodified Ag SPEs (A) before and (B) after the measurements in 1 M H₂O₂ solution. SEM images of Ag SPEs modified with DBSA/KCl (C) before and (D) after exposure to 1 M H₂O₂ solution. Accelerating voltage of 20 kV. (5.0 k x magnification).**

The progressive alteration of the surface of the DBSA/KCl modified Ag SPE following repeated exposures to H_2O_2 is shown in Fig. 3.18. After 1 h exposure to H_2O_2 there were still many of the spheroidal structures formed following DBSA/KCl modification remaining on the electrode surface, as can be seen in Fig. 3.18b. However, when the electrode was further exposed to H_2O_2, the size of these structures diminished from approx. 1 µm after 1 h exposure to 100 – 300 nm after 3h, as can be observed from Fig. 3.18b-d. This enforces the notion of the involvement of the spheroidal structures created on the electrode surface after DBSA/KCl modification in the H_2O_2

decomposition reaction, and also that the change in their morphology over time is associated with a decrease in catalytic activity.
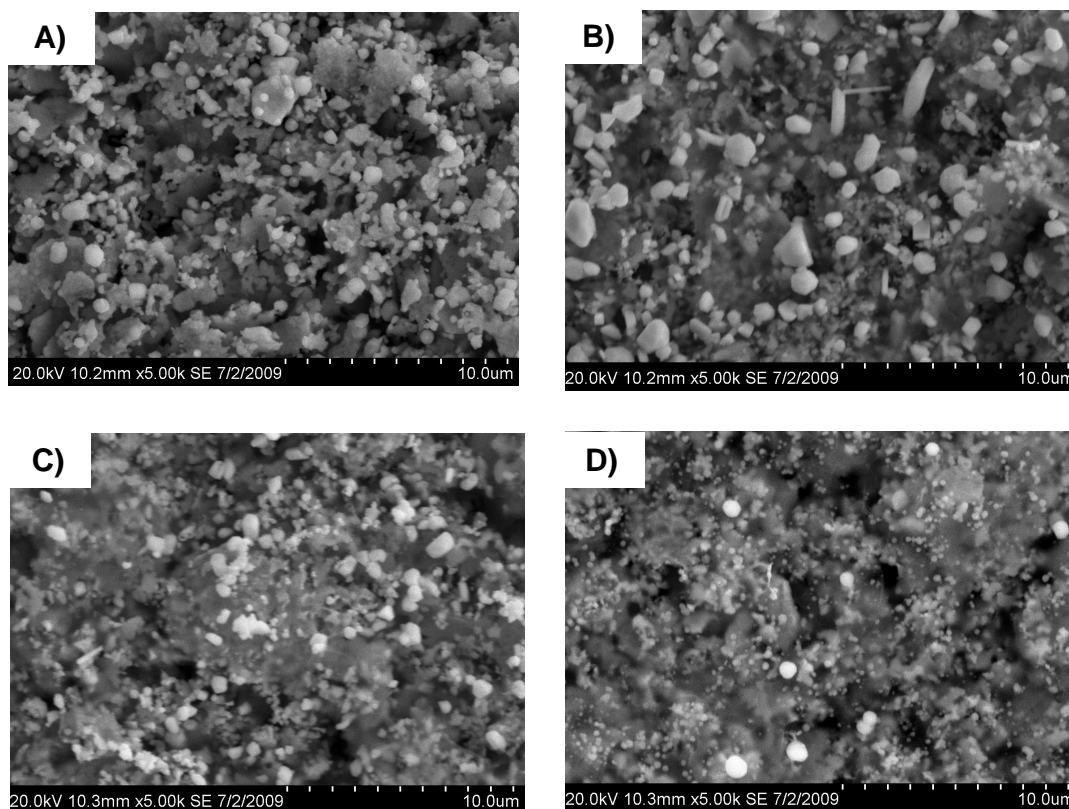
Figure 3.18. **SEM images of Ag SPEs modified with DBSA/KCl (A) before exposure to 1 M H_2O_2; and after (B) 1 h, (C) 2 h and (D) 3 h exposure to 1 M H_2O_2 solution. Accelerating voltage of 20 kV. (5.0 k x magnification)**

3.2.4. Study of the effect of surfactant type and Group I metal chloride salt in the modification solutions on electroreduction of H_2O_2

Given the catalytic effect that had been observed towards H_2O_2 reduction when Ag SPEs were modified with DBSA/KCl solutions, several other surfactants were studied to see what effect this would have on the catalytic process. Initially, sodium dodecyl sulphate (SDS) was assessed. This surfactant showed physical characteristics similar to

DBSA: both of them possess a long hydrophobic alkyl chain and a hydrophilic anionic head. The salt used as a co-partner for SDS modifying solutions was NaCl as opposed to KCl with DBSA. The aim was to check if catalysis towards H_2O_2 reduction was observed when Ag SPEs are pre-treated with SDS solutions and to evaluate the role of the salt in this effect. Therefore, Ag SPEs were dipped into solutions with different concentrations of SDS ($0.5 – 10^{-7}$ M), with and without 0.1 M NaCl for 3 h. Once rinsed, the electrodes were placed in the working cell (containing 10 ml PBS pH 6.8) and amperometry was performed. Cathodic current data from the amperometric responses to $5·10^{-3}$ M H_2O_2 were correlated with SDS concentration. Fig. 3.19 shows the comparison between modification with and without NaCl.
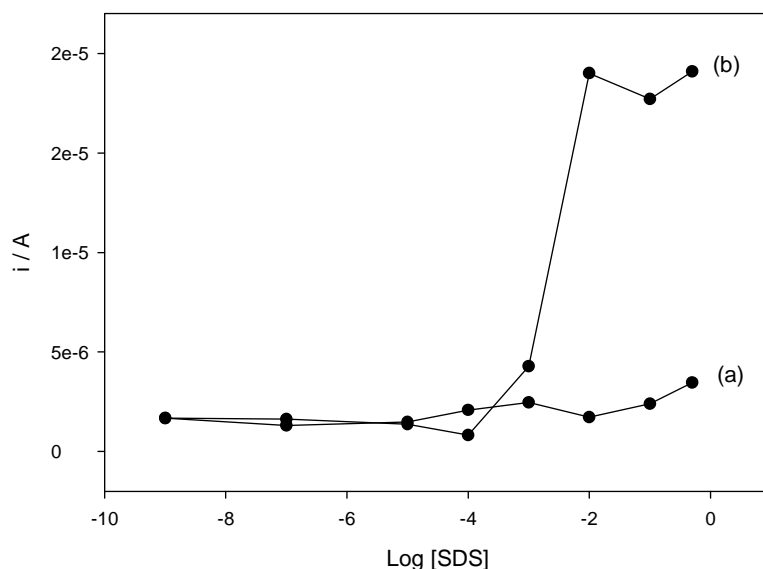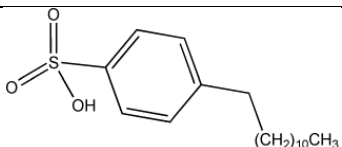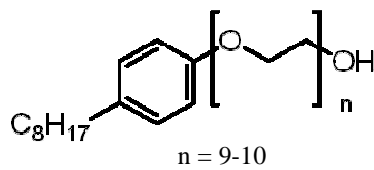
Figure 3.19. **Plot of current vs log [SDS] obtained during amperometric measurements of Ag SPEs at –0.1 V (vs Ag/AgCl) at $5·10^{-3}$ M H_2O_2. The electrodes were modified (a) only with SDS or (b) SDS and 0.1 M NaCl.**

As with DBSA, Ag SPEs modified solely with SDS solutions showed little catalytic effect towards H_2O_2 reduction, even though SDS concentration was increased to 1.5 M. However, the presence of NaCl in the modification solutions caused a noticeable

enhancement in the cathodic current when Ag SPEs were measured in the presence of $5 \cdot 10^{-3}$ M H_2O_2. At 0.1 M NaCl a significant rise in cathodic current was observed from 10^{-4} to 10^{-2} M SDS, where it reached a plateau. Consequently, the SDS concentration was fixed at $3.3 \cdot 10^{-2}$ M, to enable comparison with earlier DBSA data, and to investigate the effect of different concentrations of NaCl. At the same time, other surfactants were assessed in combination with an appropriate salt in the modification solution. Surfactant concentration used to pre-treat Ag SPEs was kept constant at $3.3 \cdot 10^{-2}$ M and the salt concentrations were varied. However, CTAB was used with a final concentration of $3.3 \cdot 10^{-3}$ M as at higher concentrations, insoluble aggregates were formed.

Table 3.2. Structure and characteristics of several surfactants.

Surfactant	Type[a]	CMC[b] / mM	Structure	Salt
Dodecyl Benzene Sulphonic Acid (DBSA)	A	1.6-2[15, 16]		KCl
Sodium Dodecyl Sulphate (SDS)	A	8-9[13, 14]		NaCl
Cetyl Trimethylammonium Bromide (CTAB)	C	0.9-1[13, 14]		NaBr
Triton X-100	N	0.2-0.3[13, 14]		KCl

[a] A, anionic; C, cationic; N, non-ionic.

[b] CMC – Critical Micelle Concentration.

Table 3.2 shows the structures and main characteristics of the surfactants under study. The Group I halogen salt used with the surfactants in the modification solutions are also presented in Table 3.2.

Cathodic current data from amperometric measurements using $5 \cdot 10^{-3}$ M H_2O_2 are shown in Fig. 3.20. Ag SPEs exposed to the different surfactant solutions showed enhanced catalysis in a manner similar to that seen with DBSA/KCl and SDS/NaCl. No remarkable enhancement effect was noticed when the concentration of the respective salt in the modification solutions remained below 10^{-5} M. However, above this concentration, a significant catalytic effect towards H_2O_2 reduction was observed, providing the highest reduction current values at salt concentrations in the modifying solutions of 10^{-2} to 1.5 M.
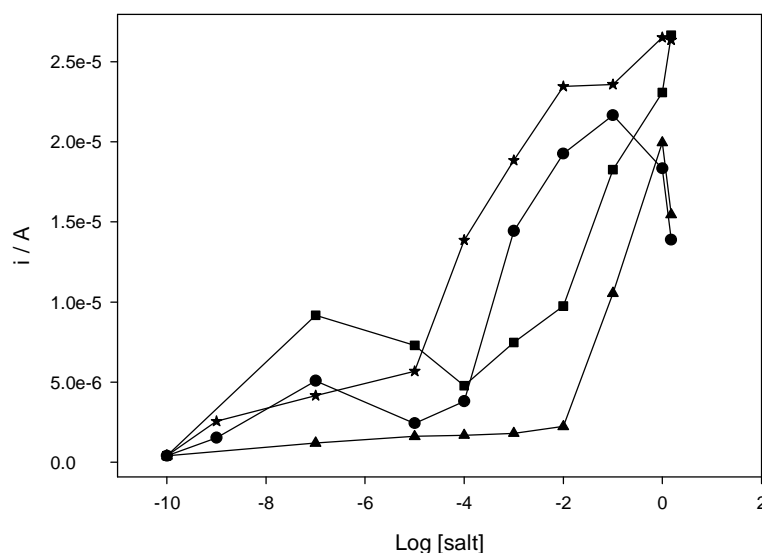
Figure 3.20. **Plot of current vs log [salt] obtained during amperometric measurements of Ag SPEs at –0.1 V (vs Ag/AgCl) at $5 \cdot 10^{-3}$ M H_2O_2. Electrodes were modified with (●) $3.3 \cdot 10^{-2}$ M DBSA/KCl; (★) $3.3 \cdot 10^{-2}$ M Triton X-100/ KCl; (■) $3.3 \cdot 10^{-3}$ M CTAB/NaBr or (▲) $3.3 \cdot 10^{-2}$ M SDS/NaCl. Salt concentration ranged from 1.5 to 10^{-7} M. Value at log [salt] = – 10 corresponds to the unmodified Ag SPEs.**

Although the overall behaviour of all the surfactant solutions was the same, there were some differences. One of these was the salt concentration at which H_2O_2 catalytic effect was observed. Triton X-100 required the lowest salt concentration to induce enhanced catalysis, being 10^{-4} M KCl, whereas SDS required the highest concentration of 0.1 M NaCl. DBSA required at least 10^{-3} M KCl to show a noticeable increase in catalysis, whereas CTAB showed a slight catalytic effect at very low NaBr concentrations in the modification solutions (10^{-7} M), although 0.1 M was required to obtain the most significant effect. Therefore, the surfactants under study in this work could be ordered from the lowest to the highest salt concentration required in the modification solution to show enhanced catalysis towards H_2O_2 reduction as reported below:

Triton X-100 < DBSA < CTAB < SDS

With the exception of CTAB, surfactants followed the same relative order as their respective critical micelle concentrations (CMC):

Triton X-100 (0.2-0.24) < CTAB (0.9-1) < DBSA (2) < SDS (7-10)

The different behaviour observed with CTAB could be explained as a result of the lower concentration of CTAB ($3.3 \cdot 10^{-3}$ M) employed for the modification solutions, which was ten times lower than that for the other surfactants ($3.3 \cdot 10^{-2}$ M). It is also worth noting that this was the only one with Br^- as counter-ion, which might lead to alterations or different behaviours during the formation of surfactant aggregates.

As is well-known, surfactants can form several types of organized structures in aqueous solutions as a function of concentration and/or experimental conditions.[13-15, 38] Typical surfactant aggregate structures are shown in Fig. 3.21.
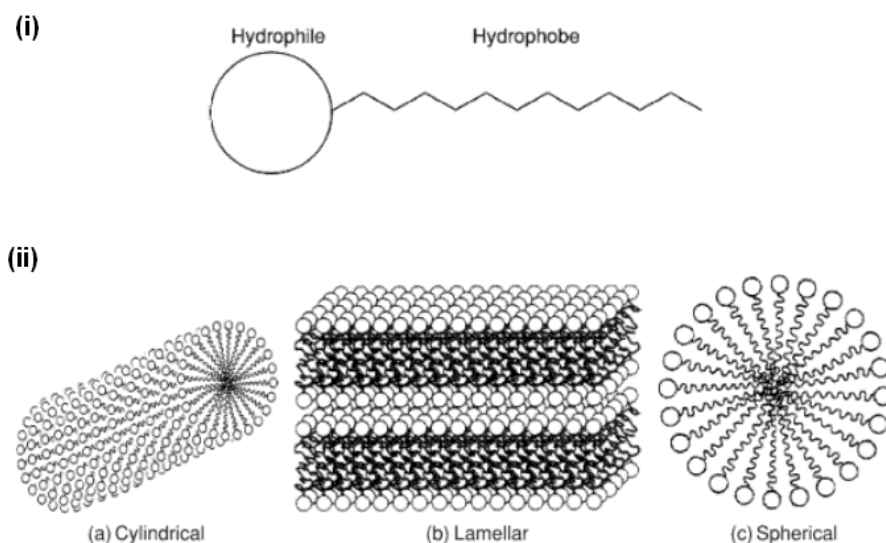
Figure 3.21. **(i). Simplified surfactant structure. (ii). Typical surfactant aggregates: (a) cylindrical structures, (b) lamellar structures and (c) spherical micelles.**[41]

Spheroidal micelles are the simplest aggregates formed by surfactants at low concentrations. When the surfactant concentration increases, cylindrical structures are observed, and above 30–40% (w/v) of surfactant, liquid crystalline phases are formed. These structures result from the aggregation of surfactant molecules into large domains, often of hexagonal or lamellar structures. However, surfactant concentration is not the only cause of changes in shape and structure. There are also other methods of inducing aggregate growth, which includes the addition of a salt such as NaCl, the addition of cosurfactants, changes in the counterions and the use of surfactant mixtures. Moreover, whereas solutions containing spherical micelles have low viscosity, the liquid crystalline phase (especially the hexagonal phase) exhibit very high viscosity values.[13]

The transition of micelles of the anionic surfactant sodium dodecylbenzenesulphonate (NaDBS) into lamellar aggregates by the addition of alkali metal chlorides was studied in dilute aqueous solution by Sein and Engberts.[15] The behaviour of NaDBS was described as a function of salt concentration, where the salt was varied along the lyotropic series (LiCl to CsCl). The cation hydration changes

dramatically along this series, from highly hydrated for Li^+ to weakly hydrated for Cs^+. On a molecular level, an increase in alkali metal cation concentration induced the packing of molecules into lamellar structures, which was facilitated by the increase in counterion binding and by the dehydration of the headgroup due to the addition of a salting-out electrolyte. Both effects would encourage a closer packing of the surfactant headgroups, which produced the rearrangement from micelles into lamellae. Less hydrated ions led to an increase in counterion binding, i.e. a decreasing electrolyte concentration from LiCl to CsCl was required to induce the packing in a lamellar array.

In the present work, both DBSA and SDS modification of, or exposure to Ag SPEs, in the presence of an alkali chloride salt (KCl and NaCl, respectively) produced similar catalytic responses when H_2O_2 reduction currents were plotted versus salt concentration. The catalytic effect of the modified electrodes was only significant above a certain salt concentration. Moreover, the highest cathodic currents were detected when the viscosity from the modification solutions was increased, with the formation of precipitates in the bulk solution being noted. Therefore, the catalytic effect observed by Ag SPEs on H_2O_2 reduction following pre-treatment with these surfactant-based solutions could be related to the formation of micelles or lamellar arrays by the surfactants in the presence of increasing salt concentration. Such structures would be formed in the solution and might become subsequently deposited or assembled at the electrode surfaces. Baryla et al.[35] recently studied the adsorption mechanisms and aggregation properties of CTAB and used atomic force microscopy (AFM) to image and determine the aggregate morphology of the surfactant on coated surfaces. They also reported the surfactant concentration dependence of the micellar coating on fused silica substrates as well as the effect of ionic strength on the surface assembly of CTAB. At low phosphate buffer ionic strength, CTAB formed spherical aggregates on the substrates whereas at higher ionic strength (0.1 M) a combination of short rods and spherical aggregates was observed. As has been shown previously, surfactant monomers form aggregates in aqueous solution because of the hydrophobic interactions between the long hydrocarbon chains which seek to minimise their interaction with water, and the hydrophilic head groups which favour interactions with water. The favourable interactions of adjacent amphiphiles are limited by the unfavourable electrostatic repulsion between the polar headgroups. Increasing the

ionic strength of the buffer minimizes this repulsion by ionic screening, which leads to the formation of different morphologies such as lamellae. Therefore, surfactants in such a conformation are likely to be deposited onto a surface in different morphologies depending on the salt concentration in the solution.[35, 42, 43] This effect could explain the dependence of the catalytic reduction current (i_{cat}) with [XCl] observed in the present work. To a certain extent, increasing the salt concentration in the surfactant-based modification solution would favour the formation of micelles or other highly packed aggregates, which are subsequently deposited on, or in some other way interact with the Ag SPE surface. Whatever the process, this appears to provide an appropriate environment to perform the significantly enhanced reduction of H_2O_2 observed.

3.2.4.1. Chloride salts with different Group I cations

In order to study the effect of the counter-cation size from the chloride salts used in the modification solution on catalysis, Ag SPEs were dipped into solutions containing $3.3 \cdot 10^{-2}$ M DBSA with a range of concentrations of the respective chloride salts (XCl, X = Li, Na, K or Cs). Then, the electrodes were rinsed and placed in PBS pH 6.8, where amperometric measurements were performed at –0.1 V (vs Ag/AgCl) in $5 \cdot 10^{-3}$ M H_2O_2 (Fig. 3.22).

Ag SPEs modified with different alkaline salts combined with $3.3 \cdot 10^{-2}$ M DBSA showed similar patterns of catalysis with an onset above approx. 10^{-4} M salt and peaking at 10^{-1} M, except DBSA/LiCl peaking at 1 M salt concentration. At 10^{-3} M, the cathodic currents obtained for all DBSA/salt modification solutions were similar and ranged between $1.4\text{-}1.7 \cdot 10^{-5}$ A. When the salt concentration in the modification solution increased, the cathodic current interval was spread, showing significant differences depending on the salt type in the modification solution. At 10^{-2} M, the highest catalytic activity was shown by the electrode exposed to DBSA/NaCl, with $2.2 \cdot 10^{-5}$ A, followed by KCl ($1.9 \cdot 10^{-5}$ A), LiCl ($1.7 \cdot 10^{-5}$ A) and CsCl ($1.3 \cdot 10^{-5}$ A). The greatest cathodic current were obtained at 10^{-1} M salt concentration, with $2.4 \cdot 10^{-5}$ A for NaCl, $2.2 \cdot 10^{-5}$ A for KCl and $2.0 \cdot 10^{-5}$ A for CsCl whereas the maximum value for LiCl, $2.1 \cdot 10^{-5}$ A, was obtained at 1 M concentration. DBSA/KCl combination was chosen for further

modifications as it presented cathodic currents in the same order than the rest of DBSA/XCl combinations and have already been proven as a catalyst for H_2O_2 decomposition as well.
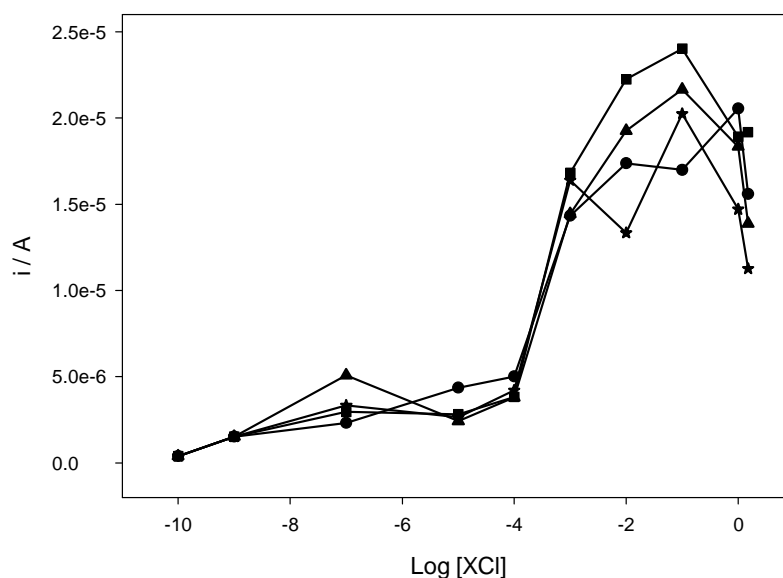
Figure 3.22. **Plot of current vs log [XCl] obtained during amperometric measurements of Ag SPEs at –0.1 V (vs Ag/AgCl) at $5 \cdot 10^{-3}$ M H_2O_2. The electrodes were modified with mixtures of $3.3 \cdot 10^{-2}$ M DBSA and different concentrations of: (●) LiCl ; (■) NaCl ; (▲) KCl or (★) CsCl. Salt concentration ranged from 1.5 to 10^{-7} M. Value at log [salt] = – 10 corresponds to the unmodified Ag SPEs.**

Moreover, the fact that all the salts resulted in catalytic activity in the same concentration range in the modification solution might be related again to the formation of surfactant aggregation in the solution. As was mentioned earlier, Sein and Engberts[15] studied the transition of surfactant micelles into lamellar structures when the concentration of alkali chloride in solution was increased. They observed that in the concentration range of approx. $0.05 \cdot 10^{-3}$ M for CsCl to $1.1 \cdot 10^{-3}$ M for LiCl, surfactant aggregates changed from micelles to unilamellar or flocculated multilamellar structures. This salt concentration range agrees with that of the enhanced H_2O_2 reduction process

observed in the present study and shown in Fig. 3.22. At $3.3 \cdot 10^{-2}$ M DBSA, more than ten times the DBSA CMC, surfactant is found as micelle aggregates in the modification solution. Dominguez[38] has also recently reported the formation of hemicylindrical aggregates of SDS molecules on graphite surfaces at different salt (NaCl)/water solutions. He performed a molecular dynamics simulation study and the results were compared to those obtained experimentally by atomic force microscopy (AFM). Again, the aggregates exhibited different structures as the salt concentration was increased. Without salt, the hemicylindrical aggregates showed only two well-defined layers due to the adsorption of the SDS tails on the graphite surface. At low NaCl concentration, a third layer was observed, which vanished at high salt concentration. Any change in solution properties which causes a reduction in the effective size of hydrophilic head groups, i.e. the addition of an electrolyte, will change the aggregate size and shape of the micelle structures.[44] When a salt is added to the modification solution, unilamellar or multilamellar structures are formed, which interact with the Ag SPE electrodes providing an enhanced ability for H_2O_2 reduction. The higher the salt concentration, the greater the catalytic activity shown by the Ag SPEs. At [salt] > 1 M, the catalytic currents decreased, which might be explained by the breaking-down of the surfactant aggregates in the modification solution or the decreasing interaction between the latter and the electrode surface.[38]

3.2.5. Detailed insights of the catalytic process

The modification of Ag SPEs with a surfactant/salt combined solution has shown to improve notably both the electrochemical reduction and decomposition of H_2O_2. That phenomenon was first detected following the exposure of the electrodes to a DBSA/KCl solution. The formation of spheroidal structures on the electrode surfaces was observed after the modification. The fact that the catalytic effect was only significant above a certain salt concentration and that surfactant concentrations in solution were above their CMC led to the conclusion that the formation of micelles or other highly packed aggregates was occurring in the solutions. Those structures would be subsequently deposited on, or in some other way interact with the Ag SPE surface, providing an

enhanced surface for H_2O_2 reactions. So far, surfactant, salt and Ag seem to be implicated in the modification and catalytic process, although other materials such as the binder from the Ag ink can not be neglected, which may serve as a surface for orientation of the hydrophobic tails of the surfactant. As will be commented on in Chapter 4, pure metallic electrodes (Au, Pt and even Ag), where the binder was not present, did not exhibit such significant catalytic enhancement after the surfactant/salt modification. Therefore, the binder might play an important role in the modification of Ag SPEs, at least.

As was suggested above, a possible explanation of the catalytic phenomenon would imply the formation of lamellar structures in the surfactant/salt solution, which interact with the Ag SPE electrode surface. That would explain the dependence on the salt and surfactant concentration in solution. That would also explain the increase in the non-faradaic current of the cyclic voltammograms of the Ag SPEs after the modification due to the formation of a surfactant-salt film which would change the dielectric constant of the surface. Moreover, the decrease of the surface area by BET analysis would agree with the formation of a film, which would block gas adsorption and would show lower available surface area.

Such a film might lead to the formation or stabilization of OH_{ads} or OH radical that are generally implicated in the electrochemical reduction and decomposition of H_2O_2. Thus, the following mechanism has been proposed by several authors for the electrochemical reduction of H_2O_2 on Ag:[3, 45]

$$H_2O_2 + e^- \rightarrow OH_{ads} + OH^-$$
$$OH_{ads} + e^- \leftrightarrow OH^-$$
$$2OH^- + 2H^+ \leftrightarrow 2H_2O$$
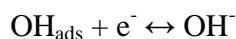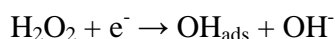
with the first step as the rate-determining one.[45] Therefore, any structure that stabilizes OH_{ads} would favour the reaction.

The increase of surface area as the explanation for the catalysis observed did not seem to be supported by BET analysis or any other solid evidence. However, the presence of a surfactant/salt film might hinder the measurements of surface area,

although be permeable to H_2O_2. Therefore, the possibility of an increase of the surface area can not be completely rejected, although is not very probable.

SEM and EDX analysis showed the presence of spheroidal structures and Cl on the surface after the modification. Those structures seemed to be reduced and Cl washed off the surface after the electrochemical reduction of H_2O_2. The interaction of the lamellar structures with the Ag SPE electrode surface, maybe through the binder, might lead to the formation of these structures with Ag and Cl. This does not mean that AgCl is formed. Ag metallic and Cl$^-$ might be confined inside, or surrounded by, the lamellar structures. During the electrochemical reduction of H_2O_2, Ag would be oxidized to Ag$^+$ and AgCl would be formed, precipitating into the solution. That would explain that no Cl would be detected after the electrochemical reduction.

The formation of a "head-up" surfactant/salt structures on the surface would justify the higher hydrophilicity of the modified electrodes compared to the unmodified ones.

In regards to the decomposition process, there was no evidence that the electrochemical reduction was coupled with the former. Only the modification of the spheroidal structures after both processes might suggest that those structures were involved in both phenomena, but not necessary following a common pathway. Some authors in the literature have reported the effect of H_2O_2 decomposition during the electrochemical reduction of H_2O_2. Welch et al.[3] attributed the shoulder exhibited at -0.7 V vs. SCE (approx. -0.66 V vs. Ag/AgCl) in the reduction wave to the electron-reduction of oxygen, produced via the silver-catalysed decomposition of H_2O_2. That phenomenon was only observed when the silver nanoparticles demonstrated a determined small size because only then did the relative rate of this process become sufficiently raised for its current to be seen. Guascito et al.[9] observed a new reduction process between 0 and -0.1 V vs. SCE for H_2O_2 concentrations larger than $2.5 \cdot 10^{-3}$ M when H_2O_2 was reduced on a Pt electrode modified with a polyvinyl alcohol (PVA) film with Ag nanoparticles in it. They related that process to the oxygen reduction formed from H_2O_2 decomposition catalyzed by silver and it was confirmed with a Clark electrode. In the present work, no evidences of O_2 influence during H_2O_2 electrochemical reduction was detected. Amperometric measurements were performed in the presence and absence of O_2 in the solution and no noticeable differences were

observed, maybe due to the low H_2O_2 concentrations (1 to $5 \cdot 10^{-3}$ M) used for the electrochemical measurements.

In the case of the decomposition, the surface modification might decrease the energy of activation (Ea) required due to a surface structure that stabilises the intermediate for H_2O_2. Strictly, a catalyst is a substance that accelerates a reaction but undergoes no net chemical change. The catalyst lowers the activation energy of the reaction by providing an alternative path that avoids the slow, rate-determining step of the uncatalysed reaction.[46, 47] Therefore, the surfactant-salt structures formed onto the Ag SPEs might provide an alternative path that requires lower Ea and increase the rate of the reaction respect to the unmodified ones, as will be seen in Chapter 4. However, as will be commented, the catalytic surfaces seemed to lose their properties over a number of decomposition reactions. That could be due to the direct implication of the modification on the decomposition process. Thus, many substances classified as catalysts are destroyed either as a result of the process that gives them their catalytic activity or because of subsequent combination with the products. From a practical point of view, a catalyst can be considered as a substance that changes the rate of a desired reaction, regardless of the fate of the catalyst itself.[48]

Regarding the electrochemical reduction, the modified electrodes provided an increase of approx. 100-fold in the cathodic currents respect to the unmodified ones. However, the differences in mass after 8 min in 1 M H_2O_2 was only 16-fold higher for the modified electrode compared to the unmodified one. Such a difference might indicate that the catalyst seemed to further enhance the electrochemical catalysis over H_2O_2 decomposition. But it is worth highlighting that the former was performed at H_2O_2 concentrations from 1 to $5 \cdot 10^{-3}$ M whereas the latter was carried out at 1 M H_2O_2. High H_2O_2 concentrations might destroy the surface modification, which result in a poorer apparent H_2O_2 decomposition process. As will be commented on in Chapter 5, surface modification seems to be very sensitive to other reactions occurring in the bulk solution. It will demonstrate a significant decrease in the electrochemical H_2O_2 response occurring on the modified electrodes after the enzymatic reaction glucose oxidase (GOx)-glucose was performed in the solution.

3.3. CONCLUSIONS

Hydrogen peroxide reduction was shown to be enhanced on Ag SPEs after their modification with DBSA/KCl solutions. Modification with $3.3 \cdot 10^{-2}$ M DBSA and 0.1 M KCl for 3 h has been presented as the optimum conditions in order to obtain the highest cathodic current, assessed in the presence of $5 \cdot 10^{-3}$ M H_2O_2. Moreover, the reduction process was highly favoured in basic solutions for the modified electrodes. SEM images presented the formation of spheroidal structures on the modified surfaces, which consisted of Ag and Cl, which were affected after the electrochemical H_2O_2 reduction on them, remaining as only Ag-based structures, as was evidenced by EDX. Two possible explanations to the catalytic effect shown by DBSA/KCl modified Ag SPEs have been suggested. On one hand, the surfactant/salt combination may undergo changes on the Ag morphology with the subsequent formation of nanostructures, which would increase the active surface area available to perform the electrochemical H_2O_2 reduction. On the other hand, the micellar or lamellar structures possibly formed by the DBSA/KCl in solution may have become deposited onto the Ag SPE in some way, creating an enhanced surface for the catalytic processes. The catalytic process was also shown to occur with other combinations of surfactants and group I halide salts and is not specific for DBSA and KCl.

The surfactant-based modification on Ag SPEs also seemed to induce an enhancement on H_2O_2 decomposition. The greater differences of mass due to the release of O_2 during H_2O_2 decomposition after the electrodes were treated with DBSA/KCl showed the surfactant-based solution produced an improvement in the catalytic process.

To sum up, Ag SPEs after the modification with DBSA/KCl resulted in a potential alternative to electrochemically quantify H_2O_2 concentration. The potential simplicity and low cost of manufacture makes this non-enzymatic device a unique platform for H_2O_2 sensing.

3.4. REFERENCES

1. L. Gorton, *Analytica Chimica Acta*, 1985, **178**, 247-253.
2. A. A. Karyakin, E. A. Puganova, I. A. Budashov, I. N. Kurochkin, E. E. Karyakina, V. A. Levchenko, V. N. Matveyenko and S. D. Varfolomeyev, *Analytical Chemistry*, 2003, **76**, 474-478.
3. C. M. Welch, C. E. Banks, A. O. Simm and R. G. Compton, *Analytical and Bioanalytical Chemistry*, 2005, **382**, 12-21.
4. A. Morrin, F. Wilbeer, O. Ngamna, S. E. Moulton, A. J. Killard, G. G. Wallace and M. R. Smyth, *Electrochemistry Communications*, 2005, **7**, 317-322.
5. A. Ambrosi, A. Morrin, M. R. Smyth and A. J. Killard, *Analytica Chimica Acta*, 2008, **609**, 37-43.
6. O. Ngamna, A. Morrin, A. J. Killard, S. E. Moulton, M. R. Smyth and G. G. Wallace, *Langmuir*, 2007, **23**, 8569-8574.
7. K. Crowley, A. Morrin, A. Hernandez, E. O'Malley, P. G. Whitten, G. G. Wallace, M. R. Smyth and A. J. Killard, *Talanta*, 2008, **77**, 710-717.
8. S. A. Kumar and S.-M. Chen, *Journal of Molecular Catalysis A: Chemical*, 2007, **278**, 244-250.
9. M. R. Guascito, E. Filippo, C. Malitesta, D. Manno, A. Serra and A. Turco, *Biosensors & Bioelectronics*, 2008, **24**, 1057-1063.
10. A. E. Radi, X. Munoz-Berbel, M. Cortina-Ping and J. L. Marty, *Electroanalysis*, 2009, **21**, 696-700.
11. M. Yemini, P. Xu, D. L. Kaplan and J. Rishpon, *Electroanalysis*, 2006, **18**, 2049-2054.
12. A. Karyakin, *Electroanalysis*, 2001, **13**, 813-819.
13. E. Pramauro and E. Pelizzetti, *Surfactants in Analytical Chemistry. Applications of organized amphiphilic media*, Elsevier, The Netherlands, 1996.
14. M. J. Rosen, *Surfactants and interfacial phenomena*, 2nd edn., John Wiley & Sons, 1989.
15. A. Sein and J. B. F. N. Engberts, *Langmuir*, 1995, **11**, 455-465.
16. V. Rumbau, J. A. Pomposo, J. A. Alduncin, H. Grande, D. Mecerreyes and E. Ochoteco, *Enzyme and Microbial Technology*, 2007, **40**, 1412-1421.
17. E. S. Brandt, *Journal of Electroanalytical Chemistry*, 1983, **150**, 97-109.
18. J. A. Cox and R. K. Jaworski, *Analytical Chemistry*, 1989, **61**, 2176-2178.
19. C. M. A. Brett and A. M. O. Brett, *Electroanalysis*, Oxford Science Publications, 1998.
20. A. Safavi, N. Maleki and E. Farjami, *Electroanalysis*, 2009, **21**, 1533-1538.
21. S. M. Senthil Kumar and K. Chandrasekara Pillai, *Electrochemistry Communications*, 2006, **8**, 621-626.
22. S. Abdollah, M. Leyla, H. Rahman and M. Hussein, *Electroanalysis*, 2008, **20**, 1760-1768.
23. G. Flätgen, S. Wasle, M. Lübke, C. Eickes, G. Radhakrishnan, K. Doblhofer and G. Ertl, *Electrochimica Acta*, 1999, **44**, 4499-4506.
24. R. Raymond & Co and S. distributor, Editon edn., Electrodag PF-410 product specification, vol. 20-01-2011.

25. S. C. Hung, Y. L. Wang, B. Hicks, S. J. Pearton, D. M. Dennis, F. Ren, J. W. Johnson, P. Rajagopal, J. C. Roberts, E. L. Piner, K. J. Linthicum and G. C. Chi, *Applied Physics Letters*, 2008, **92**, 193903-193903.

26. D. E. Watson and D. M. Yee, *Electrochimica acta*, 1969, **14**, 1143-1153.

27. F. Yalcinkaya and E. T. Powner, *Med. Eng. Phys.*, 1997, **19**, 299-301.

28. W. Lian, L. Wang, Y. Song, H. Yuan, S. Zhao, P. Li and L. Chen, *Electrochimica Acta*, 2009, **54**, 4334-4339.

29. P. Kalimuthu and S. A. John, *Journal of Electroanalytical Chemistry*, 2008, **617**, 164-170.

30. F. F. Peng, Y. Zhang and N. Gu, *Chinese Chemical Letters*, 2008, **19**, 730-733.

31. S. Brunauer, P. H. Emmett and E. Teller, *Journal of the American Chemical Society*, 1938, **60**, 309-319.

32. X. Ji, C. E. Banks, D. S. Silvester, A. J. Wain and R. G. Compton, *The Journal of Physical Chemistry C*, 2006, **111**, 1496-1504.

33. P. Boonme, K. Kravel, A. Graf, T. Rades and V. B. Junyaprasert, *AAPS PharmSciTech.*, 2006, **7**, 45.

34. M. Yamashita, K. Kameyama, R. Kobayashi, A. Asahina, S. Aita and K. Ogura, *J Electron Microsc (Tokyo)*, 1996, **45**, 461-462.

35. N. E. Baryla, J. E. Melanson, M. T. McDermott and C. A. Lucy, *Analytical Chemistry*, 2001, **73**, 4558-4565.

36. E. J. Wanless and W. A. Ducker, *The Journal of Physical Chemistry*, 1996, **100**, 3207-3214.

37. S. Manne and H. E. Gaub, *Science*, 1995, **270**, 1480-1482.

38. H. Dominguez, *Langmuir*, 2009.

39. K. Grennan, A. J. Killard and M. R. Smyth, *Electroanalysis*, 2001, **13**, 745-750.

40. H. F. Schmidt, M. Meuris, P. W. Mertens, A. L. P. Rotondaro, M. M. Heyns, T. Q. Hurd and Z. Hatcher, 1994 International Conference on Solid State Devices and Materials (SSDM 94), Yokohama, Japan, 1994.

41. R. J. Farn, *Chemistry and Technology of Surfactants*, 1st edn., Blackwell Publishing, Oxford, 2006.

42. J.-F. Liu and W. A. Ducker, *The Journal of Physical Chemistry B*, 1999, **103**, 8558-8567.

43. V. Subramanian and W. A. Ducker, *Langmuir*, 2000, **16**, 4447-4454.

44. R. J. Farn, *Chemistry and technology of surfactants*, Wiley-Blackwell, 2006.

45. M. Honda, T. Kodera and H. Kita, *Electrochimica Acta*, 1986, **31**, 377-383.

46. P. Atkins and J. de Paula, *Atkins' Physical chemistry*, 8th edn., Oxford University Press, Oxford, 2006.

47. G. C. Bond, *Heterogeneous catalysis. Principles and applications*, 2nd edn., Oxford University Press, Oxford, 1987.

48. J. W. Moore and R. G. Pearson, *Kinetics and Mechanism*, 3rd edn., John Wiley & Sons, New York, 1981.

Chapter 4

Investigation of the effect of the nature of the metallic electrode on the chemical decomposition and electrocatalytic reduction of hydrogen peroxide following modification with surfactant/salt

4.1. INTRODUCTION

Chapter 3 demonstrated the catalytic activity of surfactant/salt modified Ag SPEs on the electrochemical reduction and decomposition of H_2O_2 at silver paste electrodes. It was suggested that the combination of surfactant and salt may form stabilized lamellar structures. Those structures were proposed to interact with the Ag SPE electrode surface, leading to the formation of structures that catalyze both processes. The creation of spheroidal structures on the surface after the exposure to the surfactant/salt solution seemed to be related to the catalysis as they were diminished after the electrode reaction with H_2O_2. However, the nature of such an interaction between the surfactant/salt structures and the electrode surfaces was not fully understood. Ag ink used to fabricate the screen printed electrodes is a complex material made of metallic Ag as well as organic solvents and thermoplastic resin binders to maintain the structure of the ink and make it printable.[3] The possibility that the binder present in the Ag ink played a role in the formation of the more catalytic surface was considered. To simplify the surface and understand the relationship between the metal conductor and the surfactant/salt modification, metallic electrodes were employed to investigate the nature of the catalysis.

In the present work, therefore, a range of materials including Ag-based and other metallic electrodes are used to help understand what was happening on the electrode surfaces after the surfactant/salt modification. The effect of the modification on the H_2O_2 reduction and decomposition was assessed mainly by amperometry. In addition, Scanning Electron Microscopy (SEM) measurements were performed to characterize the electrode surfaces before and after the surfactant-based modification. Comparison of H_2O_2 detection by Ag-based electrodes of varying quality and other metal-based electrodes such as Au and Pt are shown and the effect of their modifications was also studied. A kinetic study of the H_2O_2 decomposition process on the above-mentioned metallic surfaces was also carried out. The apparent and heterogeneous rate constants for these processes were calculated and the values compared with the data already existing in the literature.

4.2. RESULTS AND DISCUSSION

After the study of DBSA/KCl modification of Ag SPEs and their catalytic activity towards H_2O_2 decomposition and electrochemical reduction, the same effect on other metallic electrodes was subsequently investigated. Other silver-based electrodes such as metallic Ag (99.9%) or sterling Ag (92.5%), as well as gold and platinum-based electrodes were assessed and their catalytic activity on H_2O_2 reactions was compared to Ag SPEs.

4.2.1. Silver-based electrodes

4.2.1.1. Electrochemical characterization

Planar Ag (99.9%) metallic electrodes were used to study the catalytic effect on H_2O_2 following their modification with DBSA/KCl. The electrodes were polished using 0.3 μm first and then 0.05 μm of alumina powder, and sonicated in distilled water for 5 min to remove any possible impurities on the surface. Next, they were dipped into $3.3 \cdot 10^{-2}$ M DBSA/ 0.1 M KCl solutions for 3 h, rinsed copiously with distilled water and placed in a working cell containing 10 ml PBS, pH 6.8. Cyclic voltammograms and amperometric measurements were performed in $0-5 \cdot 10^{-3}$ M H_2O_2. The measurements obtained with the modified electrodes were compared to those from the unmodified ones (Fig. 4.1). As can be observed, no enhancement was observed following the modification. Thus, the cathodic currents obtained with the unmodified and modified Ag (99.9%) electrodes in the presence of $5 \cdot 10^{-3}$ M H_2O_2 were $1.13 \cdot 10^{-7}$ A and $1.15 \cdot 10^{-7}$ A, respectively. The metallic silver (99.9%) electrodes were also pre-treated in HCl at +1 V (vs Ag/AgCl) for 2 s to electrochemically form AgCl on the electrode surface,[4] but no enhancement of the amperometric responses was obtained.
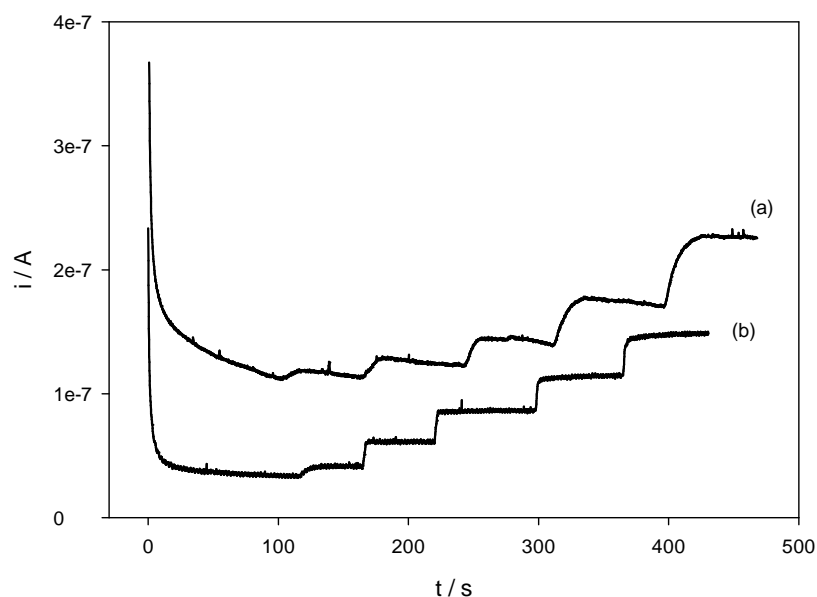
Figure 4.1. **Amperometric responses of planar Ag (99%) metallic electrodes measured at –0.1 V (vs Ag/AgCl) in PBS pH 6.8: (a) unmodified; (b) 3h DBSA/KCl modified, at H_2O_2 concentrations from 1 to $5 \cdot 10^{-3}$ M.**

SEM imaging of the metallic Ag (99.9%) electrodes was performed before and after DBSA/KCl modification. Metallic Ag (99.9%) did not show the formation of any surface structures or increasing roughness after the pre-treatment in DBSA/KCl for 3h, as is observed by comparing Fig. 4.2a and 4.2b. This data was in agreement with the lack of catalytic effect on H_2O_2 reduction. It reinforces the belief that the creation of the spheroidal structures on the Ag SPE surface after DBSA/KCl modification is related to the enhancement of H_2O_2 reduction.

The same procedure performed with Ag SPEs and planar metallic Ag (99.9%) electrodes was also applied to other available silver-based substrates, such as 0.5 mm diameter Ag wire (99.9%) and sterling Ag (92.5%). The electrodes were modified in DBSA/KCl for 3 h and then placed in a working cell containing 10 ml PBS pH 6.8, where amperometric measurements were performed at –0.1 V. Cathodic currents from

$5 \cdot 10^{-3}$ M H_2O_2 were recorded and compared to those obtained for Ag SPEs and planar metallic Ag (99.9%) electrodes.
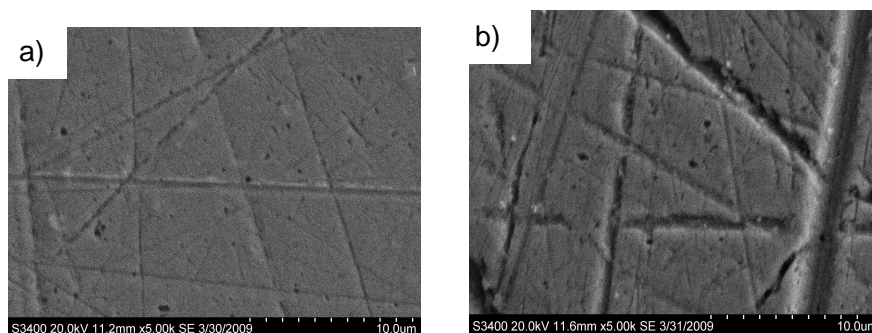
Figure 4.2. **SEM images using SE detection of metallic Ag (99.9%) electrodes (a) unmodified and (b) DBSA/KCl modified after 3h. Accelerating voltage of 20 kV. (5.0k x magnification).**

As with planar metallic Ag (99.9%) electrode substrates, little enhancement in the reduction currents were observed with the DBSA/KCl modified Ag wire and sterling Ag (92.5%) electrodes with respect to the unmodified ones. Thus, the unmodified Ag wire exhibited a cathodic current of $4.7 \cdot 10^{-8}$ A at $5 \cdot 10^{-3}$ M H_2O_2 whereas the DBSA/KCl modified one showed $4.1 \cdot 10^{-8}$ A (Fig. 4.3).

AgCl was also electrochemically formed onto the Ag wire electrodes by applying the same conditions mentioned above[4] and the electrodes were subsequently tested in the presence of H_2O_2 (Fig. 4.3). The increased deposition of AgCl on the Ag wire electrode did lead to an increase in the catalytic current. Thus, the cathodic current at $5 \cdot 10^{-3}$ M H_2O_2 was $1.0 \cdot 10^{-6}$ A for a Ag wire electrode after 2 s in 0.1 M HCl and reached $2.3 \cdot 10^{-6}$ A after 3 x 5 s exposures in 0.1 M HCl. The formation of AgCl on the surface also led to an increase in the background noise and current. For the latter, $4.6 \cdot 10^{-8}$ A was observed for the unmodified electrode whereas $2.7 \cdot 10^{-6}$ A was exhibited by the electrode modified 5 s in 0.1 M HCl three times, which reflected the increasing level of surface modification.
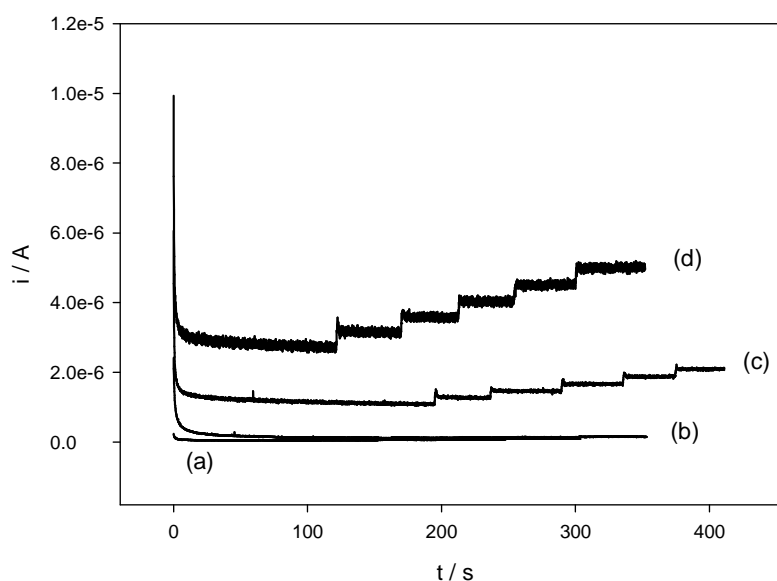
Figure 4.3. **Amperometric responses of Ag wire electrodes measured at –0.1 V (vs Ag/AgCl) in PBS pH 6.8: (a) unmodified; (b) DBSA/KCl modified; (c) AgCl electrochemical formation after 2 s at +1 V (vs Ag/AgCl) in 0.1 M HCl (d) AgCl electrochemical formation after 5 s at +1 V (vs Ag/AgCl) in 0.1 M HCl three times, at H_2O_2 concentrations from 1 to $5 \cdot 10^{-3}$ M.**

This catalytic effect on H_2O_2 reduction after the electrochemical formation of AgCl on the surface could be due to the increase of the electrode surface area, as has been previously reported. Lian et al.[1] reported the increased roughness of Ag electrodes by electrochemical oxidation-reduction cycles in a KCl solution. During the anodic process, Ag was oxidized to form a Ag-Cl complex, which was very helpful for the subsequent formation of Ag nanoparticles during the cathodic process. The roughened electrode did show noticeable increases of the amperometric responses to H_2O_2. That would explain the increase in the catalytic response of the Ag wire electrode after AgCl formation. However, there is no direct evidence that relate the formation of AgCl with the spheroidal structures that appeared on the electrode surfaces following DBSA/KCl

exposure, which are though to be in part responsible of the catalytic activity towards H_2O_2 decomposition and electrochemical reduction shown in Chapter 3.

4.2.1.2. H_2O_2 decomposition

H_2O_2 decomposition was then analysed on Ag metallic electrodes (92.5% and 99.9%) using the same conditions as for the Ag SPEs. The initial aim was to check if the catalytic effect was also observed on these substrates and to assess the influence of Ag surface on the H_2O_2 decomposition process. The mass differences were expressed per unit area (g/cm^2). The area values used in the experiments were the geometric areas because the narrow potential range in which Ag is not electroactive prevented the accurate calculations of their electroactive areas electrochemically.

The measurements of the 92.5% and 99.9% metallic electrodes (before and after modification) are shown in Fig. 4.4 and 4.5, respectively.
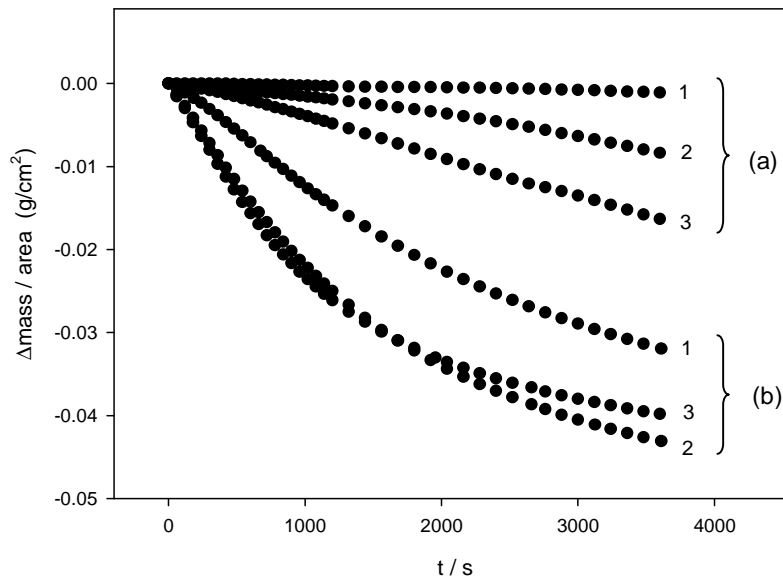
Figure 4.4. **Change of mass per unit area versus time for (a) unmodified and (b) modified 92.5% Ag electrodes upon repeated exposure to 1 M H_2O_2 solution for 1 hour. The number of exposures is indicated besides each graph.**

Unlike SPEs, the metallic Ag electrodes did not show decreased responses after multiple H_2O_2 exposures. On the contrary, higher mass decreases were observed on the unmodified 92.5% Ag electrodes as the number of exposures increased and a steady-state was shown by the same electrodes after DBSA/KCl modification. The 99.9% metallic Ag electrodes also showed a stable response after being exposed to H_2O_2 solution for 1 hour, either in the modified or unmodified state. Overall, the 99.9% Ag electrodes showed significantly higher mass reductions than the 92.5% Ag, irrespective of the state of modification. These differences were approximately ten-fold after 1 hour of exposure to H_2O_2. Again, the non-linearity of the modified 92.5% electrode seems significant – in instances where modification has enhanced the catalysis, this seems to be non-linear in nature.
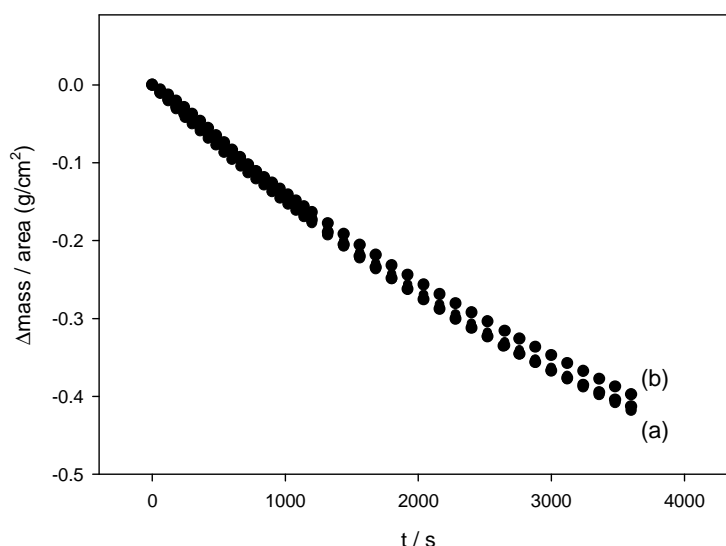
Figure 4.5. **Change of mass per unit area versus time for (a) unmodified and (b) modified 99.9% metallic Ag electrodes upon exposure to 1 M H_2O_2 solution for 1 hour.**

Figure 4.6 shows the compiled responses of SPEs and metallic 92.5% and 99.9% Ag electrodes, before and after the DBSA/KCl modification. The data correspond to the

initial exposure of each electrode to H_2O_2. The catalytic effect observed after surfactant-base modification of Ag SPEs appears to be partially observed in the 92.5% Ag electrodes. However, the catalytic responses after modification were only three times higher than before for the 92.5% Ag electrodes, whereas this was about eight times better in the case of SPEs. No enhancement in H_2O_2 decomposition was observed on the 99.9% Ag electrode after surfactant-based modification.
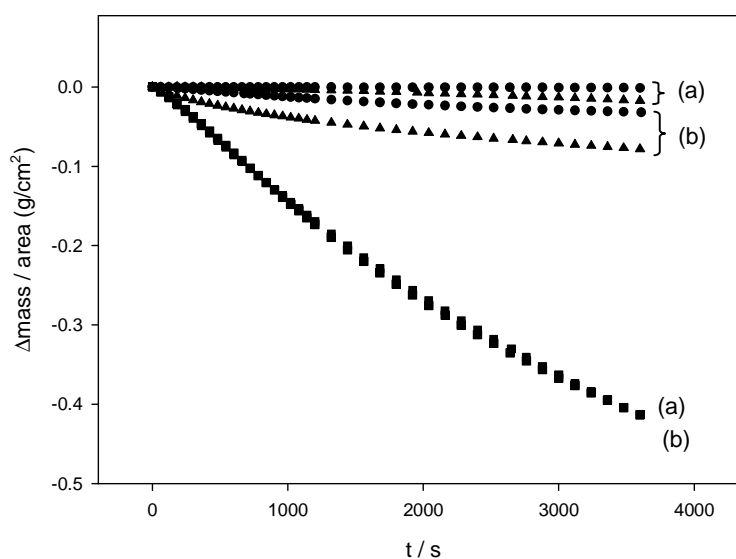
Figure 4.6. **Hydrogen peroxide decomposition rate for (a) unmodified and (b) modified (circle) 92.5%, (triangle) SPE and (square) 99.9% Ag electrodes when exposed to 1 M H_2O_2 solution for 1 hour. These data correspond to the first repetition of each electrode.**

Therefore, DBSA/KCl modification seemed to enhance H_2O_2 decomposition only on Ag SPE and metallic 92.5% Ag electrodes whereas no improved catalytic process was observed on metallic 99.9% Ag electrodes.

Scanning electron microscopic images of the unmodified metallic 92.5 and 99.9% Ag electrodes were obtained before and after exposure to 1 M H_2O_2 solution (Fig. 4.7). As can be observed, the unmodified 92.5 and 99.9% Ag metallic electrodes presented

smoother surfaces than the SPE electrodes (Chapter 3, Fig. 3.17). Between these two electrodes, the 99.9% Ag metallic seemed to be the smoothest one and only some scratches were shown on its surface possibly due to the polishing process whereas the 92.5% Ag metallic surface showed many surface defects, pitting, etc.
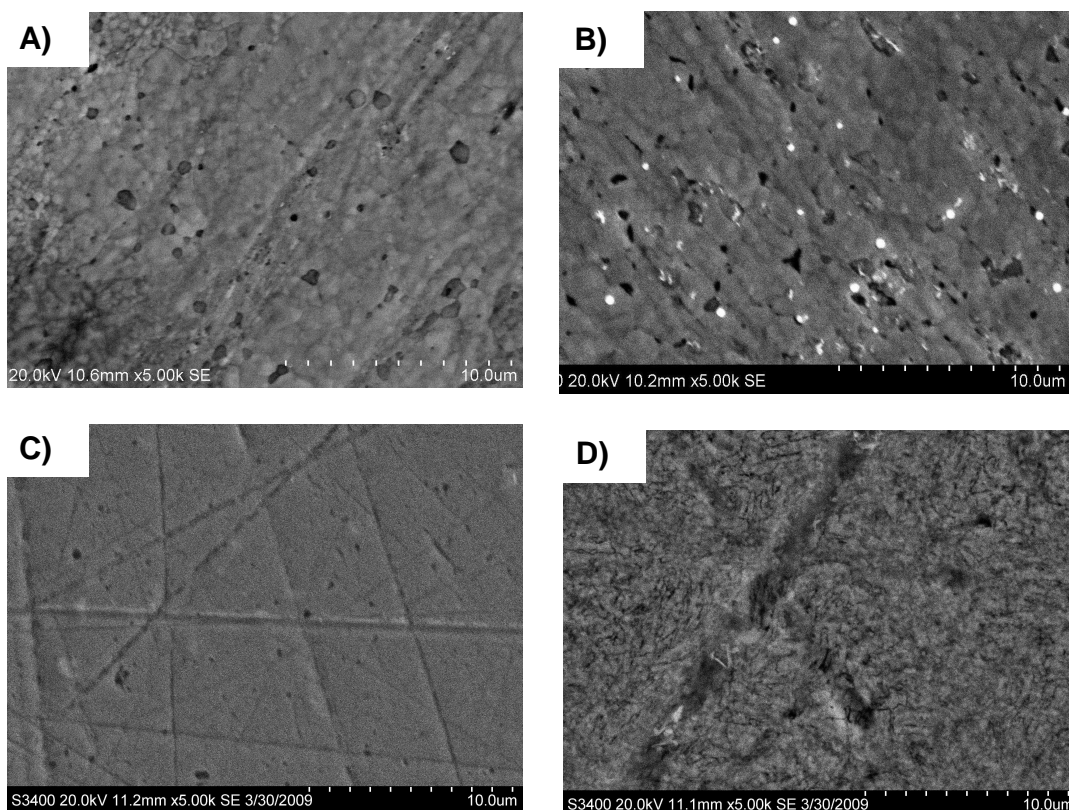
Figure 4.7. **SEM images of unmodified sterling 92.5% Ag electrodes (A) before and (B) after being exposed to 1 M H_2O_2 solution and 99.9% Ag metallic electrodes (C) before and (D) after H_2O_2 decomposition measurements. Accelerating voltage of 20 kV. (5.0 k x magnification)**

Following exposure to H_2O_2, the formation of reaction products which increased surface roughness was again observed. However, the 92.5% Ag metallic surface seems to be less affected by H_2O_2, which agrees with the low differences of mass obtained with this electrode. On the other hand, 99.9% Ag electrode shows the roughest surface after

H_2O_2 decomposition in comparison with the surface before as well as the highest differences of mass observed for that process.

Fig. 4.8 shows SEM images of the modified metallic electrode before and after exposure to H_2O_2.
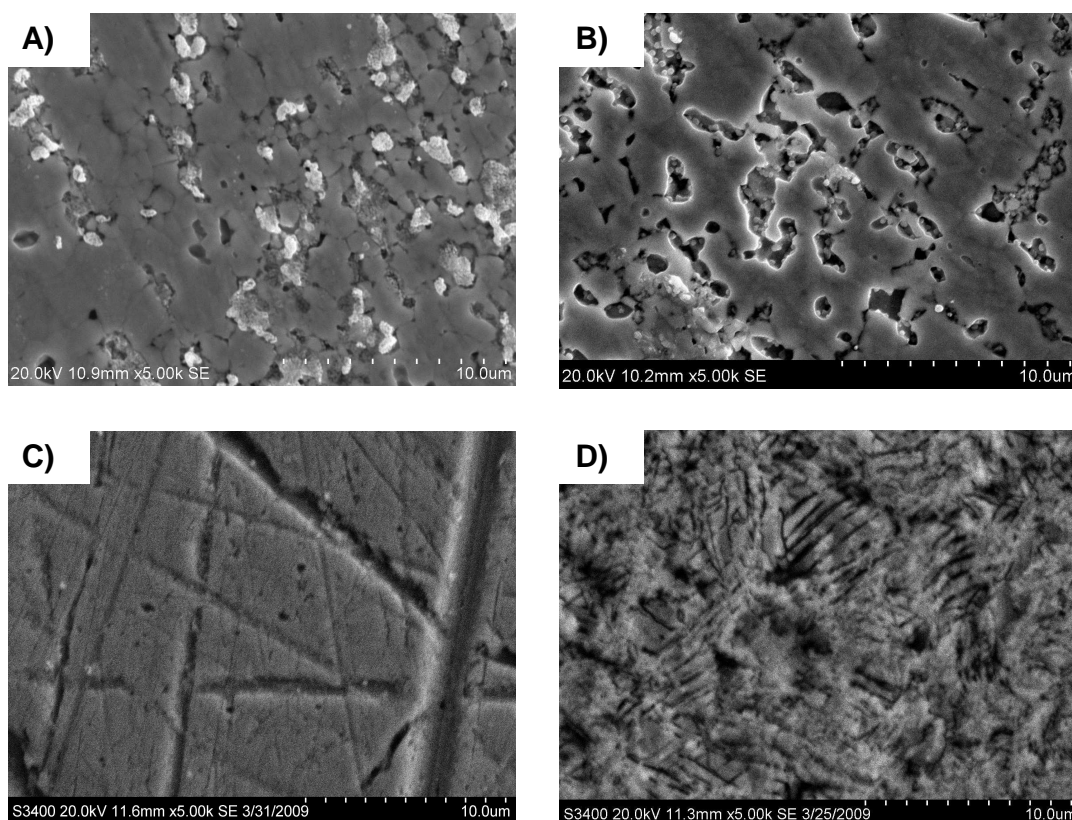
Figure 4.8. **SEM images of modified sterling 92.5% Ag electrodes (A) before and (B) after exposure to 1 M H_2O_2 solution and 99.9% Ag (C) before and (D) after H_2O_2 decomposition measurements. Accelerating voltage of 20 kV. (5.0 k x magnification)**

As with Ag SPEs, similar high contrast clusters were observed on the sterling 92.5% Ag electrodes after DBSA/KCl modification, which appeared to be associated with the surface defects of the Ag, whereas 99.9% Ag electrode surfaces did not show any such structures after the surfactant-based modification. Again the formation of rougher

surfaces after the reaction with H_2O_2 was observed in all the Ag electrodes with the difference that either the formation of holes or the creation of reaction products on sterling 92.5% Ag electrodes was more pronounced (Fig. 4.7b and 4.8b) whereas no noticeable changes relative to the unmodified substrates were shown by metallic 99.9% Ag electrodes (Fig. 4.7d and 4.8d). During the H_2O_2 decomposition reaction, sterling 92.5% Ag electrodes did show greater levels of O_2 evolution after modification, which agreed with the rougher surfaces exhibited by the electrode in comparison with the unmodified one. The high contrast clusters evident before exposure to H_2O_2 were no longer evident, but were replaced with the edges of the surface defects on the silver showing a high contrast which suggests some structural modification at these sites. Although not quantified, the surface defects seemed to be etched and larger in size following H_2O_2 decomposition.

In contrast, the 99.9% Ag electrode showed no difference in surface morphology before and after DBSA/KCl treatment, suggesting a lack of any surface modification. However, both surfaces showed a significantly different morphology following exposure to H_2O_2 with what appeared to be a roughened surface with an apparently crystalline morphology. The nature of these structures was not determined.

Therefore, as was observed before for Ag SPEs, the formation of structures on the electrode surface following DBSA/KCl treatment seemed to be directly implicated in the enhancement of the H_2O_2 decomposition reaction.

4.2.2. Gold-based electrodes

4.2.2.1. Electrochemical characterization

Other noble metallic substrates were assessed in order to check if it was an isolated effect from Ag surfaces or a general behaviour from this group of metallic elements. Several gold-based electrodes were evaluated and their responses compared to those obtained with silver-based electrodes. In addition, the relationship between metallic Au electrodes and Au paste electrodes was also assessed.

Gold screen printed electrodes (Au SPEs) were directly exposed to $3.3 \cdot 10^{-2}$ M DBSA/ 0.1 M KCl for 3 h without any prior pre-treatment, rinsed with distilled water and placed in a working cell containing 10 ml PBS, pH 6.8, where cyclic voltammetry and amperometry were performed. Three types of Au SPEs were assessed. The current densities of these electrodes to $5 \cdot 10^{-3}$ M H_2O_2 at –0.1 V (vs. Ag/AgCl) are shown in Table 4.1, before and after DBSA/KCl modification.

Table 4.1. Cathodic current densities of Au SPEs to $5 \cdot 10^{-3}$ M H_2O_2 at –0.1 V (vs. Ag/AgCl) before and after DBSA/KCl treatment. These are also compared with Ag SPE and Au (99.9%).

Electrode	Area / cm^2	j_{unmod} (x10^6) / Acm^{-2}	j_{mod} (x10^6) / Acm^{-2}	j_{mod}/j_{unmod}
Au SPE AT (Dropsens)	0.126	0.7	8.0	12.2
Au SPE BT (Dropsens)	0.126	0.3	0.5	1.9
Au SPE (DuPont)	0.045 (unmod)/ 0.040 (mod)	1.7	11.2	6.6
Ag SPE	0.126	3.1	273.6	88.8
Au (99.9%)	0.031	41.1	31.7	0.8

Au SPEs showed some enhancement of the H_2O_2 reduction current after the modification with DBSA/KCl, although this effect was not so marked as that shown by Ag SPEs. Thus, the highest ratio of cathodic current density obtained for a modified Au SPE compared to an unmodified one was approx. 12, whereas almost 90 was the ratio obtained with Ag SPEs. Regarding the Au electrodes from Dropsens, Au SPE AT (cured at high temperature) showed a more noticeable catalytic effect after DBSA/KCl pre-treatment, with approx. $8.0 \cdot 10^{-6}$ Acm^{-2}, than Au SPE BT (cured at low temperatures), on which the cathodic current was only $0.5 \cdot 10^{-6}$ Acm^{-2}. Although there was already a three-fold difference between their cathodic currents in the unmodified state, this contrast was

more remarkable after the modification, with a sixteen-fold difference. The variation between both electrodes could be a consequence of the different surface roughness or type of binder used in the preparation of the electrodes.

Generally, electrodes cured at higher temperature show rougher surfaces because the organic compounds presented in the printable ink are evaporated from the substrates when the temperature increases.[5] However, in this case, Au SPEs BT exhibited rougher surfaces[6] may be because the application of low temperature but high enough to evaporate the solvent would lead to the formation of smaller Au particles on the surface. Thus, Au SPEs AT might be more prone to DBSA/KCl modification because the surfaces seemed to present higher amount of binder exposed than Au SPEs BT. This would favour the interaction of the lamellar structures with the electrode surfaces with the subsequent enhancement of such modified surfaces towards H_2O_2 decomposition. Alternatively, the catalysis may depend on the nature of the binder used for ink fabrication which may favour the formation of surfactant/salt lamellar structures. In any case, the catalytic effect obtained by the gold-based SPEs was very low in comparison to that of Ag SPEs. One possible explanation is the higher tendency of Cl^- in the modification solution to form AgCl rather than AuCl (standard enthalpies of formation of AgCl and AuCl are -127.0 and -34.7 $kJmol^{-1}$, respectively),[7] which was previously observed as a likely important step in the subsequent enhancement of H_2O_2 reduction. However, the relevance of Cl^- in the catalytic process is still far from certain. The other possible explanation is that Au is just inherently less catalytic for H_2O_2 than Ag, either modified or unmodified.[8]

Planar metallic Au (99.9%) electrodes (A = 0.031 cm^2) were also assessed. They were polished using first 0.3 μm and later 0.05 μm alumina. Then, they were rinsed and sonicated in distilled water. Once cleaned, they were exposed to $3.3 \cdot 10^{-2}$ M DBSA/ 0.1 M KCl for 3 h. The amperometric responses at –0.1 V (vs Ag/AgCl) obtained in PBS pH 6.8 before and after DBSA/KCl modification are shown in Fig. 4.9 and the data given in Table 4.1. DBSA/KCl modification did not seem to improve the catalytic properties of metallic Au (99.9%) electrodes, as can be observed by comparing the amperometric responses from the unmodified and DBSA/KCl modified electrodes. While $41.1 \cdot 10^{-6}$ Acm^{-2} was achieved with the unmodified Au metallic electrode in the presence of $5 \cdot 10^{-3}$

M H_2O_2, only $31.7 \cdot 10^{-6}$ Acm^{-2} was obtained following DBSA/KCl modification. On the other side, comparison of these data with those for unmodified Ag SPEs, metallic Au (99.9%) showed higher reduction current values, which is probably due to the higher available metallic surface area. However, the Ag SPEs showed greater increases in catalytic currents when treated with DBSA/KCl than did metallic Au. This may relate to availability of surface defects for the deposition/modification sites not available on planar metallic Au (99.9%) as well as for the absence of binder.
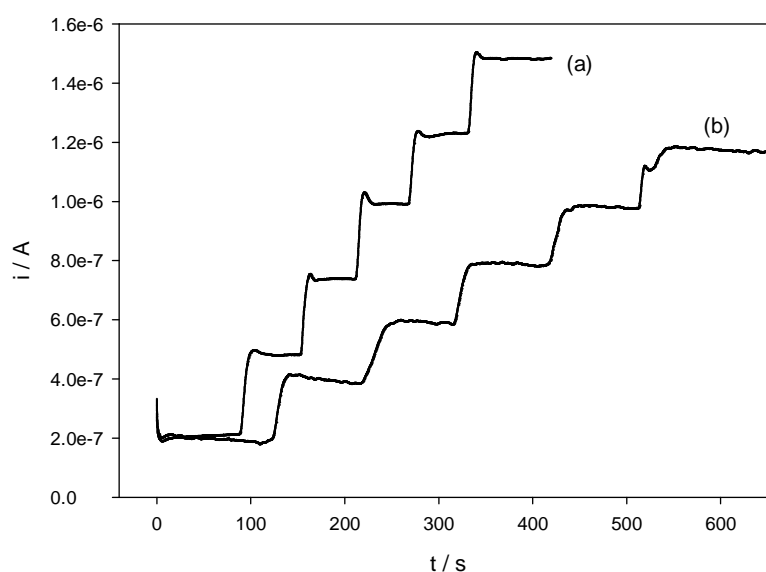
Figure 4.9. **Amperometric responses of metallic Au (99.9%) electrodes measured at –0.1 V (vs. Ag/AgCl) in PBS pH 6.8: (a) unmodified and (b) DBSA/KCl modified, at H_2O_2 concentrations from 1 to $5 \cdot 10^{-3}$ M.**

4.2.2.2. H_2O_2 decomposition

Further to the study of the catalytic decomposition effect of H_2O_2 on silver-based electrodes, the same effect was also studied on the gold-based electrodes. Metallic Au (99.9%) electrodes were polished using 0.3 and 0.05 μm alumina, and subsequently

rinsed with distilled water and sonicated for 5 min in order to clean the surfaces before the modification. Then, they were immersed in fresh $3.3 \cdot 10^{-2}$ M DBSA/ 0.1 M KCl solution for 3 hours. Au SPEs were directly dipped into the surfactant-based solution without any pre-treatment. Subsequently, H_2O_2 decomposition was analyzed by submerging the electrodes in 1 M H_2O_2 solution for 1 h. Mass differences were registered every minute and compared to the previously obtained decomposition data for silver-based electrodes. The data from the metallic Au and SPEs are presented in Fig. 4.10 and Fig. 4.11, respectively. All gold-based electrodes showed little differences in H_2O_2 decomposition rates before and after DBSA/KCl modification.
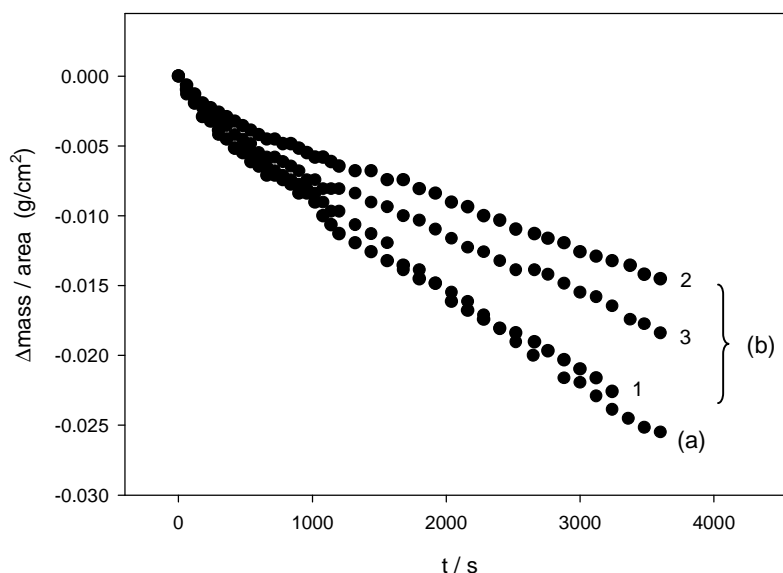
Figure 4.10. **Hydrogen peroxide decomposition rate for (a) unmodified and (b) modified metallic Au (99.9%) electrodes upon repeated exposure to 1 M H_2O_2 solution for 1 hour. The number of exposures is indicated besides each graph.**

Thus, unmodified metallic Au (99.9%) electrode showed a change in mass per unit area of 0.026 gcm^{-2} after a 1 h reaction in 1 M H_2O_2 whereas the same electrode after the modification showed only 0.023 gcm^{-2} for the first measurement. Subsequent exposures

resulted in changes of 0.015 and 0.018 gcm^{-2}, respectively. This indicated that the modification did not enhance the catalytic behaviour of this type of Au electrodes towards H_2O_2 decomposition. This supports the earlier finding in which there was little difference in the cathodic currents upon reduction of H_2O_2 before and after modification. Similarly, unmodified Au SPEs exhibited changes of 0.006 gcm^{-2} after H_2O_2 reaction whereas the modified ones showed 0.008 and 0.007 gcm^{-2} after the first and second exposure to H_2O_2, respectively.
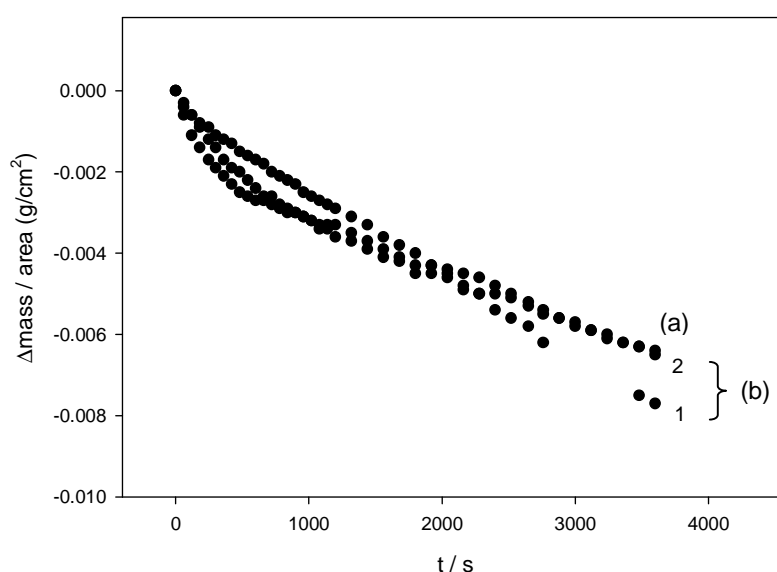
Figure 4.11. **Hydrogen peroxide decomposition rate for (a) unmodified and (b) modified Au SPEs after exposure to 1 M H_2O_2 solution for 1 hour. The number of exposure is indicated besides each graph.**

Both types of electrode did not exhibit improved catalytic effect on H_2O_2 decomposition after the modification or noticeable changes following repeated measurements. However, greater decomposition rates were obtained using the metallic Au (99.9%) electrodes compared to the Au SPEs, as was commented on before and which is shown in Fig. 4.12. This behaviour was already observed for the silver-based electrodes, where the rates of decomposition obtained for the metallic electrode were inherently greater than those obtained for the SPE or sterling (92.5%) Ag electrodes. In

that case, an approx. 20-fold greater rate of decomposition was obtained with the unmodified metallic 99.9% Ag electrode, reaching a total loss of 0.414 gcm[-2], whereas only 0.026 gcm[-2] was observed with the metallic Au electrode. These results were expected because Ag is a known catalyst of H_2O_2 decomposition whereas no similar behaviour has been reported for gold-based materials.
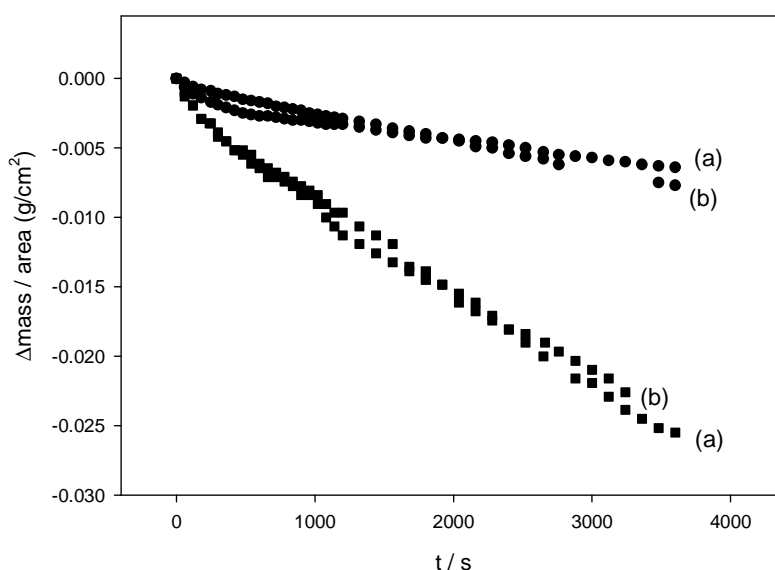
Figure 4.12. **Hydrogen peroxide decomposition rate for (a) unmodified and (b) modified (square) Au (99.9%) metallic electrodes and (circle) Au SPEs upon exposure to 1 M H_2O_2 solution for 1 hour. These data correspond to the first repetition of each electrode.**

4.2.3. Platinum-based electrodes

4.2.3.1. Electrochemical characterization

Platinum screen printed electrodes (Pt SPEs) from two different sources were modified following the same procedure as that used for Ag and Au SPE pre-treatment. After the modification in $3.3 \cdot 10^{-2}$ M DBSA/ 0.1 M KCl solution, amperometry was

performed and the cathodic currents obtained for $5 \cdot 10^{-3}$ M H_2O_2 are shown in Table 4.2. Pt is the best known catalyst for H_2O_2 reduction, and this fact is supported by the cathodic current data obtained even with unmodified Pt SPEs. Comparing the values obtained for the different metallic substrates before any modification, Pt SPEs yielded up to three orders of magnitude greater responses to H_2O_2 reduction than Au SPEs and up to two orders of magnitude greater than Ag SPEs, as is shown in Table 4.1 and 4.2. Thus, the cathodic current densities of the unmodified Pt SPE (Dropsens) at $5 \cdot 10^{-3}$ M H_2O_2 was $481.0 \cdot 10^{-6}$ Acm^{-2}, whereas the responses for Au AT and Ag SPEs were $0.7 \cdot 10^{-6}$ and $3.1 \cdot 10^{-6}$ Acm^{-2}, respectively.

Table 4.2. Cathodic current densities of Pt SPEs at $5 \cdot 10^{-3}$ M H_2O_2, –0.1 V vs Ag/AgCl, before and after DBSA/KCl treatment.

Electrode	Area (cm^2)	j_{unmod} (x10^6)/ (Acm^{-2})	j_{mod} (x10^6)/ (Acm^{-2})
Pt SPE (Dropsens)	0.126	481.0	956.3
Pt SPE (Dupont)	0.035	959.4	910.0

However, after DBSA/KCl modification, Ag SPEs achieved reduction current densities of $273.6 \cdot 10^{-6}$ Acm^{-2}, which is in the same order of magnitude to that of Pt SPEs, being $956.3 \cdot 10^{-6}$ Acm^{-2}; only a 3.5-fold difference. This showed the remarkable catalytic effect of DBSA/KCl modification on Ag SPEs compared to other metal-based electrodes. Thus, Pt showed little relative enhancement in H_2O_2 reduction after the surfactant-based pre-treatment, and gold-based electrodes only presented a moderate effect, as was shown earlier. Only silver-based electrodes, and particularly Ag SPEs, seemed to be highly improved by DBSA/KCl modification. Once again, it is worth noting the discrepancy between the two Pt inks, one where there was no enhancement and one where there was a two-fold enhancement after DBSA/KCl treatment. A possible explanation would be the use of different type of binders for the manufacture of the Pt

SPEs from the two different companies. This would reinforce the involvement of the ink binder in the catalytic process.

4.2.3.2. H_2O_2 decomposition

Despite the fact that Pt is a well known catalyst for H_2O_2 decomposition, Pt SPEs were modified with DBSA/KCl in order to analyze whether the catalytic effect observed with the silver-based electrodes was also exhibited by the Pt pastes. The electrodes were modified following the same procedure previously reported for Ag and Au SPEs and were subsequently immersed in 1 M H_2O_2 (2 ml) for 1 h. The results for the unmodified and modified substrates are presented in Fig. 4.13. Pt SPEs modified with the DBSA/KCl solution showed at least ten-fold greater rates of catalytic decomposition when they were exposed to 1 M H_2O_2 than those achieved for the unmodified substrates. Thus, changes in decomposition rate of 0.005 gcm^{-2} were registered by the unmodified electrodes whereas 0.046 gcm^{-2} were reported by the modified ones. Moreover, it seemed that the decomposition process was enhanced over time because the result obtained during the second measurement was significantly greater than that obtained during the first measurement, being 0.093 gcm^{-2} after 2 h in 1 M H_2O_2. This result, and the downward curvature of the decomposition rate curves suggests an accelerating decomposition upon exposure to the modification. This will be discussed further in the next section.

Comparing the data obtained for different metal SPEs, both Ag and Pt showed an enhancement in the H_2O_2 decomposition process after being treated with DBSA/KCl solutions. The decomposition rates after 1 hour reaction time were approx. 8 and 10 times higher than those obtained by the same unmodified Ag and Pt electrodes, respectively. However, Au SPEs did not show any enhancement from modification.
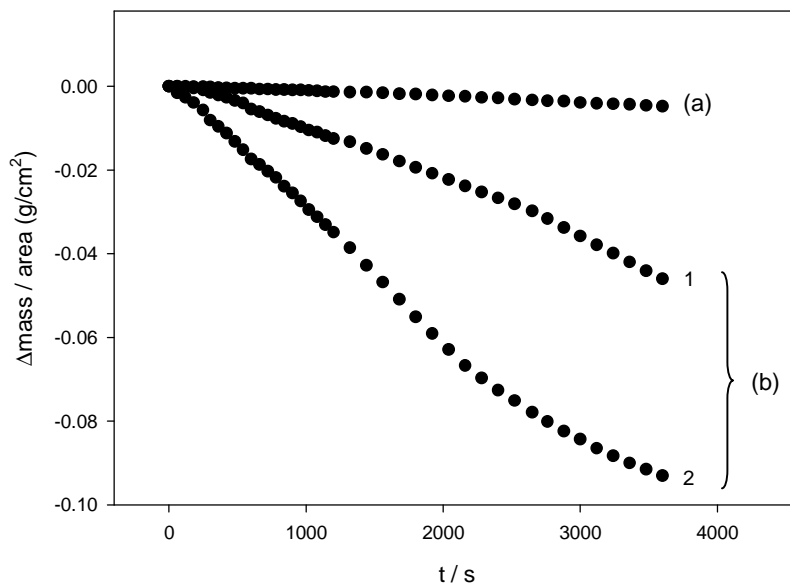
Figure 4.13. **Hydrogen peroxide decomposition rates for (a) unmodified and (b) modified Pt SPEs upon repeated exposure to 1 M H₂O₂ solution for 1 hour. The number of exposures is indicated besides each graph.**

4.2.4. Kinetic study of H_2O_2 decomposition on unmodified and DBSA/KCl modified metallic surfaces

As is well-known, a catalyst is a substance that participates in a chemical reaction by increasing the rate of that reaction. In order to compare the catalytic effect of the above-mentioned metallic electrodes on H_2O_2 decomposition before and after the modification process, apparent rate constants of the decomposition reactions were calculated.

The reaction rate is defined as the change in the advancement of the reaction with time, i.e. the change in the number of moles of a given species (reactant or product) with time:

$$R = \frac{1}{v_i} \frac{d[i]}{dt}$$

(Equation 4.1)

where R is the intensive reaction rate, v_i is related to the stoichiometric coefficient of species i and $[i]$ is the molarity of species i. The rate of a reaction will generally depend on the temperature, pressure and concentrations of species involved in the reaction as well as the phase or phases in which the reaction occurs. The empirical relationship between reactant concentrations and the rate of a chemical reaction is known as a rate law, and it is written as:

$$R = k \, [\text{A}]^{\alpha} \, [\text{B}]^{\beta} \ldots \qquad \text{(Equation 4.2)}$$

where $[\text{A}]$ is the concentration of reactant A, $[\text{B}]$ is the concentration of reactant B, and so forth. The constants α and β are the reaction orders with respect to A and B, respectively, and k is referred to as the rate constant for the reaction. The rate constant is independent of concentration, but dependent on pressure and temperature.[9]

The apparent rate constant of H_2O_2 decomposition was determined by measuring the mass of O_2 liberated as a function of time at room temperature. The mass data were rearranged to be expressed as the H_2O_2 concentration remaining in the vial versus time to study the kinetics of the reaction. There are many studies in the literature about H_2O_2 decomposition and the effect of transitions metals as catalysts but still no definitive understanding of the true mechanism involved has been reported. It has been shown that catalytic decomposition of H_2O_2 by ferric ions in solution can be first or second order[10, 11] with respect to the peroxide concentration whereas supported metal catalysts decompose H_2O_2 by first order kinetics.[12-15] Assuming that H_2O_2 decomposition followed pseudo first-order kinetics in the present work:

$$-\frac{d[H_2O_2]}{dt} = k_{app}[H_2O_2] \qquad \text{(Equation 4.3)}$$

and thus,

$$\ln\frac{[H_2O_2]_t}{[H_2O_2]_0} = -k_{app}t \qquad \text{(Equation 4.4)}$$

where k_{app} is the apparent first-order H_2O_2 decomposition rate constant, and $[H_2O_2]_t$ and $[H_2O_2]_0$ are the concentrations of H_2O_2 in the solution at time t and time zero, respectively. The data from Ag SPEs before and after modification with DBSA/KCl are shown in Fig. 4.14.
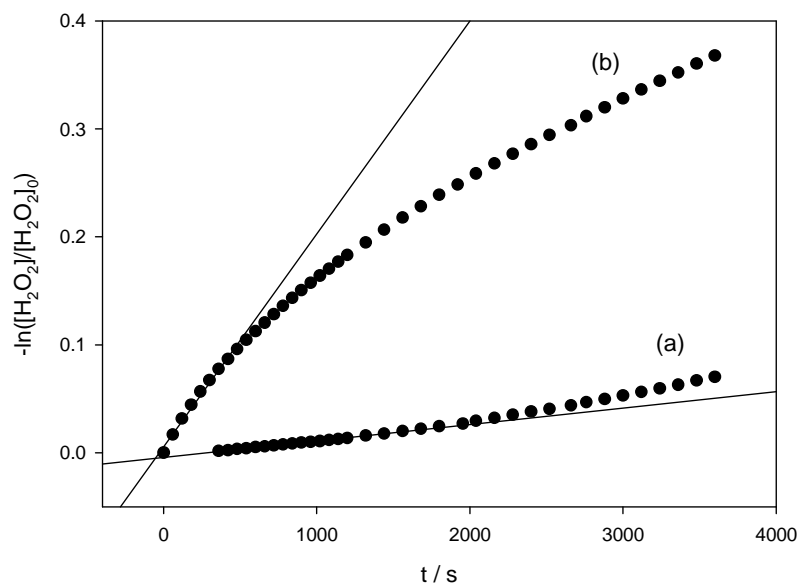
Figure 4.14. **Plot -ln $[H_2O_2]/[H_2O_2]_0$ versus time for (a) unmodified and (b) modified Ag SPEs after exposure to 1 M H_2O_2 solution for 1 hour.**

As was mentioned above, the data appears to be linear during the first ten minutes, after which it deviates from linearity. This observation could be as a result of the formation of a diffusion layer at the surface, which could become a limitation of the reaction, or as a result of bulk substrate limitation (mass transport) because the trapping of O_2 as air bubbles and its dissolution in the water. As the measurements with the unmodified and modified Ag SPEs were performed in a vial containing 2 ml 1 M H_2O_2, the maximum mass of O_2 which could be released was 0.034 g. After 1 hour reaction time, the difference of mass observed with the modified electrode was approx. 0.010, which meant that almost a third of the H_2O_2 in the solution had been decomposed. The rapid decomposition of H_2O_2 in the vicinity of the electrode surface could result in the

shape observed in the plots as H_2O_2 does not diffuse as fast towards the surface as it decomposes. Changes or losses of the surface catalytic activity over time could also lead to deviations from the linear behaviour. More precise and detailed determination of the heterogeneous rate constant would require treatment of the diffusion processes at the heterogeneous interface. For simplicity, however, further analysis was based on initial constants using the initial linear portion of the responses. Initial rates for Ag SPEs are shown in Fig. 4.15.
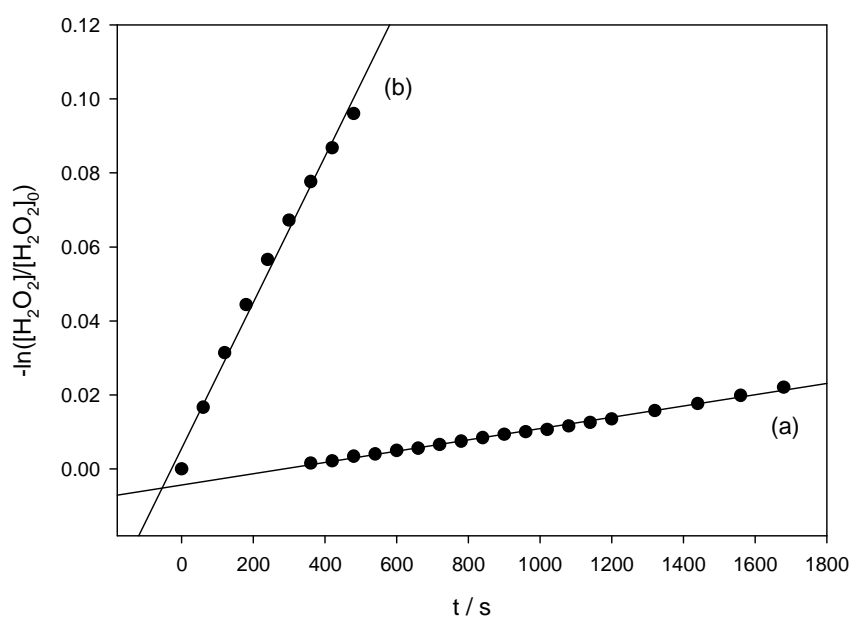
Figure 4.15. **Kinetics of H_2O_2 decomposition on (a) unmodified and (b) modified Ag SPEs.**

The same study was carried out using 92.5% and 99.9% Ag as well as SPE and metallic Au electrodes and Pt SPE. The apparent rate constants obtained with each electrode are summarized in Table 4.3. The apparent initial H_2O_2 decomposition rate constants obtained for Ag SPEs after the modification with DBSA/KCl were ten times (for the first measurement, R1), four times (for the second, R2 and third repeats, R3) higher than those obtained for the same electrodes without any modification,

respectively. Thus, apparent rate constants of 1.52, 2.96 and 1.41 s^{-1} were obtained by the unmodified Ag SPEs after the first, second and third exposures to 1 M H_2O_2, respectively whereas 19.7, 8.12 and 4.11 s^{-1} were obtained by the modified electrodes under the same measurement conditions. The decrease in the catalytic responses observed for the modified electrodes as a function of the number of repeat exposures might be explained as a result of the progressive loss of the surface modification or surface inactivation (loss of catalytic activity) with time, even though, H_2O_2 decomposition was up to four times faster than the same process carried out on the unmodified electrodes.

Table 4.3. Apparent initial rate constants k_{app} for H_2O_2 decomposition on different metallic catalysts following multiple repeat exposures (R1 to R3).

		Ag			Au		Pt
		SPE (A=0.126cm^2)	92.5% (A=0.6cm^2)	99.9% (A=0.031cm^2)	SPE (A=0.1cm^2)	99.9% (A=0.031cm^2)	SPE (A=0.1cm^2)
Unmod. k_{app} (x10^{-5} s^{-1})	R1	1.52	0.68	1.04	0.40	0.05	0.43
	R2	2.96	2.94	1.06	--	--	--
	R3	1.41	5.66	--	--	--	--
DBSA/KCl k_{app} (x10^{-5} s^{-1})	R1	19.70	29.2	1.08	0.64	0.04	3.91
	R2	8.12	53.7	0.97	1.20/5.2	0.03	9.95
	R3	4.11	57.8	--	--	0.03	--

R1 – repeat 1; R2 – repeat 2; R3 – repeat 3

More remarkable is the catalytic effect observed on the sterling (92.5%) Ag electrodes after the modification. The unmodified electrode showed some increase in decomposition rate following repeat exposure to substrate. Thus, this electrode exhibited an initial rate constant of 0.68 s^{-1} for the first measurement and 2.94 and 5.66 s^{-1} for the second and third exposures to 1 M H_2O_2, respectively. A similar growth trend was also observed for the modified electrodes, although in this case the apparent rate constants were thirty times higher than those obtained with the unmodified electrodes, being 29.2, 53.7 and 57.8 s^{-1} respectively. Unlike the SPEs and the 92.5% Ag electrodes, no differences in the kinetic data were observed with 99.9% Ag electrodes before and after

the modification. Apparent rate constants of 1.04 and 1.06 s^{-1} were obtained from the unmodified electrodes after the first and second exposures to H_2O_2, respectively, whereas 1.08 and 0.97 s^{-1} were obtained for the modified electrodes. The apparent rate constant for the unmodified electrode was approx. the same order of magnitude as that obtained from the unmodified SPE and 92.5% Ag and this did not change after exposure to the DBSA/KCl solution. With regard to the gold-based electrodes, they did not show any enhancement on H_2O_2 decomposition after DBSA/KCl modification. Moreover, the apparent rate constants obtained using metallic 99.9% Au electrodes (0.05 s^{-1}) were quite low relative to those exhibited by Ag electrodes. This agrees with the fact that silver is a known catalyst for H_2O_2 decomposition[13] whereas no similar data have been reported for Au. On the other hand, Pt SPEs also showed a catalytic enhancement to H_2O_2 decomposition after their treatment with DBSA/KCl, leading to a ten-fold greater k_{app} on the modified surfaces relative to the same unmodified substrates.

To more accurately compare the catalytic activity of the different metallic substrates, the apparent rate constants must be normalized to the surface area of the catalysts and the volume of the solution used. Therefore, the heterogeneous rate constant can be expressed as:

$$k_s \text{ (cm s}^{-1}) = V_{liq}k_{app}/A_{cat} \qquad \text{(Equation 4.5)}$$

where V_{liq} is the volume of solution (in ml), and A_{cat} the surface area of the catalyst (cm^2).[14, 16]

The heterogeneous rate constants of the studied metallic substrates are reported in Table 4.4. Unmodified metallic 99.9% Ag showed the highest heterogeneous rate constant for H_2O_2 decomposition and this did not change after its treatment with DBSA/KCl. Unlike metallic 99.9% Ag, SPE and sterling 92.5% Ag electrodes improved their H_2O_2 decomposition responses for the first repeat by over 10 and 40 times, respectively, following exposure to the modification solution. Similar enhancement was achieved with the Pt SPEs after being modified with DBSA/KCl.

Table 4.4. Heterogeneous rate constants k_s for H_2O_2 decomposition on different metallic catalysts.

		Ag			Au		Pt
		SPE (A=0.126cm²) V_{liq}=2ml	**92.5%** (A=0.6cm²) V_{liq}=2ml	**99.9%** (A=0.031cm²) V_{liq}=27ml	**SPE** (A=0.1cm²) V_{liq}=2ml	**Metallic** (A=0.031cm²) V_{liq}=27ml	**SPE** (A=0.1cm²) V_{liq}=2ml
Unmod. k_s (x10⁻⁴ cm·s⁻¹)	R1	2.4	0.2	90.0	0.8	4.3	0.9
	R2	4.7	1.0	92.0	--	--	--
	R3	2.2	1.9	--	--	--	--
DBSA/KCl k_s (x10⁻⁴ cm·s⁻¹)	R1	31.0	9.7	94.0	1.3	3.9	7.8
	R2	13.0	18.0	84.0	2.4/1.0	2.2	20.0
	R3	6.5	19.0	--	--	2.7	--

R1 – repeat 1; R2 – repeat 2; R3 – repeat 3

The heterogeneous rate constant values obtained with unmodified gold-based electrodes were close to those shown by the other metallic electrodes under study, except for metallic 99.9% Ag. However, no improvements were observed after the surfactant-based modification, as is shown by no change in the heterogeneous rate constants before and after the modification. The overall data from the unmodified electrodes were of the same order of magnitude than those previously reported.[14]

4.2.5. Further insights in the decomposition process

The decomposition of H_2O_2 in the presence of catalysts has been widely investigated and many mechanisms have been proposed. The first explanation for the decomposition of H_2O_2 was given by Haber and Weiss based on a radical mechanism.[17] Since then, several mechanisms have been proposed for this reaction. Many of them are based on a cyclic electron-transfer process, which is initiated by either the transfer of an electron from a reduced site on the surface of the catalyst to the peroxide to yield an OH˙ radical or the transfer of an electron from the peroxide to an oxidized site on the surface of the catalyst, to produce an HO₂˙ radical. The reactions might be:[16]

$$cat(red) + HO_{2(ads)}^{-} + H_2O \rightarrow 2OH^- + OH^{\cdot} + cat\ (ox) \qquad \text{(reaction 4.1)}$$

and

$$cat(ox) + HO_2^- \rightarrow HO_2^{\cdot} + cat(red) \qquad \text{(reaction 4.2)}$$
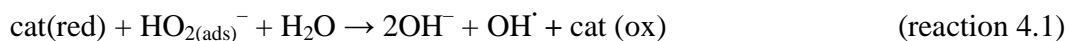
Thus, a more recent mechanism for the decomposition of H_2O_2 catalyzed by a Co(II)-silica-based catalyst and considering that both ions and free radicals may be involved simultaneously in the process was:[11, 12]

$$H_2O_2 \rightleftarrows O_2H^- + H^+ \quad \textit{(fast)} \qquad \text{(reaction 4.3)}$$

$$cat\text{-}H_2O + O_2H^- \rightleftarrows cat\text{-}O_2H^- + H_2O \quad \textit{(fast)} \qquad \text{(reaction 4.4)}$$

$$cat\text{-}O_2H^- \leftrightarrow \text{intermediate product (active species)} \quad \textit{(slow)}$$

$$\rightleftarrows cat + 2OH^- + O_2 \quad \textit{(fast)} \qquad \text{(reaction 4.5)}$$

$$2OH^- + 2H^+ \rightleftarrows 2H_2O \quad \textit{(fast)} \qquad \text{(reaction 4.6)}$$

$$Cat + H_2O \rightleftarrows cat\text{-}H_2O \quad \textit{(fast)} \qquad \text{(reaction 4.7)}$$
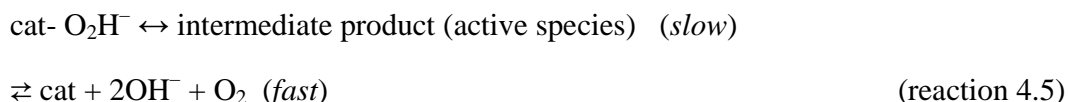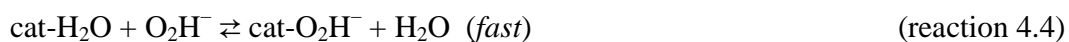
Silver has already been proven to be a catalyst for the decomposition of H_2O_2, as has been shown in this chapter and also reported in the literature.[18-20] From Chapter 3, the DBSA/KCl modification of Ag SPEs led to an enhancement in the electrochemical reduction and decomposition of H_2O_2. The formation of lamellar structures in the surfactant/salt solution and its subsequent interaction to the electrode surface was assessed. A possible explanation proposed was that the modification structures created on the surface brought about the formation or stabilization of OH_{ads} or OH radical, generally implicated in the electrochemical reduction. This might also be an explanation for the decomposition process as OH radical is a typical intermediate of the reaction, as was reported above. Moreover, the electrodes seemed less affected as catalysts after the electrochemical reduction than after the decomposition. Besides the difference in H_2O_2 concentrations employed, this might be related to the possible regeneration of Ag(0)

during the amperometric process due to the cathodic potential applied (–0.1 V vs. Ag/AgCl) whereas such a possibility would not exist for the decomposition process.

In this chapter, several metallic-based electrodes were evaluated in order to further understand the nature of the modification process. With regard to the electrochemical reduction, all the SPEs except the Pt from Dupont showed an increase in the catalysis after the DBSA/KCl treatment. Pt and Au SPEs exhibited enhancements from 2 to 10 times in their cathodic currents after modification, whereas Ag SPEs presented more than 90-fold higher reduction currents. This reinforces the possible implication of the ink binder in the formation of the catalytic surfaces. The differences in the modification between the SPEs might be attributed to differences in the nature of the binder. On metallic electrodes in the absence of a binder, the presence of defects on the surface might be associated with the formation of catalytic structures, as was observed on the Ag 92.5% electrode surface. These electrodes showed a small improvement in the electroreduction process but the greatest increase in the decomposition process, with almost 50-fold higher heterogeneous rate constant for the first repeat after the modification. Unlike the SPEs, pure metallic electrodes (99.9% Au and Ag) did not show any enhancement in the decomposition after the modification. Once again this supports the involvement of the binder in the surfactant/salt modification.

The fact that the 92.5% Ag electrodes showed such an enhancement in the decomposition might be related to the presence of defects and higher amounts of Ag available for the decomposition. Thus, the surfactant/salt modification might be related not only to the binder present in the printable inks but also with the presence of rougher surfaces or edge defects, which would favour the deposition/interaction of the lamellar structures with those surfaces.

To sum up, electrodes that showed an increase in the catalytic activity of the electrochemical reduction of H_2O_2 also exhibited an increase in the decomposition process. Therefore, both mechanisms seemed to be connected. However, the level of enhancement is not proportional for both processes. Thus, modified Ag SPEs presented the highest increase in the electrochemical reduction (approx. 90 times) whereas the heterogeneous rate constant was only 13-fold higher for the decomposition. However, 92.5% Ag did not show a significant improvement in the cathodic currents whereas it

exhibited the best enhancement in the decomposition. Further studies should be performed to fully understand the implication of the binder and the surface defects on the surface modification as well as the nature of the modification itself.

With regard to future work, Ag SPEs were shown to be the best substrates for the fabrication of further devices based on the electrochemical reduction of H_2O_2, because they provide high cathodic currents without the interferences of the decomposition process. Unmodified Pt SPEs provided the highest currents for H_2O_2 reduction; however, modified Ag SPEs led to responses in the same order of magnitude and Ag is known to be a much lower cost material than Pt. Therefore, DBSA/KCl modified Ag SPEs will be used as platforms for the development of a glucose biosensor in the following chapters.

4.3. CONCLUSIONS

In the previous chapter, the surfactant/salt modification of Ag SPEs exhibited a remarkable enhancement on the electrochemical reduction of H_2O_2. A $3.3 \cdot 10^{-2}$ M DBSA/0.1 M KCl solution was shown to provide the highest improvement on H_2O_2 catalysis. The effect of such a surfactant/salt modification solution on other metallic electrodes and their catalytic activity towards the electrochemical H_2O_2 reduction has been studied in the present chapter. Little enhancement in the reduction currents were observed with other DBSA/KCl Ag-based electrodes (metallic Ag (99.9%), sterling Ag (92.5%)) and Pt-based electrodes, compared to the unmodified ones. On the contrary, some Au SPEs presented an increase in the catalytic responses after the modification, although it was not as notable as that observed at Ag SPEs.

As with Ag SPEs, the modification also seemed to induce an enhancement on H_2O_2 decomposition on several other metallic-based electrodes. The greater differences of mass due to the release of O_2 during H_2O_2 decomposition after the electrodes were treated with DBSA/KCl showed the surfactant-based solution produced an improvement in the catalytic process. Such an enhancement was proven by the increase of the heterogeneous rate constants obtained after the kinetics study carried out on both

unmodified and modified electrodes. It showed that DBSA/KCl modification on the metallic surfaces provided an easier mechanism for H_2O_2 decomposition. On the other hand, Au and Pt substrates did not show so high catalytic effect on both electrochemical H_2O_2 reduction and H_2O_2 decomposition after DBSA/KCl modification as Ag electrodes.

4.4. REFERENCES

1. W. Lian, L. Wang, Y. Song, H. Yuan, S. Zhao, P. Li and L. Chen, *Electrochimica Acta*, 2009, **54**, 4334-4339.
2. A. A. Karyakin, E. A. Puganova, I. A. Budashov, I. N. Kurochkin, E. E. Karyakina, V. A. Levchenko, V. N. Matveyenko and S. D. Varfolomeyev, *Analytical Chemistry*, 2003, **76**, 474-478.
3. R. Raymond & Co and S. distributor, Editon edn., Electrodag PF-410 product specification, vol. 20-01-2011.
4. S. C. Hung, Y. L. Wang, B. Hicks, S. J. Pearton, D. M. Dennis, F. Ren, J. W. Johnson, P. Rajagopal, J. C. Roberts, E. L. Piner, K. J. Linthicum and G. C. Chi, *Applied Physics Letters*, 2008, **92**, 193903-193903.
5. K. Grennan, A. J. Killard and M. R. Smyth, *Electroanalysis*, 2001, **13**, 745-750.
6. DropSens, Editon edn., 2011, vol. 06-02-2011.
7. W. M. Haynes, *Handbook of Chemistry and Physics*, 91st edn., CRC Press, Taylor & Francis group, US, 2010-2011.
8. R. Zeis, T. Lei, K. Sieradzki, J. Snyder and J. Erlebacher, *Journal of Catalysis*, 2008, **253**, 132-138.
9. T. Engel and P. Reid, *Physical Chemistry*, 2006.
10. Z. M. Galbacs and L. J. Csanyi, *Journal of the Chemical Society, Dalton Transactions*, 1983, 2353-2357.
11. S. F. Oliveira, J. P. Espinola, W. E. S. Lemus, A. G. de Souza and C. Airoldi, *Colloids and Surfaces A: Physicochemical and Engineering Aspects*, 1998, **136**, 151-154.
12. R. F. de Farias, A. S. Gonçalves and C. Airoldi, *Journal of Colloid and Interface Science*, 2002, **247**, 159-161.
13. N. Kitajima, S. Fukuzumi and Y. Ono, *The Journal of Physical Chemistry*, 1978, **82**, 1505-1509.
14. R. Venkatachalapathy, G. P. Davila and J. Prakash, *Electrochemistry Communications*, 1999, **1**, 614-617.
15. Y. Ono, T. Matsumura, N. Kitajima and S. Fukuzumi, *The Journal of Physical Chemistry*, 1977, **81**, 1307-1311.
16. H. Falcon and R. E. Carbonio, *Journal of Electroanalytical Chemistry*, 1992, **339**, 69-83.
17. F. Haber and J. Weiss, *Proceedings of the Royal Society of London. Series A, Mathematical and Physical Sciences*, 1934, **147**, 332-351.
18. S. M. Joksimovic-Tjapkin and D. Delic, *Ind. Eng. Chem. Fundam.*, 1973, **12**, 33-39.
19. F. T. Maggs and D. Sutton, *Transactions of the Faraday Society*, 1958, **54**, 1861-1870.
20. F. T. Maggs and D. Sutton, *Transactions of the Faraday Society*, 1959, **55**, 974-980.

Chapter 5

Application of modified silver paste electrodes to the development of a glucose biosensor

5.1. INTRODUCTION

Electrochemical biosensors are self-contained integrated devices, which are capable of providing specific quantitative or semi-quantitative analytical information using a biological recognition element (biochemical receptor) which is retained in direct spatial contact with an electrochemical transduction element.[1] Although many different transducer types have been used in biosensor fabrication, such as optical, piezoelectric, thermal or electrochemical, the latter has been the most commercially successful because of its suitable sensitivity, reproducibility and mass production capability at low cost.[2]

Glucose biosensors alone account for about 85% of the entire biosensor market, which has recently been estimated to be worth around \$5 billion.[2, 3] The reason for such a high percentage lies in their leading role in diabetes monitoring. Diabetes is a metabolic disorder as a result of insulin deficiency and hyperglycemia and is reflected by blood glucose concentrations higher or lower than the normal range (4.4-6.6·10^{-3} M).[3] It is estimated that over 170 million people suffer from diabetes worldwide and it is a leading cause of mortality.[2] Therefore, the diagnosis and management of diabetes is vital and requires robust and consistent glycemic control. Since the fabrication of the first glucose enzyme electrode by Clark and Lyons in 1962,[4] many research activities have been focused on the development of reliable devices for diabetes control. The most commonly used enzyme in the design of glucose biosensors is glucose oxidase (GOx), which contains redox groups that change redox state during the biochemical reaction. GOx is a homodimer flavoprotein containing two active sites per molecule. GOx acts by oxidising glucose to gluconolactone, accepting electrons in the process and thereby changing to an inactivated state. The enzyme is normally returned to the active oxidised state by transferring these electrons to molecular oxygen, resulting in the production of hydrogen peroxide (H_2O_2), as is shown in equation 1:[2, 5]

$$\text{Glucose} + O_2 \xrightarrow{\text{GOx}} \text{Gluconic acid} + H_2O_2 \qquad (1)$$
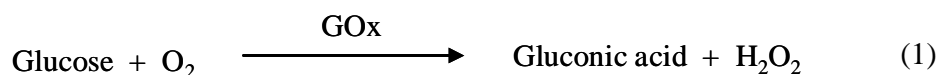
Therefore, the construction of amperometric glucose biosensors can rely on monitoring either the depletion of oxygen or the production of H_2O_2. The first commercial device consisted on a thin layer of GOx entrapped over an oxygen electrode (via a semi-permeable dialysis membrane) to screen the oxygen consumed by the enzyme-catalyzed reaction.[2, 6] However, direct measurements of oxygen were subject to errors due to fluctuations in the oxygen tension. Two oxygen working electrodes were required to correct the oxygen background variation in samples by measuring differential currents.[6, 7] Further investigations led to the determination of blood glucose based on electrochemical monitoring of the liberated H_2O_2. This could be measured at a potential of approx. +0.7 V (vs Ag/AgCl), when a Pt working electrode was used.[2, 8] Wingard et al.[9, 10] developed a potentiometric glucose biosensor by immobilizing GOx directly on a Pt electrode and using Ag/AgCl as a reference electrode. However, the amperometric measurement of H_2O_2 requires application of a potential at which species, such as ascorbic acid, uric acids or acetaminophen are also electroactive. Several membranes such as poly(phenylenediamine), polypyrrole, Nafion or cellulose acetate have been used to discriminate against coexisting electroactive compounds.[6] More recently, mediators such as ferrocene derivatives, ferricyanide, conducting organic salts or quinine compounds have been successfully utilised for the fabrication of commercial glucose biosensors. They shuttle electrons from the redox center of the enzyme to the electrode surface, replacing the oxygen as the electron acceptor for the enzymatic reaction.[2, 6, 11] Simultaneously, mediators decrease the applied electrode potential of the sensor, eliminating possible electroactive interferences such as ascorbic acid.[8] Thus, Cass et al.[12] reported the development of a ferrocene-mediated biosensor for the amperometric determination of glucose. Unlike previous reports, the mediator was incorporated into the graphite electrode together with the GOx, which facilitated the electron transfer between the enzyme and the ferricinium ion. More recently, Miao et al.[13] developed a glucose biosensor by immobilising GOx and ferrocene as a mediator onto a carbon paste electrode by means of a double chitosan film. Ghica and Brett[14] reported the fabrication of an amperometric enzyme electrode sensitive to glucose, where the enzyme was cross-linked with glutaraldehyde and immobilized together with

the redox mediator, methyl viologen, with a Nafion film. The calibration curves for the sensor were performed at -0.5 V (vs. Ag/AgCl).

Commercial blood glucose self-testing meters generally rely on the use of ferrocene or ferrricyanide as mediators. However, most *in vivo* devices are mediatorless due to potential leaching and toxicity of the mediator.[6] Besides that, mediator systems are unsuitable for detection of low glucose concentrations because of high noise current (ferrocene primary oxidation).[15] Other developments have focused on the electrocatalytic reduction of the liberated H_2O_2 which has allowed shifting the detection potential to the optimal region (0.0 to –0.2 V vs. Ag/AgCl) where most unwanted reactions are negligible.[6] Karyakin et al.[15] reported the fabrication of an amperometric glucose biosensor based on a PB-modified glassy carbon electrode. The glucose detection was carried out at 0.18 V (vs. Ag/AgCl). Zhu et al.[16] developed a glucose biosensor by means of a PB nanoparticle and multiwall carbon nanotubes (PB/MWNTs) composite deposited on a glassy carbon electrode. GOx was then immobilized on the PB/MWNTs platform by an electrochemically polymerized o-phenylenediamine (OPD) film and the resulting biosensor was applied for glucose determination at 0 V (vs. Ag/AgCl).

Several materials have been used as electrode substrates in the fabrication of glucose biosensors based on GOx, such as Pt,[9, 17] glassy carbon (GC),[16, 18] ITO-glass[19] and carbon fibers.[20] These materials have been previously modified with metal nanoparticles,[17, 18, 21] multiwall carbon nanotubes,[18] PB[15, 22] and so on before enzyme immobilization to improve their catalytic activity towards glucose determination. For example, Salimi et al.[23] reported the fabrication of a glucose biosensor by co-deposition of GOx and nickel-oxide (NiO) nanoparticles onto a glassy carbon electrode. The so-fabricated biosensor showed excellent bioelectrocatalytic activity of immobilized enzyme towards glucose oxidation when ferrocenmethanol was used as an artificial redox mediator. Yin et al.[24] developed a glucose biosensor based on layer-by-layer (LBL) self-assembling of chitosan and GOx on a PB-modified gold electrode. Glucose determination was then performed by amperometry at approx. –0.05 V (vs. Ag/AgCl). Luque et al.[25] fabricated a glucose biosensor based on a carbon nanotube paste electrode

modified with GOx and metallic particles such as cupper and iridium. The working potential of the so-formed biosensor was –0.1 V (vs. Ag/AgCl).

The need for inexpensive and reproducible methods for the mass manufacture of blood glucose devices for home testing has led to the widespread use of a single technique, namely screen printing.[2, 26-28] Screen printing has made low cost, large scale biosensor production possible, thanks to the precision, speed and scalability of the method.[19] The majority of personal blood glucose monitors rely on disposable screen printed enzyme electrode test strips. The screen printing technology involves printing patterns of conductors, insulators and active biological and non-biological reagents onto the surface of planar solid (plastic or ceramic) substrates based on pressing the corresponding inks through a patterned mask.[3] Vaughan et al.[29] determined acetaminophen (paracetamol) in whole blood by means of a disposable, single use, screen-printed dry-strip. The working electrode was printed as an aqueous carbon-based paste incorporating aryl acylamidase, enzyme responsible of the hydrolysis of acetaminophen to form 4-aminophenol. The latter was amperometrically detected by oxidation at the working electrode. Wang and Zhang[30] developed a disposable glucose biosensor based on the dispersion of cupric-hexacyanoferrate and GOx within a screen-printable carbon ink. The use of cupric-hexacyanoferrate as a catalyst permited H_2O_2 detection at applied potential around –0.1 V (vs. Ag/AgCl) as well as a stable response at physiological pH (7.4). The dispersion of both the enzyme and the catalyst within the ink resulted in a one-step fabrication, simplifying greatly the sensor fabrication. More recently, Gonzalo-Ruiz et al.[31] employed a carbon screen printed electrode as a platform for the fabrication of an amperometric biosensor for glucose determination in grape juice. GOx and horseradish peroxidise (HRP) were coimmobilized onto the electrode by cross-linking with glutaraldehyde (GA). Amperometry at –0.1 V (vs Ag/AgCl) was carried out in the presence of ferrocyanide as a mediator in the enzymatic reaction of HRP and H_2O_2. Kotzian et al.[32] developed a glucose biosensor using a modified carbon screen printed electrode as a substrate. The carbon ink was initially mixed with RhO_2 and then screen printed onto ceramic supports. After drying, GOx solution was pre-mixed with Nafion and directly applied onto the electrodes for enzyme immobilization. The biosensor worked at applied potential of –0.2 V (vs Ag/AgCl), where contributions

from other interfering species was neglected and was investigated as a glucose detector in flow injection analysis. It should also be noted that the development of glucose biosensors using GOx are an excellent surrogate to establish operational proof of concept that can be applicable to a wide range of other oxidase-based biosensor systems.

The most critical point in fabricating a biosensor is to achieve a working architecture, i.e. a favourable immobilization of the enzyme on the device which allows good communication between enzyme and electrode. The four main approaches to enzyme immobilization are: (a) adsorption; (b) gel entrapment; (c) covalent coupling and (d) cross-linking.[8, 33] It is worth noting that some systems did not truly immobilise the enzyme as it becomes free when solvated with the blood sample. The choice of the specific method partly defines the operational characteristics of the biosensor. Adsorption is a very simple process and rarely leads to loss of enzyme activity but changes of pH, ionic strength and temperature may detach the enzyme. Cross-linking is also a simple procedure that provides a strong chemical binding of the enzyme. However, enzymatic activity may be diminished by chemical alterations of the catalytically active sites of the protein.[8] In covalent bonding, the mass and activity of the immobilized enzyme can be quite carefully controlled by strong chemical bonds, leading to highly stable devices. Nevertheless, that technique may bring about a decrease in the overall activity of the biomolecule due to blockage of active sites by chemical bonds or misorientation of the enzyme. Entrapment in a polymeric film allows the biomolecules to keep as close to their native state as possible since they do not undergo covalent attachements.[34] The type of immobilization process will have a key impact on many characteristics of the biosensor, such as sensitivity, selectivity, stability, analytical range and response time, i.e. the feasibility of the device.

In the present work, a mediatorless glucose biosensor was created based on the novel electrocatalytic materials developed in Chapters 3 and 4. This was fabricated by the immobilization of GOx onto the DBSA/KCl modified silver screen printed electrodes (Ag SPEs). Possible interferences of the enzyme/glucose interaction in the catalytic activity of the sensor to H_2O_2 reduction were identified and several membranes were assessed to overcome these drawbacks. Other immobilization parameters were

optimized and LOD, sensitivity and reproducibility of the biosensor were evaluated. Scanning Electron Microscopy was performed to characterize the electrode surface.

5.2. RESULTS AND DISCUSSION

As was mentioned earlier, most of the enzymatic glucose biosensors in the literature are fabricated by immobilizing the enzyme GOx onto the electrode surface by means of several techniques. GOx catalyses the oxidation of β–D-glucose to gluconic acid, with the simultaneous reduction of oxygen to H_2O_2. Therefore, good catalysts for H_2O_2 detection are generally used as platforms in the production of glucose biosensors which exploit H_2O_2 as the detected species. The catalytic enhancement of DBSA/KCl modified Ag SPEs to H_2O_2 sensing led to a feasibility study of such a material for biosensor fabrication. An analysis of the compatibility of the electrode material with the glucose biosensing mechanism was thus required before enzyme immobilization.

5.2.1. Preliminary solution-phase assay evaluation

The DBSA/KCl modified Ag SPEs were initially evaluated as a glucose biosensor by performing glucose determination using the enzyme in solution. Time-based amperometry was performed at –0.1 V (vs Ag/AgCl) in PBS pH 6.8, in the presence or absence of GOx in solution. Initially, the electrode was measured in buffer in the absence of enzyme. In order to first evaluate the electrode's catalytic activity towards H_2O_2 reduction, the final H_2O_2 concentration in the solution ranged from $1 \cdot 10^{-3}$ to $5 \cdot 10^{-3}$ M. Subsequently, the electrode was placed in a cell with 2 ml of a stirred solution containing 1 mg/ml GOx to which glucose was added to final concentrations from 0 to $5 \cdot 10^{-3}$ M. Finally, the catalytic activity of the electrode to H_2O_2 reduction was again measured in the absence of enzyme and compared to the initial results (Fig. 5.1). As can be seen, the modified electrode before glucose sensing showed cathodic currents of approx. $3.5 \cdot 10^{-5}$ A in the presence of $5 \cdot 10^{-3}$ M H_2O_2 whereas the current obtained after glucose sensing only reached approx. $1.9 \cdot 10^{-5}$ A. Such current is similar to that exhibited by the same electrode for $5 \cdot 10^{-3}$ M glucose in the presence of GOx in solution, $1.6 \cdot 10^{-5}$ A. That was expected as the stoichiometry of the reaction is 1:1 for glucose: H_2O_2.
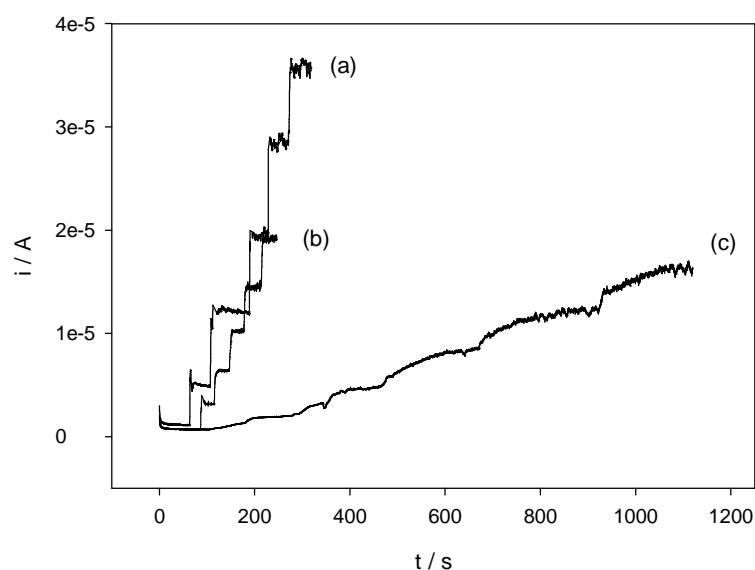
Figure 5.1. **Amperometric responses of a DBSA/KCl modified Ag SPE measured at –0.1 V (vs Ag/AgCl) in PBS pH 6.8: (a) before, and (b) after glucose sensing, at H_2O_2 concentrations from 1 to $5 \cdot 10^{-3}$ M; and (c) glucose sensing with 1 mg/ml GOx in solution, at glucose concentration from 1 to $5 \cdot 10^{-3}$ M.**

Thus, the catalytic activity of the electrode was significantly reduced following glucose determination, resulting in a halving of the catalytic response to H_2O_2. Moreover, the steady state background current exhibited by the modified electrode prior to glucose sensing (approx. $1.13 \cdot 10^{-6}$ A) was also higher than that shown by the same electrode after the enzymatic reaction (approx. $6.9 \cdot 10^{-7}$ A). As was already observed in Chapter 3, the background current from the amperometric responses appeared to be related to the modification of the Ag SPEs by DBSA/KCl. Thus, a decrease in the steady state background might be related to some change or loss in the DBSA/KCl modification from the electrode surface after glucose determination.

In order to prove whether the decrease in the cathodic current was due to the presence of the enzyme in the solution or to the glucose sensing process itself, the catalytic activity to H_2O_2 reduction was assessed in the presence and absence of the

enzyme in the bulk solution. The corresponding amperometric responses are shown in Fig. 5.2.
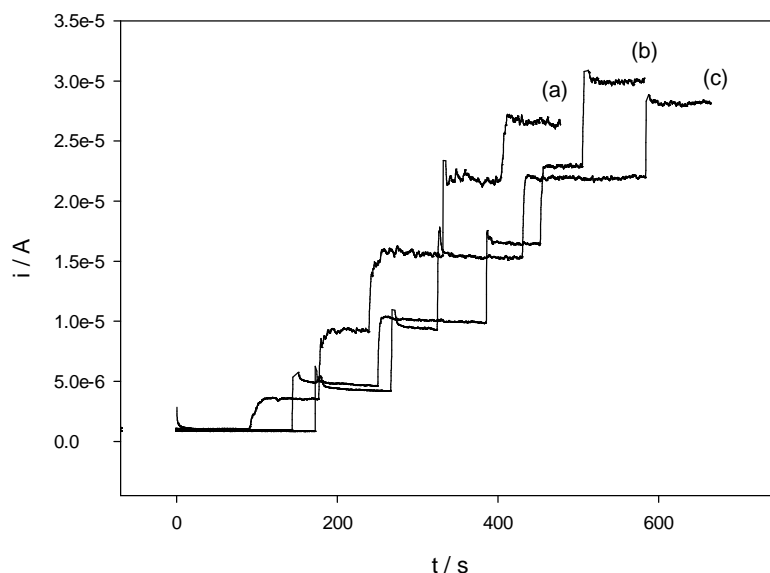
Figure 5.2. **Amperometry of a DBSA/KCl modified Ag SPEs measured at –0.1 V (vs Ag/AgCl) in PBS pH 6.8: (a) prior to exposure to enzyme; (b) in the presence of 1 mg/ml GOx and (c) following exposure to enzyme at H_2O_2 concentrations from 1 to $5 \cdot 10^{-3}$ M.**

As can be observed, the presence of GOx in solution did not seem to affect the catalytic activity of the modified electrode towards H_2O_2 reduction. Thus, the cathodic currents provided by the electrode in the presence of $5 \cdot 10^{-3}$ M H_2O_2 were $2.6 \cdot 10^{-5}$ A, $2.9 \cdot 10^{-5}$ A and $2.7 \cdot 10^{-5}$ A in the absence of enzyme, in the presence of 1 mg/ml GOx and in the absence of enzyme again, respectively. Also, the background currents from the amperometric responses ($1.0 \cdot 10^{-6}$ A, $9.5 \cdot 10^{-7}$ A and $8.6 \cdot 10^{-7}$ A, respectively) were comparable. These results suggested that the DBSA/KCl modification remained unaffected after the exposure of the electrode to a solution of GOx. Further experiments such as H_2O_2 sensing in the presence of glucose alone or in the presence of gluconolactone and gluconic acid were also performed and again, no effect on the

amperometric responses were observed. Therefore, it appeared that it was the enzymatic mechanism for glucose determination itself that was responsible for the decrease in the catalytic activity to H_2O_2 reduction observed in Fig. 5.1.

Having established that catalysis was lost only when GOx and glucose were present and interacted at the modified electrode surface simultaneously, with the assumption that they somehow impaired the catalysis via some surface phenomenon, a strategy was chosen that would maintain the separation of these two components from the surface. One such design approach could be the immobilization of the enzyme on the electrode surface. However, such metallic electrode surfaces are generally incompatible materials where proteins undergo denaturation upon immobilization and consequently lose their activities.[23] It is known that several heavy metal ions, such as Ag^+, Hg^{2+} and Cu^{2+} exhibit a marked inhibition on the activity of enzymes.[17, 35] Therefore, employment of a membrane was investigated as a means to stabilise and control enzyme concentration, keep it close to the electrode surface, while also prevent it from coming in contact with the catalytic layer. However, its effect on the electrode system also had to be determined, particularly the issue of diffusion of electroactive substances (i.e., H_2O_2) to the electrode surface and loss of catalytic effect.

Several types of membrane have been used in the literature for the fabrication of glucose biosensors, e.g. cellulose acetate (CA).[36-38] Barsan and Brett[37] developed a glucose biosensor based on a carbon/ CA composite with a poly(neutral red) (PNR) phenazime layer polymerized on top. The latter was used as an electron acceptor to transfer electrons from the redox active centre of GOx to the electrode surface. The enzyme was then immobilized by cross-linking with glutaraldehyde (GA), providing glucose biosensors with high reproducibility and sensitivities of $3.15 \cdot 10^{-2}$ $AM^{-1}cm^{-2}$. Chitosan is also an interesting natural material than can be used for biosensor fabrication. Due to its advantageous properties as a biopolymer, e.g. low cost, biocompatibility for biomolecular entrapment, chemical inertness and low toxicity, numerous applications using chitosan to immobilize enzymes have been reported.[13, 39, 40] For example, Miao et al.[13] described a glucose biosensor fabricated by means of GOx and mediator immobilization in the following "sandwich" configuration: chitosan-ferrocene/GOx/chitosan. High enzyme loadings were enabled due to the cross-linking

reaction between the amino group of chitosan and aldehyde group of glutaraldehyde. A carbon paste electrode was used as a platform to prepare the biosensor, which exhibited a high stability and sensitivity of $1.8 \cdot 10^{-3}$ AM^{-1}. Nafion films have also been used for the production of biosensors.[22] They have been extensively used as protective coating materials and as supports for enzyme immobilization due to their high stability, good ionic conductivity and biocompatibility. Norouzi et al.[41] reported the fabrication of an electrochemical glucose biosensor, where GOx was immobilized on to a glassy carbon electrode by means of a Nafion matrix. Prior to GOx deposition, a glassy carbon surface was modified with gold nanoparticles and multiwall carbon nanotubes to improve the biosensor response. A LOD as low as $3 \cdot 10^{-8}$ M was obtained using Fast Fourier transformation continuous cyclic voltammetry (FFTCCV), where ferrocene methanol was used as an electron-transfer mediator.

In this work the three membrane materials (CA, Nafion and chitosan) were evaluated taking into account the residual catalytic response to H_2O_2 of the DBSA/KCl modified electrodes after their deposition. Preliminary work showed that all of them led to good retention of catalytic activity after their immobilization. Thus, the electrode modified with chitosan displayed a cathodic current in the presence of $5 \cdot 10^{-3}$ M H_2O_2 of $2.5 \cdot 10^{-5}$ A which equates to retention of 75% of the initial activity ($3.3 \cdot 10^{-5}$ A). For the Nafion membrane, the remaining catalytic activity to H_2O_2 of the electrode after its immobilization was 81 % whereas for CA it was 93%. Therefore, CA seemed to result in the highest residual activity following membrane deposition. Besides that, several preliminary GOx immobilization protocols were evaluated on the three types of membrane, resulting in a positive response only with the CA modified electrode. Therefore, CA was chosen as the membrane for more detailed evaluation in the fabrication of a glucose biosensor. The CA-modified DBSA/KCl modified Ag SPEs were initially assessed with enzyme in the solution. As stated above, the cathodic response of the CA-modified electrode in the presence of $5 \cdot 10^{-3}$ M H_2O_2 was $3.9 \cdot 10^{-5}$ A, which was equivalent to 93% of the current response of DBSA/KCl modified Ag SPE alone, or $4.2 \cdot 10^{-5}$ A. The electrode was subsequently tested in 1 mg/ml GOx solution in PBS pH 5, showing a reduction response at -0.1 V (vs. Ag/AgCl) of $1.5 \cdot 10^{-5}$ A in the presence of $5 \cdot 10^{-3}$ M glucose. The catalytic activity of the electrode to H_2O_2 after

glucose sensing was checked and a cathodic current of $3.1 \cdot 10^{-5}$ A was observed in the presence of $5 \cdot 10^{-3}$ M H_2O_2, i.e. 79% activity remaining after the enzymatic reaction which appeared to demonstrate retention of the catalytic properties of the electrode. Thus, deposition of a membrane layer and subsequent introduction of enzyme and substrate did not lead to the eradication of catalytic activity which further enforces the observation that this loss of activity was the result of both enzyme and glucose coming into contact with the modified electrode layer.

Subsequently, several parameters such as CA and GOx concentrations, immersion time in cellulose acetate solution during the formation of the membrane and other aspects of the immobilization protocols were optimized to achieve a reproducible glucose biosensor device.

5.2.2. Optimisation of GOx immobilization onto DBSA/KCl modified Ag SPEs

The feasibility of the DBSA/KCl modified Ag SPEs following CA deposition to be used for glucose determination with the enzyme in solution was previously verified by amperometry as shown above. Subsequently, optimisation of the immobilization of GOx at the electrode was investigated. Among the available methods for enzyme immobilization that were mentioned before, covalent coupling to the surface generally provides the best activity stability and avoids enzyme leaching from the sensor surface.[42] However, two main difficulties may be encountered: low levels of activated surface groups on the support and denaturation of enzyme if covalent bonding is performed through functional groups essential to the enzyme catalytic activity. Unlike other membranes such as collagen films, CA membranes of different thickness may be easily prepared and exhibit significant permselectivity towards anions, which has made them amenable as supports for *in vivo* implantable glucose sensors.[43] Besides that, GOx contains multiple tertiary NH_2 groups, which can be used to covalently anchor the enzyme to CA membranes after successive copolymerisation processes.[36-38] Some immobilization processes found in the literature involve covalent coupling of bovine serum albumin (BSA)[44] to a CA membrane and a subsequent reaction of the membrane with GOx, which had previously been activated with an excess of *p*-benzoquinone in

some cases.[43] Good sensitivity and LOD were obtained with these biosensors, although the use of another protein might hinder analyte diffusion to the electrode surface and make the resulting device more expensive. More recently, Portaccio et al.[36] reported the covalent attachment of GOx onto a CA film by means of hexamethylenediamine (HMDA) and glutaraldehyde (GA) as spacer and coupling agent, respectively. The immobilization procedure was quite straightforward and the resulting biosensors displayed analogous results to those obtained by a commercial glucometer when both real sample and *in vivo* measurements were performed. Therefore, the latter protocol was adopted and optimised for GOx immobilization on DBSA/KCl modified Ag SPEs in the present work.

5.2.2.1. Preparation of GOx biosensor by covalent enzyme immobilization

Unlike the buffer used in the earlier amperometric measurements, all enzyme solutions used in this work were prepared in 0.1 M phosphate buffer, pH 5. Such a pH was chosen rather than pH 6.8 because GOx has been reported to work more efficiently in slightly acidic solutions.[45, 46] However, acidic media lower than pH 4 led to GOx denaturation.

A cellulose acetate layer was deposited onto the DBSA/KCl modified Ag SPEs by immersing the electrodes in a cellulose acetate solution (0.02% w/v cellulose acetate in acetic acid) for 3 s.[36] The electrodes were then immersed in cold water for 10 min to accelerate the polymer solidification phase and rinse the surface of any remaining unbound polymer. The so-formed cellulose membrane was activated by immersing the electrodes in a 5% (w/v) hexamethylenediamine (HMDA) aqueous solution for 20 min. After rinsing the surfaces with distilled water, the electrodes were placed in a 2.5% (v/v) glutaraldehyde (GA) aqueous solution for 20 min. After further washing with distilled water, GOx was immobilized by keeping the electrodes at 3ºC overnight in a 25 mg/ml GOx solution in PBS pH 5. DBSA/KCl modified Ag SPEs with a cellulose acetate membrane will be referred to as Ag/ DBSA/KCl/ CA. Those electrodes with GOx immobilized on the surface will be referred to as Ag/ DBSA/KCl/ CA/ GOx.

A scheme of the entire membrane fabrication and enzyme immobilization process is shown in Fig. 5.3.
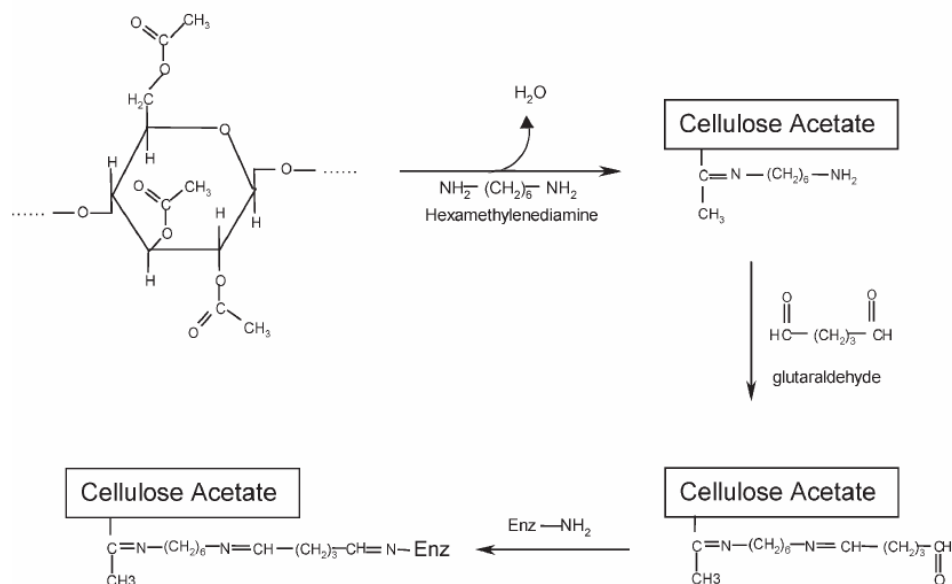
Figure 5.3. **Scheme of the process of membrane fabrication and covalent immobilisation of glucose oxidase to the cellulose acetate membrane.[36]**

Once the enzyme was immobilized onto the electrode, its glucose biosensing activity was tested using amperometry. The electrode was placed in a cell containing 2.5 ml PBS, pH 6.8 and amperometry was performed at –0.1 V (vs Ag/AgCl). Glucose concentrations in the solution were from $1 \cdot 10^{-3}$ to $5 \cdot 10^{-3}$ M. Then, H_2O_2 was added to the solution to a final concentration of $1 \cdot 10^{-3}$ M as before, to assess the residual catalysis. Fig. 5.4 shows the amperometric responses for the sensing of glucose using Ag/ DBSA/KCl/ CA/ GOx. As can be observed, although the biosensor showed a response towards glucose, this was significantly lower than that obtained for H_2O_2 reduction.
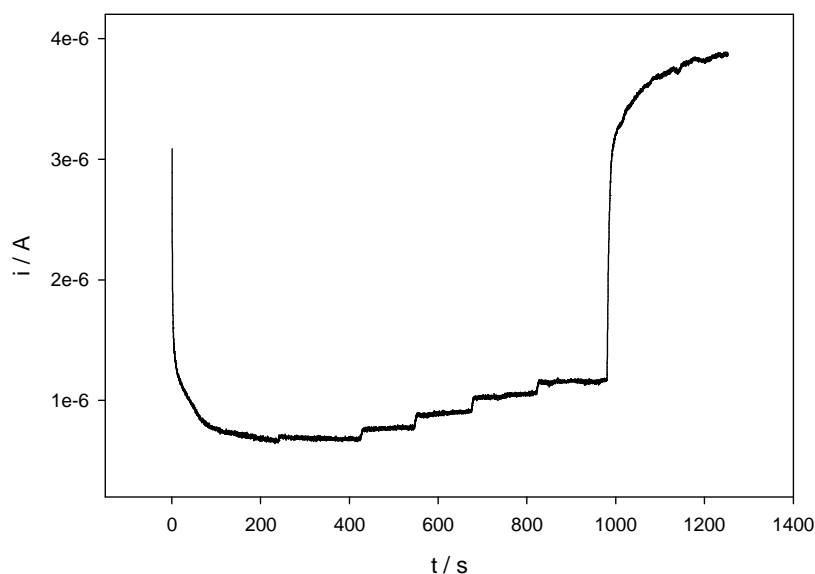
Figure 5.4. **Amperometric responses of a Ag/ DBSA/KCl/ CA/ GOx electrode measured at –0.1 V (vs Ag/AgCl) in PBS pH 6.8, at glucose concentration from 1 to $5 \cdot 10^{-3}$ M. At t = 1000s, H_2O_2 ($1 \cdot 10^{-3}$ M) was added to the solution.**

Thus, the cathodic current from the amperometric curve in the presence of $1 \cdot 10^{-3}$ M H_2O_2 was approx. $3.21 \cdot 10^{-6}$ A, after subtracting the background current, whereas the current obtained in the presence of $1 \cdot 10^{-3}$ M glucose reached only approx. $1.0 \cdot 10^{-7}$ A. This difference of more than one order of magnitude might be as a result of either a low amount of enzyme immobilized on the CA membrane or a partial loss of activity from the deposited enzyme. As is well known, the immobilization process reduces enzyme activity to a large extent. The enzyme molecules are suspended unprotected in the polymer layer at the electrode surface, leading to a limitation of the conformational freedom of the molecules and a partial deformation/deactivation.[8, 47] Such enzyme inactivation might be attributed to conformational changes induced by the number and types of enzyme-support interactions.[48] Cross-linkers such as GA are also well-known to highly cross-link the enzyme, reducing its activity. Immobilization also brings about diffusion-related restrictions associated with the immobilized enzyme and a decrease in

enzyme mobility can also affect the mobility of substrates and cofactor.[49] Also, glucose diffusion to the enzyme active site might become difficult, which would also decrease the electrochemical response. Notwithstanding these deficiencies, however, the system was responding to glucose additions and so was a feasible platform for glucose detection. Further methodological optimisation was performed to improve the response characteristics of the biosensor.

5.2.2.2. Optimization of the membrane deposition and GOx immobilization process

The initial inter-electrode variability observed for the biosensors might be attributed to a number of parameters such as the variability in the catalytic response of the underlying DBSA/KCl modified electrodes and all the steps involved in the membrane deposition and enzyme immobilization processes. This section focuses on the optimization of the latter, starting with the CA membrane deposition method. CA concentration and modification time as well as the solvent for the solution are assessed. Later, parameters involved in the GOx immobilization method, such as modification time in HMDA and GA solution are optimized.

5.2.2.2.1. Optimization of CA concentration for membrane deposition

The main purpose of this work was to create a high-quality CA layer which would enable the immobilization of an optimal concentration of enzyme to achieve maximum activity while not reducing glucose/ H_2O_2 diffusion to inhibitory levels. Some DBSA/KCl modified Ag SPEs were immersed in CA solutions of several concentrations (0.02 to 20% w/v) in acetic acid for 3 s. The electrodes were then immersed in cold water for 10 min and rinsed again before measuring. Thicker CA membranes might show decreases in the response to H_2O_2 due to diffusion limitation. Plot of the cathodic currents at $5\cdot10^{-3}$ M H_2O_2 vs log[CA] used for CA membrane deposition are shown in Fig. 5.5. Amperometric responses of DBSA/KCl modified electrodes with and without CA membranes of different concentration solutions are shown in the inset of Fig. 5.5.
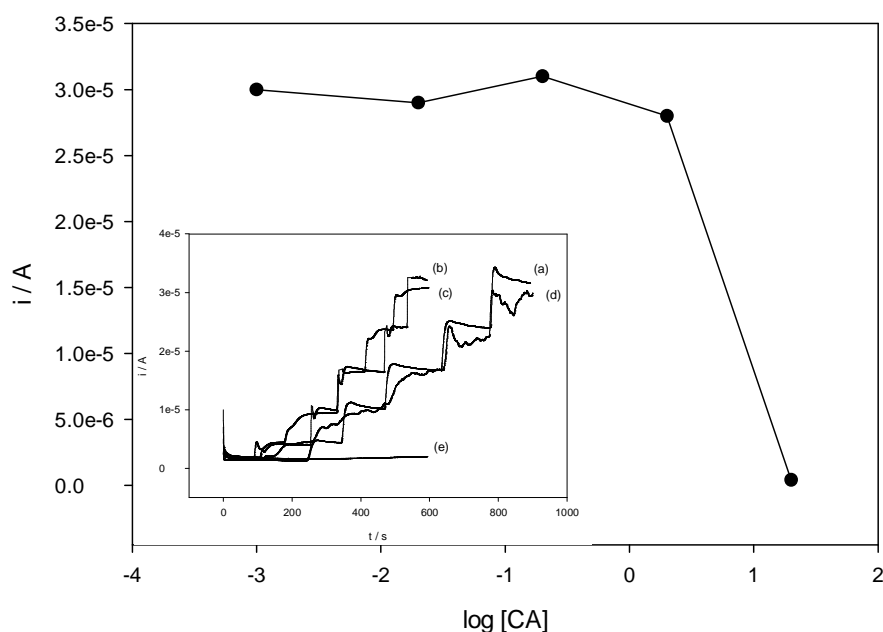
Figure 5.5. **Plot of catalytic currents at 5·10^{-3} M H$_2$O$_2$ vs log[CA]. Data at log[CA] = -3 corresponding to the cathodic current of the electrode without CA membrane. Inset: Amperometric responses of the reduction of 1 to 5·10^{-3} M H$_2$O$_2$ at DBSA/KCl modified Ag SPEs measured at –0.1 V (vs Ag/AgCl) in PBS pH 6.8: CA concentrations of (a) 0; (b) 0.2; (c) 0.02; (d) 2 and (e) 20% (w/v).**

Electrodes modified with CA membranes generated from 0.02% (w/v) and 0.2% (w/v) CA solutions seemed to maintain full catalytic activity towards H$_2$O$_2$ reduction, although the quality of signal produced was poor compared to that in the absence of membrane. Thus, the cathodic currents obtained in the presence of 5·10^{-3} M H$_2$O$_2$ were 2.9·10^{-5} A and 3.1·10^{-5} A for 0.02% (w/v) and 0.2% (w/v) CA concentrations, respectively, whereas the reduction current for a DBSA/KCl modified electrode before CA deposition was 3.0·10^{-5} A. The DBSA/KCl modified electrode treated with a 2% (w/v) CA solution provided a similar cathodic current of 2.8·10^{-5} A. However, the quality of the amperometric responses was increasingly noisy at these higher CA concentrations, which might be a result of a thicker layer that may have formed on the

electrode surface. At 20% (w/v) CA the current response was significantly reduced to approx. $4.2 \cdot 10^{-7}$ A. This electrode also showed a significant increase in response time. Both effects were assumed to relate to the formation of a thick, dense polymer film on the electrode which decreased the H_2O_2 diffusion rate from the solution to the electrode surface. These data suggested that films prepared from CA concentrations of the order of 1 or 2% (w/v) would not significantly impact diffusion of substrate to the electrode surface, although electrodes modified with 2% (w/v) showed noisy amperometric responses. Generally, CA concentrations around 1-2% (w/v) have been used in the literature for the deposition of CA membranes for the fabrication of glucose biosensors.[38, 50, 51] Initially, the standard protocol adopted here for enzyme attachment employed 20% (w/v) CA solution for membrane formation.[36] However, it was shown above that such a high concentration was not optimal in the present system as it hindered substrate diffusion and brought about a significant increase in response time.

Therefore, 1% (w/v) CA in acetic acid was selected as the optimum concentration for the deposition of a CA membrane as it maintained high catalytic activity on H_2O_2 reduction and provided a suitable platform for GOx immobilization.

5.2.2.2.2. *Optimization of the formation time for CA membrane formation*

Another parameter of the CA deposition process which needed to be optimized and studied was the formation time, i.e. the time DBSA/KCl modified Ag SPEs were immersed in the CA solution before GOx immobilization procedure. Several DBSA/KCl modified electrodes were immersed into 1% (w/v) CA solutions for different periods of time, from 5 to 20 s. The electrodes were washed thoroughly with distilled water as before. The viability of the CA membranes was evaluated by time-based amperometry of the glucose biosensors fabricated from them. The sensitivity for glucose determination as well as the remaining activity towards H_2O_2 reduction after enzyme immobilization for the four electrodes is shown in Table 5.1.

Table 5.1. Effect of membrane formation time on H_2O_2 response in 1% (w/v) CA solution.

Modification time/s	Before GOx i_1^a/x10^{-6} A	After GOx i_2^b/ x10^{-6} A	%Ratio i_1/i_2	$i_{1mM\ glucose}$ / x10^{-9} A	Sensitivity/ AM^{-1}cm^{-2}
5	3.49	2.93	84	9.0	$1.3 \cdot 10^{-4}$
10	4.02	1.71	43	8.3	$1.7 \cdot 10^{-4}$
15	4.29	1.66	39	11.0	$1.2 \cdot 10^{-4}$
20	4.61	1.81	39	6.3	$8.7 \cdot 10^{-5}$

^{a} cathodic current in the presence of $1 \cdot 10^{-3}$ M H_2O_2 before GOx immobilization

^{b} cathodic current in the presence of $1 \cdot 10^{-3}$ M H_2O_2 after GOx immobilization

As can be observed, the catalytic activity towards H_2O_2 reduction after GOx immobilization decreased remarkably as the immersion time in CA solution increased. Moreover, the sensitivity of the glucose biosensor displayed a similar tendency with the immersion time. 10 s seemed to be the optimum immersion time, providing biosensors with the highest sensitivity towards glucose determination. These results suggested that longer exposures to CA solutions resulted in the formation of thicker, denser layers, hindering both H_2O_2 and glucose catalytic processes. It might also relate the immersion time to a negative effect from glacial acetic acid used as a solvent for the CA solutions onto DBSA/KCl modification. It is worth remarking here that the 10 s modification time followed by washing might result in significant fabrication process variability. The obvious alternative then would be to reduce concentration and increase time. However, longer exposure to solvent (glacial acetic acid) was found to be damaging to the surface modification, so exposure times were kept short. Further studies about such solvent effects will be performed and commented upon later in this section.

A major requirement for good sensor device performance is inter-electrode reproducibility.[52, 53] Reproducibility studies were carried at this point, which demonstrated significant inter-electrode variability when prepared under the conditions described above (1% w/v CA for 10 s, 25 mg/ml GOx in PBS, pH 5 overnight). In order

to improve the reproducibility of the GOx immobilization procedure, nine electrodes were processed simultaneously prior to immersion in the enzyme solution. The electrodes were first modified with DBSA/KCl at the same time and then immersed in 1% (w/v) CA solution for 10 s and subsequently in cold water for 10 min in order to accelerate the CA solidification phase. Further modifications were then performed following the established protocol for GOx immobilization. The response of the biosensors to glucose determination was subsequently evaluated at –0.1 V (vs Ag/AgCl). Ag/ DBSA/KCl/ CA/ GOx electrodes were placed in a cell containing 2.5 ml PBS pH 6.8 and aliquots of 0.2 M glucose were successively added to the solution so glucose concentrations in the bulk increased from $1 \cdot 10^{-3}$ to $6 \cdot 10^{-3}$ M. After that, 1 M H_2O_2 was added to the solution to a final concentration of $1 \cdot 10^{-3}$ M as a performance check. The responses of the electrodes to glucose are shown in Fig. 5.6 and Table 5.2. Current data corresponding to $1 \cdot 10^{-3}$ M glucose were not considered for the regression line.
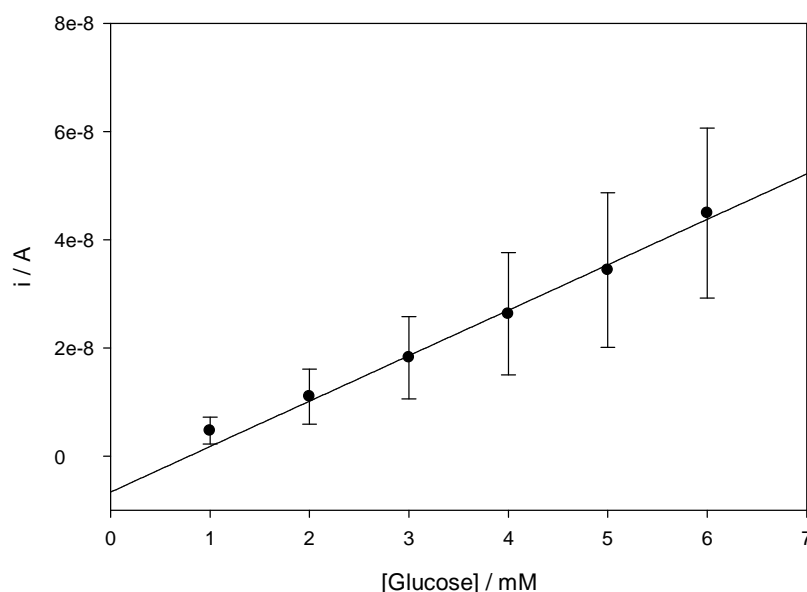
Figure 5.6. **Measurement of glucose using the Ag/ DBSA/KCl/ CA/ GOx electrodes (n=9) at –0.1 V (vs Ag/AgCl) in PBS pH 6.8. CA membrane deposited after 10 s immersion in 1% (w/v) CA solution in glacial acetic acid. (slope = $8.4 \cdot 10^{-9}$ AmM^{-1}; sensitivity = $6.7 \cdot 10^{-5}$ AM^{-1}cm^{-2}).**

From the data in Fig. 5.6 and Table 5.2, it is evident that the inter-electrode variability was significant for all glucose concentrations tested, varying from 35% at $6 \cdot 10^{-3}$ M to 53% at $1 \cdot 10^{-3}$ M. One possible explanation could be that electrodes did not reach the steady state background current before glucose was added to the solution. That would lead to signal-to-noise responses lower than three for the first glucose additions, which justify that at the beginning of the glucose sensing process ($1 \cdot 10^{-3}$ M glucose in solution) the inter-electrode reproducibility was lower than that observed at the last stage of the amperometric curves ($6 \cdot 10^{-3}$ M glucose in solution).

Table 5.2. Average and standard deviation for Ag/ DBSA/KCl/ CA/ GOx (n=9).

[Glucose] / 10^{-3} M	i_{cat} (average) / A	Standard deviation / A	% error
1	$4.7 \cdot 10^{-9}$	$2.5 \cdot 10^{-9}$	53
2	$1.10 \cdot 10^{-8}$	$5.1 \cdot 10^{-9}$	46
3	$1.82 \cdot 10^{-8}$	$7.6 \cdot 10^{-9}$	42
4	$2.63 \cdot 10^{-8}$	$1.13 \cdot 10^{-8}$	43
5	$3.44 \cdot 10^{-8}$	$1.43 \cdot 10^{-8}$	42
6	$4.49 \cdot 10^{-8}$	$1.57 \cdot 10^{-8}$	35

Delaying the first glucose addition during amperometry might improve the signal-to-noise and reproducibility at low glucose concentrations. However, that would imply addition times longer than 900 s, which is unacceptable from a commercial point of view. Other electrochemical methods such as potential stepping or chronocoulometry might resolve some of these issues. Besides that, the variability observed by the biosensors even at high glucose concentrations in solution was excessive compare to that expected for this type of devices. For instance, Miao et al.[13] developed a glucose biosensor that provided an inter-reproducibility of 6.5% (r.s.d.) in the presence of $3.92 \cdot 10^{-3}$ M glucose (n=6). Basically, the biosensor showed the following "sandwich" structure: chitosan-ferrocene/GOx/cross-linked chitosan using a carbon paste electrode as the basic electrode. To avoid loss of immobilized GOx, the biosensor surface was cross-linked with glutaraldehyde. The repeatability of response of a single glucose enzyme biosensor was also investigated at $3.92 \cdot 10^{-3}$ M glucose, leading to an intra-

reproducibility value of 4.2% (n=9). Zuo et al.[54] reported the fabrication of a disposable glucose biosensor by immobilizing GOx into silver nanoparticles-doped silica sol-gel and polyvinyl alcohol hybrid film on a Prussian blue-modified screen-printed electrode. The presence of silver nanoparticles led to a remarkable improvement of the film conductivity and a subsequent enhancement of the biosensor sensitivity. The inter-electrode reproducibility studied was carried out in the presence of $5 \cdot 10^{-2}$ M glucose, providing a relative standard deviation of 7.6% (n=12), whereas the intra-reproducibility was 6.3%. Hence, further optimization studies of the GOx immobilization procedure were performed to improve the biosensor reproducibility in the present work.

5.2.2.2.3. Optimization of the solvent for CA membrane dissolution

Due to the high inter-electrode variability observed between biosensors, the effect of the solvent used to dissolve CA was assessed.

CA is relatively inert and does not interact with or impede the movement of proteins, making it a useful component for a support medium. Generally, CA is prepared by treating cellulose with acetic anhydride (acetylation of cellulose). That is, acetyl groups become linked to the hydroxyl groups (negative charges) on sugar molecules that are the building blocks for cellulose.[55] The solubility of CA depends on the degree of substitution (DS), e.g. the most common form of CA has an acetate group on approx. 2-2.5 of every three hydroxyls (DS = 2-2.5). This type is soluble in acetone, dioxane and methyl acetate; higher acetylated types are soluble in dichloromethane. Acetic acid is generally a good solvent for CAs with DS greater than 0.8.[56] CA used in the present work presented a DS of approx. 1.2, therefore, glacial acetic acid was first used as a solvent. Acetic acid is a weak acid that in its pure, water-free formulation (glacial acetic acid) is quite corrosive. Therefore, it might interact with the Ag SPE electrode surface, removing the binder from the ink and causing further surface modifications. In order to evaluate its effect, amperometric responses at –0.1 V (vs Ag/AgCl) in PBS, pH 6.8 were performed for a DBSA/KCl modified Ag SPE before and after 10 s immersion in glacial acetic acid. The effect of the acid on the DBSA/KCl modification and, consequently,

H_2O_2 catalysis was estimated by comparison of the cathodic currents provided by the electrode in the presence of $5 \cdot 10^{-3}$ M H_2O_2 (Fig. 5.7).
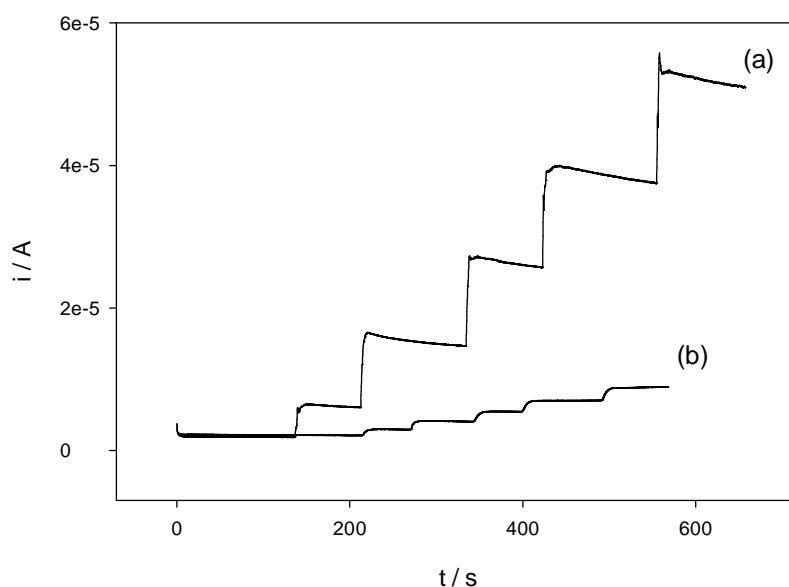
Figure 5.7. **Amperometric responses of a DBSA/KCl modified Ag SPEs measured at –0.1 V (vs Ag/AgCl) in PBS pH 6.8: (a) before and (b) after 10 s immersion in glacial acetic acid, at H_2O_2 concentration from 1 to $5 \cdot 10^{-3}$ M.**

As can be observed, acetic acid had a significant negative impact on H_2O_2 catalysis from DBSA/KCl modified Ag SPEs. Thus, the cathodic current shown by the electrode at $5 \cdot 10^{-3}$ M H_2O_2 after immersion in acetic acid was approx. $6.8 \cdot 10^{-6}$ A, almost one order of magnitude lower than that shown by the same electrode before acetic acid treatment, $4.9 \cdot 10^{-5}$ A. That negative effect of the acetic acid on DBSA/KCl modified electrodes can be also observed in the SEM pictures in Fig. 5.8. An etching effect on the electrode surfaces was observed after the immersion in both acetic acid solutions, alone and with CA, as is shown in Fig. 5.8B and 5.8C. The spheroidal structures that appeared on the surface following DBSA/KCl modification (Fig. 5.8A) were not so evident on electrodes after acetic acid treatment (Fig. 5.8B and 5.8C). The presence of the CA membrane might have reduced the etching process from the solvent, which would explain the

higher catalytic responses obtained by the CA-modified electrodes respect to those exposed just to acetic acid solutions (Figs. 5.5 and 5.7). However, a CA membrane would not be visible by SEM. This decrease in the catalytic activity after immersion in a solution containing acetic acid might explain the further variability obtained between glucose biosensors. Therefore, a different solvent for the preparation of CA solutions was required.
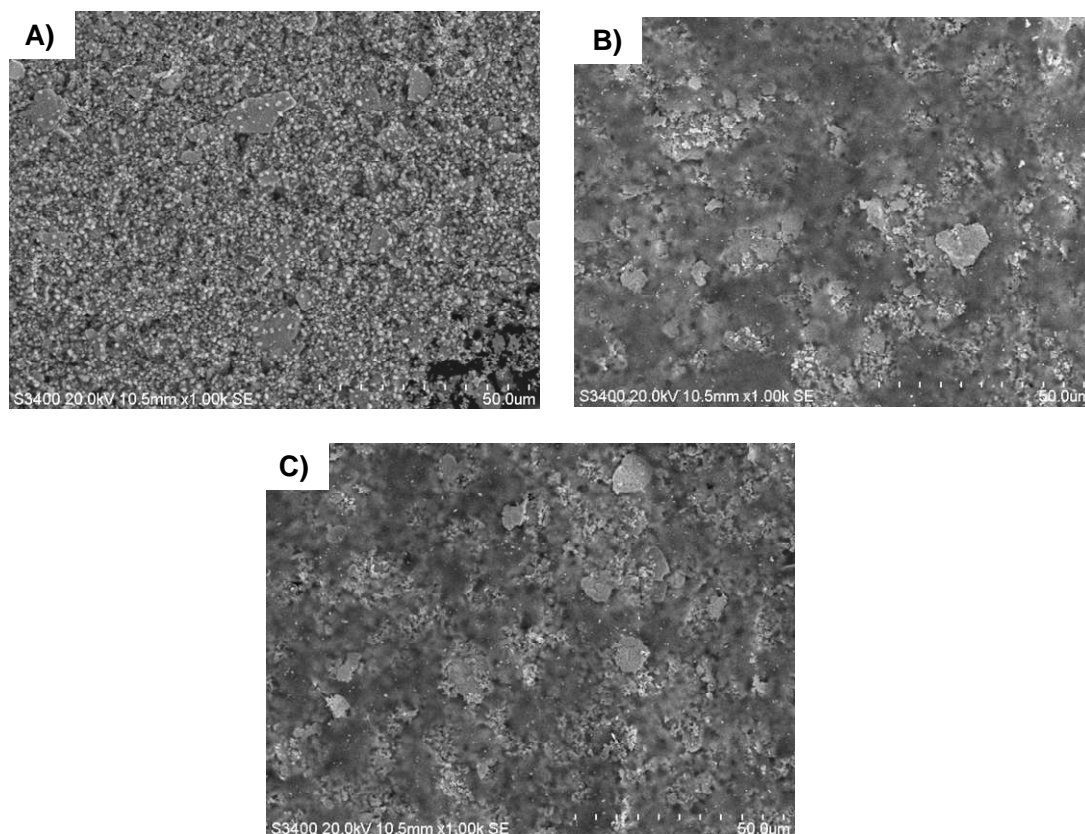
Figure 5.8. **SEM images of DBSA/KCl modified electrodes (A) without any further modification, (B) after 10 s immersion in 1%** (w/v) **CA in acetic acid and (C) after 10 s immersion in glacial acetic acid. Accelerating voltage of 20 kV. (1.0 k x magnification).**

Acetone is a colourless, flammable liquid, miscible with water and used as an important solvent for many industrial applications. As was mentioned above, CA is readily soluble in acetone, so this solvent was evaluated as a suitable alternative to glacial acetic acid for cellulose membrane formation. In order to check the effect of CA/acetone on DBSA/KCl modification, amperometric responses and SEM images of surfactant-modified electrodes were taken before and after their immersion in an acetone-based solution. A DBSA/KCl modified Ag SPE was first measured in PBS, pH 6.8 in the presence of 1 to $5 \cdot 10^{-3}$ M H_2O_2 by amperometry at -0.1 V (vs Ag/AgCl). After that, the electrode was dipped into a 2% (w/v) CA in acetone solution for 1 min. After washing thoroughly with distilled water, the electrode was placed in a cell containing PBS, pH 6.8 and amperometry was again performed in the presence of H_2O_2. The effect of just acetone on DBSA/KCl modification was also checked by the immersion of the electrode in acetone for 10 s. Fig. 5.9 shows the amperometric responses of a DBSA/KCl modified electrode before and after the immersion in CA/acetone solution and after the immersion in just acetone. DBSA/KCl modified electrode before immersion in CA solution exhibited a cathodic current of approx. $6.4 \cdot 10^{-5}$ A in the presence of $5 \cdot 10^{-3}$ M H_2O_2 whereas the same electrode after CA membrane deposition showed approx. $2.3 \cdot 10^{-5}$ A. When immersed only in acetone for 10 s the cathodic current was $5.0 \cdot 10^{-6}$ A. Therefore, the decrease in the catalytic current shown by the electrode after the immersion in CA/acetone could be attributed to the etching effect of the acetone diminished by the presence of CA.

As can be seen, the cathodic current of the DBSA/KCl modified electrode is simply three-fold higher than that after CA deposition and over an order of magnitude greater than that after acetone immersion.
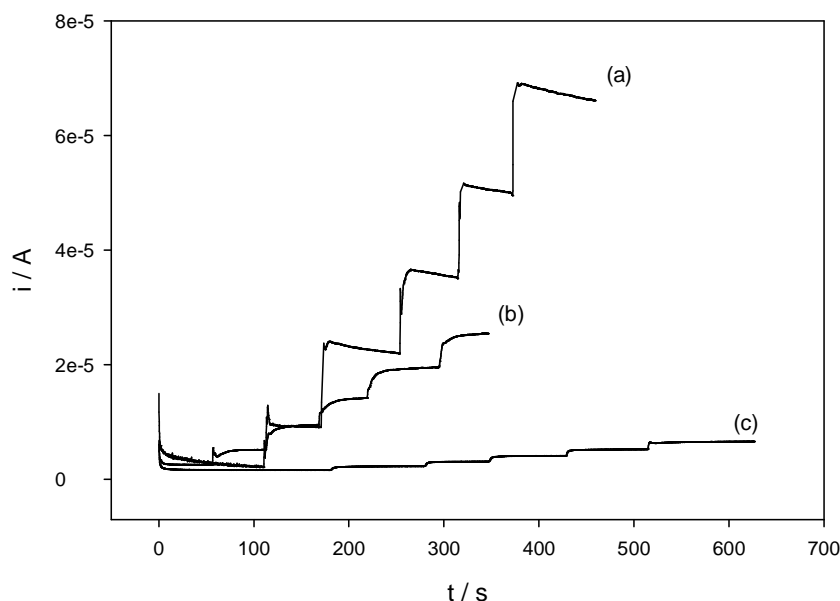
Figure 5.9. **Amperometric responses of DBSA/KCl modified Ag SPEs measured at –0.1 V (vs Ag/AgCl) in PBS pH 6.8: (a) without any further treatment (b) after 1 min immersion in 2%** (w/v) **CA in acetone solution and (c) after 10 s in acetone, at H_2O_2 concentration from 1 to $5 \cdot 10^{-3}$ M.**

The etching effect of acetone on the electrode surface was also observed in the SEM images shown in Fig. 5.10. Surface areas from electrodes after treatment in acetone-based solution alternated silver paste areas with blurred ones, as can be observed in Fig. 5.10B and 5.10C. Again, the presence of CA might have diminished the etching effect of the solvent, as can be observed by the higher catalytic responses towards H_2O_2 of the CA-modified electrodes respect to those just exposed to acetone (Fig. 5.9). However, the CA membrane is not conductive, which made difficult its detection by SEM microscopy without any metal sputtered on top. Nevertheless, the negative effect of acetone on DBSA/KCl modification was evident from the amperometric responses and the SEM images. Such effects have been previously reported in the literature. Thus, Polan et al.[51] developed a glucose biosensor by immobilizing GOx onto carbon screen printed electrodes with CA. Solutions at concentrations from 0.05 to 3% of CA in acetone were used. They realized that acetone dissolved the binder in the carbon ink (of a resin type),

which caused partial washing of the electrode. In this case, that could be a further evidence for the presence of the binder playing a role in the H_2O_2 catalysis observed after DBSA/KCl modification. The etching effect of the acetone might remove the binder with the consequent loss of the DBSA/KCl modification.
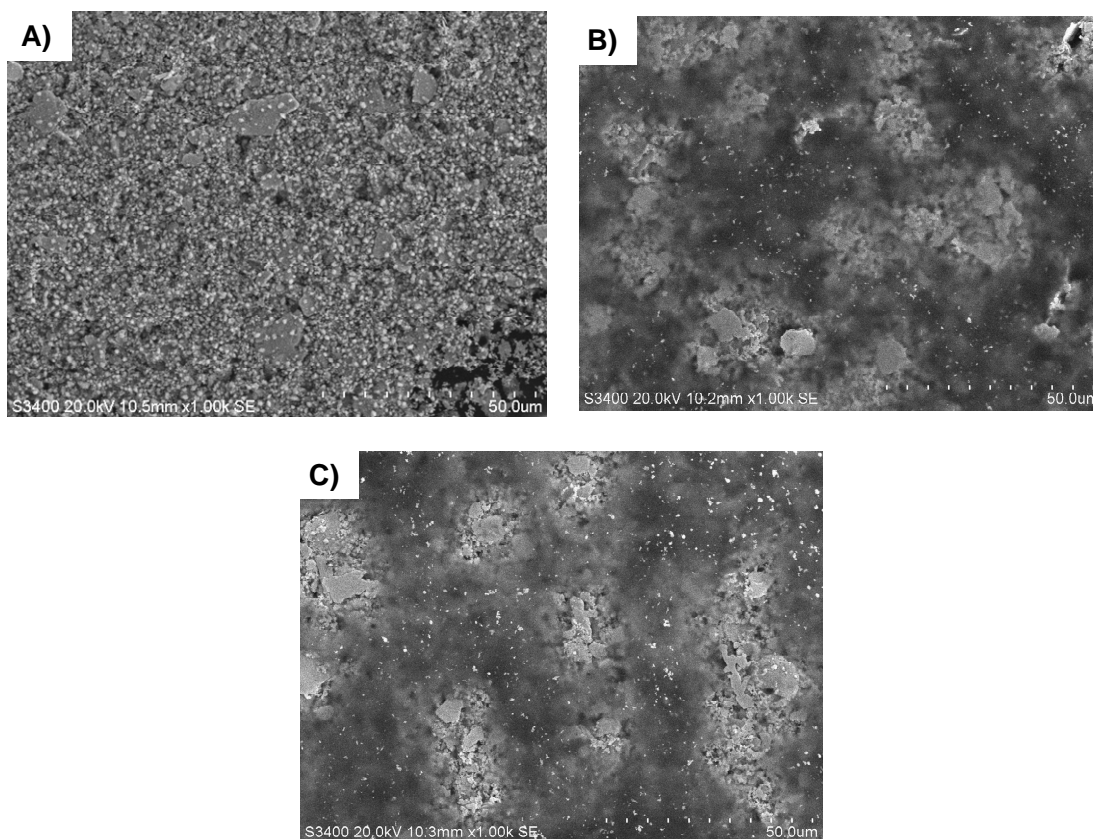
Figure 5.10. **SEM images of DBSA/KCl modified electrodes (A) without any further modification, (B) after 1 min immersion in 2% (w/v) CA in acetone and (C) after 10 s immersion in acetone. Accelerating voltage of 20 kV. (1.0 k x magnification).**

Despite the observed effect of the acetone, a glucose biosensor was fabricated from a DBSA/KCl modified electrode by immersion in a 2% (w/v) CA in acetone solution for 1

min. The electrode was then washed thoroughly with distilled water and subjected to modification steps according to the established GOx immobilization process. Amperometry at –0.1 V (vs Ag/AgCl) in PBS, pH 6.8 was carried out at glucose concentrations from 1 to $6 \cdot 10^{-3}$ M. H_2O_2 was then added to the bulk to a final concentration of $1 \cdot 10^{-3}$ M. Varying the solvent from CA solution during GOx immobilization procedure did alter the catalytic response towards glucose determination shown by the biosensor devices, as is illustrated in Fig. 5.11.
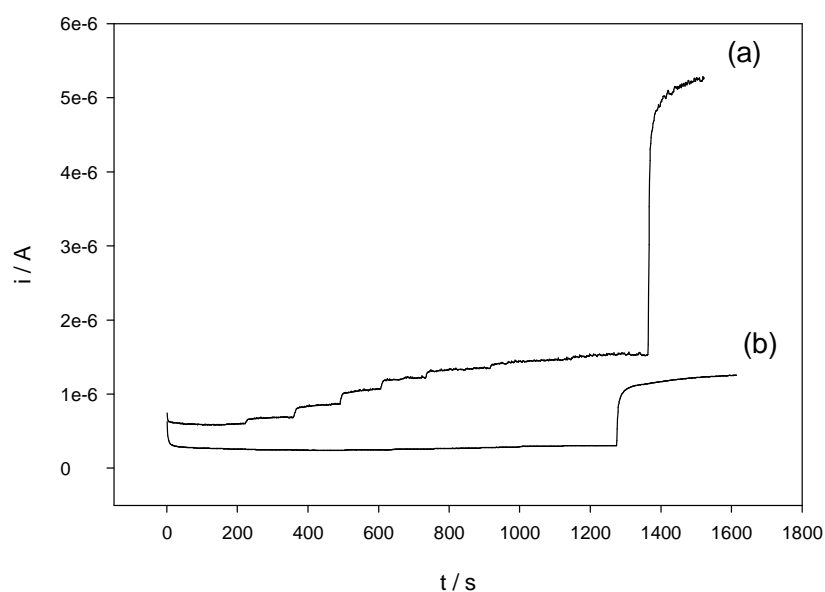
Figure 5.11. **Amperometric responses of Ag/ DBSA/KCl/ CA/ GOx electrodes measured at –0.1 V (vs Ag/AgCl) in PBS pH 6.8, at glucose concentration from 1 to $5 \cdot 10^{-3}$ M. Later, H_2O_2 ($1 \cdot 10^{-3}$ M) is added to the solution. Ag/ DBSA/KCl/ CA/ GOx electrodes were prepared by immersion in: (a) 2%** (w/v) **CA solution in acetone for 1 min and (b) 1%** (w/v) **CA in glacial acetic acid solution for 10 s.**

CA dissolved in acetone seemed to provide better membranes on the DBSA/KCl modified electrodes compared to acetic acid. The cathodic current shown by the former was approx. $8.6 \cdot 10^{-7}$ A in the presence of $6 \cdot 10^{-3}$ M glucose whereas the latter exhibited

approx. $6.6 \cdot 10^{-8}$ A. The catalytic enhancement of the reduction current using acetone as solvent for CA was not only observed in glucose determination but also in H_2O_2 sensing. A near five-fold greater cathodic current in the presence of $1 \cdot 10^{-3}$ M H_2O_2 was obtained by the acetone modified electrode ($4.7 \cdot 10^{-6}$ A), than by the acetic acid modified one ($1.0 \cdot 10^{-6}$ A). Therefore, acetone was selected as the solvent in the CA solution in further work as it exhibited larger responses during both glucose and H_2O_2 sensing processes.

5.2.2.2.4. Optimization of modification times in 5% HMDA and 2.5% GA solutions

Following the optimisation of the CA membrane formation step, the next step in the GOx immobilization process was considered. Thus, several Ag/ DBSA/KCl/ CA electrodes were immersed in 5% HMDA in aqueous solution for different periods of time, from 1 to 20 min. After intensive washing with distilled water, the electrodes were placed in PBS, pH 6.8 and amperometry at –0.1 V (vs Ag/AgCl) was carried out. Fig. 5.12 shows the amperometric responses of the HMDA-treated electrodes in the presence of H_2O_2 ($0-5 \cdot 10^{-3}$ M). Varying the time of exposure to 5% HMDA aqueous solution did not seem to bring about noticeable changes in the cathodic currents in the presence of $5 \cdot 10^{-3}$ M H_2O_2. In this way, $7.8 \cdot 10^{-6}$ A was the cathodic current at that concentration shown by a Ag/ DBSA/KCl/ CA electrode after 1 min immersion in HMDA solution whereas an electrode immersed for 20 min provided $8.2 \cdot 10^{-6}$ A. The currents exhibited by electrodes immersed in 5 and 10 min in HMDA solution were $8.1 \cdot 10^{-6}$ A and $6.7 \cdot 10^{-6}$ A, respectively. However, those currents were approx. 4-fold lower than that obtained by a DBSA/KCl modified Ag SPE in the presence of $5 \cdot 10^{-3}$ M H_2O_2, being $3.5 \cdot 10^{-5}$ A.

Figure 5.12. **Amperometric responses of Ag_DBSA/KCl_CA electrodes measured at -0.1 V (vs Ag/AgCl) in PBS pH 6.8 after immersion in 5% HMDA aqueous solution for: (a) 1 min; (b) 5 min (c) 10 min and (d) 20 min, at H_2O_2 concentration from 1 to $5 \cdot 10^{-3}$ M.**

Further studies varying immersion times in 2.5% GA aqueous solutions did not lead to any improvement in reproducibility or sensitivity of the glucose biosensor whereas the cathodic current provided for the catalytic reduction of H_2O_2 were even lower. Thus, Ag/ DBSA/KCl/ CA electrodes immersed in 2.5% GA solution for 1, 5, 10 and 20 min showed cathodic currents of $3.7 \cdot 10^{-6}$ A, $3.1 \cdot 10^{-6}$ A, $3.8 \cdot 10^{-6}$ A and $3.1 \cdot 10^{-6}$ A, in the presence of $5 \cdot 10^{-3}$ M H_2O_2. Amperometric responses corresponding to these experiments are shown in Fig. 5.13.
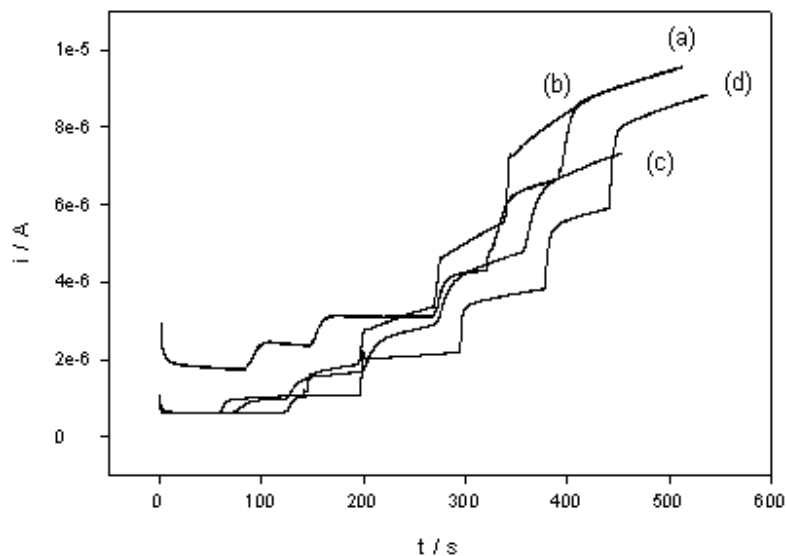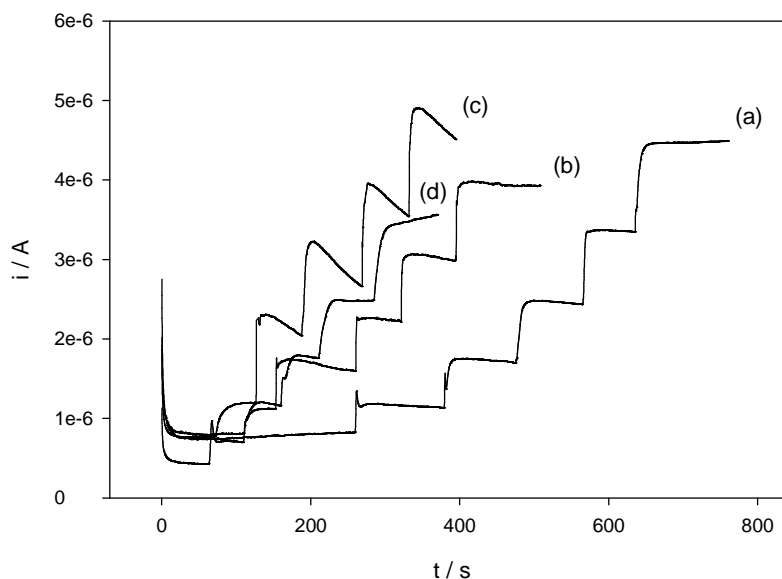
Figure 5.13. **Amperometric responses of Ag/ DBSA/KCl/ CA electrodes measured at –0.1 V (vs Ag/AgCl) in PBS pH 6.8, at H_2O_2 concentration from 1 to $5 \cdot 10^{-3}$ M. Electrodes were first modified in 5% HMDA aqueous solution for 1 min and then in 2.5% GA for: (a) 1 min; (b) 5 min (c) 10 min and (d) 20 min.**

5.2.2.3. Analytical characterisation of the glucose biosensor

Subsequently, the feasibility of Ag/ DBSA/KCl/ CA/ GOx electrodes to be used as glucose biosensors was evaluated and LOD, sensitivity and reproducibility studies were performed. Six DBSA/KCl modified electrodes were treated according to the adopted standard protocol, using acetone as solvent in CA solutions. After rising, they were measured in PBS, pH 6.8. Amperometric responses to glucose from 0.4 to $4 \cdot 10^{-3}$ M were plotted versus glucose concentration and regression lines for each electrode were calculated. Fig. 5.14 shows the amperometric response and the calibration curve acquired with one of the electrodes as an example. LOD and sensitivity were calculated from the regression line obtained from the plot of the cathodic currents vs glucose concentration, with a signal-to-noise ratio of 3.[57] These data are presented in the inset of

Fig. 5.14. LOD and sensitivity obtained for this particular electrode were found to be $8.4 \cdot 10^{-5}$ M and $1.36 \cdot 10^{-3}$ $AM^{-1}cm^{-2}$, and the average values for the six electrodes were $8.9 \cdot 10^{-5}$ M and $1.2 \cdot 10^{-3}$ $AM^{-1}cm^{-2}$, respectively (Fig. 5.15). A comparison of the analytical parameters of the developed glucose biosensor with other devices reported in the literature is shown in Appendix 3.
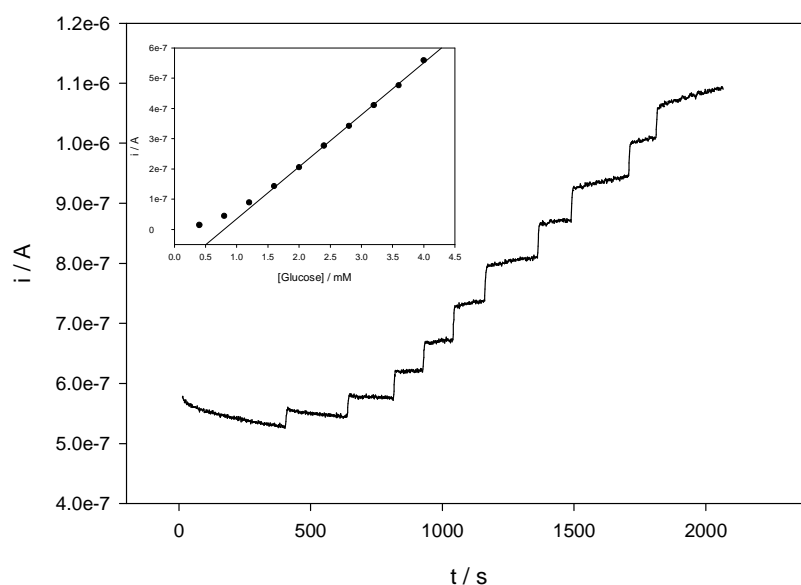
Figure 5.14. **Amperometric responses of a Ag/ DBSA/KCl/ CA/ GOx electrode in $0.4 \cdot 10^{-3}$ M aliquots of glucose (0.4 - 4 $\cdot 10^{-3}$ M) at –0.1 V (vs Ag/AgCl) in PBS pH 6.8. Input: Plot of cathodic current vs glucose concentration at –0.1 V (vs Ag/AgCl) in PBS pH 6.8.**

Those values were improved with regard to other LODs and sensitivities obtained with biosensors based on screen-printed electrodes. For example, Lee et al.[58] developed a glucose biosensor based on carbon screen printed electrodes with hexacyanoferrato (III) as an electron transfer mediator. A mixture solution of chitosan oligomers (COs) and the mediator (Ferri) was drop-coated onto the carbon screen printed electrodes and GOx was subsequently deposited on top, creating a GOx/Ferri-COs glucose biosensor.

Several parameters such as GOx loadings, COs concentrations, pH solution and applied potential were studied in order to provide a high sensitivity and good reproducibility biosensor device. A LOD of $1.38 \cdot 10^{-3}$ M and a sensitivity of $6.77 \cdot 10^{-4}$ AM^{-1} were obtained at an applied potential of 0.3 V. Ricci et al.[22] also reported the fabrication of a glucose biosensor based on GOx deposition onto a modified graphite screen printed electrode. Prior to enzyme immobilization, electrodes were chemically modified with ferric hexacyanoferrato (Prussian Blue), which allowed H_2O_2 detection at low applied potential (0 V vs Ag/AgCl). Both the Prussian Blue layer and the assembled biosensor showed high operational and storage stability. After optimization, the glucose biosensor exhibited a LOD of $2.5 \cdot 10^{-5}$ M, which is in the same order of magnitude as that obtained in the present work. Lower LODs, in the order of 10^{-6} M, were also described in the literature meanly corresponding to systems based on gold nanoparticles (GNp) modified Pt electrodes. For instance, Wu et al.[39] developed a glucose biosensor based on the layer-by-layer assembled chitosan/gold nanoparticles/GOx film onto Pt electrodes, which exhibited a LOD of $7 \cdot 10^{-6}$ M at an applied potential of 0.6 V (vs Ag/AgCl). The same group[59] also fabricated another glucose biosensor based on multilayer films composed of multi-wall carbon nanotubes (MWCNTs), GNp and GOx for the specific detection of glucose. This system provided a lower LOD, $6.7 \cdot 10^{-6}$ M at also lower applied potential, 0.35 V (vs Ag/AgCl).

Data of averages and standard deviations of the cathodic currents obtained by the six electrodes are shown in Fig. 5.15 and Table 5.3. Current data corresponding to 0.4-$1.2 \cdot 10^{-3}$ M glucose were not considered for the regression line. As can be observed, low glucose concentrations led to higher standard errors in the cathodic currents than high glucose concentrations. However, the variability shown by the electrodes modified by CA in acetone was far lower than that previously observed when the electrodes were immersed in CA solution containing acetic acid. Standard error for acetone-based solution at $4 \cdot 10^{-3}$ M glucose was approx. 21% whereas the error for the electrodes modified with the acetic acid-based solution was 43%.
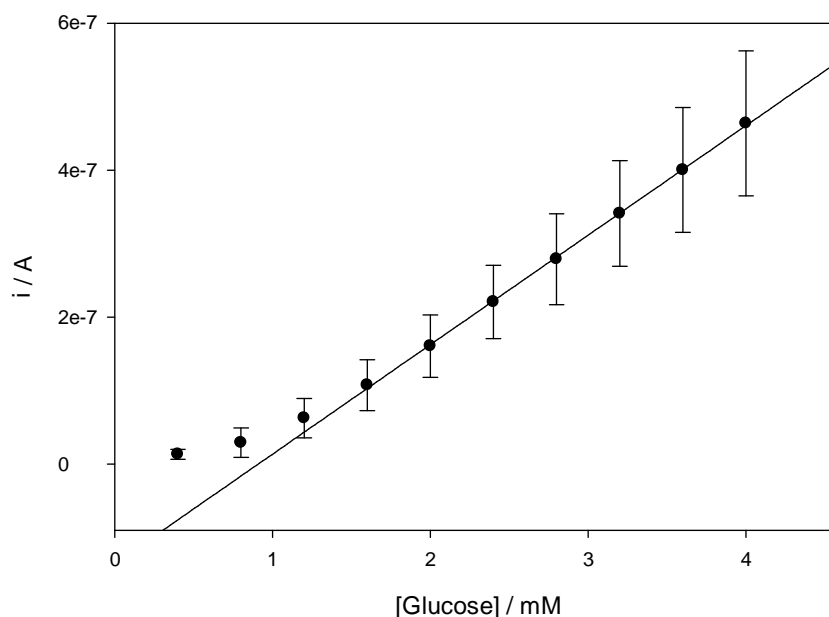
Figure 5.15. **Measurements of glucose using the Ag/ DBSA/KCl/ CA/ GOx electrodes (n=6) at –0.1 V (vs Ag/AgCl) in PBS pH 6.8. CA membrane deposited after 1 min immersion in 2% (w/v) CA solution in acetone. (slope = $1.491 \cdot 10^{-7}$ AmM^{-1}; sensitivity = $1.18 \cdot 10^{-3} AM^{-1}cm^{-2}$).**

An enhancement in the sensitivity of the electrodes was also exhibited when the CA membrane was deposited from the acetone-based solution. The latter provided an average cathodic current of $4.64 \cdot 10^{-7}$ A in the presence of $4 \cdot 10^{-3}$ M glucose whereas the average for the electrodes modified with the acetic acid-based solution was $2.63 \cdot 10^{-8}$ A. Such difference represented an almost 20-fold enhancement in the catalytic response of the electrodes treated with the acetone-based solution towards glucose. However, the variability shown by the latter was still high in comparison with other systems in the literature. As was mentioned above, Barsan and Brett[37] reported the development of a new carbon/CA composite material used as a platform in the fabrication of a glucose biosensor. The enzyme was immobilized by cross-linking with glutaraldehyde on the top of poly(neutral red) (PNR) modified CA-graphite composite electrodes. The

reproducibility obtained with this CA-based glucose biosensor was approx. 5% (r.s.d.), depending on the type of graphite applied in the composite fabrication.

Table 5.3. Average and standard deviation for Ag/ DBSA/KCl/ CA/ GOx (n=6)

[Glucose] / 10^{-3} M	i_{cat} (average) / A	Standard deviation / A	% error
0.4	$1.3 \cdot 10^{-8}$	$7 \cdot 10^{-9}$	54
0.8	$2.9 \cdot 10^{-8}$	$2.0 \cdot 10^{-8}$	69
1.2	$6.3 \cdot 10^{-8}$	$2.7 \cdot 10^{-8}$	43
1.6	$1.07 \cdot 10^{-7}$	$3.5 \cdot 10^{-8}$	33
2.0	$1.61 \cdot 10^{-7}$	$4.2 \cdot 10^{-8}$	26
2.4	$2.21 \cdot 10^{-7}$	$5.0 \cdot 10^{-8}$	23
2.8	$2.79 \cdot 10^{-7}$	$6.2 \cdot 10^{-8}$	22
3.2	$3.41 \cdot 10^{-7}$	$7.2 \cdot 10^{-8}$	21
3.6	$4.00 \cdot 10^{-7}$	$8.5 \cdot 10^{-8}$	21
4.0	$4.64 \cdot 10^{-7}$	$9.9 \cdot 10^{-8}$	21

As was mentioned above, the responses detected by the amperometric glucose biosensors developed in the present work corresponded to H_2O_2 released after the enzymatic reaction. Glucose responses obtained by the Ag/ DBSA/KCl/ CA/ GOx electrodes were in part dependent on the initial catalytic activity of those electrodes towards H_2O_2 reduction as illustrated in Chapters 3 and 4. Therefore, the variability of the catalysis of the DBSA/KCl-modified electrode surface would be a contribution to the lack of reproducibility shown by the biosensor devices. To assess this, data corresponding to glucose determination were ratioed with respect to the response of each electrode to $1 \cdot 10^{-3}$ M H_2O_2. Averages and standard deviation for the normalized data were determined and are shown in Fig. 5.16 and Table 5.4. Current data corresponding to $0.4-1.2 \cdot 10^{-3}$ M glucose were not considered for the regression line. As can be observed, standard errors for the normalized data were significantly lower than those calculated from the raw data. Such improvement in reproducibility was more noticeable at high glucose concentrations, where standard deviations were less than half those for the raw data.
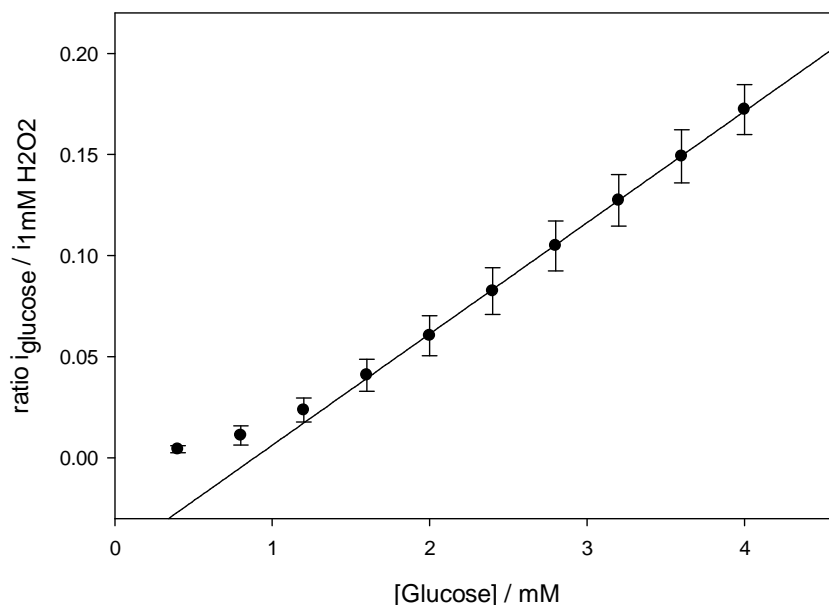
Figure 5.16. **Plot of average and standard deviation of the ratios glucose/1·10^{-3} M H$_2$O$_2$ responses vs glucose concentration for Ag/ DBSA/KCl/ CA/ GOx electrodes (n=6). Data were obtained by amperometry at –0.1 V (vs Ag/AgCl) in PBS pH 6.8. CA membrane deposited after 1 min immersion in 2% (w/v) CA solution in acetone. (slope = 5.5·10^{-2} mM^{-1}).**

The fact that better reproducibility was obtained with the normalized data pointed to the fact that the enzymatic immobilization process was not the only factor responsible of the inter-electrode variability observed, but also changes in DBSA/KCl modification. DBSA/KCl modified electrodes had undergone several modification steps during the GOx immobilization process, which might partially reduce the catalytic activity towards H$_2$O$_2$ reduction. Moreover, the manual nature of the surface modification might contribute to the poor reproducibility of the biosensors. Such issues could be improved by the use of inkjet printing for DBSA/KCl modification and material deposition by controlling and reducing reagent exposure times and reducing and precisely controlling deposited reagent volumes.

Table 5.4. Average and standard deviation for normalized data of Ag/ DBSA/KCl/ CA/ GOx (n=6)

[Glucose] / 10^{-3} M	Ratio $i_{glucose}/i_{1mM}$ $_{H2O2}$ (average)	Standard deviation	% error
0.4	0.004	0.002	50
0.8	0.011	0.005	45
1.2	0.024	0.006	25
1.6	0.041	0.008	20
2.0	0.060	0.010	17
2.4	0.083	0.012	14
2.8	0.105	0.012	11
3.2	0.127	0.013	10
3.6	0.149	0.013	9
4.0	0.172	0.012	7

The use of acetone as a CA solvent might also be responsible of the relatively poor reproducibility of the biosensors. Polan et al.[51] reported the uneven distribution of CA onto carbon screen-printed electrodes when acetone was used as a solvent. They attributed that effect to the volatility of the acetone, which vaporized very quickly while CA was spread onto the electrode surface. In the present work, the membrane was formed by immersion in a CA solution and subsequently in cold distilled water. However, the period of time employed to move the electrodes from one solution to the next one might be enough to introduce a relative variability in the membrane deposition.

Although the biosensors fabricated following the established protocol exhibited acceptable analytical performance parameters for determination of glucose compared to other devices in the literature, further studies should be carried out to obtain a more amenable GOx immobilization procedure.

5.3. CONCLUSIONS

DBSA/KCl modified Ag SPEs as developed in Chapter 3 have been used as a platform for the fabrication of a glucose biosensor. Previous investigations had shown the enhancement of the catalytic activity towards H_2O_2 undergone by Ag SPEs after

surfactant-based modification. This phenomenon was employed here for the construction of an enzymatic device for glucose determination. The feasibility of DBSA/KCl modified Ag SPEs was first assessed in the presence of the enzyme GOx in solution by amperometry. The catalytic activity of the electrodes to H_2O_2 reduction seemed to be affected by the enzymatic reaction of the glucose. Therefore, a protective membrane was required to avoid any damages on DBSA/KCl modification and simultaneously to facilitate GOx immobilization. Cellulose acetate (CA) was selected as the isolating layer and a first glucose biosensor was built by covalent attachment of GOx using hexamethylenediamine (HMDA) and glutaraldehyde (GA). Poor reproducibility was obtained with the initial values of the adopted immobilization protocol. Therefore, several parameters such as CA concentrations and appropriate solvent for its solutions, modification times in HMDA and GA were further studied. 1 min in 2% (w/v) CA in acetone, 20 min in 5% (w/v) HMDA aqueous solution and 20 min in 2.5% GA aqueous solution turned to be the optima parameters for the biosensor. An average LOD of $8.9 \cdot 10^{-5}$ M and sensitivity of $1.2 \cdot 10^{-3}$ $AM^{-1}cm^{-2}$ were obtained when glucose concentration ranged from 0.4 to $4 \cdot 10^{-3}$ M. An improved reproducibility in the measurements was reached when the cathodic currents corresponding to glucose sensing were normalized respect to the catalytic response to $1 \cdot 10^{-3}$ M H_2O_2. R.S.D. of up to 7% was obtained by six electrodes when glucose concentration was $4 \cdot 10^{-3}$ M. Such enhancement in the normalized data respect to the raw one showed the negative effect that acetone as a solvent for CA induced on the DBSA/KCl modification as well as the variability of the DBSA/KCl modified electrodes as platforms. The application of more accurate deposition technique such as inkjet printing for the surfactant-based modification first and the subsequent fabrication of a glucose biosensor will be further studied and discussed in Chapter 6.

5.4. REFERENCES

1. D. Thevenot, K. Toth, R. Durst and G. Wilson, *Analytical Letters*, 2001, **34**, 635.
2. J. D. Newman and A. P. F. Turner, *Biosensors and Bioelectronics*, 2005, **20**, 2435-2453.
3. J. Wang, *Chemical Reviews*, 2008, **108**, 814-825.
4. L. Clark, Jr. and C. Lyons, *Ann. NY Acad. Sci.*, 1962, **102**, 29.
5. G. Kouassi, J. Irudayaraj and G. McCarty, *BioMagnetic Research and Technology*, 2005, **3**, 1.
6. J. Wang, *Electroanalysis*, 2001, **13**, 983-988.
7. S. J. Updike and G. P. Hicks, *Nature* 1967, **214**, 986-988.
8. F. Scheller and F. Schubert, *Biosensors*, Elsevier Science Publishers B.V., The Netherlands, 1992.
9. L. B. Wingard, C. C. Liu, S. K. Wolfson, S. J. Yao and A. L. Drash, *Diabetes Care*, 1982, **5**, 199-202.
10. R. A. Peura, Medical Instrument Design, 1991. IEEE Case Studies in, 1991.
11. J. E. Frew and H. A. O. Hill, *Analytical Chemistry*, 1987, **59**, 933A-944A.
12. A. E. G. Cass, G. Davis, G. D. Francis, H. A. O. Hill, W. J. Aston, I. J. Higgins, E. V. Plotkin, L. D. L. Scott and A. P. F. Turner, *Analytical Chemistry*, 1984, **56**, 667-671.
13. Y. Miao, L. S. Chia, N. K. Goh and S. N. Tan, *Electroanalysis*, 2001, **13**, 347-349.
14. M. E. Ghica and C. M. A. Brett, *Analytica Chimica Acta*, 2005, **532**, 145-151.
15. A. A. Karyakin, O. V. Gitelmacher and E. E. Karyakina, *Anal. Chem.*, 1995, **67**, 2419-2423.
16. L. Zhu, J. Zhai, Y. Guo, C. Tian and R. Yang, *Electroanalysis*, 2006, **18**, 1842-1846.
17. S. Ma, J. Mu and L. Jiang, *Journal of Dispersion Science & Technology*, 2008, **29**, 682-686.
18. H. J. Wang, C. M. Zhou, F. Peng and H. Yu, *Int. J. Electrochem. Sci.*, 2007, **2**, 508-516.
19. E. Crouch, D. C. Cowell, S. Hoskins, R. W. Pittson and J. P. Hart, *Biosensors and Bioelectronics*, 2005, **21**, 712-718.
20. L. Mauko, B. Ogorevc and B. Pihlar, *Electroanalysis*, 2009, **21**, 2535-2541.
21. Z. Cao, Y. Zou, C. Xiang, L.-X. Sun and F. Xu, *Analytical Letters*, 2007, **40**, 2116-2127.
22. F. Ricci, D. Moscone, C. S. Tuta, G. Palleschi, A. Amine, A. Poscia, F. Valgimigli and D. Messeri, *Biosensors and Bioelectronics*, 2005, **20**, 1993-2000.
23. A. Salimi, E. Sharifi, A. Noorbakhsh and S. Soltanian, *Biosensors and Bioelectronics*, 2007, **22**, 3146-3153.
24. B. Yin, R. Yuan, Y. Chai, S. Chen, S. Cao, Y. Xu and P. Fu, *Biotechnology Letters*, 2008, **30**, 317-322.
25. G. L. Luque, N. F. Ferreyra and G. A. Rivas, *Microchimica Acta*, 2006, **152**, 277-283.

26.   W.-J. Guan, Y. Li, Y.-Q. Chen, X.-B. Zhang and G.-Q. Hu, *Biosensors and Bioelectronics*, 2005, **21**, 508-512.

27.   J. Gine Bordonaba and L. A. Terry, *Journal of Agricultural and Food Chemistry*, 2009, **57**, 8220-8226.

28.   M. Tudorache and C. Bala, *Analytical and Bioanalytical Chemistry*, 2007, **388**, 565-578.

29.   P. A. Vaughan, L. D. L. Scott and J. F. McAller, *Analytica Chimica Acta*, 1991, **248**, 361-365.

30.   J. Wang and X. Zhang, *Analytical Letters*, 1999, **32**, 1739 - 1749.

31.   J. Gonzalo-Ruiz, M. Asunción Alonso-Lomillo and F. Javier Muñoz, *Biosensors and Bioelectronics*, 2007, **22**, 1517-1521.

32.   P. Kotzian, P. Brázdilová, S. Řezková, K. Kalcher and K. Vytřas, *Electroanalysis*, 2006, **18**, 1499-1504.

33.   S. A. Barker, *Biosensors: Fundamentals and Applications*, Oxford University Press, Oxford, 1987.

34.   A. J. Killard and M. R. Smyth, *Biomolecular Films. Design, Function and Applications.*, Marcel Dekker, Inc., New York, 2003.

35.   S. Nakamura and Y. Ogura, *Flavins and Flavoproteins*, University of Tokyo Press, Tokyo, 1968.

36.   M. Portaccio, D. Durante, A. Viggiano, S. Di Martino, P. De Luca, D. Di Tuoro, U. Bencivenga, S. Rossi, P. Canciglia, B. De Luca and D. G. Mita, *Electroanalysis*, 2007, **19**, 1787-1793.

37.   M. M. Barsan and C. M. A. Brett, *Bioelectrochemistry*, 2009, **76**, 135-140.

38.   X. Ren, D. Chen, X. Meng, F. Tang, A. Du and L. Zhang, *Colloids and Surfaces B: Biointerfaces*, 2009, **72**, 188-192.

39.   B.-Y. Wu, S.-H. Hou, F. Yin, J. Li, Z.-X. Zhao, J.-D. Huang and Q. Chen, *Biosensors and Bioelectronics*, 2007, **22**, 838-844.

40.   K. Sugawara, T. Takano, H. Fukushi, S. Hoshi, K. Akatsuka, H. Kuramitz and S. Tanaka, *Journal of Electroanalytical Chemistry*, 2000, **482**, 81-86.

41.   P. Norouzi, F. Farnoush, B. Larijani and M. R. Ganjali, *Int. J. Electrochem. Sci.*, 2010, **5**, 1213-1224.

42.   A. F. Collings and F. Caruso, *Rep. Prog. Phys.*, 1997, **60**, 1397-1445.

43.   R. Sternberg, D. S. Bindra, G. S. Wilson and D. R. Thevenot, *Anal. Chem.*, 1988, **60**, 2781-2786.

44.   D. S. Jiang, E. Liu and J. Huang, *Key Engineering Materials*, 2003, **249**, 425-428.

45.   H. B. Yildiz, S. Kiralp, L. Toppare and Y. Yagci, *International Journal of Biological Macromolecules*, 2005, **37**, 174-178.

46.   S. Sungur, E. Emregul, G. Gunendi and Y. Numanoglu, *Journal of Biomaterials Applications*, 2004, **18**, 265-277.

47.   Y. Fu, C. Chen, Q. Xie, X. Xu, C. Zou, Q. Zhou, L. Tan, H. Tang, Y. Zhang and S. Yao, *Analytical Chemistry*, 2008, **80**, 5829-5838.

48.   M. Tortajada, D. Ramon, D. Beltran and P. Amoros, *Journal of Materials Chemistry*, 2005, **15**, 3859-3868.

49.   I. Wilson, *Handbook of Analytical Separations vol.4. Bioanalytical Separations*, Elsevier science B.V., The Netherlands, 2003.

50.   P. G. Osborne, O. Niwa, T. Kato and K. Yamamoto, *Current Separations*, 1996, **15**, 19-23.
51.   V. Polan, J. Soukup and K. Vytras, *Enzyme research*, 2011, **(in press)**.
52.   Y. H. Lee and R. Mutharasan, *Sensor Technology Handbook*, Elsevier, 2005.
53.   J. Tkáč, P. Gemeiner and E. Šturdík, *Biotechnology Techniques*, 1999, **13**, 931-936.
54.   S. Zuo, Y. Teng, H. Yuan and M. Lan, *Analytical Letters*, 2008, **41**, 1158-1172.
55.   J. Stanley, *Essentials of immunology and serology*, Delmar, Thomson Learning, 2002.
56.   S. Fischer, K. Thümmler, B. Volkert, K. Hettrich, I. Schmidt and K. Fischer, *Macromolecular Symposia*, 2008, **262**, 89-96.
57.   C. M. A. Brett and A. M. O. Brett, *Electroanalysis*, Oxford Scienc Publications, 1998.
58.   S.-H. Lee, H.-Y. Fang and W.-C. Chen, *Sensors and Actuators B: Chemical*, 2006, **117**, 236-243.
59.   B.-Y. Wu, S.-H. Hou, F. Yin, Z.-X. Zhao, Y.-Y. Wang, X.-S. Wang and Q. Chen, *Biosensors and Bioelectronics*, 2007, **22**, 2854-2860.

Chapter 6

**Development of a glucose biosensor based on a
surfactant/salt-modified silver-based electrocatalyst
fabricated by inkjet printing**

6.1. INTRODUCTION

The fabrication of biosensors and other related biomedical devices requires the localised interaction of biological molecules and biomaterials with an analyte contained in a sample fluid. This necessitates the placing of the biomolecule in a defined location in the biosensor device. In the past, sensors and biosensors were relatively complex devices in terms of the diversity of parts and techniques required to assemble them. This led to high device manufacturing costs. In recent years, the production of biosensors has moved to fabrication and production processes that allow for high throughput, highly parallel, mass manufacture. Such processes have had the common feature of a system of production based on a flexible, planar manufacturing platform inspired by the traditional print media industry, particularly screen printing.

In more recent times, inkjet printing has become one of the most promising techniques capable of manufacturing low cost electronic biosensor platforms. In terms of patterning, inkjet printing is one of the most versatile methods available for prototyping. It also allows the deposition of very small volumes of ink (picolitres) in a rapid procedure, achieving high pattern precision and resolution with greater reproducibility than that of other techniques such as screen-printing.[1] Moreover, the fact that no mask is required to pattern the ink and the absence of physical contact between printhead and printed substrate further facilitate the printing process.

Inkjet printing operates by the highly controlled ejection of low volumes of ink from a printhead employing a single nozzle or a series of nozzles. It permits the deposition of tiny droplets (≥ 1 pl) onto a substrate (glass, plastic, metal, etc.) with high precision and reproducibility. Resolutions higher than 1200 dpi (dots-per-inch) can be reached with the modified desktop Olivetti system, which means a dot diameter of approx. 15-40 μm, depending on printing material and substrate.[1]

Four techniques exist to bring about ejection of droplets from a printhead. These are thermal, piezoelectric, electrostatic and acoustic.[2, 3] However, the most common inkjet printers are based on either drop-on-demand thermal and piezoelectric printheads (Fig. 6.1).
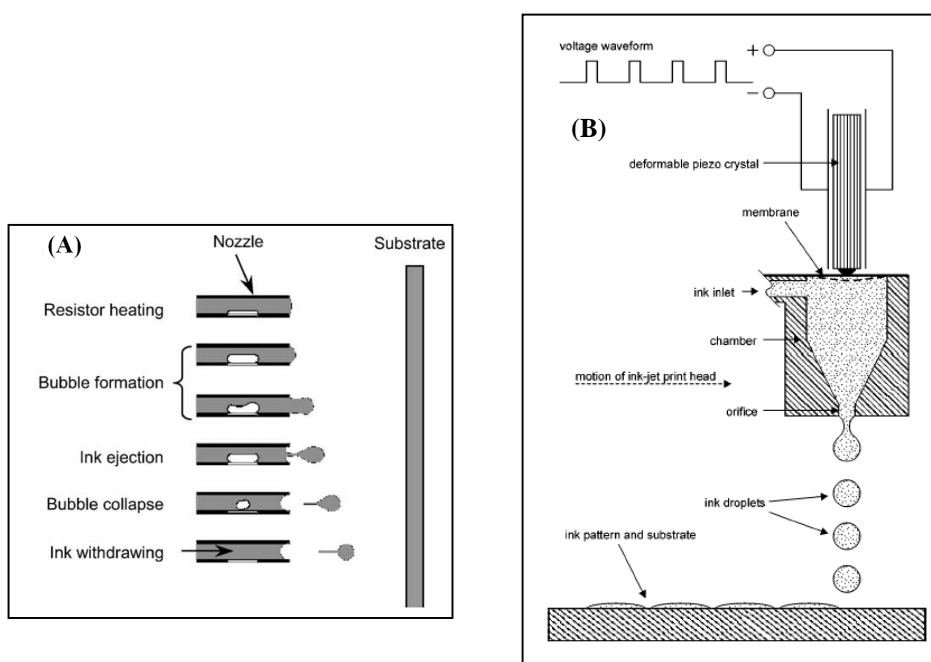
Figure 6.1. **Principles of operation of (A) Thermal[4] and (B) Piezoelectric[5] inkjet printing ejection mechanisms.**

To develop an ink that is printable, rheological properties such as viscosity and surface tension are critical. As a droplet is expelled from the orifice of a nozzle, energy goes into viscous flow, surface tension of the drop and kinetic energy. The viscosity must be low enough to allow the channel to be refilled in about 100 μs.[6] The surface tension must be high enough and the pressure low enough, to hold the ink in the nozzle without dripping. The viscosity of the ink should be in the range of 3-20 cP and the surface tension between 20 and 70 dyncm^{-1} to avoid clogging or dripping and to ensure continuous film formation onto the substrate surface in a piezoelectric inkjet printing system.[7, 8] These precise characteristics depend on the ejection mechanism and the end-application for the printed films.[9, 10] It is often necessary to add wetting agents, pigments and polymeric compounds to improve resolution and printed film quality.[1, 8, 11]

The range of functional ink materials that can be printed has increased greatly during the last number of years. Inks can be printed directly to an unmodified substrate or after

a pre-treatment in order to induce air-stability and solution processability. For example, PEDOT can be doped with PSS to permit its dispersion in water to obtain a printable ink.[4, 12, 13] Resulting polymer films possess good conductivities (1-10 S cm^{-1})[13] and high stability in the solid film form and have been used for the fabrication of biosensors,[1] thin film transistors[12] and other electronic circuits.[14] Surfactant-dispersed PANI nanoparticles have been inkjet printed using a piezoelectric device by Morrin et al.[15] Conducting polymers such as PANI are important promising materials in terms of both optical and electrochemical sensing and are being extensively researched at a nanostructured level, where processability can be significantly improved.

Most large-scale applications for inkjet printing carried out to date have been based on high value or high volume products such as solar panels, OLED displays, electronic components, graphics, packaging and other industrial marking. However, many are now turning to its application in biosensing devices, for both industrial and R&D purposes. Thus, as well as conducting polymer and organic materials, new biological materials including enzymes, single-stranded DNA (ssDNA) oligomers[16, 17] and human cells[18] have been developed and printed using this technique.

Although inkjet printing technology has been exploited for the last number of years for the printing of functional materials, new applications, especially in the biosensing field, are constantly emerging. Its unique characteristics, range of materials that can be printed, non-contact mode and its simple handling make this technique feasible to large-scale production. In addition, inkjet printing permits the use of environmentally friendly solvents and the waste production is minimal as small quantities of printed material are required, as opposed to more traditional deposition techniques such as screen-printing. Therefore, inkjet printing has proven to be a useful technique to pattern a high variety of material simply and quickly; key characteristics for the application of any deposition technique.

In the present work, inkjet printing was used to deposit DBSA/KCl solution onto Ag SPEs and its catalytic effect towards H_2O_2 reduction was assessed. The previous chapter had shown a lack of reproducibility between glucose biosensors, partially attributed to the poor reproducibility of the modification steps due to their manual nature. The use of inkjet printing for DBSA/KCl deposition might improve the variability of the sensing

devices by enhancing the control of the reagent volume and exposure times. Cyclic voltammetry and amperometry were performed to compare the catalytic activity on H_2O_2 of electrodes modified by both inkjet printing and dip-coating techniques. Inkjet printing parameters such as ejection volume, solution concentrations and nozzle voltage were subsequently optimised. Scanning Electron Microscopy was performed to characterize electrode surfaces modified by both deposition mechanisms. GOx was then immobilized onto the inkjet printed DBSA/KCl modified electrodes following the standard protocol adopted in the previous chapter and its catalytic activity on glucose determination was evaluated. Analytical parameters such as LOD, sensitivity and inter-electrode reproducibility were calculated and contrasted with other data in the literature.

6.2. RESULTS AND DISCUSSION

As was observed in previous chapters, the DBSA/KCl modification of Ag SPEs led to an enhancement of the catalytic characteristics of that material towards H_2O_2 electrochemical reduction. Up to now, such modification was carried out by immersing the electrodes in the surfactant-based modification solution for approx. 3 h. However, higher reproducibility, shorter modification times, and better production processing might be reached by using a technique such as inkjet printing. The application and optimization of such a technique for DBSA/KCl modification is discussed and its application to a glucose biosensor assessed.

6.2.1. Modification of the silver electrode by the inkjet print deposition of DBSA/KCl

DBSA/KCl Ag SPEs modified by inkjet printing were compared to those modified by dip-coating in the surfactant-based solution by means of cyclic voltammetry and amperometry. These electrochemical techniques were first performed on the unmodified electrodes in PBS, pH 6.8 as controls. Subsequently, Ag SPEs were either dipped into a solution of $3.3 \cdot 10^{-2}$ M DBSA/ 0.1 M KCl for 3 h or the modification solution was inkjet printed onto the electrodes. Five layers of surfactant-based solution were inkjet printed at a nozzle voltage of 18 V by means of a 16-nozzle head cartridge. The excess of modification solution was removed from the surfaces by rinsing the electrodes thoroughly with distilled water. The inkjet printed solution was allowed to dry for five minutes before washing. The modified electrodes were then subjected to cyclic voltammetry and amperometry in PBS, pH 6.8. Final H_2O_2 concentrations in the solution ranged from $1 \cdot 10^{-3}$ to $5 \cdot 10^{-3}$ M. Fig. 6.2 shows the cyclic voltammograms for unmodified, dip-coated DBSA/KCl modified and inkjet printed DBSA/KCl modified Ag SPEs in the absence of H_2O_2. As can be observed, the non-faradaic or charging current from the cyclic voltammograms was much higher for the modified electrodes than for the unmodified one. To be precise, dip-coated DBSA/KCl modified electrode showed a non-faradaic current of $2.4 \cdot 10^{-5}$ A at –0.1 V whereas the current for the unmodified

electrode was $3.6 \cdot 10^{-7}$ A at the same potential. As was previously mentioned in Chapter 3, the almost 70-fold difference in the charging current indicated that Ag SPEs had undergone a surface modification after immersion into the surfactant/salt solution. The non-faradaic current corresponding to the inkjet printed DBSA/KCl modified electrode was $2.1 \cdot 10^{-5}$ A, which was only marginally lower than the dip-coated electrode. Such similarity illustrated that DBSA/KCl modified electrodes by inkjet printed seemed to also undergo a surface modification comparable with that carried out by the dip-coating technique employed initially.
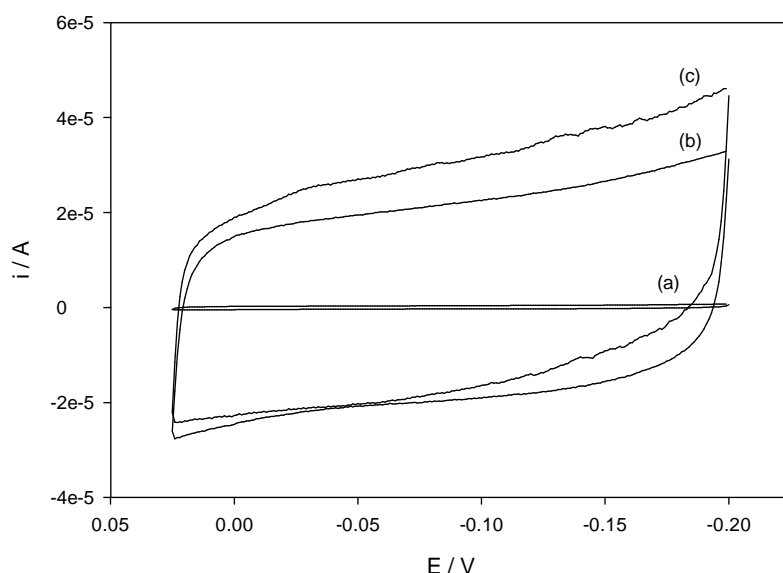
Figure 6.2. **Cyclic voltammograms of Ag SPEs measured in PBS pH 6.8 solution, in the absence of H_2O_2: (a) unmodified; (b) $3.3 \cdot 10^{-2}$ M DBSA/ 0.1 M KCl modified by inkjet printing and (c) $3.3 \cdot 10^{-2}$ M DBSA/ 0.1 M KCl modified by dip-coating.**

Typical amperometric responses for the unmodified and DBSA/KCl modified electrodes in H_2O_2 are shown in Fig. 6.3. These were performed at –0.1 V (vs Ag/AgCl) in PBS pH 6.8. The cathodic currents exhibited by the unmodified, dip-coated and inkjet printed DBSA/KCl modified Ag SPEs in the presence of $5 \cdot 10^{-3}$ M H_2O_2 were $1.7 \cdot 10^{-7}$ A,

$5.6 \cdot 10^{-5}$ A and $3.1 \cdot 10^{-5}$ A, respectively. As was previously suggested by the non-faradaic currents from the cyclic voltammograms, inkjet printed DBSA/KCl modified Ag SPE underwent a surface modification which led to an enhancement in its catalytic activity towards H_2O_2 reduction. Although the modification time was remarkably reduced by the inkjet printing process (from 3 h to 10 min), the cathodic current shown by the dip-coated modified electrode was only some two-fold higher than that provided by the inkjet printed modification. However, the initial charging current and the background current were lower for the electrode modified by inkjet printing, as well as reaching steady state more quickly. Several printing parameters such as ejection volume, DBSA and KCl concentrations in the cartridge, nozzle voltage and the effect of washing after printing were investigated to further improve the inkjet deposition methodology.
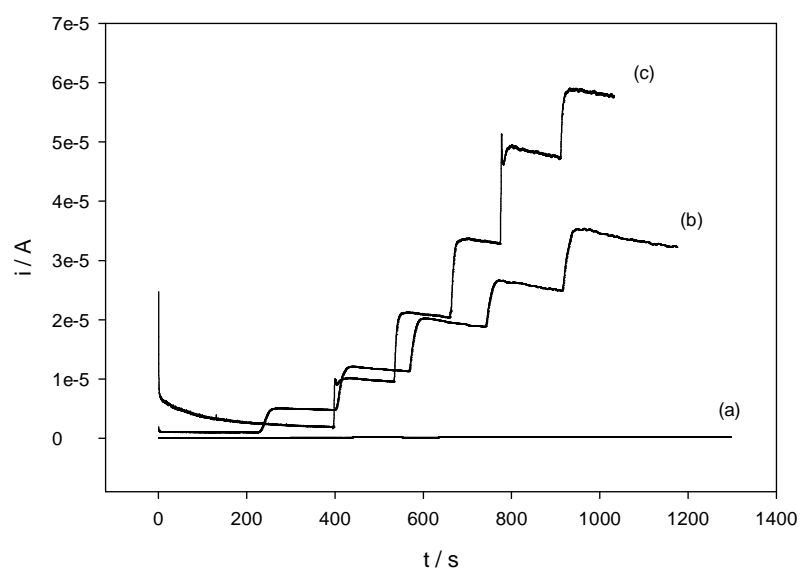
Figure 6.3. **Amperometric responses of Ag SPEs measured at –0.1 V (vs Ag/AgCl) in PBS pH 6.8: (a) unmodified; (b) $3.3 \cdot 10^{-2}$ M DBSA/ 0.1 M KCl modified by inkjet printing and (c) $3.3 \cdot 10^{-2}$ M DBSA/ 0.1 M KCl modified by dip-coating, at H_2O_2 concentration from 1 to $5 \cdot 10^{-3}$ M.**

6.2.1.1. Optimization of the ejection volume

Drop-on-demand piezoelectric inkjet printing is based on the application of a pressure pulse generated by an electromechanical actuator to a chamber of liquid behind a printing aperture. The printhead is previously positioned where required and drops are generated "on demand" when necessary in order to create the established pattern.[19] The mass of modifying agent that is deposited is a combination of the concentration and the volume of liquid per unit area that can be deposited, which is in turn dependent on the contact angle of the liquid on the surface. One of the ways of increasing the mass of modification solution that the surface is exposed to is to increase the number of prints, assuming that the concentration remains constant. Multiple overprints can be performed automatically as required.[20] The greater the number of prints, the greater the total amount of material ejected onto the substrate. There are generally two modes of depositing materials by an inkjet printer. The first one is a firing mode and consists of just ejecting material at a fixed position whereas the second one allows simultaneous pattern deposition on several electrodes. The first mode can be used to calculate the drop volume, simply by weighing the substrate before and after the deposition of a certain amount of drops and approximating the material density to that of water ($1 \ g \cdot ml^{-1}$). This mode allows deposition of larger quantities of material, which reduces the error in the volume calculation due to evaporation, but does not allow pattern formation. However, the second method permits the generation of any pre-defined or customized pattern. The material is here deposited layer-by-layer and generally the amount of material is so small that this leads to significant errors in volume estimations. This error is generally enhanced by the high evaporation rate due to the high solution area exposed to air.

The aim in the present work was the development of a protocol for the inkjet printing of the DBSA/KCl modification solution and its subsequent use in the development of a glucose biosensor. The ejection volume was evaluated according to the number of prints deposited, assuming solution concentration remains invariable.

The optimum number of prints was assessed by amperometry, contrasting the catalytic response of the modified electrodes in H_2O_2. The concentrations in the modification solution for the inkjet printing procedure were the same as those used for

dip-coating being $3.3 \cdot 10^{-2}$ M DBSA/ 0.1 M KCl. Five electrodes were modified with the same number of prints simultaneously and the average and standard deviation for the cathodic currents were calculated. Fig. 6.4 shows the average and standard deviation for the catalytic response of Ag SPEs modified by inkjet printing versus the number of prints of material deposited. As can be observed, one print of surfactant-based solution onto Ag SPEs was enough to enhance the catalytic response of the electrodes towards H_2O_2 reduction. As was presented in the previous section, the cathodic current provided by an unmodified Ag SPE in the presence of $5 \cdot 10^{-3}$ M H_2O_2 was $7.0 \cdot 10^{-7}$ A whereas the average current after one print of DBSA/KCl was $1.91 \cdot 10^{-5}$ A. This difference of almost two orders of magnitude in the response demonstrated the immediate modification of the electrode surface after its contact with the DBSA/KCl solution. In Chapter 3, the rapidity of the modification phenomenon was already noted, and is reinforced by the inkjet printed solution as well as the little amount of solution required for the modification being effective.
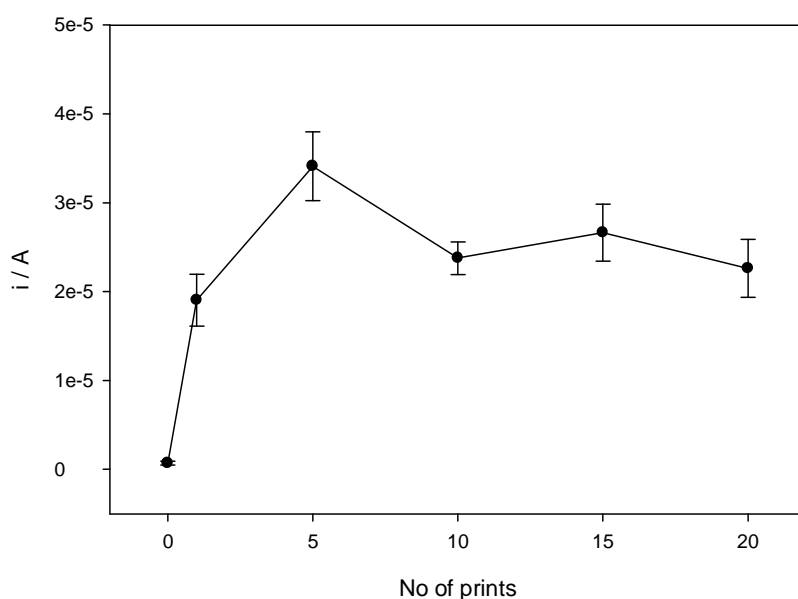
Figure 6.4. **Plot average cathodic current and standard deviation at $5 \cdot 10^{-3}$ M H_2O_2 vs no of prints of DBSA/KCl inkjet deposited onto Ag SPEs. The data at 0 prints corresponds to the unmodified Ag SPE.**

The catalytic response of the electrodes seemed first to increase from 1 to 5 prints and then decrease above this, as can be seen in Fig. 6.4. Thus, the cathodic current at –0.1 V (vs Ag/AgCl) in the presence of $5 \cdot 10^{-3}$ M H_2O_2 showed by Ag SPE following five prints of modification solution deposition was $3.41 \cdot 10^{-5}$ A whereas the corresponding currents after 10, 15 and 20 prints inkjet printed were $2.38 \cdot 10^{-5}$ A, $2.67 \cdot 10^{-5}$ A and $2.26 \cdot 10^{-5}$ A, respectively. A possible explanation for this behavior might be related to the amount of DBSA/KCl solution required for the modification. The adsorption of the DBSA/KCl to the electrode surface would follow an adsorption isotherm. The volume of modification solution on the electrode surface would act as a reservoir from which DBSA/KCl is adsorbed. This would then deplete the solution of DBSA/KCl. It would appear that five prints allowed sufficient adsorption of DBSA/KCl to the electrode to result in its complete modification. Above this, this effect was either not apparent, or actually slightly reduced the performance of the electrode due, possibly, to inhibitory concentrations of the modification material.

Thus, five prints of the surfactant-based solution seemed to be optimum to achieve the highest enhancement in H_2O_2 catalysis. Therefore, five prints of DBSA/KCl solution, which were equivalent to $1.0 \cdot 10^{-8}$ l, were used in further optimization experiments.

6.2.1.2. Re-optimization of the DBSA and KCl concentrations in the modification solution

Having established that five cycles of inkjet printing of the modification solution were necessary to observe the highest catalytic responses, the concentrations of DBSA and KCl were re-assessed to establish whether the concentrations used for dip-coating were also optimal for inkjet printing. Cyclic voltammetry and amperometry were first performed in the presence of $3.3 \cdot 10^{-2}$ M DBSA over a range of KCl concentrations followed by 0.1 M KCl over a range of DBSA concentrations. The cathodic responses to $5 \cdot 10^{-3}$ M H_2O_2 were correlated with DBSA or KCl concentrations. Fig. 6.5 shows the responses of Ag SPEs after five prints of $3.3 \cdot 10^{-2}$ M DBSA/KCl were deposited. As can be observed, the catalytic effect on H_2O_2 reduction increased with KCl concentration in

the modification solution to be printed, with an optimum value reached at 0.1 M KCl. The cathodic currents for $4 \cdot 10^{-3}$ M, $4 \cdot 10^{-2}$ M and 0.1 M KCl in the presence of $5 \cdot 10^{-3}$ M H_2O_2 were $2.6 \cdot 10^{-6}$ A, $1.99 \cdot 10^{-5}$ A and $3.11 \cdot 10^{-5}$ A, respectively. Higher concentrations of KCl did not lead to an improvement in H_2O_2 catalysis. This was the same concentration established for dip-coating. Therefore, the optimum KCl concentration in the modification solution for inkjet printing was 0.1 M.
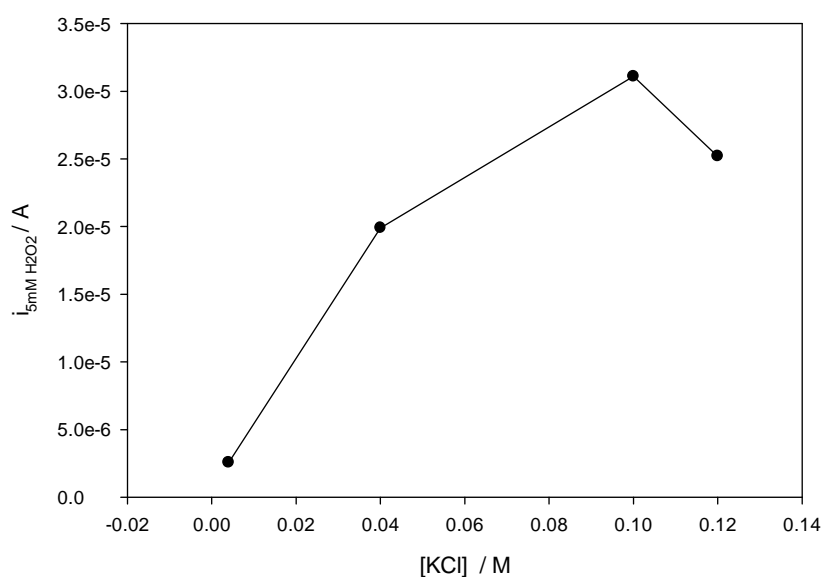
Figure 6.5. **Plot of current vs [KCl] obtained during amperometric measurements of inkjet printed modified Ag SPEs at –0.1 V (vs Ag/AgCl) at $5 \cdot 10^{-3}$ M H_2O_2. The electrodes were modified with a mixed solution of $3.3 \cdot 10^{-2}$ M DBSA and KCl.**

Fig. 6.6 shows the results of a similar study, using 0.1 M KCl and a range of DBSA concentrations. The enhancement of the H_2O_2 reduction current was shown to be dependent on DBSA concentrations with an increasing catalytic effect observed at higher DBSA concentration. Thus, at $3.3 \cdot 10^{-3}$ M DBSA the cathodic current observed in the presence of $5 \cdot 10^{-3}$ M H_2O_2 was $1.08 \cdot 10^{-5}$ A whereas at $1.67 \cdot 10^{-2}$ M DBSA the reduction current was $1.52 \cdot 10^{-5}$ A. The optimum DBSA concentration in the

modification solution was found to be approx. $3.3 \cdot 10^{-2}$ M, where the cathodic current for the studied electrode reached a value of $1.86 \cdot 10^{-5}$ A. Further increases in DBSA concentrations did not provide higher catalytic responses on H_2O_2 reduction, e.g. the cathodic current observed for $6.7 \cdot 10^{-2}$ M DBSA was $1.59 \cdot 10^{-5}$ A. Again, this was identical to that established for dip-coating.
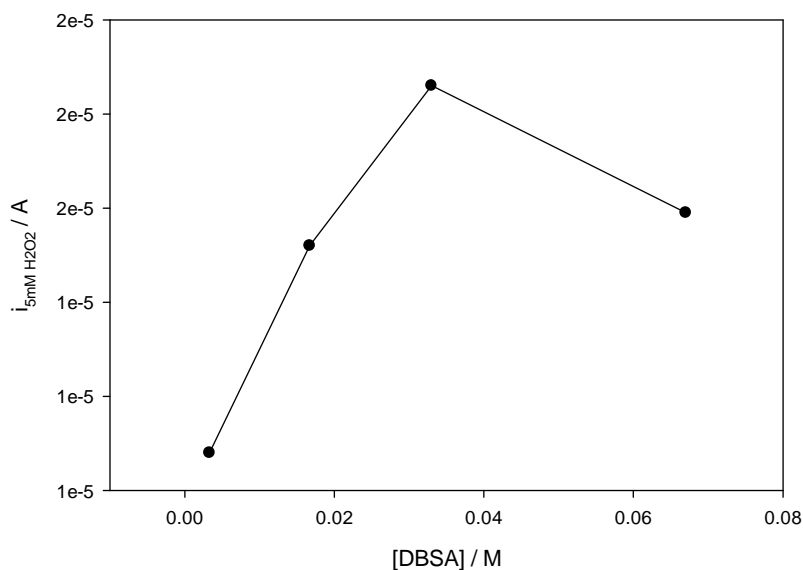
Figure 6.6. **Plot of current vs [DBSA] obtained during amperometric measurements of inkjet printed modified Ag SPEs at –0.1 V (vs Ag/AgCl) at $5 \cdot 10^{-3}$ M H_2O_2. The electrodes were modified with a mixed solution of 0.1 M KCl and DBSA.**

Hence, a solution of $3.3 \cdot 10^{-2}$ M DBSA and 0.1 M KCl was established as the optimum modification solution for the treatment of Ag SPEs by inkjet printing and this was used in subsequent experiments. These data further suggest that the optimum concentration of the DBSA/KCl is a critical feature of the surface modification process as increases in either do not result in further enhanced catalysis, even when the volume of the modification solution is limiting as is the case in the inkjet printed methodology. This lends further weight to the argument that the DBSA/KCl solution forms structures

that are deposited at the electrode surface. It also suggests that this ratio of concentrations are also most appropriate for deposition using inkjet printing and that the DBSA/KCl survives the inkjet printing process, at least to a significant degree.

To assess the effect of the contact time of the modification solution with the electrode surface, some electrodes were rinsed immediately after inkjet printing at a nozzle voltage of 30 V, whereas the rest were left unwashed for 4 hours (Fig. 6.7).
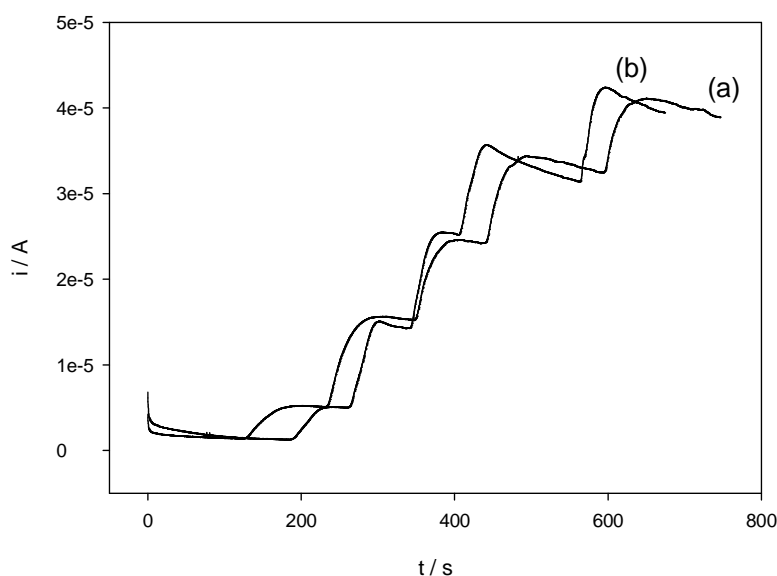
Figure 6.7. **Amperometric responses of Ag SPEs measured at –0.1 V (vs Ag/AgCl) in PBS pH 6.8, at H_2O_2 concentration from 1 to $5 \cdot 10^{-3}$ M. Electrodes were modified with DBSA/KCl by inkjet printing and then rinsed with distilled water (a) immediately or (b) 4 h after the printing process. Nozzle voltage: 30 V.**

This suggests that longer exposure times to the inkjet printed DBSA/KCl solution did not seem to lead to higher catalytic effect towards H_2O_2 electrochemical reduction. In Chapter 3, 3h dip-coated in the DBSA/KCl solution was chosen as the optimum modification time. In this case, the printing technique might limit the modification process and no further enhancement was observed with time. Thus, the small amounts of

DBSA/KCl solution deposited compared to those used for the dip-coating process might lead to a quick evaporation of the water and a decrease in the number of lamellar structures formed in the solution, even a partial breaking-down. That would lead to lower catalytic responses and no further influence of the modification time.

The cathodic current obtained in the presence of $5 \cdot 10^{-3}$ M H_2O_2 by the electrode washed immediately after inkjet printing was $3.84 \cdot 10^{-5}$ A whereas the reduction current from the electrode washed 4 h later was $3.83 \cdot 10^{-5}$ A. The steady state background currents exhibited by both electrodes were also analogous, being $1.4 \cdot 10^{-6}$ A and $1.3 \cdot 10^{-6}$ A, respectively.

6.2.1.3. Optimization of nozzle voltage

Nozzle voltage can also influence the level of catalytic activity of the modification solution on Ag SPEs by affecting two parameters: the actual voltage felt by the solution and the volume of deposited material. Increasing the printing voltage has been found to increase both drop velocity and drop mass when the deposition time is kept constant.[18, 21] Hence, by controlling the excitation voltage applied to the piezoelectric transducer, it is possible to vary the quantity of ejected solution.

DBSA/KCl solution was printed onto a pre-weighed container for 60 s at 5 kHz frequency with the application of a range of nozzle voltages. The number of drops was estimated by multiplying the ejection time by the frequency and by the number of working nozzles. The drop mass was then calculated by dividing the mass of solution ejected by the number of drops. The results for each nozzle voltage are shown in Table 6.1. The plot of drop mass versus nozzle voltage for the inkjet printing process is illustrated in Fig. 6.8. As can be seen, the drop mass did increase with nozzle voltage in a non-linear fashion. For example, the drop mass obtained applying 25 V, $14.85 \cdot 10^{-11}$ g, was only two-fold higher than that achieved applying 13 V, $7.14 \cdot 10^{-11}$ g, whereas at 30 V the drop mass was found to be more than four-fold higher at $31.82 \cdot 10^{-11}$ g.

Table 6.1. Data related to nozzle voltage and the amount of material ejected.

Nozzle voltage / V	No. of working nozzles	No. of drops ejected in 60 s	Mass difference / g	Drop mass / g
13	7	$2.1 \cdot 10^6$	$1.5 \cdot 10^{-4}$	$7.14 \cdot 10^{-11}$
16	9	$2.7 \cdot 10^6$	$1.1 \cdot 10^{-4}$	$4.07 \cdot 10^{-11}$
20	11	$3.3 \cdot 10^6$	$4.4 \cdot 10^{-4}$	$13.33 \cdot 10^{-11}$
25	11	$3.3 \cdot 10^6$	$4.9 \cdot 10^{-4}$	$14.85 \cdot 10^{-11}$
30	11	$3.3 \cdot 10^6$	$10.5 \cdot 10^{-4}$	$31.82 \cdot 10^{-11}$
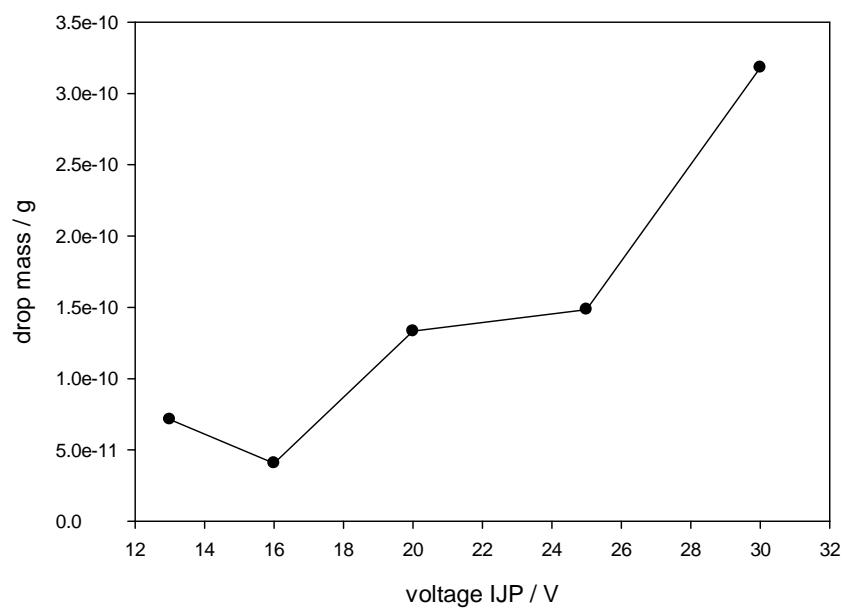
Figure 6.8. **Plot of drop mass vs nozzle voltage applied during the inkjet printing process of $3.3 \cdot 10^{-2}$ M DBSA/ 0.1 M KCl solution.**

The effect of the nozzle voltage on H_2O_2 catalysis was then studied. DBSA/KCl modification solution was inkjet printed on Ag SPEs applying several nozzle voltages. The electrodes were then rinsed thoroughly with distilled water and amperometry at –0.1

V (vs Ag/AgCl) in PBS pH 6.8 was performed. Fig. 6.9 illustrates the plot of the effect of the nozzle voltage on the resulting catalytic response to H_2O_2. The effect of exposure time of the modification solution is again evaluated here. Once again, the exposure time following printing did not change the catalytic response. With regard to nozzle voltage, a voltage of 10 V was not strong enough to cause the ejection of the solution and so, therefore, did not show any catalysis. Little change in catalytic current was observed between 13 and 30 V suggesting that nozzle voltage did not have any effect on the formation of the catalytic surface. As was already commented earlier, DBSA/KCl volumes above a certain level did not improve the catalytic activity of Ag SPEs towards H_2O_2.
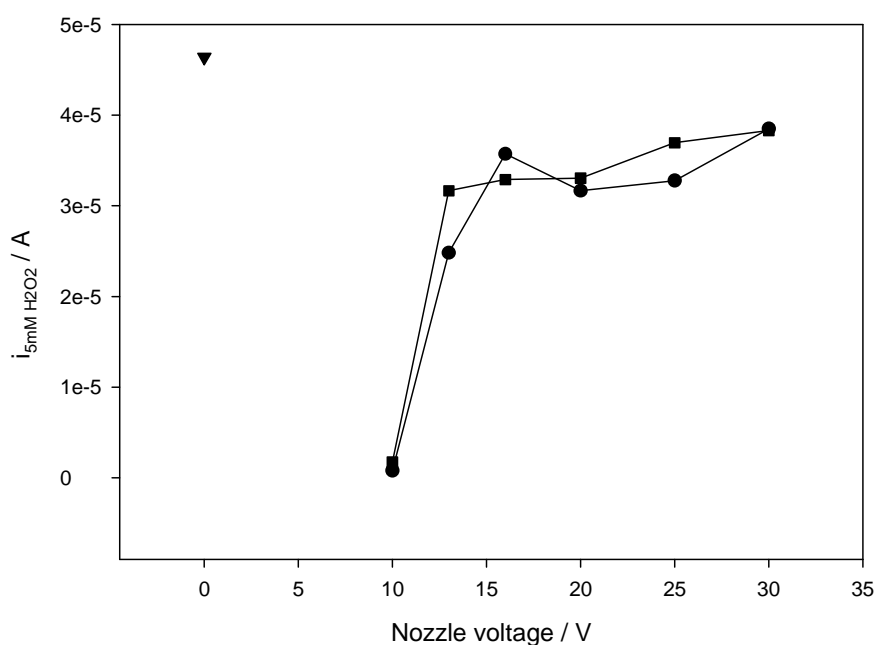
Figure 6.9. **Plot of current vs nozzle voltage obtained during amperometric measurements of Ag SPEs at –0.1 V (vs Ag/AgCl) at $5 \cdot 10^{-3}$ M H_2O_2. The electrodes were inkjet printed modified with $3.3 \cdot 10^{-2}$ M DBSA/ 0.1 M KCl solution and (●) washed immediately or (■) 4 h after the printing process. Data at nozzle voltage 0 V (▼) corresponds to dip-coated modified electrodes.**

The highest catalytic activity was detected at 30 V, $3.9 \cdot 10^{-5}$ A. This value was only some 1.2-fold lower than that showed by the dip-coated modified electrode, $4.6 \cdot 10^{-5}$ A. Such similarity illustrated that inkjet printed technique was a feasible method for DBSA/KCl modification of Ag SPEs. However, such difference between techniques might imply that the application of any voltage, even 13 V, to DBSA/KCl solution already have an effect on it, leading to the 1.2-fold reduction in catalysis observed. 16 V was selected as the optimum nozzle voltage for further DBSA/KCl deposition as it provided sufficient enhancement of catalysis. Since the catalytic effect towards H_2O_2 reduction did not appear to be significantly affected by exposure time, electrodes were subsequently prepared by the deposition of 5 rounds of printing, immediately followed by rinsing and drying.

6.2.2. Comparison of DBSA/KCl modification by inkjet printing and dip-coating

Having established five prints ($1.0 \cdot 10^{-8}$ l), $3.3 \cdot 10^{-2}$ M DBSA/ 0.1 M KCl and a 16 V nozzle voltage as the optimal parameters for DBSA/KCl modification of Ag SPEs by inkjet printing, a final comparison between this method and dip-coating was performed. A reproducibility study was first carried out. Ag SPEs were immersed in DBSA/KCl solution for 3 h (n=10). The same modification solution was inkjet-printed simultaneously onto Ag SPEs (n=8). All the electrodes were then rinsed with distilled water and amperometric responses to H_2O_2 at –0.1 V (vs Ag/AgCl) in PBS, pH 6.8 were monitored (Fig. 6.10 and Table 6.2). The DBSA/KCl modified electrodes prepared by dip-coating showed consistently higher catalytic responses towards H_2O_2 reduction than those electrodes treated by inkjet printing. Thus, the average reduction currents in the presence of $1 \cdot 10^{-3}$ M H_2O_2 were $5.6 \cdot 10^{-6}$ A and $3.5 \cdot 10^{-6}$ for dip-coated and inkjet-printed, respectively, whereas the average cathodic responses at $5 \cdot 10^{-3}$ M H_2O_2 were $4.64 \cdot 10^{-5}$ A and $2.79 \cdot 10^{-5}$ A, respectively. Subsequently, the average sensitivity calculated for the inkjet printed modified electrodes was $4.9 \cdot 10^{-2}$ AM^{-1}cm^{-2}, which was 1.6-fold lower than that obtained for the dip-coated modified electrodes at $8.1 \cdot 10^{-2}$ AM^{-1}cm^{-2}. Despite all the optimization steps performed to improve the catalytic activity of the inkjet-printed modification of the electrodes, dip-coated electrodes provided higher reduction currents

for H_2O_2. One possible explanation might be an as yet identified impact that inkjet printing technique has on the DBSA/KCl solution. It was observed that voltages lower than 13 V did not allow solution deposition. Higher nozzle voltages however led to DBSA/KCl deposition but it might be in some measure altered after the printing process, bringing about a different behaviour of the modified electrodes towards H_2O_2 reduction. In previous chapters, the catalytic enhancement observed on Ag SPEs after DBSA/KCl treatment was partially attributed to the interaction of micellar/lamellar structures from the solution with the screen printed electrode surface. If the printing process affected the structure of the modification solution, that would change its catalytic effect and would diminish the catalytic enhancement towards H_2O_2.
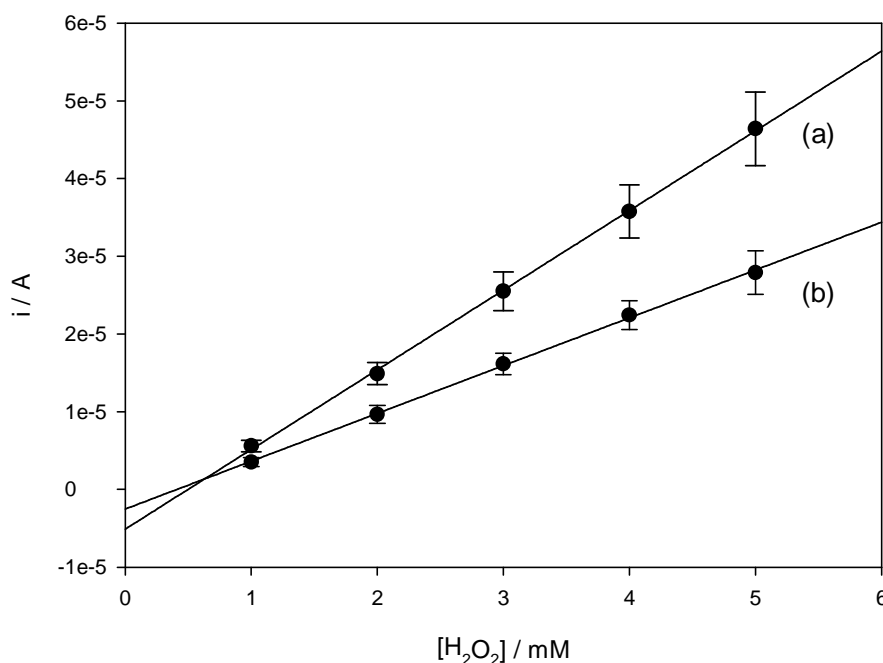
Figure 6.10. **Measurements of H_2O_2 at –0.1 V (vs Ag/AgCl) in PBS pH 6.8 using the DBSA/KCl modified Ag SPEs (a) by dip-coating (n = 10) or (b) by inkjet printing (n = 8).**

Regarding the variability of the modification methods, both techniques exhibited similar relative reproducibility in the measurements, with improved data at higher H_2O_2 concentrations. Thus, the variability in the cathodic currents found in the presence of $1 \cdot 10^{-3}$ M H_2O_2 were 17% and 13% for the inkjet printing and dip-coating method, respectively, whereas the reproducibility increased up to 10% in both cases at $5 \cdot 10^{-3}$ M H_2O_2. However, comparing % error, the lower signals achieved by the inkjet printed sensor were not taking into account, as will be commented on below.

Table 6.2. Statistical data corresponding to the catalytic activity to H_2O_2 reduction of DBSA/KCl modified Ag SPEs by inkjet printing and dip-coating.

[H_2O_2] / mM	INKJET PRINTING			DIP-COATING		
	i_{cat} (avrg) / A	Stand dev	% error	i_{cat} (avrg) / A	Stand dev	% error
1	$3.5 \cdot 10^{-6}$	$0.6 \cdot 10^{-6}$	17	$5.6 \cdot 10^{-6}$	$0.7 \cdot 10^{-6}$	13
2	$9.7 \cdot 10^{-6}$	$1.2 \cdot 10^{-6}$	12	$1.49 \cdot 10^{-5}$	$1.4 \cdot 10^{-6}$	9
3	$1.61 \cdot 10^{-5}$	$1.4 \cdot 10^{-6}$	9	$2.55 \cdot 10^{-5}$	$2.5 \cdot 10^{-6}$	10
4	$2.42 \cdot 10^{-5}$	$1.9 \cdot 10^{-6}$	8	$3.58 \cdot 10^{-5}$	$3.4 \cdot 10^{-6}$	9
5	$2.79 \cdot 10^{-5}$	$2.8 \cdot 10^{-6}$	10	$4.64 \cdot 10^{-5}$	$4.7 \cdot 10^{-6}$	10

These reproducibility and sensitivity values were in line with data reported in the literature for other enzyme-modified screen printed electrodes for the detection of H_2O_2. Thus, Li et al.[22] developed a disposable amperometric H_2O_2 biosensor based on carbon screen-printed electrodes and horseradish peroxidase (HRP) entrapped in a polypyrrole film deposited on the surface. The biosensor showed a sensitivity of $3.324 \cdot 10^{-2}$ $AM^{-1}cm^{-2}$ and a reproducibility of 10.24% r.s.d. (n = 5). Improved analytical parameters were obtained with other screen printed based H_2O_2 sensors. Ricci et al.[23] employed a PB modified carbon screen printed electrode to detect H_2O_2 at an applied potential of –0.05 V (vs an internal screen printed Ag pseudoreference electrode). The electrode provided a sensitivity of 0.234 $AM^{-1}cm^{-2}$ and a LOD of 10^{-7} M, and the r.s.d. was up to 5% (n = 6).

The modified screen printed electrodes were then used as a platform for the immobilization of enzymes such as glucose oxidase or choline oxidase. Xu et al.[24] described the fabrication of a disposable H_2O_2 biosensor by the immobilization of HRP on a colloidal gold modified carbon screen printed electrodes. The biosensor exhibited a sensitivity of 0.307 $AM^{-1}cm^{-2}$ and r.s.d. of 2.7 and 2.3% (n = 10) at 8 and 20·10^{-6} M H_2O_2, respectively. Higher sensitivities were obtained by PB modified Au and Pt screen printed electrodes. De Mattos et al.[25] reported the development of amperometric sensors selective for H_2O_2 detection by galvanostatically depositing a PB film on both Au and Pt screen printed electrodes. The sensors displayed sensitivities towards H_2O_2 of 1 and 2 $AM^{-1}cm^{-2}$ for the Pt and Au based electrodes, respectively. The sensors were subsequently employed for the construction of glucose biosensors by crystallised GOx immobilization in a Nafion membrane. Although slightly lower, the reproducibility of the H_2O_2 sensors created by dip-coated or inkjet printed DBSA/KCl modification of Ag SPEs seems to be in the same range than other systems found in the literature. Although the inkjet printing process did not necessarily improve the reproducibility, it did not make it worse. Therefore, the issue of the reproducibility may be as a result of the electrode surface. During the dip-coating technique, the process is homogeneous so it may be the heterogeneity of the electrode surface that is the underlying cause of the response variability. On the other side, the surfactant-based sensor developed here does not require expensive noble metals or enzymatic systems that hinder its mass production application. Therefore, addressing the reproducibility issue would lead to the development of a competitive H_2O_2 to be introduced in the market.

Fig. 6.11 shows the steady state background currents from electrodes prepared with either inkjet printing or dip-coating. The dip-coated modified electrodes displayed higher background currents than the electrodes modified by inkjet printing, which was in agreement with the greater catalytic activity towards H_2O_2 previously exhibited by the former. Thus, the average baseline current calculated for the inkjet printed modified electrodes was 1.07·10^{-6} A whereas the dip-coated modified electrodes showed 1.88·10^{-6} A. However, the inkjet printing technique resulted in much better inter-electrode variability in the steady state background currents, being 2.5% (r.s.d.), as compared to dip-coating which was 17% (r.s.d.). These data suggest that, while inkjet printing did not

lead to higher overall catalytic responses, it did lead to more reproducible DBSA/KCl modification on the Ag SPEs, and that the residual variability in the sensor devices is due to the inherent variability of the silver surface upon which the electrocatalytic response is dependent.
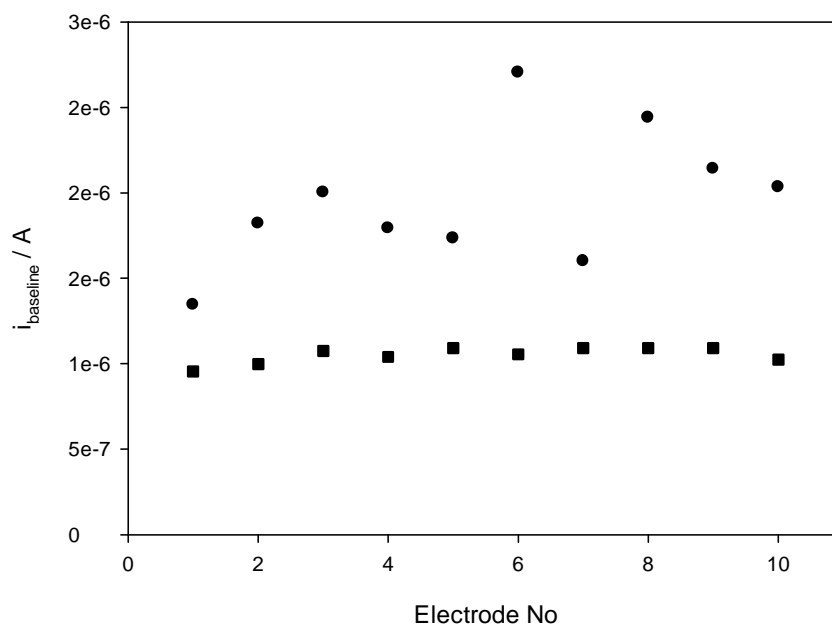
Figure 6.11. **Plot of steady state background current vs electrode number obtained during amperometric measurements of Ag SPEs at –0.1 V (vs Ag/AgCl) in PBS pH 6.8. The electrodes were modified with 3.3·10^{-2} M DBSA/ 0.1 M KCl solution: (●) by dip-coating or (■) by inkjet printing technique.**

Table 6.3 shows the signal-to-background (S/B) data calculated from the catalytic response data in Table 6.2 and the average background currents observed for both set of modified electrodes (dip-coated and inkjet printed) in Fig. 6.11. These data showed that although the absolute cathodic currents obtained by the dip-coated modified electrodes were higher than those from the inkjet printed electrodes, S/B levels were slightly better in the case of the inkjet-printed electrodes. The fact that the steady-state background

current was lower and more reproducible for the inkjet-printed electrodes means greater precision and lower achievable limits of detection.

Table 6.3. Signal to background (S/B) data corresponding to the catalytic activity to H_2O_2 reduction of DBSA/KCl modified Ag SPEs by inkjet printing and dip-coating.

	INKJET PRINTING		DIP-COATING	
[H_2O_2] / mM	i_{cat} (avrg) / A	S/B	i_{cat} (avrg) / A	S/B
1	$3.5 \cdot 10^{-6}$	3.3	$5.6 \cdot 10^{-6}$	3.0
2	$9.7 \cdot 10^{-6}$	9.1	$1.49 \cdot 10^{-5}$	7.9
3	$1.61 \cdot 10^{-5}$	15.1	$2.55 \cdot 10^{-5}$	13.6
4	$2.42 \cdot 10^{-5}$	22.6	$3.58 \cdot 10^{-5}$	19
5	$2.79 \cdot 10^{-5}$	26.1	$4.64 \cdot 10^{-5}$	24.7

A plot of the sensitivity of each electrode towards H_2O_2 reduction versus the background current was also performed and is shown in Fig. 6.12. Electrodes modified by dip-coating presented a linear correlation between the sensitivity to H_2O_2 reduction and the baseline current. In the case of the dip-coated electrodes, higher steady state background currents clearly correlated with higher levels of H_2O_2 reduction. Thus, sensitivity increased from $7.2 \cdot 10^{-2}$ to $9.4 \cdot 10^{-2}$ $AM^{-1}cm^{-2}$ when the baseline current ranged from $1.34 \cdot 10^{-6}$ to $2.70 \cdot 10^{-6}$ A. Unlike dip-coating, inkjet printed electrodes did not show any remarkable correlation between these parameters.

Figure 6.12. **Plot of sensitivity vs steady state background (baseline) current obtained during amperometric measurements of Ag SPEs at –0.1 V (vs Ag/AgCl) in PBS pH 6.8, at H_2O_2 concentration from 1 to $5 \cdot 10^{-3}$ M. The electrodes were modified with $3.3 \cdot 10^{-2}$ M DBSA/ 0.1 M KCl solution: (●) by dip-coating or (■) by inkjet printing technique.**

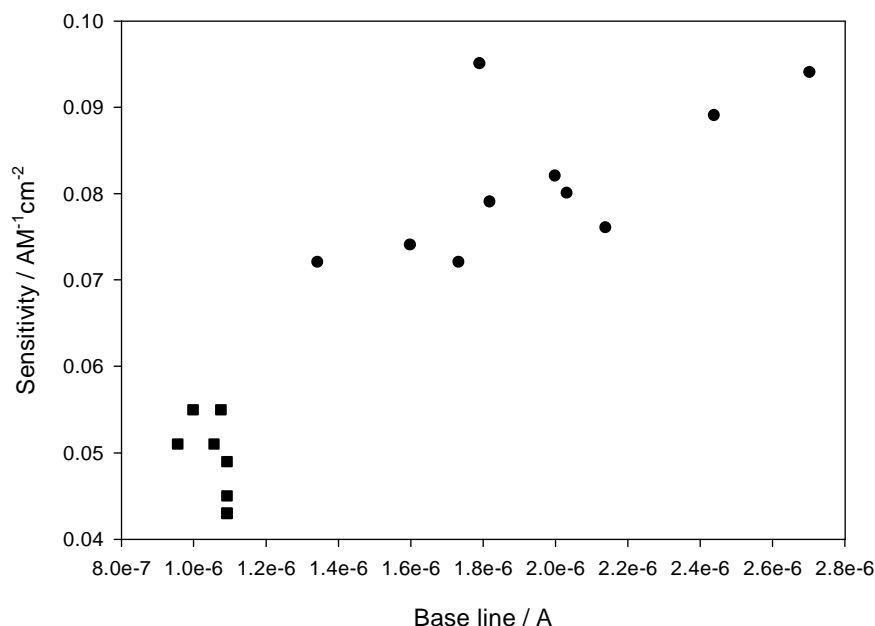In order to further understand the distinct behaviours of the DBSA/KCl modified Ag SPEs treated either by dip-coating or inkjet printing, surface characterization of the electrodes was performed. Scanning electron micrographs of Ag SPEs modified by both techniques, before and after H_2O_2 sensing were carried out and are shown in Fig. 6.13. The spheroidal structures observed on electrode surfaces following DBSA/KCl modification by dip-coating were not clearly evident on the electrode surfaces modified by inkjet printing, as can be seen comparing Fig. 6.13B and 6.13C. At first, Ag SPEs modified by inkjet printing exhibited electrode surfaces analogous to the unmodified electrode, as is observed in Fig. 6.13A and 6.13B. Moreover, the morphology of the spheroidal structures appeared to change following the H_2O_2 sensing process, as is

shown in Fig. 6.13E and was previously reported in Chapter 3. Such variation in the structures was then explained by a possible interaction between H_2O_2 and the structures during the reduction process. Comparing Fig. 6.13B and 6.13D, electrodes modified by inkjet printing did not present any apparent change after H_2O_2 catalysis. However, they still showed a noticeable enhancement on H_2O_2 reduction with respect to the unmodified Ag SPEs. Two possible phenomena might explain such different surface characteristics and catalytic activities of the inkjet printed modified electrodes: the volume of DBSA/KCl that the surface is actually exposed to; and the deposition technique itself. Although the previous voltage study suggested that increasing the voltage did not make catalysis worse, maybe catalysis was already impacted even at low voltages. On the other hand, the driving force of the modification adsorption process may still not be as effective when performed in smaller volumes. Therefore, it might be assumed that the phenomenon is not different, but more limited and harder to visualize when DBSA/KCl is deposited by inkjet printing.

The difference on both modifications might be explained in terms of possible damage or break-down of the hexagonal or lamellar structures formed in the surfactant-based solution and that were considered to be the responsible of the catalytic effect on H_2O_2 observed after DBSA/KCl treatment. However, as the cathodic responses and the sensitivities of the inkjet printed modified electrodes were only 1.6-fold lower than those exhibited by the electrodes following dip-coating procedure, and appear to result in improved electrode reproducibility, the former method might be yet feasible for further studies. Inkjet printing will be applied as a technique to modify Ag SPEs, which subsequently will be used as platforms for the fabrication of glucose biosensors.
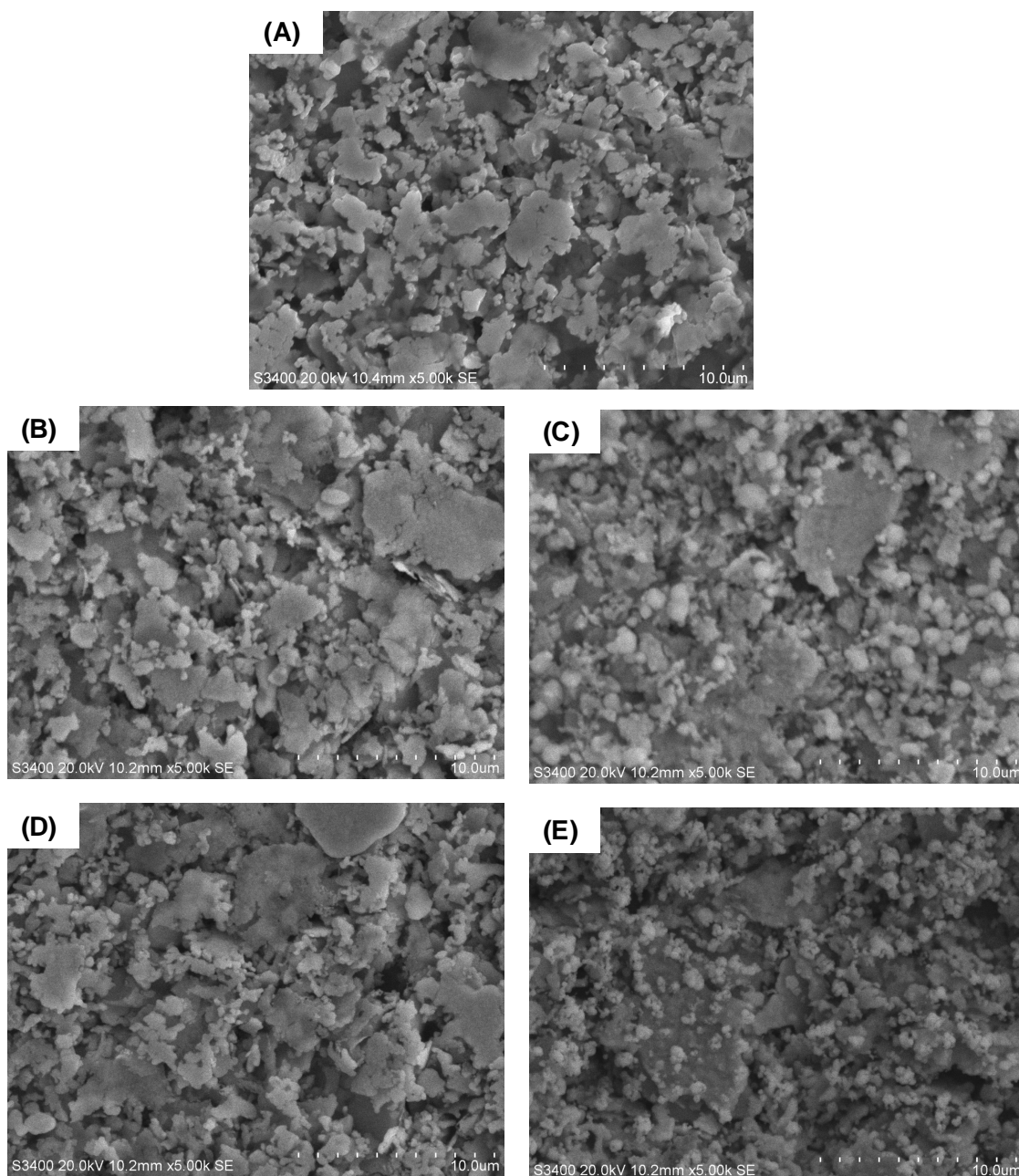
Figure 6.13. **SEM images using secondary electron (SE) detection of Ag SPEs (A) unmodified; (B) DBSA/KCl modified by inkjet printed, before H_2O_2; (C) DBSA/KCl modified by dip-coating, before H_2O_2; (D) DBSA/KCl modified by inkjet printed, after electrochemical reduction of $5 \cdot 10^{-3}$ M H_2O_2 and (E) DBSA/KCl modified by dip-coating, after electrochemical reduction of $5 \cdot 10^{-3}$ M H_2O_2. Accelerating voltage of 20 kV. (5.0k x magnification).**

6.2.3. Application of the inkjet printed DBSA/KCl modified Ag SPEs to the fabrication of a glucose biosensor

A glucose biosensor was fabricated using the inkjet printed DBSA/KCl modified Ag SPE as a platform for the GOx attachment. Five prints of freshly prepared DBSA/KCl solution were inkjet printed at 16 V on a Ag SPE and subsequently the electrode was washed thoroughly with distilled water. GOx was then immobilized onto the electrode surface following the standard protocol established in Chapter 5. Briefly, the electrode was immersed in a 2% CA solution in acetone for 1 min and then rinsed with distilled water, 20 min immersion in 5% HMDA aqueous solution followed by 20 min immersion in 2.5% GA aqueous solution were then before being transferred to a 25 mg/ml GOx solution in PBS pH 5 overnight. Amperometry at -0.1 V (vs Ag/AgCl) in PBS, pH 6.8 was performed in the presence of glucose from 1 to $8 \cdot 10^{-3}$ M. In order to assess the catalytic activity of the biosensor towards H_2O_2 following GOx immobilization, $1 \cdot 10^{-3}$ M H_2O_2 was added to the cell. Fig. 6.14 shows the amperometric responses of the inkjet printed and dip-coated electrodes to glucose. The cathodic responses exhibited by the electrodes modified by dip-coating were higher than those shown by the inkjet printed modified ones at low glucose concentrations. For example, $1.77 \cdot 10^{-7}$ A was the reduction current obtained by a dip-coated modified electrode in the presence of $2 \cdot 10^{-3}$ M glucose whereas the cathodic current shown by an inkjet printed modified one was $1.35 \cdot 10^{-7}$ A. However, from $4 \cdot 10^{-3}$ M glucose concentration and on electrodes modified by inkjet printed provided greater catalytic responses for glucose determination and that difference increased with the concentration. Thus, the cathodic currents for an inkjet printed and a dip-coated modified electrodes in the presence of $5 \cdot 10^{-3}$ M glucose were $5.57 \cdot 10^{-7}$ A and $4.77 \cdot 10^{-7}$ A, respectively, whereas at $8 \cdot 10^{-3}$ M glucose the reductions currents were $9.76 \cdot 10^{-7}$ A and $7.23 \cdot 10^{-7}$ A, respectively. Therefore, inkjet printed modified electrode showed better total responses to glucose than dip-coated modified electrodes in this case.
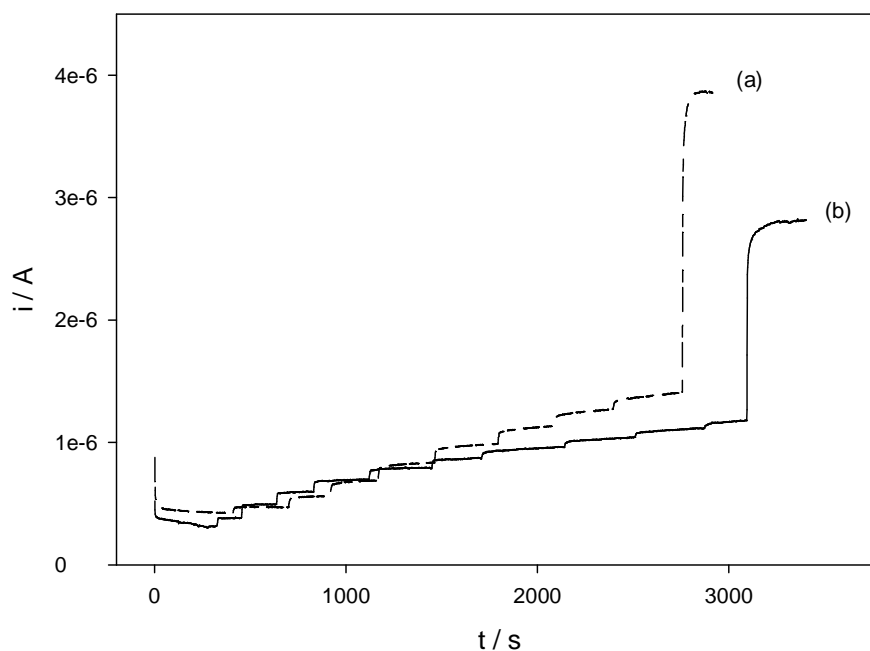
Figure 6.14. **Amperometric responses of Ag/ DBSA/KCl/ CA/ GOx electrodes measured at –0.1 V (vs Ag/AgCl) in PBS pH 6.8, where DBSA/KCl modification was performed by (a) inkjet printing or (b) dip-coating. Glucose concentration ranges (a) from 1 to 8·10^{-3} M or (b) from 1 to 10·10^{-3} M. At the end, H$_2$O$_2$ (1·10^{-3} M) was added to the solution.**

Catalytic responses corresponding to dip-coated modified electrodes seemed to reach saturation currents at lower glucose concentration than the electrodes modified by inkjet printing. That would explain the decrease observed in the cathodic responses of dip-coated modified electrodes respect to the inkjet printed ones as glucose concentration in the bulk increased. As was seen in Chapter 5, the dip-coated modified electrodes provided linear catalytic responses in the glucose concentration range from 0.4 to 4·10^{-3} M. However, when higher glucose concentrations were added to the bulk solution, saturated responses were achieved for glucose concentrations above 6·10^{-3} M. Unlike dip-coating, inkjet printing led to biosensors with broader range of linear catalytic

responses, up to $8 \cdot 10^{-3}$ M as minimum. The normal range of blood glucose concentration varies from 4.4 to $6.6 \cdot 10^{-3}$ M whereas diabetic people presented concentrations higher or lower than that.[26] Therefore, using inkjet printing for DBSA/KCl modification brought about a remarkable improvement in the linearity of the biosensor response and the subsequent device application for blood glucose determination.

A reproducibility study of the glucose biosensors fabricated by inkjet printing was performed (n=6). DBSA/KCl modification solution was deposited simultaneously onto Ag SPEs using the established inkjet printing methodology. After rinsing thoroughly, GOx was immobilized following the established standard protocol.

Tabla 6.4. Statistical data for the glucose biosensors based on DBSA/KCl inkjet printed modification (n=6).

[Glucose] / mM	i_{cat} (average) / A	Standard deviation	% error
1	$2.5 \cdot 10^{-8}$	$0.7 \cdot 10^{-8}$	28
2	$6.7 \cdot 10^{-8}$	$2.5 \cdot 10^{-8}$	37
3	$1.40 \cdot 10^{-7}$	$3.6 \cdot 10^{-8}$	26
4	$2.28 \cdot 10^{-7}$	$4.8 \cdot 10^{-8}$	21
5	$3.23 \cdot 10^{-7}$	$6.6 \cdot 10^{-8}$	20
6	$4.15 \cdot 10^{-7}$	$7.8 \cdot 10^{-8}$	19
7	$5.12 \cdot 10^{-7}$	$9.0 \cdot 10^{-8}$	18
8	$6.01 \cdot 10^{-7}$	$9.7 \cdot 10^{-8}$	16

Amperometry at -0.1 V (vs Ag/AgCl) in PBS, pH 6.8 was carried out. Final glucose concentrations in the bulk ranged from 1 to $8 \cdot 10^{-3}$ M. After that, H_2O_2 was added to the solution as a reference to H_2O_2 concentration of $1 \cdot 10^{-3}$ M. Plots of the cathodic currents versus glucose concentration were performed and the values were fitted to regression lines. Analytical parameters such as LOD and sensitivity were calculated from those regression lines and compared to those provided by electrodes based on dip-coated DBSA/KCl modification. Table 6.4 and Fig. 6.15 show the averages of the cathodic

currents and the standard deviation obtained for the six modified electrodes. Current data corresponding to $1 \cdot 10^{-3}$ M glucose were not considered for the regression line.
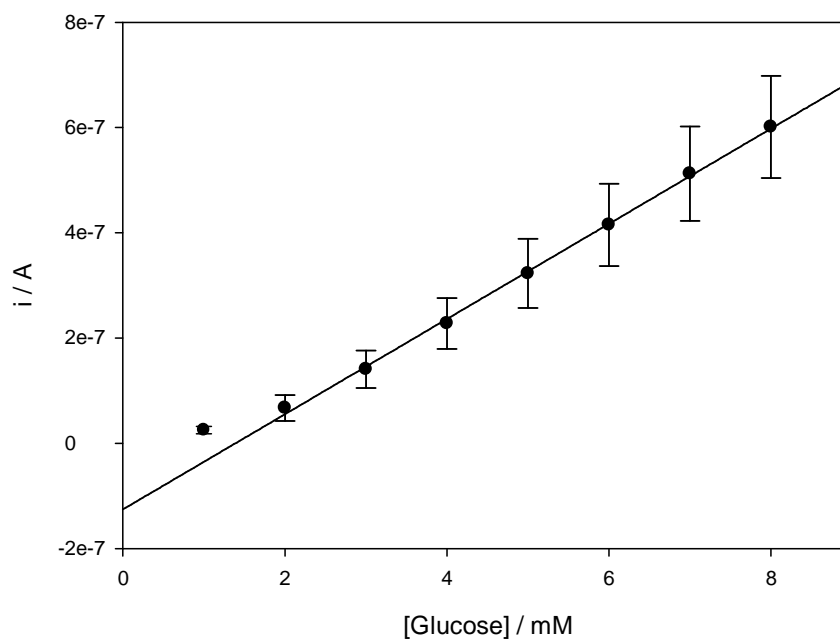
Figure 6.15. **Measurements of glucose using the Ag/ DBSA/KCl/ CA/ GOx electrodes (n=6) at –0.1 V (vs Ag/AgCl) in PBS pH 6.8. DBSA/KCl modification was performed by inkjet printing. (slope = 9.05·10^{-8} AmM^{-1}; sensitivity = 7.2·10^{-4} AM^{-1}cm^{-2}).**

The LOD of the inkjet printed glucose biosensor was found to be $1.55 \cdot 10^{-4}$ M, with a 5% r.s.d. This was slightly higher than that obtained in Chapter 5 for the biosensor fabricated using dip-coating and drop-casting, being $8.9 \cdot 10^{-5}$ M (22% r.s.d), although both values were in the same order of magnitude and the reproducibility was better for the inkjet printing modified sensor. Regarding sensitivity, biosensors based on the inkjet printed sensor provided an average sensitivity of $7 \cdot 10^{-4}$ AM^{-1}cm^{-2}, with a 30% r.s.d., whereas the value obtained by the dip-coated modified electrodes was $1.2 \cdot 10^{-3}$ AM^{-1}cm^{-2}, with a 17% r.s.d.. These LOD and sensitivity values were similar to those found in the

literature for other glucose biosensors. For example, Crouch et al.[27] reported the fabrication of an amperometric glucose biosensor by screen-printing of a water-based carbon ink containing GOx and cobalt phthalocyanine (CoPC). The latter was used as an electrocatalyst for the electrochemical oxidation of H_2O_2 at approx. 0.55 V (vs Ag/AgCl). The sensitivity of the biosensor was found to be $1.3 \cdot 10^{-2}$ $AM^{-1}cm^{-2}$, with a LOD of $2.5 \cdot 10^{-5}$ M. The resulting device was evaluated in commercially available samples of bovine serum providing a variability of 3.3% (n = 6). Chiu et al.[28] developed a glucose sensing electrode based on a poly(4,5-ehylenedioxythiophene)(PEDOT)/PB bilayer modification of a carbon screen printed electrode. The PB layer was electrodeposited first for H_2O_2 determination whereas the PEDOT layer was electrodeposited to entrap GOx. The biosensor showed a reproducibility of 2.54% (r.s.d.) and a sensitivity of $2.67 \cdot 10^{-3}$ $AM^{-1}cm^{-2}$, which was further improved by the incorporation of multi-walled carbon nanotubes before PB film deposition. Ricci et al.[29] produced planar glucose biosensors based on the PB modification of carbon screen printed electrodes and subsequent GOx immobilization by cross-linking employing glutaraldehyde and Nafion. The device was tested in a continuous flow system at low applied potentials (ca. 0 V vs Ag/AgCl), displaying a sensitivity of $5.4 \cdot 10^{-2}$ $AM^{-1}cm^{-2}$ and a LOD of $2.5 \cdot 10^{-5}$ M whereas the reproducibility was approx. 7% (n = 5). Therefore, the analytical parameters corresponding to inkjet printed DBSA/KCl modified biosensors were to some extent poorer than those obtained by the all dip-coated modified devices but still in the same order of magnitude.

As can be also observed, the glucose biosensors possessed significant inter-electrode variability, which decreased when the glucose concentration in the bulk increased. This phenomenon was already reported in Chapter 5 for the dip-coated modified electrodes. A possible explanation was that the electrodes did not reach the complete steady state background before glucose was added to the bulk. Therefore, initial glucose additions provided higher variability as the electrodes were not at the same stage. After a period of time, when more glucose aliquots were added to the solution, similar responses were exhibited by the electrodes. Another explanation may be related with an instrumental/experimental issue. The cathodic currents registered at low glucose concentrations are very low (in the order of 10^{-8} A) and they might be at the limit of the

precision of the instrument, so precision would be proportionately worse at these current levels.
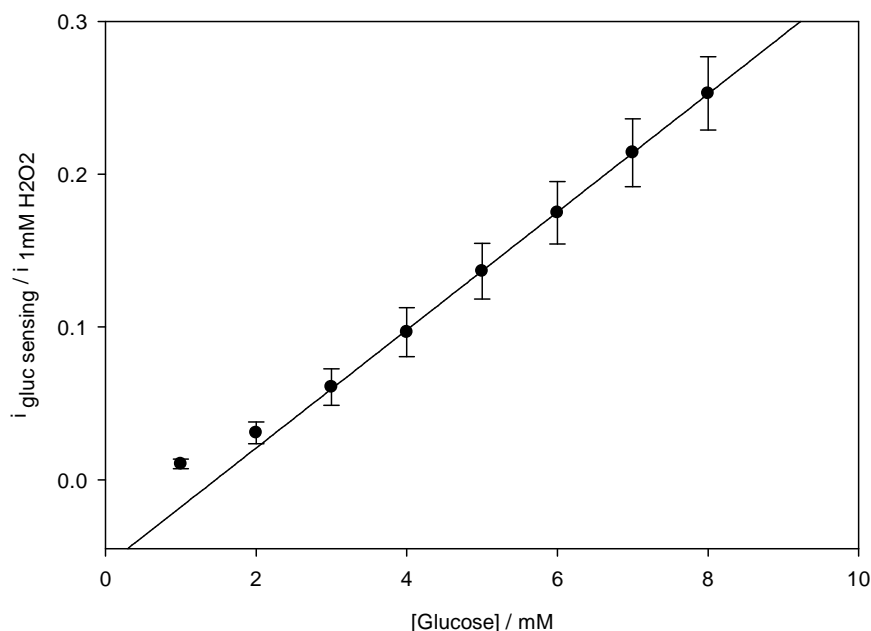

Figure 6.16. **Normalized data for the measurement of glucose using the Ag/ DBSA/KCl/ CA/ GOx electrodes (n=6) at –0.1 V (vs Ag/AgCl) in PBS pH 6.8. DBSA/KCl modification was carried out by inkjet printing (slope = 3.86·10^{-2} mM^{-1}).**

The reproducibility data observed for the biosensors based on inkjet printed DBSA/KCl Ag SPEs were very poor showing around 16-30% r.s.d. across the whole range of glucose concentrations. However, the reproducibility data provided here were similar to those obtained by the all dip-coated modified electrodes at analogous glucose concentrations in the previous chapter. It was also observed in Chapter 5 that the inter-electrode variability decreased when the cathodic currents for glucose sensing were normalized with respect to the reduction current obtained in the presence of $1 \cdot 10^{-3}$ M H_2O_2. As was previously highlighted, the biosensors developed in the present work were based on H_2O_2 detection released after the enzymatic reaction of GOx and glucose in the

presence of oxygen. Hence, the sensitivity of the electrode towards H_2O_2 reduction might affect its sensitivity to glucose determination.

Fig. 6.16 and Table 6.5 show the averages of the cathodic currents and the standard deviation for the normalized data. Current data corresponding to 1 and $2 \cdot 10^{-3}$ M glucose were not considered for the regression line. A significant increase in the reproducibility can be observed with respect to data in Table 6.3. As was previously mentioned in Chapter 5, the notable improvement in the reproducibility after normalization might indicate that changes in DBSA/KCl modification contributed to a large extent to the variability of the biosensors. Regarding the all dip-coated modified biosensors studied in Chapter 5, inkjet printed modified electrodes showed higher variability than the former for similar concentrations. Thus, variability observed by the inkjet printed modified electrodes was 23 and 17% r.s.d. at 2 and $4 \cdot 10^{-3}$ M, respectively, whereas the all dip-coated modified electrodes showed 17 and 7% r.s.d., respectively, for the same concentrations. However, there was no improvement at the low concentration range, which may again suggest an instrumental issue and limit of precision on the methodology.

Table 6.5. Statistically normalized data for the glucose biosensors based on DBSA/KCl inkjet printed modification.

[Glucose] / mM	$i_{cat\ normalized}$(average) / A	Standard deviation	% error
1	$1.04 \cdot 10^{-2}$	$3.1 \cdot 10^{-3}$	30
2	$3.08 \cdot 10^{-2}$	$7.1 \cdot 10^{-3}$	23
3	$6.07 \cdot 10^{-2}$	$1.19 \cdot 10^{-2}$	20
4	$9.66 \cdot 10^{-2}$	$1.60 \cdot 10^{-2}$	17
5	$1.365 \cdot 10^{-1}$	$1.83 \cdot 10^{-2}$	13
6	$1.747 \cdot 10^{-1}$	$2.04 \cdot 10^{-2}$	12
7	$2.141 \cdot 10^{-1}$	$2.22 \cdot 10^{-2}$	10
8	$2.529 \cdot 10^{-1}$	$2.39 \cdot 10^{-2}$	9

The all dip-coated electrodes were assessed in the range of 0.4 to $4 \cdot 10^{-3}$ M glucose because the cathodic currents seemed to reach a saturated value at higher glucose concentrations. Hence, higher variability was showed at lower concentrations (0.4 to $1.2 \cdot 10^{-3}$ M) whereas at 2 or $4 \cdot 10^{-3}$ M the variability was much lower. However, the inkjet printed modified electrodes measured glucose concentrations ranged from 1 to $8 \cdot 10^{-3}$ M, so high variability was still shown at 2 or $4 \cdot 10^{-3}$ M. That might explain the difference in reproducibility between the two sets of electrodes.

An intra-electrode reproducibility study was also performed for the glucose biosensor. A single Ag SPE was modified following the established standard protocol and then measured six consecutive times in PBS pH 6.8 in the presence of 1 to $8 \cdot 10^{-3}$ M glucose. The cathodic currents from the amperometric curves at 1 to $8 \cdot 10^{-3}$ M glucose concentration and $1 \cdot 10^{-3}$ M H_2O_2 are shown in Table 6.6.

Table 6.6. Cathodic currents of a glucose biosensor based on DBSA/KCl inkjet printed modification (Intra-electrode reproducibility study)

[Glucose] / mM	Rep1[a] i_{cat} / A	Rep2 i_{cat} / A	Rep3 i_{cat} / A	Rep4 i_{cat} / A	Rep5 i_{cat} / A	Rep6 i_{cat} / A
1	$3.6 \cdot 10^{-8}$	$4.0 \cdot 10^{-8}$	$4.2 \cdot 10^{-8}$	$4.6 \cdot 10^{-8}$	$2.2 \cdot 10^{-8}$	$3.7 \cdot 10^{-8}$
2	$1.09 \cdot 10^{-7}$	$1.21 \cdot 10^{-7}$	$1.13 \cdot 10^{-7}$	$1.20 \cdot 10^{-7}$	$6.1 \cdot 10^{-8}$	$7.7 \cdot 10^{-8}$
3	$2.12 \cdot 10^{-7}$	$2.29 \cdot 10^{-7}$	$2.14 \cdot 10^{-7}$	$2.42 \cdot 10^{-7}$	$1.23 \cdot 10^{-7}$	$1.44 \cdot 10^{-7}$
4	$3.29 \cdot 10^{-7}$	$3.54 \cdot 10^{-7}$	$3.39 \cdot 10^{-7}$	$3.66 \cdot 10^{-7}$	$1.95 \cdot 10^{-7}$	$2.14 \cdot 10^{-7}$
5	$4.45 \cdot 10^{-7}$	$4.86 \cdot 10^{-7}$	$4.58 \cdot 10^{-7}$	$4.92 \cdot 10^{-7}$	$2.70 \cdot 10^{-7}$	$2.98 \cdot 10^{-7}$
6	$5.45 \cdot 10^{-7}$	$6.07 \cdot 10^{-7}$	$5.65 \cdot 10^{-7}$	$6.01 \cdot 10^{-7}$	$3.38 \cdot 10^{-7}$	$3.71 \cdot 10^{-7}$
7	$6.36 \cdot 10^{-7}$	$7.12 \cdot 10^{-7}$	$6.64 \cdot 10^{-7}$	$6.74 \cdot 10^{-7}$	$3.95 \cdot 10^{-7}$	$4.37 \cdot 10^{-7}$
8	$6.98 \cdot 10^{-7}$	$7.96 \cdot 10^{-7}$	$7.32 \cdot 10^{-7}$	--	$4.41 \cdot 10^{-7}$	$4.94 \cdot 10^{-7}$
1mM H_2O_2	$3.160 \cdot 10^{-6}$	$3.500 \cdot 10^{-6}$	$3.311 \cdot 10^{-6}$	--	$2.655 \cdot 10^{-6}$	$2.753 \cdot 10^{-6}$

[a] Rep=repeat number.

As can be observed, the cathodic currents from the first four repetitions were quite alike, providing approx. 5% r.s.d. However, after repetition 5 (Rep5), the biosensor

underwent an approx. 40% loss of sensing activity towards glucose determination. That decrease in the catalytic activity was also exhibited with respect to H_2O_2 reduction, with an approx. 20% loss from Rep5. The difference in activity loss with respect to glucose sensing might be attributable to a partial inactivation or loss of the enzyme immobilized onto the electrodes.

In summary, DBSA/KCl treatment of Ag SPEs using inkjet printing resulted in an effective procedure for electrode modification, resulting in glucose biosensors with more reproducible steady state background currents and comparability in glucose measurement compared to the dip-coated modified electrodes. LOD and sensitivity were lower but in the same order of magnitude than those obtained by the dip-coating method.

6.3. CONCLUSIONS

The application of inkjet printing for the deposition of DBSA/KCl modification solution onto Ag SPEs has been studied. The catalytic activity of the so-formed electrodes towards H_2O_2 reduction was assessed and compared to that displayed by dip-coated DBSA/KCl modified electrodes. Optimal printing parameters such as volume ejected, DBSA and KCl concentrations in the solution and nozzle voltage were defined, being 5 prints ($1.0 \cdot 10^{-8}$ l), $3.3 \cdot 10^{-2}$ M DBSA/ 0.1 M KCl modification solution and 16 V nozzle voltage. Inkjet printing turned out to be a suitable technique for the deposition of the surfactant/salt solution, leading to cathodic currents only marginally lower than those shown by the dip-coated modified electrodes, whereas the modification time was remarkably reduced. Similar reproducibility data where shown by the electrodes modified by both techniques (approx. 10%), although the inkjet-printed modification resulted in lower and more reproducible background currents. SEM images of the inkjet printed modified electrode surfaces did not show the same observable spheroidal structures analogous to those observed on dip-coated modified electrodes and considered responsible of the H_2O_2 catalytic process, although electrochemical evidence suggests surface modification has certainly taken place. The possibility of a potentially negative impact of the voltage applied during the printing process, together with the smaller

volumes of modification solution in contact with the electrode surface may explain these differences.

Inkjet-printed DBSA/KCl modified electrodes were subsequently used as a platform for GOx immobilization, following the standard protocol established in Chapter 5. A LOD of $1.55 \cdot 10^{-4}$ M and sensitivity of $7 \cdot 10^{-4}$ $AM^{-1}cm^{-2}$ were obtained. These values were only 1.7-fold lower than those obtained with the dip-coated modified electrodes. After normalization, inkjet printed modified biosensors presented inter-electrode variability higher than that shown by the dip-coated modified electrodes. However, the former permitted measurement of a wider glucose concentration range of measurements (1 to $8 \cdot 10^{-3}$ M) prior to saturation current was achieved.

To sum up, inkjet printing resulted in a feasible technique for DBSA/KCl modification of Ag SPEs, providing H_2O_2 sensor and subsequent glucose biosensors with analogous characteristics than those fabricated by dip-coating. Further studies should be performed to provide an all-inkjet printed glucose biosensor amenable for mass production.

6.4. REFERENCES

1. L. Setti, A. Fraleoni-Morgera, B. Ballarin, A. Filippini, D. Frascaro and C. Piana, *Biosensors and Bioelectronics*, 2005, **20**, 2019-2026.
2. L. Setti, C. Piana, S. Bonazzi, B. Ballarin, D. Frascaro, A. Fraleoni-Morgera and S. Giuliani, *Analytical Letters*, 2004, **37**, 1559 - 1570.
3. R. Parashkov, E. Becker, T. Riedl, H. H. Johannes and W. Kowalsky, *Proceedings of the IEEE*, 2005, **93**, 1321-1329.
4. B. Ballarin, A. Fraleoni-Morgera, D. Frascaro, S. Marazzita, C. Piana and L. Setti, *Synthetic Metals*, 2004, **146**, 201-205.
5. S. B. Fuller, E. J. Wilhelm and J. M. Jacobson, *Microelectromechanical Systems, Journal of*, 2002, **11**, 54-60.
6. P. Calvert, *Chemistry of Materials*, 2001, **13**, 3299-3305.
7. B.-J. de Gans and U. S. Schubert, *Macromolecular Rapid Communications*, 2003, **24**, 659-666.
8. O. Ngamna, A. Morrin, A. J. Killard, S. E. Moulton, M. R. Smyth and G. G. Wallace, *Langmuir*, 2007, **23**, 8569-8574.
9. S. Shigematsu, Y. Ishida, N. Nakashima and T. Asano, *Japanese Journal of Applied Physics Letters*, 2008, **47**, 5109-5112.
10. Y. Kim, S. Son, J. Choi, D. Bym and S. Lee, *J. Semic. Tech. Sci.*, 2008, **8**, 121-127.
11. A. M. J. van den Berg, A. W. M. de Laat, P. J. Smith, J. Perelaer and U. S. Schubert, *Journal of Materials Chemistry*, 2007, **17**, 677-683.
12. H. Sirringhaus, T. Kawase, R. H. Friend, T. Shimoda, M. UInbasekaran, W. Wu and E. P. Woo, *Science*, 2000, **290**, 2123-2126.
13. L. Groenendaal, F. Jonas, D. Freitag, H. Pielartzik and J. R. Reynolds, *Advanced Materials*, 2000, **12**, 481-494.
14. B. Chen, T. Cui, Y. Liu and K. Varahramyan, *Solid-State Electronics*, 2003, **47**, 841-847.
15. A. Morrin, F. Wilbeer, O. Ngamna, S. E. Moulton, A. J. Killard, G. G. Wallace and M. R. Smyth, *Electrochemistry Communications*, 2005, **7**, 317-322.
16. T. Okamoto, T. Suzuki and N. Yamamoto, *Nature Biotechnology*, 2000, **18**, 438-441.
17. a. Bietsch, J. Y. Zhang, M. Hegner, H. P. Lang and C. Gerber, *Nanotechnology*, 2004, **15**, 873-880.
18. R. E. Saunders, J. E. Gough and B. Derby, *Biomaterials*, 2008, **29**, 193-203.
19. T. Wang, C. Cook and B. Derby, in *2009 Third International Conference on Sensor Technologies and Applications*, Athens, Glyfada, Editon edn., 2009, vol. 18-23 June 2009 pp. 82-85.
20. I. Fujifilm Dimatix, *Dimatix Materials Printer DMP-2800 series User Manual*.
21. R. M. Meixner, D. Cibis, K. Krueger and H. Goebel, *Microsyst Technol*, 2008, **14**, 1137-1142.
22. G. Li, Y. Wang and H. Xu, *Sensors*, 2007, **7**, 239-250.
23. F. Ricci, A. Amine, G. Palleschi and D. Moscone, *Biosensors and Bioelectronics*, 2003, **18**, 165-174.
24. X. Xu, S. Liu and H. Ju, *Sensors*, 2003, **3**, 350-360.

25.   I. L. de Mattos, L. Gorton and T. Ruzgas, *Biosensors and Bioelectronics*, 2003, **18**, 193-200.
26.   J. Wang, *Chemical Reviews*, 2008, **108**, 814-825.
27.   E. Crouch, D. C. Cowell, S. Hoskins, R. W. Pittson and J. P. Hart, *Biosensors and Bioelectronics*, 2005, **21**, 712-718.
28.   J.-Y. Chiu, C.-M. Yu, M.-J. Yen and L.-C. Chen, *Biosensors and Bioelectronics*, 2009, **24**, 2015-2020.
29.   F. Ricci, D. Moscone, C. S. Tuta, G. Palleschi, A. Amine, A. Poscia, F. Valgimigli and D. Messeri, *Biosensors and Bioelectronics*, 2005, **20**, 1993-2000.

Chapter 7

Future developments

7.1. FURTHER UNDERSTANDING OF AND IMPROVEMENTS TO THE HYDROGEN PEROXIDE ELECTROCATALYST (CHAPTERS 3 & 4)

The development of a H_2O_2 electrocatalyst based on the DBSA/KCl modification of Ag SPEs has brought about several advantages compared to other devices existing in the literature, such as fabrication simplicity, the absence of biological substrates (proteins, enzymes) and the cost effectiveness of the involved materials. However, as was observed in previous chapters, the sensitivity and reproducibility of the so-formed H_2O_2 sensors might still not be the appropriate for its introduction in the mass production market. In order to improve those parameters and create a more competitive sensor for the sensitive direct detection of H_2O_2, a more intensive study of the electrocatalytic characteristics of the material will be developed. As was seen above, the surfactant/salt-based modification of the Ag SPEs led to changes on the electrode surface together with the formation of small spheroidal structures made principally of Ag and Cl (data from the structural analysis). Both phenomena were related to the enhancement in the H_2O_2 catalytic activity observed on the electrodes after exposure to DBSA/KCl solutions. In order to improve the analytical parameters of the H_2O_2 sensors as well as try to understand the basic mechanism behind the modification, further improvements will be performed. It was clear from this work that a significant underlying limitation of the electrode's performance is its inherent variability and sensitivity which is believed to relate directly to the ill-defined and disordered nature of the silver paste electrode material. Any improvement in performance must investigate this matter. For example, the fabrication of nanostructured Ag SPEs with an enhanced homogeneity of the metal particles will be achieved by the fabrication of customized Ag inks. These inks will be created by mixing previously created Ag nanoparticles (Ag NPs) and other ingredients such as binders, solvents, surfactants and salts in optimized ratios to provide higher and more reproducible responses to H_2O_2. The use of a pre-formed nanostructured material might homogenise surface behaviour, result in benefits from surface area enhancements, decrease the background noise and increase the magnitude and reproducibility of the cathodic responses. These inks will be characterized by surface analysis techniques, such as SEM, EDX, XPS and TEM and they will be related to the catalytic properties of the

materials by cyclic voltammetry, amperometry and impedance spectroscopy. The improved system will be used not only for the development of biosensors but also for the measurement of H_2O_2 in industrial process water and wastewater.

The exact mechanism of the catalysis and the role of all the materials involved in the process also need further elucidation. The involvement of other components of the silver paste such as binder needs to be clarified and the type of surface structures formed at the electrode after surfactant/salt modification need to be determined, possibly through x-ray scattering techniques. Also, a greater understanding of the thermodynamics of the process and the reaction route that is used needs to be established. A more complete understanding of the materials and mechanisms involved may lead to the identification of other hybrid organic/inorganic materials with similar heterogeneous catalytic and electrocatalytic properties.

Other enhancements can also be envisaged using the surfactant/salt modification, particularly in combination with precision deposition techniques such as ink jet printing. For example, ink jet printing could be used to create effective microcatalytic electrode arrays in which isolated droplets of surfactant/salt create catalytic microelectrode islands which will benefit from semi-infinite radial diffusion. This will benefit from classical microelectrode array behaviours including improved signal-to-background responses.

7.2. ALTERNATIVE IMMOBILIZATION STRATEGIES FOR THE DEVELOPMENT OF AN AMPEROMETRIC GLUCOSE BIOSENSOR (CHAPTER 5)

The catalytic enhancement towards H_2O_2 reduction of DBSA/KCl modified Ag SPEs was exploited in Chapter 5 for the development of an electrochemical glucose biosensor. After several attempts, GOx was covalently immobilized onto the electrodes after the deposition of a cellulose acetate (CA) layer, which both isolated the DBSA/KCl modification from the negative effect of the enzymatic reaction and was used as a platform for GOx attachment. The standard protocol adopted in that section for GOx immobilization involved the use of glutaraldehyde (GA) and hexamethylenediamine

(HMDA), which did not seem to hinder the electrochemical glucose detection. However, the deposition of the CA layer brought about additional problems. The solvents used to dissolved CA (glacial acetic acid and acetone) showed to induce damage to the electrode surface that led to a significant decrease in the amperometric H_2O_2 responses of the sensors as well as an increase in the variability of the measurements.

The use of less aggressive techniques for the enzyme immobilization process particularly regarding the membrane layer may lead to a significant improvement in the biosensor characteristics as the glucose determination is directly related to the catalytic response of the device to H_2O_2.[1] For example, Nafion and chitosan were also evaluated in Chapter 5 as possible separation membranes taking into account the residual catalytic response to H_2O_2 of the modified electrodes after their deposition. At that stage, CA was chosen because it showed the highest retention of activity (93%), but the other two membranes also exhibited good retention of catalysis after their deposition (75% and 81% for chitosan and Nafion, respectively). Moreover, solvents used during the preparation of chitosan and Nafion solutions were diluted acetic acid (0.8% v/v) and a mixture of lower aliphatic alcohols and water, respectively. These solvents seem to be less damaging than the glacial acetic acid and acetone used for CA. Also, there are many other examples in the literature using chitosan[2, 3] or Nafion[4, 5] as membranes for enzyme deposition and many other strategies for enzyme deposition apart from covalent attachment. Therefore, chitosan or Nafion will be tested as membranes for GOx deposition and other methods such as entrapment in a matrix or cross-linking with GA will be assessed for GOx immobilization.

Alternatively, a non-covalent immobilisation strategy could be investigated, depending on the final application of the biosensor. For instance, single use, electrode strips have a very small sample volume (microlitres) and so dilution of non-covalently deposited enzyme into the bulk is not significant and so can avoid the need to attach to the surface.

7.3. GLUCOSE OXIDASE DEPOSITION BY INKJET PRINTING: TOWARDS AN ALL-PRINTED GLUCOSE BIOSENSOR (CHAPTER 6)

Chapter 6 showed that inkjet printing could be a powerful fabrication technique for biosensor fabrication. However, it was not fully exploited in this work and could be utilised further.

Once a glucose biosensor had been created by drop-coating, inkjet printing was used to improve the reproducibility of material deposition as well as decrease the fabrication time. Chapter 6 reported the DBSA/KCl modification process of Ag SPEs by inkjet printing and compared the resulting H_2O_2 sensors to those generated by dip-coating. Several optimization steps led to the construction of an inkjet printed H_2O_2 sensor with analogous analytical characteristics to those from the dip-coated sensor. In order to further optimise the glucose biosensing device, an attempt at GOx deposition by inkjet printing was carried out.

As was mentioned in Chapter 6, the inkjet printing technique has already been applied to enzyme deposition during the biosensor fabrication process. In order to evaluate enzyme (protein) concentrations in solution after the printing process, the bicinchoninic acid (BCA) assay was used. Basically, the BCA assay is based on the formation of a Cu^{2+} -protein complex under alkaline conditions, followed by reduction of the Cu^{2+} to Cu^{1+}. Cysteine, cystine, tryptophan, tyrosine and the peptide bond are able to reduce Cu^{2+} to Cu^{1+}, being the amount of reduction proportional to protein present. BCA forms a purple-blue complex with Cu^{1+} in alkaline solution, thus providing a basis to monitor the reduction of alkaline Cu^{2+} by proteins and to calculate the amount of protein in solution.[6] 1 mg/ml solution of GOx in PBS pH 5 was inkjet printed at 16 V onto a PET substrate and the ejected solution was transferred to an eppendorf vial for the BCA assay. After the incubation time, UV measurements of the samples were carried out and GOx concentrations in solution were calculated by using the previously established calibration curve of the system. Data for the theoretical and calculated GOx concentrations of five samples are shown in Table 7.1. Except for in the case of sample 1, more than 70% of the enzyme was found in solution after the printing process.

Tabla 7.1. Data from BCA assay to calculate [GOx] in solution after inkjet printing process.

Tube no.	1	2	3	4	5
$C(GOx)_{theor}$ / μgml^{-1}	2.50	2.50	2.50	2.50	3.75
$C(GOx)_{calc}$ / μgml^{-1}	1.54	1.84	2.41	1.85	3.52
% GOx after IJP[a]	62	74	96	74	94

[a] Inkjet Printing

GOx solution was then inkjet printed onto DBSA/KCl modified Ag SPEs and the catalytic responses of the so-formed biosensors were evaluated by amperometry. Several GOx concentrations (1 to 25 mg/ml) and solution amounts (1 to 10 prints) were evaluated but invalid or poor responses towards glucose determination were acquired. The best catalytic response was observed after 5 prints of 5 mg/ml GOx solution. Comparison of the cathodic currents of two glucose biosensors fabricated by inkjet printing and dip-coating, respectively, are shown in Fig. 7.1. DBSA/KCl modification was performed by dip-coating in both cases. As can be observed, the steady state background for the inkjet printed modified electrode was higher than that from the dip-coated one. This might be explained by a thicker layer of enzyme deposited onto the electrodes, which would increase the non-faradaic current. With regard to the catalytic activity, electrodes modified by inkjet printed GOx seemed to provide higher responses in the presence of glucose, although the cathodic current reached a saturation value faster than GOx dip-coated modified electrodes. Thus, the reduction current displayed by the former in the presence of $5 \cdot 10^{-3}$ M glucose was $2.07 \cdot 10^{-7}$ A whereas the current provided by the latter was $6.4 \cdot 10^{-8}$ A. However, electrodes modified by inkjet-printed GOx seemed to become saturated at $4 \cdot 10^{-3}$ M glucose and above whereas the dip-coated modified biosensor displayed a stable response until glucose concentration in the bulk was $10 \cdot 10^{-3}$ M. That could be justified by the diverse conformations that the enzyme would present on the electrode surface due to the different deposition methods. The catalytic responses of these systems were lower than that provided by the optimized all dip-coated device, where approx. $7.5 \cdot 10^{-7}$ A were obtained in the presence of $5 \cdot 10^{-3}$ M

glucose. Higher GOx concentrations in the solution to be printed did lead to higher but very slow cathodic responses, maybe due to the higher thickness of the GOx layer deposited on the electrode surface.
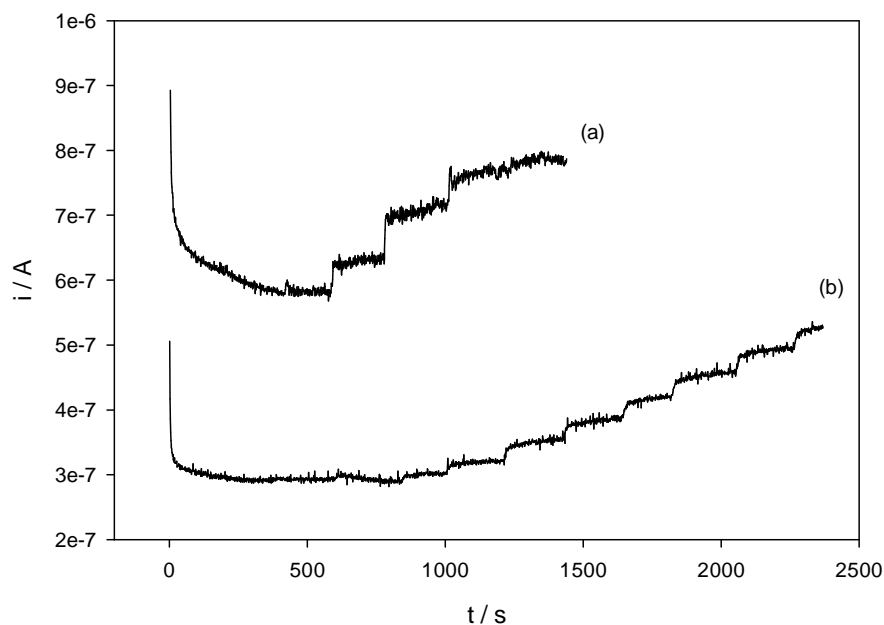
Figure 7.1. **Amperometric responses of Ag/ DBSA/KCl/ CA/ GOx electrodes measured at –0.1 V (vs Ag/AgCl) in PBS pH 6.8, where 5 mg/ml GOx in PBS pH 5 solution was deposited by (a) inkjet printing or (b) dip-coating. Glucose concentration ranges (a) from 1 to $5·10^{-3}$ M or (b) from 1 to $10·10^{-3}$ M.**

Therefore, initial attempts of using inkjet printing to deposit the enzyme have led to positive results, although further studies must be performed to improve the enzyme behaviour after immobilization. GOx was inkjet printed and enzyme concentration after the process was evaluated, providing an average of 70% recovery. Glucose biosensors fabricated by enzyme inkjet printing seemed to provide higher catalytic responses than those created by dip-coating, although the former reached saturations values at lower glucose concentrations.

7.4. OTHER APPLICATIONS

7.4.1. Other enzyme biosensors

As was mentioned in Chapter 1, H_2O_2 is the by-product of many enzymatic reactions and its concentration may be used as an indicator of the progress of a reaction or for the analytical determination of a certain substrate.[7]

Recently, there has been an increasing concern about the determination of cholesterol levels in blood as abnormal levels are directly related to clinical disorders such as hypertension, heart disease, arteriosclerosis, cerebral thrombosis, etc. In the fabrication of a cholesterol biosensor, the enzyme cholesterol oxidase (ChOx) is most commonly used as the biosensing element.[8] ChOx catalyzed the oxidation of cholesterol by dissolved molecular oxygen, releasing H_2O_2 as a side product of the reaction. Therefore, cholesterol can be analyzed indirectly by monitoring H_2O_2 generated in the enzymatic reaction using voltammetry or amperometry.[9] The catalytic properties towards H_2O_2 reduction observed in the Ag SPEs following exposure to DBSA/KCl can be used for the development of a cholesterol biosensor. The enzyme would be first investigated in solution and subsequently attached to the electrode surface by means of an appropriate immobilization method. Several parameters such as buffer, pH and enzyme load would be assessed in order to provide optima analytical parameters for the sensor, e.g. sensitivity, LOD and reproducibility. Finally, both DBSA/KCl and ChOx would be inkjet printed and comparisons with the dip-coated biosensor would be performed.

7.4.2. Fuel cells/printed fuel cells

Fuel cells provide a possibility for high energy density due to a refuelling capability. As was previously mentioned, in order to achieve an acceptable performance of fuel cells, it is necessary the use of electrode materials with high catalytic activity for the electrochemical reduction of oxygen.[10, 11] That implied the use of expensive precious metals and very low oxygen diffusion through the solution phase. These drawbacks have

been generally addressed by using porous electrodes fabricated with high-area carbon as a conductive support and a catalyst for the oxygen reduction. To decrease the cathodic polarization and to enhance the electrode life, it is critical to eliminate effectively the peroxide form during the oxygen reduction.[11] Therefore, DBSA/KCl modified Ag SPEs may be employed as catalysts for H_2O_2 reduction in the manufacture of fuel cells that use oxygen reduction. However, a fundamental problem with the use of oxygen (or any gaseous reactant) is the availability of the reactant at the active catalyst site on the electrode surface. Liquids reactants are notably more abundant at the active site than gaseous reactants, so the use of H_2O_2 as the fuel-cell oxidant is an alternative that have been already used in the literature.[12, 13] Thus, Ag SPEs following modification with DBSA/KCl may be used for the fabrication of fuel cells that directly employ H_2O_2 as the fuel. The catalyst might be produced by dip-coating or inkjet printing, depending on the substrate required for the fuel cell.

7.5. SUMMARY AND OVERALL CONCLUSIONS

The remarkable enhancement in the electrocatalytic activity towards H_2O_2 reduction observed on Ag SPEs after exposure to DBSA/KCl solutions has led to the development of novel H_2O_2 sensors and biosensors. This phenomenon was also exhibited by the electrodes after modification with other surfactant/salt combinations, although the highest activity was shown following exposure to DBSA/KCl on which most development was based. The electrode surfaces were characterized by SEM, EDX and XPS techniques. The modification process appeared related to the formation of spheroidal structures (mainly made of Ag and Cl) on the electrode surface which seemed to be involved in the catalysis and which showed structural changes after the electrode contact with H_2O_2 solutions. The formation of lamellar structures in the surfactant/salt solutions and their subsequent interaction with the electrode surface seemed to be a possible explanation for the noticeable enhancement showed by Ag SPEs towards the electrochemical reduction and decomposition of H_2O_2. An attempt to understand the phenomenon that brought about those results was performed. The modification of the electrode surface might lead to a surface that stabilized any of the intermediates for both processes. The change in the spheroidal structures after both phenomena seemed to interconnect the pathways for the reactions. However, the fact that a different level of enhancement was observed would suggest that both processes followed diverse mechanisms, as would be expected. Therefore, the modification of the surface might stabilize one common intermediate and then the reactions would go along their own mechanism.

The binder present in the printing inks and the presence of rough or defects on the electrode surfaces were considered as possible explanations for the interaction/deposition of the lamellar structures on the electrode. In order to prove that theory, other metal substrates such as several silver electrodes, gold and platinum were also evaluated. All the SPEs also showed potential enhanced catalysis with the surface modification. Indeed, all modified electrodes that showed an increase in the catalytic activity on the electrochemical reduction also exhibited an enhancement in the decomposition process, although the improvements were not proportional. However, the

pure metallic electrodes (99.9% Ag and Au) did not show any particular enhancement after the modification. That again reinforced the possible involvement of the binder in the modification process.

Silver, and particularly silver paste was the material that provided the greatest increase in catalytic responses to H_2O_2 reduction following modification. At the same time, these sensors exhibited low cost and easy manufacture characteristics that made them suitable to be used as platforms for the development of glucose biosensors. Surprisingly, it was found that the presence of both GOx and glucose at the modified electrode surface resulted in the destruction of the catalytic behaviour of the electrode, but either component alone did not cause this effect. To avoid this problem, a CA membrane was first deposited onto the modified electrodes. GOx was then covalently attached to the CA layer by means of HMDA and GA. The resulting biosensors showed a good LOD at a low applied potential (–0.1V vs. Ag/AgCl), which would make it effective in the presence of interferences such as ascorbic acid. However, the devices exhibited low reproducibility due partially to the high variability of the catalysis of the DBSA/KCl-modified electrodes. In order to improve such parameters, inkjet printing technique was used for DBSA/KCl deposition, leading to wider glucose concentration range of measurements (1 to $8 \cdot 10^{-3}$ M) and more stable background currents. However, the catalytic activity of the sensors towards H_2O_2 was reduced in comparison to the dip-coating DBSA/KCl modification. This result may be attributable to either the breakdown of the micellar/lamellar structure of the DBSA/KCl during the printing process, which would decrease the level of electrode modification, or the low volumes of modification solution in contact to the surface, which would lead to an incomplete modification process.

To sum up, the discovery of the enhancement of the catalytic activity of Ag SPEs to the decomposition and electrochemical reduction of H_2O_2 following modification by DBSA/KCl represents the beginning of a new generation of direct H_2O_2 sensors and biosensors. Combined with inkjet printing as a means of sensor fabrication, this has the potential to result in novel, low cost, mass producible electrochemical devices for a range of applications.

7.6. REFERENCES

1.   J. D. Newman and A. P. F. Turner, *Biosensors and Bioelectronics*, 2005, **20**, 2435-2453.
2.   Y. Miao, L. S. Chia, N. K. Goh and S. N. Tan, *Electroanalysis*, 2001, **13**, 347-349.
3.   B.-Y. Wu, S.-H. Hou, F. Yin, J. Li, Z.-X. Zhao, J.-D. Huang and Q. Chen, *Biosensors and Bioelectronics*, 2007, **22**, 838-844.
4.   P. Norouzi, F. Farnoush, B. Larijani and M. R. Ganjali, *Int. J. Electrochem. Sci.*, 2010, **5**, 1213-1224.
5.   F. Ricci, D. Moscone, C. S. Tuta, G. Palleschi, A. Amine, A. Poscia, F. Valgimigli and D. Messeri, *Biosensors and Bioelectronics*, 2005, **20**, 1993-2000.
6.   Sigma-Aldrich, *QuantiPro™ BCA Assay Bulletin*
7.   C. M. Welch, C. E. Banks, A. O. Simm and R. G. Compton, *Analytical and Bioanalytical Chemistry*, 2005, **382**, 12-21.
8.   S. K. Arya, M. Datta and B. D. Malhotra, *Biosensors and Bioelectronics*, 2008, **23**, 1083-1100.
9.   J.-P. Li and H.-N. Gu, *Journal of the Chinese chemical society*, 2006, **53**, 575-582.
10.   H. Falcon and R. E. Carbonio, *Journal of Electroanalytical Chemistry*, 1992, **339**, 69-83.
11.   R. Venkatachalapathy, G. P. Davila and J. Prakash, *Electrochemistry Communications*, 1999, **1**, 614-617.
12.   D. N. Prater and J. J. Rusek, *Applied Energy*, 2003, **74**, 135-140.
13.   Y. Yamada, Y. Fukunishi, S. Yamazaki and S. Fukuzumi, *Chem. Commun,*, 2010, **46**, 7334-7336.

LIST OF PUBLICATIONS AND PRESENTATIONS

Scientific Publications

- **Laura Gonzalez-Macia**, Malcolm R. Smyth, Aoife Morrin and Anthony J. Killard.
  Enhanced electrochemical reduction of hydrogen peroxide at metallic electrodes modified with surfactant and salt. (Manuscript in preparation)

- **Laura Gonzalez-Macia**, Malcolm R. Smyth, Aoife Morrin and Anthony J. Killard.
  Enhanced electrochemical reduction of hydrogen peroxide on silver paste electrode modified with surfactant and salt. *Electrochimica Acta*, 2011, **56**, 4146-4153.

- **Laura Gonzalez-Macia**, Aoife Morrin, Malcolm R. Smyth and Anthony J. Killard.
  Advanced printing and deposition methodologies for the fabrication of biosensors and biodevices. *Analyst,* 2010, **135**, 845-867.

Conference Participations

- **The 59th Annual Meeting of the International Society of Electrochemistry**

  University of Seville, Seville, Spain, 7-12 September 2008.

  "Polyaniline Nanoparticles for Sensing Applications" (Poster)

  Laura Gonzalez-Macia, Aoife Morrin, Malcolm R. Smyth, Anthony J. Killard

- **42nd IUPAC Congress Chemistry Solutions**

  SECC, Glasgow, UK, 2-7 August 2009.

  "Study of Hydrogen Peroxide Decomposition and Reduction on Metallic Surfaces" (Poster)

  Laura Gonzalez-Macia, Aoife Morrin, Malcolm R. Smyth, Anthony J. Killard

- **The 61st Annual Meeting of the International Society of Electrochemistry**

  Acropolis Conference Center, Nice, France, 26 September-1 October 2010.

  "Enhancement of Hydrogen Peroxide Reduction by Surfactant/Salt Modified Silver Electrodes" (Poster)

  Laura Gonzalez-Macia, Aoife Morrin, Malcolm R. Smyth, Anthony J. Killard

- **Eirelec'11: Electrochemistry – The Future?**

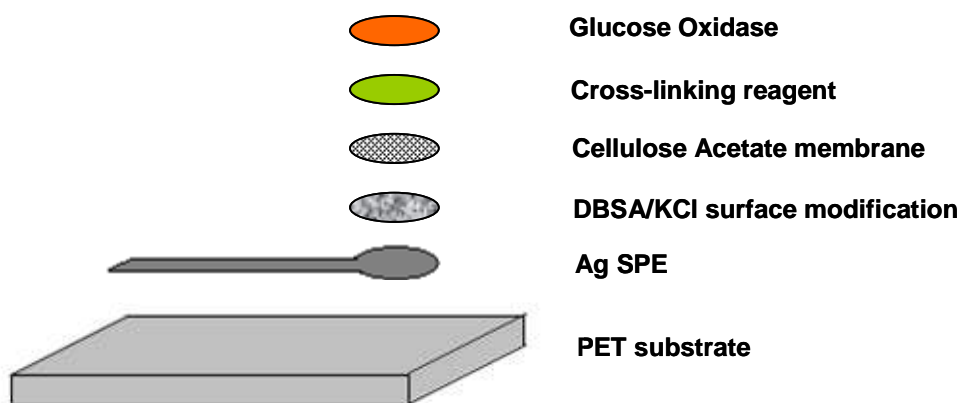 Adare, Ireland, 16-18 May 2011.

  "Application of a Novel Hydrogen Peroxide Electrocatalyst to the Development of a Glucose Biosensor" (Poster)

  Laura Gonzalez-Macia, Malcolm R. Smyth and Anthony J. Killard

APPENDICES

APPENDIX 1. Silver screen printed electrode design

Glucose Oxidase

Cross-linking reagent

Cellulose Acetate membrane

DBSA/KCl surface modification

Ag SPE

PET substrate

APPENDIX 2. A comparison of the developed hydrogen peroxide sensor with other devices reported in the scientific literature

Electrode	LOD/ M	Sensitivity/ $AM^{-1}cm^{-2}$	% r.s.d.	E_{app}/ V vs. Ag/AgCl	Chapter/ Ref. (pg)
HRP entrapped in a PPy film on C SPE	--	$3.3 \cdot 10^{-2}$	10.24 (n=5)	-0.3	1/ 29 (7) 6/ 22 (173)
HRP on a colloidal Au-modified C SPE	--	0.307	2.3-2.7 (n=10)	--	6/ 24 (174)
PB modified C SPE	$1.0 \cdot 10^{-7}$	0.234	5 (n=6)	-0.05	6/ 23 (173)
PB modified Au and Pt SPE	--	2 (Au) 1 (Pt)	--	-0.05	1/ 30 (7)
GC modified with a composite of thionine, EDTA, MWCNTs and CHIT	$6.5 \cdot 10^{-8}$	--	5.6 (n=3)	-0.4	1/ 31 (7)
Electropolymerization of aniline and SWCNTs on Pt	$1.2 \cdot 10^{-6}$	--	--	-0.35	1/ 41 (11)
Electroroughened Ag	$6.0 \cdot 10^{-6}$	--	4.6 (n=10)	-0.35	1/ 12 (12)
"Flowerlike" silver microspheres on GC	$1.2 \cdot 10^{-6}$	--	< 5	-0.55	1/ 43 (12)
AgNPs on GC	$2.0 \cdot 10^{-6}$	--	--	-0.7	1/ 4 (13) 3/ 3 (51)
AgNPs immobilized in a PVA film on Pt	$1.0 \cdot 10^{-6}$	--	--	-0.55	1/ 2 (14) 3/ 9 (51)
Cu-plated C SPE	$9.7 \cdot 10^{-7}$	$3.45 \cdot 10^{-2}$	1.1 (n=10)	-0.3	1/ 49 (14)
Nafion/Cu particulate modified GC	$1.6 \cdot 10^{-6}$	--	--	-0.2	1/ 50 (14)
PABS-modified GC	$1.0 \cdot 10^{-5}$	--	--	-0.7	1/ 25 (17)

AgNPs on CILE	$7.0 \cdot 10^{-7}$	--	--	-0.35	3/ 20 (51)
NAD$^+$ and SWCNTs modified GC	$1 \cdot 10^{-11}$	--	--	-0.25	3/ 22 (52)
DBSA/KCl modified Ag SPEs (Present work)	$1.1 \cdot 10^{-6}$	$7.1 \cdot 10^{-3}$	--	-0.1	3/ (50)
Dip-coated DBSA/KCl modified Ag SPEs (Present work)	--	$8.1 \cdot 10^{-2}$	9-13 (n=10)	-0.1	6/ (171)
Inkjet printed DBSA/KCl modified Ag SPEs (Present work)	--	$4.9 \cdot 10^{-2}$	8-17 (n=8)	-0.1	6/ (171)

APPENDIX 3. A comparison of the developed glucose biosensor with other devices reported in the scientific literature

Electrode	LOD/ M	Sensitivity/ $AM^{-1}cm^{-2}$	% r.s.d.	E_{app}/ V vs. Ag/AgCl	Chapter/ Ref. (pg)
GOx immobilized by cross-linking with GA and Nafion on a PB-modified C SPE	$2 \cdot 10^{-5}$	$5.4 \cdot 10^{-2}$	--	0.0	1/ 76 (23)
GOx immobilized by Nafion on a PB-modified GCE	--	$1.8 \cdot 10^{-4}$	--	0.18	5/ 15 (119)
GOx immobilized on a PB nanoparticles and MWCNTs modified GCE	$1.3 \cdot 10^{-5}$	--	4.7 (n=8)	0.0	5/ 16 (119)
GOx and NiO nanoparticles co-deposited on a GCE	$2.4 \cdot 10^{-5}$	--	--	0.3	5/ 23 (119)
Layer-by-layer deposition of GOx and chitosan on a PB-modified Au electrode	$3.1 \cdot 10^{-6}$	--	--	0.05	5/ 24 (119)
GOx and Cu-modified CNTs paste electrodes	$2 \cdot 10^{-5}$	$2.97 \cdot 10^{-5}$	12 (n=5)	-0.1	5/ 25 (119)
Cu-hexacyanoferrate and GOx dispersed within a screen-printable C ink	--	--	9.6 (n=12)	-0.1	5/ 30 (120)
GOx/Nafion immobilized on a RhO_2-C SPE	$1.1 \cdot 10^{-6}$	--	1.8 (n=5)	-0.2	5/ 32 (120)
GOx immobilized with GA on poly (neutral red) modified CA/C composite	$2.0 \cdot 10^{-6}$	$3.15 \cdot 10^{-2}$	5.0	-0.3	5/ 37 (125)
GOx immobilized into AgNP-doped silica sol-gel and PVA hybrid film on a PB-modified C SPE	$3.9 \cdot 10^{-3}$	$2.0 \cdot 10^{-2}$	7.6 (n=12)	0.0	5/ 54 (135)

GOx/ Ferri-COs modified C SPEs	$1.4 \cdot 10^{-3}$	$6.77 \cdot 10^{-4}$ AM^{-1}	--	0.3	5/ 58 (145)
GOx immobilized by GA and Nafion on a PB-modified C SPEs	$2.5 \cdot 10^{-5}$	$5.4 \cdot 10^{-2}$	7.0 (n=5)	0.0	5/ 22 (145) 6/ 29 (184)
Multilayer films of MWCNTs/GNp/GOx on Pt	$6.7 \cdot 10^{-6}$	$2.5 \cdot 10^{-3}$ AM^{-1}	2.1-5.5 (n=5)	0.35	5/ 59 (146)
GOx/CoPC/C SPE	$2.5 \cdot 10^{-5}$	$1.3 \cdot 10^{-2}$	3.3 (n=6)	0.55	6/ 27 (183)
GOx entrapped into a PEDOT layer on a PB-modified C SPE	--	$2.67 \cdot 10^{-3}$	2.54	-0.1	6/ 28 (184)
Ag SPE/ DBSA/KCl/ CA/ GOx (Present work) DBSA/KCl dip-coated	$8.9 \cdot 10^{-5}$	$1.2 \cdot 10^{-3}$	20-50 (n=6)	-0.1	5/ (144)
Ag SPE/ DBSA/KCl/ CA/ GOx (Present work) DBSA/KCl inkjet printed	$1.6 \cdot 10^{-4}$	$7.0 \cdot 10^{-4}$	16-28 (n=6)	-0.1	6/ (182)